# Bulletin

# of the

# Geological Society of America

VOLUME 48 MAY 1, 1937 NUMBER 5

## CONTENTS

PAGES

**Wapussakatoo Mountains, Labrador. By James E. Gill, Harold M. Bannerman, and Carl Tolman** ..... 567–586

**Geology of the middle part of the Sierra de Parras, Coahuila, Mexico. By Ralph W. Imlay** ..... 587–630

**Structure of the Uinta Mountains. By J. Donald Forrester** ..... 631–666

**Etch figure investigations with optically active solvents. By Arthur P. Honess and J. Robert Jones** ..... 667–722

**Subscription, $10 per year.**

**Publication Office: Florida Avenue and Eckington Place, Washington, D. C.**

**Communications for publication should be addressed to The Geological Society of America, Prof. Charles P. Berkey, Secretary, 419 West 117th Street, New York, N. Y.**

**NOTICE.—In accordance with the rules established by the Council, claims for non-receipt of the preceding part of the Bulletin must be sent to the Secretary of the Society within three months of the date of the receipt of this number in order to be filled gratis.**

---

Entered as second-class matter in the Post-Office at Washington, D. C., under the Act of Congress of July 16, 1894.

Accepted for mailing at special rate of postage provided for in Section 1103, Act of October 3, 1917, authorized on July 8, 1918.

---

PRESS OF JUDD & DETWEILER, INC., WASHINGTON, D. C.

FIGURE 1. CHARACTERISTIC TOPOGRAPHY
Star Lake in the foreground; Lake Wabush Katsao and others beyond.

FIGURE 2. WAPUSSAKATOO MOUNTAINS
Lake Wabush Katsao in the foreground.

TOPOGRAPHY OF THE WAPUSSAKATOO AREA

BULLETIN OF THE GEOLOGICAL SOCIETY OF AMERICA
VOL. 48, PP. 567-586, 7 PLS., 2 FIGS. MAY 1, 1937

# WAPUSSAKATOO MOUNTAINS, LABRADOR

BY JAMES E. GILL, HAROLD M. BANNERMAN, AND CARL TOLMAN

## CONTENTS

| | Page |
|---|---|
| Introduction | 567 |
| Location and accessibility | 568 |
| Physiography | 568 |
| General | 568 |
| Wapussakatoo area | 570 |
| Geology | 571 |
| General distribution | 571 |
| Duley Lake series | 572 |
| Gneisses, schists, and iron-bearing quartzite | 572 |
| Marble | 573 |
| Wapussakatoo series | 573 |
| Mica schists and gneisses | 573 |
| Iron-bearing formation | 574 |
| Schistose grit | 575 |
| White quartzite | 575 |
| Intrusives | 575 |
| Acid types | 575 |
| Basic types | 580 |
| Quartz veins | 581 |
| Structure | 582 |
| Relations to rocks in other districts | 583 |

## ILLUSTRATIONS

| Figure | Page |
|---|---|
| 1. Index map of the Wapussakatoo Mountain district | 569 |
| 2. Geological map of the Wapussakatoo Mountain district | 576 |

| Plate | Facing page |
|---|---|
| 1. Topography of the Wapussakatoo area | 567 |
| 2. Lake terraces and glaciated topography | 570 |
| 3. Photomicrographs of gneiss and schist | 571 |
| 4. Photomicrographs of schists of the Wapussakatoo series | 574 |
| 5. Iron-bearing formation of the Wapussakatoo series | 575 |
| 6. Grit of the Wapussakatoo series | 578 |
| 7. Photomicrographs of granite of the Wapussakatoo region | 579 |

## INTRODUCTION

During the summer of 1933, the writers were engaged in investigations near the headwaters of the Hamilton River system in western Labrador. The expedition was organized to explore for mineral deposits, and

especially to investigate certain quartz veins which were reported to exist in this area and to carry important gold values. The reported deposits proved to be of no value. The geological observations made in connection with this work extended over some 300 square miles and are the first to be recorded from this area. A report made by A. P. Low,[1] on explorations carried out for the Geological Survey of Canada, provides the only available published information on the geology of adjacent parts of Quebec and Labrador.

## LOCATION AND ACCESSIBILITY

The area discussed in this paper lies between latitudes 52° 45′ and 53° 10′ N. and longitudes 66° 35′ and 67° 05′ W., adjacent to the height of land dividing the waters of the Hamilton River system from those flowing southward to the Gulf of St. Lawrence (Fig. 1). It lies approximately 200 miles due north in an air line from the towns of Seven Islands and Moisie, on the north shore of the St. Lawrence.

Aeroplanes were used to transport the members of the expedition, field equipment and food supplies, the trip from Moisie being made in from two to three hours, depending on weather conditions. The planes were supplied by Canadian Airways Limited, and the service rendered was very satisfactory throughout the entire season.

As an alternative, the trip could be made inland by canoe, following either the St. Margaret or the Moisie rivers, the distance being about 250 miles. These are the routes followed annually toward the end of August by the Indians, who trek inland to hunt and trap, coming out the following spring to spend the summer months at Seven Islands and Moisie. Both rivers are rough, and the trip, especially going in, is time-consuming and arduous. Owing to the fact that the working season in the interior is only about three months long, the time consumed in travelling is important, and the canoe method of travel to and from the area to be worked over is not, therefore, very satisfactory for an expedition of this kind. Canoes are needed, however, for getting about most parts of the interior.

## PHYSIOGRAPHY

### GENERAL

Flying northward from Moisie, one crosses, about 50 miles from the coast, the axis of a range of mountains rising to heights of slightly more than 3000 feet. The lower slopes of these mountains are well wooded, but the tops are rocky and bare of vegetation. The drainage is southward, toward the St. Lawrence, by turbulent streams. The main ones

[1] A. P. Low: *Report on explorations in the Labrador Peninsula, along East Main, Koksoak, Hamilton, Manicuagan, and portions of other rivers in 1892–1893–1894–1895*, Geol. Surv. Canada, Ann. Rept. 1895, pt. L (1897) 311 pages.

FIGURE 1.—*Index map of the Wapussakatoo Mountain district*

flow across the range and are entrenched 1500 feet or more below the mountain summits. About 100 miles from Moisie, the elevations of the summits are noticeably lower, and the country, although still moderately rugged, falls progressively to an average height of around 2000 feet. Relief in the central part of the Labrador peninsula is, in general, not great. There are extensive flat lake and muskeg areas with low mounds and ridges at intervals. In certain places, however, groups of hills rise several hundred feet above the general level. Some of these are of such proportions as to be properly described as mountains. The Wapussakatoo mountains stand out from their surroundings in this way. The area studied covers a portion of these mountains and some of the adjacent more subdued areas. It is bounded on the south and west by the divide that separates the waters of the Hamilton River from those flowing southward to the St. Lawrence.

All of the country as far north as Ashuanipi and Wabush Katsao lakes has been intensely glaciated. The mountain summits have been rasped and scoured by the prolonged passage of slowly moving debris-burdened ice. The valleys are clogged with drift. The flatter ground in the interior is generally covered by ground moraines, with here and there groups of kame-like hills. Beautiful eskers along the upper stretches of the Hamilton River system extend north and south, generally following the valleys. Some of them can be traced for as much as 40 to 50 miles. Shore lines, marking the earlier stands of lakes, partially drained since Pleistocene time, are locally conspicuous features.

Although the local details of drainage reflect the vagaries of glacial deposition and glacial erosion, the deeply entrenched and structurally adjusted character of the main valleys, many of which run transverse to the direction of ice movement, makes it clear that the broader features of the drainage system originated long before the Pleistocene. The existence of abundant glacial drift, even in the main valleys, shows conclusively that erosion since the disappearance of the last ice sheet has been slight.

### WAPUSSAKATOO AREA

The area studied more particularly is, on the whole, of fairly rugged topography, but quite extensive lowlands exist (Pl. 1, fig. 1) in the form of broad river-cut pre-glacial valleys, somewhat clogged by glacial and lake deposits. Large and small lakes are extant in many parts of this area. Groups of hills rise 200 to 900 feet above the valley bottoms, their summits reaching an altitude of 2200 to 2900 feet above sea level. A range, referred to by the Indians as the Wapussakatoo Mountains (Pl. 1, fig. 2), in the west-central part of the area, is the most conspicuous surface feature in the district. Characteristically, the hills are rocky prominences, smooth and rounded in general aspect, but somewhat precipitous and craggy in detail. These lineaments, together with the polished and striated rock surfaces, chatter-marks, and the profusion of erratic boulders of various rock types on their summits, show beyond reasonable doubt that for some time during the Pleistocene period even the highest of these hills was overridden by ice.

Bed-rock exposures are found mainly along the summits of the ridges, where, too, are found the more resistant rocks. The highest ridges, which lie in the western part of the area, are held up by massive quartzite. Secondary ridges, in the same area, are formed of siliceous iron-bearing strata and, in a few instances, of large intrusive masses of gabbro or diabase. Toward the south, are mesas of marble; toward the southeast, abrupt cuestas of garnetiferous gneiss stand out in strong relief. The glaciated outcrop surfaces are remarkably fresh-looking. Even where they have been rendered somewhat friable by the ravages of mechanical

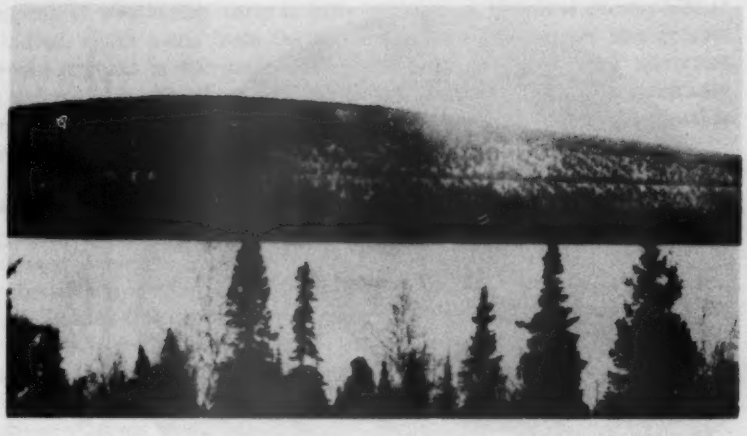

FIGURE 1. LAKE TERRACES ON SLOPES RISING FROM LAKE WABUSH KATSAO

FIGURE 2. CHARACTERISTIC BARE ICE-SCOURED SUMMITS
Slopes covered with reindeer moss and scattered evergreens.

LAKE TERRACES AND GLACIATED TOPOGRAPHY

FIGURE 1. CYANITE GNEISS OF THE DULEY LAKE SERIES
Conspicuous crystals of cyanite showing cleavage, and standing in relief, dark flakes of biotite, clear particles of quartz, and altered albite. Note the orientation of the biotite at an angle to the other linear elements. Ordinary light, x 20.

FIGURE 2. QUARTZ-BIOTITE SCHIST OF THE WAPUSSAKATOO SERIES
Flakes of biotite, most of which are aligned, in a mosaic of quartz. Ordinary light, x 20.

PHOTOMICROGRAPHS OF GNEISS AND SCHIST

agents of weathering, there is little evidence of chemical decomposition. Indeed, slides made from the various feldspathic gneisses and igneous rocks exposed in the area are conspicuously free from such alteration products as kaolin, chlorite, and limonitic stains, which are so commonly found in the weathered portions of similar rocks in the regions farther south.

The slopes rising from Wabush Katsao Lake are interrupted by conspicuous terraces (Pl. 2, fig. 1), which speak of a time, presumably late glacial, when the lake was much more extensive than now. The upper terrace is approximately 100 feet above the present lake level. It is ostensibly a wave-washed shore line. It marks the upper limit of the lake beds in this part of the region, and it is made particularly noticeable on the steeper slopes by the presence of many large erratics, from among which the finer sediment has been washed. Lower benches, which are essentially depositional features, mark in a general way the top of the apron of sands and silts that were deposited on the shoreward slopes of the ancestral lake basin. Ordinarily, they slope lakeward. They are not at a constant elevation, but rise higher in the side valleys, where streams built deltas in the lake, and they are quite indistinct where the shores of the present lake rise abruptly.

## GEOLOGY

### GENERAL DISTRIBUTION

The rocks in the district are shown in the following table of formations, the oldest at the bottom and the youngest at the top:

| | |
|---|---|
| Unconsolidated | Glacial drift, lake and outwash deposits, muskeg |
| Basic intrusives | Olivine gabbro and diabase |
| Acid intrusives | Biotite and biotite-hornblende granite; microcline granite; pegmatite, aplite, and porphyritic granite dikes |
| Basic intrusives | Diorite, gabbro |
| Wapussakatoo series | White quartzite<br>Schistose grit<br>Iron-bearing formation<br>Mica schists and gneisses, injection gneiss |
| Duley Lake series | Marble<br>Gneisses, schists, and iron-bearing quartzite |

The sequence shown for the meta-sediments is only tentative. All the rocks are considered to be pre-Cambrian in age, except the unconsolidated superficial deposits, which are Pleistocene and Recent.

The distribution of the rock groups distinguished in the District is shown in Figure 2. It will be observed there that the Duley Lake series occupies the southeastern part of the area and the Wapussakatoo series the mountainous western and northwestern parts. There is a sharp contrast in structure between these two areas as well as in rock composition and physiographic forms.

### DULEY LAKE SERIES

*Gneisses, schists, and iron-bearing quartzite.*—A great variety of metamorphic types is found within the Duley Lake series. They range from medium-grained quartz-garnet-cyanite schist or quartz-mica schist, to coarse-grained feldspathic quartz-garnet-sillimanite gneiss and almost massive quartz-hornblende-garnet rock.

The formation exhibits atttitudes ranging from flat-lying to steeply inclined, but low dips are the rule. Bedding is well preserved even where metamorphism was intense. The rocks are generally foliated, with foliation planes parallel to the bedding, or nearly so.

Bands of quartz-mica schist flank the west shore of Lake Wabush Katsao and have been observed in isolated outcrops in the area south of this lake. In places, these carry much carbonate and oxide of iron. They are interbedded with quartz-garnet-mica schists and quartz-garnet-hornblende schist.

Coarse-grained garnet-cyanite gneiss is developed most extensively near the southeastern boundary of the sheet, where the prevailing structure is flat-lying. A thin section of cyanite gneiss from this area is composed essentially of quartz, albite, and biotite, with cyanite, muscovite, graphite, sillimanite, zircon, garnet, and possibly cordierite (Pl. 3, fig. 1). The rock has a well-developed gneissic structure, emphasized mainly by the parallel orientation of muscovite, cyanite, and the elongation of the quartz crystals. The biotite flakes, on the other hand, are rudely aligned at approximately 60 degrees to this direction, and in thin section, are found to be accompanied in this alignment by the twinning in the albite and a marked streakiness in the quartz—the latter feature being due to a system of fractures in the quartz, along which tiny cavities are strung out, which, in ordinary magnifications, resemble specks of opaque minerals. The biotite is distinctly later than the cyanite, as is shown by consistent moulding of the biotite on the cyanite. The garnet is older than the sillimanite, as the latter is wrapped around or is moulded on the broken garnet crystals.

Bands of impure quartzite were noted at several localities in the Duley Lake series. Ordinarily, they are well-bedded hornblende-actinolite or biotite-garnet-bearing rocks, but in a few places, notably on the west shore, near the south end of Wabush Katsao Lake, and on the shoulders

of the hills 2 miles south of this lake, a facies carries so much magnetic oxide of iron as to seriously deflect the compass needle. This particular facies is apparently local in extent, for in the southeastern part of the area, where the amphibole and garnet-mica gneisses are most common, the iron-bearing quartzite was not recognized. Usually, the iron-rich beds are not more than 6 to 8 feet thick, and they seem prone to appear among the quartz-amphibole type of quartzite. In thin section, they are found to consist of fairly coarse-grained quartz, some carbonate, and upward to 20 per cent magnetite. Some of the magnetite is coarse, but most of it is finer grained than, and interstitial to, the quartz.

*Marble.*—A large part of the area south and east of Duley Lake is underlain by marble. For the most part, it is a thickly bedded, medium- to coarse-grained, pale buff to white aggregate. In part, however, it is thinly bedded and siliceous. Characteristically, it exhibits many thin silicified bands, which either follow the planes of stratification or pass at low angles from one bed to another. It contains also many concretion-like nodules of quartz. Near the base, a band 40 feet thick is composed mainly of fine-grained, well-bedded quartzite. In some places the formation is streaked with actinolite and other greenish minerals, in other places with fibrous tremolite. Beautiful specimens of these metamorphic minerals can be collected at various points. The thickness of the limestone member has not been accurately determined, but it is at least 250 feet. Structurally, these beds show only moderate disturbance. The bedding is gently undulating, with few dips more than 25 degrees.

### WAPUSSAKATOO SERIES

*Mica schists and gneisses.*—Mica schists and gneisses of the Wapussakatoo group have a wide distribution. They are best exposed in the mountainous western and northwestern parts of the area. Typically, they are thinly bedded, strongly schistose rocks, grading from black to greenish or grayish black. Some of the gray and green bands proved to be quartz-tremolite and quartz-actinolite schists. Locally, they are interbedded with iron-rich bands, indistinguishable from the overlying carbonate iron-bearing formation, and, occasionally, particularly near the base of the series, the schists contain some beds of fine-grained impure garnet-bearing quartzite. In most instances, the original bedding is preserved, and the schistosity is approximately parallel to it.

South of Sunday Lake and along the height of land west of Narrow Lake, they are cut by small dikes of granite, and, here, local developments of biotite-staurolite schists and biotite-feldspar gneiss are found. Toward the head of Rivière aux Fraises, exposures near the granite batholith grade into injection gneiss, with increasing proportions of granitic material as the granite is approached.

Thin sections show the most abundant micaceous schists to consist of biotite, quartz, sericite, and fresh sodic plagioclase with graphite in some bands and, rarely, chlorite (Pl. 3, fig. 2). Magnetite is locally abundant. Garnet, zircon with well-developed haloes, and staurolite are found in some slides, but are relatively rare. Tremolite, actinolite, hornblende (Pl. 4, fig. 1), augite, rutile, cordierite, and epidote were also noted. Many of the slides show effects of deformation subsequent to recrystallization, such as fractured quartz and bent mica flakes.

Well-preserved bedding structures show, without doubt, that these rocks were originally sedimentary. In common with the other sediments of this series, they are intricately folded. Their total thickness is not known, and their transition to the carbonate type of iron-bearing formation is so gradual that boundaries must be drawn arbitrarily.

*Iron-bearing formation.*—Sediments carrying large amounts of iron oxides or carbonates are interlayered with bands of mica, graphite, and hornblende schists and make up a prominent formation within the Wapussakatoo series. This formation is as much as 1000 feet thick, but, in mapping, it was not differentiated from the gneisses and schists of the series (Fig. 2). It is most widely exposed in a broad band within, and just east of, the Wapussakatoo Mountains. To the north, it is exposed on Mt. Bondurant and at several other places nearby. South of the mountains, a broad exposure lies just west of the northern portion of Mills Lake. Characteristically, these beds are folded and faulted and more or less metamorphosed. In the central part of the map area, where the formation is best exposed, folds are generally tightly compressed and overturned toward the northwest.

Several types of iron-bearing sediments are distinguishable within the formation. The most common is an interbanded quartz and iron carbonate, carrying small amounts of iron oxide and grunerite in the iron-rich beds (Pl. 4, fig. 2). In the more severely deformed portions of the range, this variety becomes essentially a quartz-grunerite schist bearing considerable specularite. In places, this rock is intricately folded (Pl. 5, fig. 1). It weathers to a deep rusty brown.

Intimately associated with this type, and apparently grading into it, is a quartz and magnetite-specularite variety, in which bands of white quartz alternate with layers of sparkling specularite and magnetite (Pl. 5, fig. 2). These beds are richer in iron than are the carbonate-bearing member, but are more local in extent.

A third type is composed mainly of quartz, magnetite, and specularite. It is rudely banded. The quartz grains in the more siliceous portions are of various shapes and sizes. Many of them are rimmed by iron oxides

FIGURE 1. HORNBLENDE-BIOTITE SCHIST
Basal sections of hornblende, flakes of biotite, and quartz. Ordinary light, x 20.

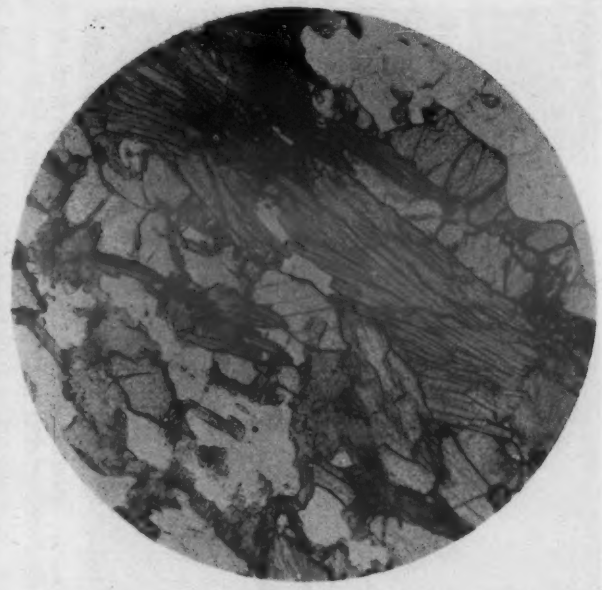

FIGURE 2. QUARTZ-GRUNERITE SCHIST OF THE IRON-BEARING FORMATION
Conspicuous grunerite showing cleavage, calcite standing in relief, and quartz. Ordinary light, x 69.

PHOTOMICROGRAPHS OF SCHISTS OF THE WAPUSSAKATOO SERIES

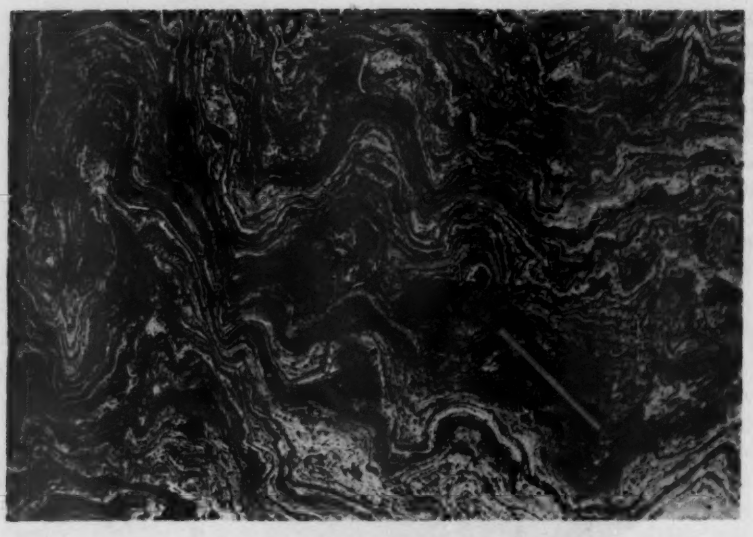

FIGURE 1. INTRICATELY FOLDED QUARTZ-GRUNERITE SCHIST
Representing metamorphosed carbonate iron-bearing beds.

FIGURE 2. BANDED QUARTZITE IRON-BEARING BEDS
Light bands are relatively pure quartzite; dark bands contain considerable specularite and magnetite.

IRON-BEARING FORMATION OF THE WAPUSSAKATOO SERIES

and packed together in a matrix of iron oxide and carbonate in a manner, in many respects, resembling an iron-rich quartzite of clastic origin. This type is quite local, and apparently is near the top of the assemblage.

No part of the iron-bearing formation observed in these areas is rich enough in iron for commercial exploitation under present conditions.

*Schistose grit.*—To the north of the Wapussakatoo Mountains, in the valley of Rivière aux Fraises, the schists and iron-bearing formation are overlain by heavy beds of grit or fine conglomerate. In its relation to the schists, this rock resembles the white quartzite, to be described next. It is, therefore, considered to be roughly equivalent in age to the quartzite. The grit possibly lies beneath the quartzite toward the north, but does not extend as far south as the mass of the Wapussakatoo Mountains.

The grit is commonly well banded (Pl. 6, fig. 1). It consists of numerous more or less rounded particles, from an eighth to half an inch in diameter, mostly of granitic material in a finer matrix that is now largely mica, but includes some quartz and a little feldspar. The rock is distinctly schistose (Pl. 6, fig. 2).

*White quartzite.*—A quartzite, remarkable for its purity, crops out on the tops of the higher ridges in the west-central part of the area. It is essentially a massive rock, made up of rather coarse interlocking grains of glassy to milky quartz, so uniform in texture, color, and composition that small exposures or boulders of the formation strongly resemble vein quartz. Large exposures, however, usually reveal streaky color banding, presumably inherited from original bedding. In some places, particularly near the base of the formation, where it is interlayered with a conglomeratic quartz-muscovite schist, excellent bedding was observed, and in several places the upper part of the exposed section contains a little carbonate of iron and streaks of iron oxide. The formation is well developed and fairly persistent in the mountainous areas, but, in common with the adjacent members of the Wapussakatoo series, it has suffered severe deformation, such that its apparent thickness has been considerably increased by folding.

### INTRUSIVES

*Acid types.*—The acidic intrusives include two petrographically different granites. One constitutes a large batholith, occupying the northwestern part of the area; the other is represented by several smaller bodies in the southern part of the area. The writers are not able to state definitely whether more than one intrusive epoch is represented by the granites, but the distribution and differences in composition suggest that such may be the case.

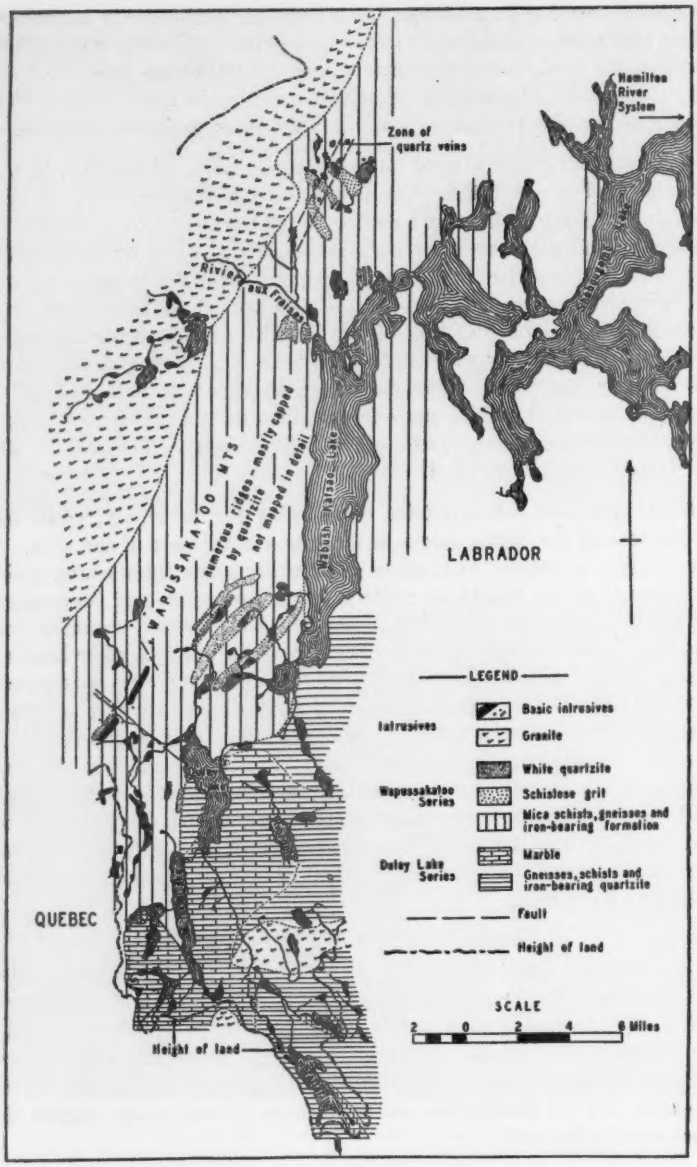


FIGURE 2.—*Geological map of the Wapussakatoo Mountain district*

The batholith in the northwestern part of the area is at least 30 miles by 25 miles in extent. Its contacts, so far as known from observations and reliable information from other sources, are shown in Figure 2.

The rock typical of the batholith is grayish, medium grained, and contains conspicuous biotite and quartz that tends to be opalescent in places. Both plagioclase and potash feldspar are prominent constituents. The plagioclase, generally in excess of the potash feldspar, has a percentage composition of about $Ab_{90}An_{10}$. The potash feldspar shows a variable amount of microcline twinning, which is distributed in such a way as to suggest a genetic relation to minute fractures traversing the feldspar. Deformation is not only indicated by the fracturing and, in places, granulation of the feldspar but also by the fracturing and marked strained extinction of the quartz. Much of the feldspar, especially where it is shattered, has been extensively sericitized. A small amount of epidote has been developed within the feldspar in some sections. Biotite, a greenish brown pleochroic variety, is the only dark mineral present in almost all sections and makes up between 7 per cent and 15 per cent of the rock in most places. A distinctive feature of the biotite in all the granite examined was the plentiful development of intersecting minute needle-like inclusions, probably rutile, along planes intersecting at 60 degrees. In a few places, minor amounts of hornblende are present with the biotite. Apatite is a common accessory, but the almost complete absence of zircon is notable (Pl. 7, fig. 1).

Analysis of a specimen typical of the granite of the eastern part of the batholith, collected 6 miles west of Lake Wabush Katsao, is as follows:

| | per cent | *Norm* | per cent |
|---|---|---|---|
| $SiO_2$ | 66.90 | Quartz | 19.32 |
| $Al_2O_3$ | 14.02 | Orthoclase | 21.13 |
| $Fe_2O_3$ | 1.46 | Albite | 34.06 |
| FeO | 3.50 | Anorthite | 9.45 |
| MgO | 2.71 | Hypersthene | 10.23 |
| CaO | 2.44 | Diopside | 1.63 |
| $Na_2O$ | 4.00 | Magnetite | 2.09 |
| $K_2O$ | 3.59 | Ilmenite | 1.22 |
| $H_2O+$ | 0.59 | Apatite | 0.34 |
| $H_2O-$ | 0.05 | | |
| $CO_2$ | 0.50 | Total | 99.47 |
| $TiO_2$ | 0.59 | | |
| $P_2O_5$ | 0.13 | C. I. P. W. symbol II, 4, 2, 4 | |
| MnO | 0.01 | | |
| Total | 100.49 | | |

Analyst, H. I. Miller.

Much of the feldspar is masked by sericite, which prevents a confident distinction being made between orthoclase and plagioclase. A Rosiwal analysis of a thin section from this specimen gives the following result:

| | per cent |
|---|---|
| Quartz | 17.9 |
| Orthoclase | 25.0 |
| Plagioclase ($An_{35}$) | 45.6 |
| Biotite | 10.9 |
| Accessory | .6 |
| | 100.0 |

Adamellite (Johannsen)

Dikes of pegmatite and aplite were observed to cut the schists bordering the granite in a number of places. These are as much as 25 feet wide and are clearly derived from the granite. The main body of granite near its contact with the schists loses its normal granitic appearance and takes on a distinct banding. This banding is believed to be an inheritance from the schists, which it has intruded and incorporated in part within its own mass. Gradual transitions from granite to schists are the rule, and, where such transitions could be observed, banding in the granites was parallel to the schistosity in the adjacent schists.

Small dikes of pale quartz-rich granite cut the schists and iron formations in the west-central part of the area mapped. Most of these dikes are 2 to 8 feet in width, but in places are as much as 25 feet wide. They cut across the foliation and bedding of the older rocks. Apparently, they are offshoots of a larger body not far distant, for the general degree of metamorphism of the schists is increased near the sections that contain these intrusive bodies. Essentially, the dikes are composed of pale gray- to buff-colored perthitic feldspar and quartz, together with small quantities of muscovite and biotite. The feldspar and quartz have undergone a certain amount of crushing, and the feldspars are drab-looking because of the development of considerable sericite. The quartz tends toward bluish tints and in places occurs as phenocrysts, but the dikes, on the whole, are not typical porphyries. Some are accompanied by small quartz veins, but they seem to be barren of metals.

The granitic rocks in the southern part of the area differ from the batholithic rocks to the north in their higher proportion of potash feldspar. They include a number of stock-like and irregularly shaped bodies with numerous dikes as follows:

Along the height of land and in the areas surrounding Duley Lake and Mills Lake, the marble and other members of the Duley Lake series are intruded at intervals by dikes of pegmatite. Some of these dikes, usually small, are as much as 40 feet in width. They are typically whitish,

FIGURE 1. BANDING IN THE WAPUSSAKATOO GRIT

FIGURE 2. PHOTOMICROGRAPH SHOWING SCHISTOSE NATURE OF THE GRIT
Eyes of feldspar and of quartz are shown in a finer-grained matrix in which biotite has been developed. Ordinary light, x 20.

GRIT OF THE WAPUSSAKATOO SERIES

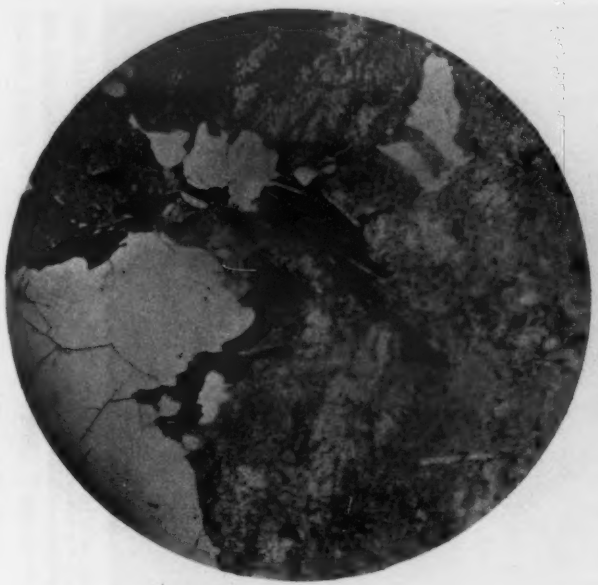

FIGURE 1. GRANITE TYPICAL OF THE WESTERN PART OF THE REGION
Note fractured quartz, biotite, and greatly sericitized feldspar. Ordinary light, x 20.

FIGURE 2. GRANITE TYPICAL OF THE SOUTHERN PART OF THE REGION, NEAR DULEY LAKE.
Quartz, microcline, and acid oligoclase can be distinguished. Crossed nicols, x 18.

PHOTOMICROGRAPHS OF GRANITE OF THE WAPUSSAKATOO REGION

some of them so white as to resemble vein quartz. Their essential composition is potash feldspar, quartz, and muscovite. The quartz is usually abundant. They are, on the whole, coarse-grained and yield fine specimens of whitish iridescent feldspar.

An oblong body of granitic gneiss underlies the eastern part of the area, about 3 miles south of Duley Lake. The long axis is oriented in a general east-west direction. The body is about 1¾ miles wide and 4 miles long within the area mapped, but extends eastward an unknown distance. This body intrudes the garnet-gneiss and limestone of the Duley Lake series. The boundaries between the garnet-gneiss and the granitic rock are gradational. The magma appears to have soaked into the sediments in a pervasive manner and to have converted them to rock essentially of granitic composition and texture. The structural trends of the foliation in the granitic gneiss and the bedding of the adjoining garnet gneiss are parallel. Some of the bands still retain remnants of the earlier mineral components, such as garnet and cyanite. These, together with the gray color and the distinctive banding of the gneiss, disappear as the section is followed toward the central part of the body, and the rock becomes an igneous gneiss in appearance. Typically, this rock is a pinkish, strongly foliated biotite-feldspar gneiss, relatively rich in quartz. In places, it is traversed by small dikes of aplite and pegmatite.

Bodies of granitic gneiss also are found along the height of land at the south end of the area. For example, portions of the garnet gneiss that forms the ridge on the west side of Gibraltar Lake are converted into hybrid rocks, apparently by lit-par-lit injection.

Another body of gneissic granite intrudes the marble near the northeast shore of Duley Lake. This body is about half a mile by a quarter of a mile in extent. Its boundaries are sharply demarked against the coarse-grained marble. The periphery of the mass is a medium-grained biotite granite gneiss, composed essentially of grayish to pinkish feldspar, quartz, and biotite. Toward the center, a pegmatitic facies appears, which is a relatively coarse-grained, quartz-rich feldspathic aggregate containing some muscovite and a little pyrite.

Thin sections of the various masses of granitic rock in the area south and east of Duley Lake, which have just been discussed, show them to be similar to one another. They have an appreciably higher potash content than has the granite of the batholith in the northwestern part of the area, and, characteristically, also, they are lower in dark mineral. Essentially, they consist of quartz and microcline, with lesser amounts of microcline perthite and occasional grains of acid plagioclase. The mica minerals are muscovite and a greenish-brown biotite. There is, also, a rela-

tively large amount of zircon, commonly showing strong pleochroic haloes (Pl. 7, fig. 2). The pegmatite dikes in this part of the area are essentially the same as the granitic bodies in mineral composition. The main feldspar is microcline, usually quite white in hand specimens. Microcline perthite, quartz, and appreciable amounts of muscovite are also present.

The following is an analysis of a specimen of the granite on the northeast shore of Duley Lake:

| | per cent |
|---|---|
| $SiO_2$ | 74.31 |
| $Al_2O_3$ | 14.08 |
| $Fe_2O_3$ | .25 |
| FeO | .30 |
| MgO | .22 |
| CaO | .46 |
| $Na_2O$ | 3.85 |
| $K_2O$ | 5.95 |
| $H_2O+$ | .23 |
| $H_2O-$ | .04 |
| $TiO_2$ | .04 |
| $P_2O_5$ | .10 |
| MnO | .01 |
| Total | 99.84 |

Analyst, R. B. Ellestad.

| *Norm* | per cent |
|---|---|
| Quartz | 27.84 |
| Orthoclase | 35.58 |
| Albite | 32.48 |
| Anorthite | 1.39 |
| Hypersthene | .86 |
| Magnetite | .46 |
| Apatite | .34 |
| Corundum | .71 |
| Total | 99.66 |

C. I. P. W. Symbol I, 4, 1, 2

| *Mode* | per cent |
|---|---|
| Quartz | 25. |
| Microcline and microperthite | 52. |
| Albite | 22. |
| Biotite | 0.9 |
| Minor minerals | 0.3 |
| Total | 100.2 |

Alaskite (Johannsen)

Other than a little pyrite, these intrusive rocks do not carry any appreciable amounts of sulphides or other metalliferous minerals.

*Basic types.*—A few basic dikes were observed in the northwestern part of the map area. Thin sections of two of these showed them to be badly altered hornblende-plagioclase rocks. One contained a little biotite as well. The plagioclase is greatly obscured by white micaceous alteration products, and there is considerable development of epidote and chlorite throughout. The hornblende, in large part at least, appears secondary. The alteration is such that it is not possible to give a significant mineralogical analysis of the rock. The age relations of these intrusives to the others in the district could not be determined, but, from the degree of alteration they exhibit, they are almost certainly older than the granites.

Numerous intrusive masses of gabbro and diabase cut the iron formations and associated rocks in the northern and central sections of the

area. Some of these are masses of considerable size, but of undetermined form. Some are large dikes. One dike in particular has a width of about 700 feet, a north-south strike, and has been traced, at intervals, for more than 4 miles. The dominant type included in this group is a medium-grained, dark, massive rock, consisting mainly of lath-shaped grayish plagioclase feldspar and black- to brownish-colored pyroxene. Considerable quantity of olivine, commonly rimmed by hypersthene, is present. Small amounts of serpentine and actinolite are found as alteration products of the olivine and hypersthene, respectively, in some of the specimens. A Rosiwal analysis of a section from a specimen from one of the intermediate-sized dikes northwest of Wapussakatoo Mountains gives the following result:

| | per cent |
|---|---|
| Plagioclase (approx. $An_{50}$) | 56.7 |
| Pyroxene (mainly augite but some hypersthene) | 18.6 |
| Olivine (partly altered to serpentine) | 5.0 |
| Magnetite (partly a product of serpentinization process) | 4.6 |
| Biotite (largely reaction rims about magnetite-plagioclase boundaries) | 2.2 |
| Serpentine, actinolite, and others | 11.4 |
| Minor minerals, mainly apatite | 1.5 |
| | 100.0 |

Gabbro (Johannsen)

These rocks are characteristically fresh and unmetamorphosed and resemble, to a marked degree, the so-called olivine diabase or "younger diabase" of the region north of Lake Huron. They are considered to be the youngest rocks in the district.

## QUARTZ VEINS

Veins of coarse glassy quartz with local nests of chlorite and variable amounts of sulphides were observed at numerous points, more particularly in the northwestern part of the area. These veins are from a few feet to more than 100 feet wide. They strike northwest and have steep dips. Most of those examined lie in a belt striking N.27°E. (Fig. 2). Pyrrhotite is the most abundant sulphide, and in it, clear, well-formed crystals of quartz are found. Locally, pyrite and chalcopyrite appear, but, in most of the veins, sulphides are not abundant. Where iron-bearing formation is in one or both walls, iron-bearing carbonates are found in the veins. At one place, brecciated, iron-bearing formation of the cherty type has been extensively replaced by sulphides (pyrite and pyrrhotite). The suggestion is strong, in such instances, that the iron forming the sulphides has come from the replaced rock, for the iron sulphides are unusually abundant, and the iron oxides of the original rock have disappeared. Some of the quartz has formed by recrystallization of cherty iron formation, for gradations from vein quartz to chert can be observed.

In the iron-rich beds, little more than sulphur had to be introduced to form the nearly massive sulphide deposits. On weathered surfaces, these deposits present an impressive display of gossan. Similar exposures are not at all uncommon in more-traveled parts of the Canadian Shield.

From the coarse glassy character of the quartz and the abundant pyrrhotite, it appears that these veins formed under high-temperature conditions.

## STRUCTURE

The conditions under which the work was carried out did not make it possible to establish conclusively the relations between the various formations. Consequently, any discussion of the structure must be liberally interspersed with question marks. All that can be done at present is to state the facts, to suggest the possible structural relations, and to point out where more detailed work should yield positive results.

In the earlier part of this paper, the meta-sedimentary rocks were divided into two series, named Duley Lake and Wapussakatoo, respectively. This grouping is based mainly on rock compositions, general field associations, and structural likenesses. The various members of each series have a similar field distribution, appear to be structurally conformable, and are similarly deformed. Between the two series, however, there is a marked lithologic and structural contrast.

The Wapussakatoo series occupies the northwest part of the area. The mica schists, iron-bearing formation, and quartzite, which are the dominant rock types, have been thrown into tight folds with axes trending N.20°E. to N.30°E. They are generally overturned toward the northwest. The only departure from the general trend is along the valley of Rivière aux Fraises, where there is a sharp local swing toward the northwest.

It is strongly suspected that thrust faults striking northeasterly and dipping southeasterly are important elements in the structure, but none was found exposed, and the mapping was not sufficiently complete to prove conclusively from indirect evidence that such faults exist.

In the area west of the south end of Lake Wabush Katsao, the outcrops are numerous, so that without much doubt the structure and stratigraphy could be determined quite accurately by additional and more detailed work.

The Duley Lake series occupies the southern and southeasterly parts of the area. The lower members are gneisses of various kinds. The upper members are mainly marbles. The gneisses and marbles show only slight folding. Dips are usually less than 30 degrees, except at a few points, where faults post-dating the folding are known to exist. Near the contact with the Wapussakatoo rocks, the prevalent strike is north-

easterly, but a few miles back from that contact the prevailing strike is almost at right angles, in a general northwesterly direction. This is shown by narrow strips of marble, preserved southeast of the main body of marble, as well as by banding in the gneisses.

The Wapussakatoo series and the Duley Lake series are in contact along an irregular line, as shown on the map (Fig. 2). As the contact was not exposed at any of the sections examined, the structural relations between the two series were not determined. It appears clear, however, from the lack of parallelism between the contact and the trend of the rock structures in the Wapussakatoo area and from the divergence of the strikes from one another on opposite sides of the contact, at certain places, that the two series are not structurally conformable. This means that the contact is at an angular unconformity or a fault.

If the two series are in contact at an angular unconformity, the older must have suffered two deformations. In the Duley Lake series, sharp changes in strike within short distances are characteristic, suggesting that the series has been folded more than once. In the Wapussakatoo area, strikes are consistently in the same general direction for long distances, and, except locally, where folds terminate, changes in trend occur gradually and affect the whole belt. Under this hypothesis, the Duley Lake series must, therefore, be considered the older.

If the contact is at a fault, a low-angle thrust with a dip toward the east is indicated by the sinuous character of the contact and the consistent overturning of the Wapussakatoo folds toward the west. On such a fault, the Duley Lake formations would, therefore, have been carried upward and northwestward, relative to the Wapussakatoo. In this instance, the age relations are in doubt, but it appears more probable that the Duley Lake series is the older.

In addition to probable thrust faults related to the folding, there are high-angle faults of later date. Two sets are prominent. These trend N.25° to 40°W. and N.55° to 70°W., respectively. The more important representatives of these sets within the mapped area are shown. Those along Ironstone River and Gibraltar Lake are particularly prominent. The influence of these fault sets on the topography in other parts of the district is suggested by the trends of the waterways, particularly the N.25°W. direction. Certain of these faults are found to have offset the younger diabase dikes, so they are considered to be the latest prominent structures in the district.

## RELATIONS TO ROCKS IN OTHER DISTRICTS

The relationship of these rocks with those in better-known parts of the Canadian Shield is a matter of great interest, but, because of the extensive

areas of unmapped country that separate these exposures from those which have been studied in detail, no precise correlation is possible. The most striking similarities are found in comparing the Duley Lake rocks with the Grenville series of the southeastern part of the Canadian Shield. Low, in his explorations, extending northeastward from the typical Grenville area, found rocks closely resembling the Grenville, as to composition, structure, and degree of metamorphism, on all the rivers traversed. He describes these rocks as follows:

"Mica-gneiss greatly predominates over all the other members of this group, and it varies from coarse-grained, well crystallized gneiss, through all gradations of texture and composition to mica-schist. Pink or white orthoclase, quartz and mica (generally biotite) are always present, and hornblende is often found in small quantities. Garnetiferous bands are frequently met with, especially in the great areas along the Manicuagan River. The gneisses are usually very quartzose, and in many places shade into an impure, garnetiferous quartzite. All are well foliated or stratified, and in many places the dip of the foliation approaches the horizontal, giving the rocks the appearance of flat-bedded, altered clastic rocks. In many places, these gneisses and schists are associated with bands of crystalline limestone."[2]

The close similarity between these rocks and those of the Duley Lake series is obvious, and it seems reasonable, in consequence, to place them tentatively together. The resemblance to the Grenville area extends to the intrusives found, though it cannot be said that all the igneous epochs of the Grenville province are represented in this northerly area. It is interesting to note, however, that true anorthosites and anorthositic gabbros are found at intervals throughout the region from the Hamilton River southwestward. Although these rocks were not found in the area mapped, Gill saw several bodies east and west of Ashuanipi River, the nearest being about 20 miles east of Duley Lake. The granites in the region occupied by the Duley Lake series are potash-rich types, resembling those in the type Grenville area and contrasting with those to the northwest of the Grenville area along the Quebec gold belt. The latter are dominantly soda-rich granites and related types, some of which are not greatly different from the granite in the extreme northwestern part of the area described in this paper.

The Wapussakatoo series, with its quartzites, sedimentary schists, and abundant carbonate and oxide iron-bearing formations, strongly resembles the older Huronian formations of the Lake Superior district.

Thus, from the scattered information at hand, it seems almost certain that, with more detailed work, it will not only be possible to determine the true relations of the two rock series to one another, but to others of similar character farther north in the Hamilton River region, which have

[2] A. P. Low: *Report on explorations in the Labrador Peninsula, along the East Main, Koksoak, Hamilton, Manicuagan, and portions of other rivers*, Geol. Surv. Canada, Ann. Rept. 1895, pt. L (1897) p. 197.

been previously described by Low, and were examined at numerous points by Gill during an earlier visit to the region (1929). Moreover, the record, when worked out, promises to present some interesting parallels to that found in the pre-Cambrian areas around Lakes Superior and Huron. A point of special interest is that, in the Hamilton River region, the field occurrence of meta-sediments of Grenville and Huronian types is such that there is every reason to believe that their age relations could be definitely established.

McGill University, Montreal, Que.; Dartmouth College, Hanover, N. H.;
Washington University, St. Louis, Mo.
Manuscript received by the Secretary of the Society, March 26, 1936.
Read before the Geological Society, December 27, 1934.

RELIEF MODEL OF THE MIDDLE PART OF THE SIERRA DE PARRAS

BULLETIN OF THE GEOLOGICAL SOCIETY OF AMERICA
VOL. 48, PP. 587-630, 14 PLS., 4 FIGS. MAY 1, 1937

# GEOLOGY OF THE MIDDLE PART OF THE SIERRA DE PARRAS, COAHUILA, MEXICO

BY RALPH W. IMLAY

CONTENTS

| | Page |
|---|---|
| Introduction | 589 |
| Location and extent of area | 589 |
| Construction of maps and sections | 589 |
| Acknowledgments | 589 |
| Earlier investigations | 590 |
| Geography | 590 |
| Topography and drainage | 590 |
| Culture | 596 |
| Water supply | 597 |
| Sedimentary rocks | 597 |
| Jurassic system | 598 |
| La Gloria formation | 598 |
| Areal extent | 598 |
| Stratigraphic and lithologic features | 599 |
| Correlation | 600 |
| La Casita formation | 600 |
| Areal extent | 600 |
| Stratigraphic and lithologic features | 601 |
| Fossils | 602 |
| Correlation | 603 |
| Cretaceous system | 605 |
| Taraises formation | 605 |
| Areal extent | 605 |
| Stratigraphic and lithologic features | 605 |
| Fossils and correlation | 605 |
| Cupido limestone | 606 |
| Definition | 606 |
| Areal extent | 606 |
| Stratigraphic and lithologic features | 606 |
| Correlation | 607 |
| La Peña formation | 607 |
| Areal extent | 607 |
| Stratigraphic and lithologic features | 607 |
| Fossils and correlation | 610 |
| Aurora limestone | 611 |
| Areal extent | 611 |
| Stratigraphic and lithologic features | 611 |
| Origin and correlation | 613 |
| Cuesta del Cura limestone | 613 |
| Areal extent | 613 |

Page

Stratigraphic and lithologic features ..... 614
Correlation ..... 615
Indidura formation ..... 615
Areal extent ..... 615
Stratigraphic and lithologic features ..... 615
Correlation ..... 616
Caracol formation ..... 616
Definition ..... 616
Areal extent ..... 616
Stratigraphic and lithologic features ..... 616
Origin ..... 618
Correlation ..... 619
Parras shale ..... 619
Areal extent ..... 619
Stratigraphic and lithologic features ..... 619
Source of sediment ..... 619
Correlation ..... 620
Quaternary system ..... 620
Mayrán formation ..... 620
Alluvium ..... 620
Igneous rocks ..... 620
Distribution and structural relations ..... 620
Petrology of the monzonite porphyry ..... 622
Petrology of the granite ..... 622
Structure ..... 622
General features ..... 622
Folds continuous from the western part of the Sierra de Parras ..... 623
Santiago anticline ..... 623
Parras anticline ..... 623
Taraises anticline ..... 623
Prieta anticline ..... 625
Juan Perez anticline ..... 625
Folds beginning in the middle part of the Sierra de Parras ..... 625
Conejo anticline ..... 625
La Gloria anticline ..... 626
Patagalana anticline ..... 626
Organo anticline ..... 626
Concordia anticline ..... 626
Berrendo anticline ..... 627
Sabinilla anticline ..... 627
Faults ..... 628
Mineral deposits ..... 628
Summary of geologic events ..... 628
Literature cited ..... 630

## ILLUSTRATIONS

Figure Page

1. Index map of northern Mexico ..... 590
2. Stratigraphic sections of the middle part of the Sierra de Parras ..... 621
3. Index map of stratigraphic sections and fossil localities in the middle part of the Sierra de Parras ..... 624
4. Summary of geologic events in the middle part of the Sierra de Parras ..... 629

| Plate | | Facing page |
|---|---|---|
| 1. | Relief model of the middle part of the Sierra de Parras | 587 |
| 2. | Cañon de la Casita | 592 |
| 3. | Canyons | 593 |
| 4. | Northern front of the Sierra de Parras | 594 |
| 5. | Anticlines and mountains | 595 |
| 6. | Folds and formations | 596 |
| 7. | Mountains and plains | 597 |
| 8. | Jurassic formations | 610 |
| 9. | Aurora limestone | 611 |
| 10. | Cretaceous formations | 614 |
| 11. | Indidura formation | 615 |
| 12. | Cretaceous formations | 616 |
| 13. | Geologic structure sections of the middle part of the Sierra de Parras | 628 |
| 14. | Geologic map of the middle part of the Sierra de Parras | 630 |


## INTRODUCTION

### LOCATION AND EXTENT OF AREA

The Sierra de Parras lies in southern Coahuila. The area mapped extends from a point about 4 miles east of Parras, eastward 45 miles to a point near the town of Fraile. The width of the range increases toward the east, varying from 8 miles, at the west end, to 12 miles in the region south of Huarichic and to 16 miles near the east end. The area mapped comprises about 550 square miles of mountainous country.

### CONSTRUCTION OF MAPS AND SECTIONS

Mapping was done by pace and compass traverse. A relief map of the northern half of the range, between Parras and Huarichic, furnished by Señor Salvador Madero, was of considerable assistance. Sections were measured with a steel tape. Altitudes were determined by an aneroid barometer.

### ACKNOWLEDGMENTS

Preparation of this report was made possible by assistance received from the Geological Society of America and from the University of Michigan. The writer has been associated with Professor Lewis B. Kellum in a program of coöperative geological studies in northern Mexico. This investigation is a contribution to the regional studies of that program. Recognition is made of the generous assistance given by certain residents of Parras, who, as in former years, have helped materially during the course of the field investigations. The writer is indebted to Professor Walter F. Hunt for checking the determinations of the rocks and to Mr. Marion V. Denny for his determination of the minerals.

## EARLIER INVESTIGATIONS

In 1923, Böse[1] defined the group of mountains along the southern margin of the Parras Basin as the Sierra de Parras and briefly discussed the structure and stratigraphy of the region from General Cepeda south-

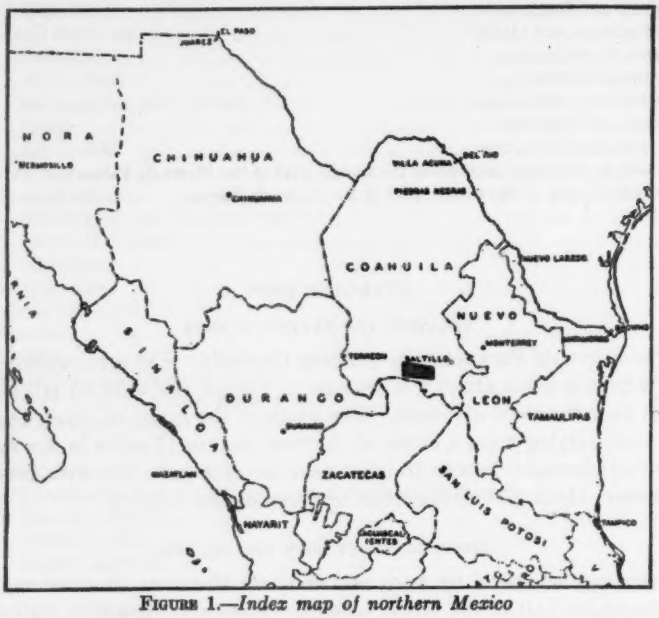


FIGURE 1.—*Index map of northern Mexico*

ward to Rancho La Casita in the heart of the range. He noted the major divisions of the Jurassic and Cretaceous systems; but some of his interpretation of the structural features do not accord with those of the writer.

## GEOGRAPHY

### TOPOGRAPHY AND DRAINAGE

The middle part of the Sierra de Parras[2] consists of many eastward-trending mountainous ridges, broken by deep cross-canyons and separated in a north-south direction by rather broad flat valleys or deep canyons. The mountainous ridges rise from a few hundred feet to five thousand feet above their bases, but their general elevation above sea

[1] Emil Böse: *Vestiges of an ancient continent in northeast Mexico*, Am. Jour. Sci., 5th ser., vol. 6 (1923) p. 329-332.

[2] For description of regional setting see R. W. Imlay: *Geology of the western part of the Sierra de Parras, Coahuila, Mexico*, Geol. Soc. Am., Bull., vol. 47 (1936) p. 1095-1097.

level increases gradually toward the east, coinciding with a rise of the plateau beneath. Altitudes of numerous localities, as obtained from aneroid readings, are presented in the following table:

TABLE 1.—*Altitudes determined by aneroid*

| Locality | Feet |
|---|---|
| Cañón de Arroyo Seco, mouth | 6325 |
| Cañón del Organo, mouth | 6935 |
| Cañón Victoria, west end at fork of roads | 6680 |
| Cañón de los Lobos, mouth | 6035 |
| Cañón Tanque Verde, mouth | 6135 |
| Cañón Tappon del Toro, north end | 7130 |
| Cañón La Casita, at east end of Sierra del Organo | 7085 |
| Cañón La Casita, mouth | 6385 |
| Cañón Salsipuedes, mouth | 5645 |
| Cañón Salsipuedes, head | 6700 |
| Cañón El Angel, mouth | 5985 |
| Cañón Sabinilla, mouth | 5215 |
| Cuesta Yeguales | 7285 |
| Cuesta Herradura | 6185 |
| Divide at head of Arroyo Gurustola | 7015 |
| La Hoya | 6325 |
| Picacho Chileverde | 9085 |
| Picacho de la Gloria, near San Marcos | 9925 |
| Peak at head of Cañón del Organo | 9925 |
| Plain at southwest end of Sierra Grullo | 4615 |
| Plain at west end of Sierra Potrillo | 6335 |
| Rancho Alto de los Remedios | 7735 |
| Rancho Astillero | 6535 |
| Rancho Cinco | 7045 |
| Rancho Concordia | 8200 |
| Rancho El Angel | 5385 |
| Rancho Garambullo | 6815 |
| Rancho La Casita | 6885 |
| Rancho La Presa | 5485 |
| Rancho Los Hoyos | 5595 |
| Rancho Majada | 6285 |
| Rancho Mesquite | 5015 |
| Rancho Palmas Altas | 6975 |
| Rancho Sabinilla | 5385 |
| Rancho San Angel | 6335 |
| Rancho San Marcos in Cañón Tanque Verde | 6735 |
| Rancho Santa Rita | 7365 |
| Rancho Victoria | 7735 |
| Sierra Astillero, top | 6535 |
| Sierra Garambullo, on trail to Rancho Gerónimo | 7825 |
| Sierra Yeso, top | 7085 |

From Parras eastward to La Presa the rise is about 400 feet in 22 miles. From La Presa eastward the rise is about 1200 feet in 25 miles. When the Sierra de Parras is viewed in profile from north to south (Pl. 13), it

is evident that, in general, the ridges along the northern part of the sierra rise to somewhat greater elevations above sea level than those along the southern part, but not necessarily any higher above their bases. This difference in elevation reflects a local reversal of the regional tilt of the plateau.

A plain, more than 4 miles wide in most places, separates the Sierra de Parras from the mountains to the south. Near the southeast corner of the area mapped, and about a mile south of the Sierra Garambullo, rises a prominent ridge, called Sierra Gerónimo, which might be considered part of the Sierra de Parras; this, however, was not studied.

The northern front of the Sierra de Parras is abrupt, steep, and trends irregularly east-southeast. This irregularity is due to the presence of several ridges, which trend at a slight angle to the front. The mountain front, from the Sierra Conejo eastward, rises steeply in an escarpment ranging from about 1500 to about 4000 feet and with several peaks rising 1000 feet higher. The greatest heights are in the region of La Casita, south of General Cepeda. Westward from Sierra Conejo the mountain front is much lower, ranging from 300 to 1500 feet in height.

The Parras Basin bounds the Sierra de Parras on the north. The southern half of the basin is partly occupied by mesas capped with conglomerate and tufa and steep-sided hills of sandstone and shale. A large mesa, called Mesa de San José, flanks the sierra from the Lomas de San Pablo, near Parras, eastward for 22 miles, to the mouth of Cañón de los Lobos. Eastward from the Mesa de San José, a belt of low hills, with nearly continuous exposures of sandstone and shale, flanks the sierra in a belt 5 or 6 miles wide. North of the hills are many long, eastward-trending ridges and tufa-capped mesas between which lie plains that merge northward and westward with the Laguna de Mayrán. The hills, small mesas, and plains east of the Mesa de San José have been formed by dissection of a former high plain, of which the Mesa de San José is a remnant. Erosion has been more active north of the highest mountain mass, which has apparently induced considerable precipitation. The preservation of the Mesa de San José can be attributed to the fairly low elevation of the mountain to the south and the consequent small rainfall. These relationships, if correctly interpreted, indicate that erosion of the mesa has been due primarily to torrential streams rather than to sheet-floods.

The mountainous ridges of the Sierra de Parras are the topographic reflections of major anticlines that have been deeply eroded. Where erosion has cut only slightly into the thick-bedded Aurora limestone, the resulting ridges are of the rounded anticlinal type. This type is found mainly in the northern half of the area mapped, and includes the Sierra

FIGURE 1. EAST WALL OF CAÑÓN DE LA CASITA

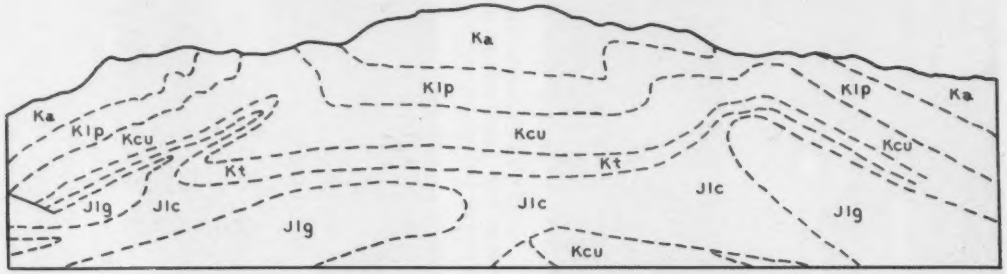


FIGURE 2. DIAGRAM OF FORMATIONS SHOWN IN FIGURE 1
(Somewhat generalized). Jlg, La Gloria formation; Jlc, La Casita formation; Kt, Taraises formation; Kcu, Cupido limestone; Klp, La Peña formation; Ka, Aurora limestone.

FIGURE 1. VIEW WESTWARD FROM EAST END OF CAÑÓN MESQUITE
Sierra Mesquite del Norte (right); Sierra Mesquite del Sur (left); Picacho Yeguales in middle distance about 18 miles. Low hills of Caracol formation (right foreground).

FIGURE 2. CAÑÓN AND SIERRA DEL ÓRGANO
From mouth of canyon. Ka, Aurora limestone; Klp, La Peña formation; Kcu, Cupido limestone; Kt, Taraises formation; Jlc, La Casita formation; Jlg, La Gloria formation.

CANYONS

de Santiago, Sierra de Patagalana, Sierra de Cabrera, Cerro Campana, Cerro Prieto, Sierra de los Pinos, Sierra Berrendo, Sierra Mesquite del Norte, Sierra Yeguales, Sierra Conejo, Sierra Boca de Domingo, part of the Sierra Escondida, Sierra Panocha, Sierra Sitio, the western part of the Sierra San Angel, Sierra de la Concordia, and most of the Sierra Cupido. Where erosion has cut deeply into the Lower Cretaceous limestones along the anticlines, hogbacks and cuestas result. Hogbacks mapped in the southern and eastern parts of the area include the Sierra de San Francisco, Sierra Mesquite del Sur, Sierra Guitarra, Sierra Garambullo, Sierra Astillero, Sierra Yeso, the eastern end of Sierra San Angel, Sierra Potrillo, Sierra del Organo, and part of Sierra de los Patos. Cuestas include the Sierra Grullo and the Sierra de la Tinaja, which are low, inconspicuous ridges. The Sierra de la Gloria is the only synclinal mountain proper in the entire northern part of the area mapped.

The Sierra de Patagalana, forming the northern front of the range 2 miles south of Patagalana, rises only about 800 feet above its base but has steep flanks (Pl. 5, fig. 2). The Sierra de Santiago, in the northwest corner of the area mapped, rises 600 to 800 feet above its base. The same ridge continues east of Puerto Gurustola as the Sierra de Cabrera, which becomes broader and higher toward the east, attaining a height of about 1200 feet above the floor of Cañón Tunal. Cerro Prieto, directly east of Cañón Tunal, rises several hundred feet higher. The same line of uplift is continued eastward 14 miles as the Sierras de los Pinos, Panocha, and Sitio, which rise from 600 to 1000 feet above their bases. The Sierra Berrendo, south of Cerro Prieto, is a small but prominent ridge about 7 miles long. Its middle part rises about 1200 feet above Cañón Berrendo to the north.

Half a mile to a mile south of the Sierras de Santiago and Cabrera, across a synclinal valley, lies the rugged Sierra Mesquite del Norte (Pl. 3, fig. 1). On the west, near Puerto Yeguales, it rises 2700 feet above Parras and about 1300 feet above the valleys to the north and to the south. Toward the east the ridge maintains about the same elevation almost to Cañón Salsipuedes. In the same interval the valley to the north rises 800 feet to a point in the vicinity of Tanque de las Palmas and then declines several hundred feet; the valley to the south, comprising Cañón Yeguales and Cañón Mesquite, however, declines eastward about 1400 feet to a point near Rancho Mesquite and then rises gradually about 400 feet in the next 7 miles. As a result, the sierra rises 2800 feet above Mesquite but only 1200 feet above the valley to the north. Eastward from Cañón Salsipuedes the sierra gradually dwindles and plunges into the plain at the west end of the broad Cañón Victoria. The eastern end of the sierra is cut by four southward-draining cross-canyons. The

western half is partly cut by two short, northward-draining canyons at Puertos del Indio and Yeguales.

The Sierra Yeguales, south of Sierra Mesquite del Norte, is narrow, and at Picacho Yeguales forms a razor-like ridge, which rises about 1800 feet above Cañón Yeguales and about 3200 feet above Parras. The north flank of the picacho is nearly vertical. The eastern end of the sierra is low and is cut by two cross-canyons. The Sierra de San Francisco is separated from the Sierra Yeguales by a narrow synclinal valley and forms the southern flank of the range. It extends westward to Cuesta del Carmen, about 5½ miles beyond the area mapped. The Sierra Mesquite del Sur rises rather steeply from 800 to 1200 feet above the plain to the north and more gently about 1600 feet above the plain to the south. The Sierra Guitarra to the southeast rises only a few hundred feet and is continuous eastward with Sierra Garambullo, which extends to the town of Fraile and rises about 1000 feet above its base. However, as the plateau on which these mountains rest rises rapidly to the east at the rate of about 100 feet to the mile, the actual altitude of the Sierra Garambullo is much greater than that of the Sierra Guitarra.

North of the Sierras Guitarra and Garambullo is Cañón Garambullo, a broad valley, which extends from a mile east of Garambullo westward to Sabinilla and descends 1400 feet. Its floor is mainly a plain of erosion, covered partly with a thin veneer of soil, and dotted with many small hills.

The Sierras Yeso and Astillero form a prominent hogback ridge along the north side of Cañón Garambullo. From Sierra Yeso eastward the ridge rises 1600 feet to a place north of Rancho Garambullo. The Sierra Yeso rises about 1600 feet above Cañón Garambullo and about 800 feet above the valley to the north; the western half of the Sierra Astillero rises about 1600 feet above Cañón Garambullo and 600 feet above the valley to the north at Las Playas; the eastern part of the Sierra Astillero rises about 1800 feet above Cañón Garambullo and about 1300 feet above the canyon to the north.

Half a mile to a mile north of the Sierras Astillero and Yeso, across a synclinal depression, is the Sierra San Angel, which is low and rounded as far east as Cuesta San Angel, but eastward consists of two prominent ridges. At Cuesta San Angel the sierra rises about 700 feet above Cañón Victoria and 1400 feet above the canyon to the south. At the Cuesta San Isabel, it rises 600 feet above Las Playas. In the vicinity of Rancho Victoria, it rises about 1000 feet above Cañón Victoria and about 1400 feet above the valley to the south.

The mountains north of the Sierra San Angel and east of Cerro Zapatero, about 2 miles southeast of Huarichic, have been formed by erosion of a

FIGURE 1. MOUTH OF CAÑÓN DE LA CASITA
Ka, Aurora limestone; Kc, Cuesta de Cura limestone; Ki, Indidura formation; Kca, Caracol formation; Kp, Parras shale.

FIGURE 2. SIERRA DE LOS PATOS

FIGURE 3. PUERTO BOCA DE DOMINGO

NORTHERN FRONT OF THE SIERRA DE PARRAS

FIGURE 1. EAST SIDE OF CERRO ZAPATERO
(a) Crest of Órgano Anticline; (b) crest of overturned Patagalana Anticline.

FIGURE 2. LOW NORTHERN FRONT OF THE SIERRA DE PARRAS NEAR HUARICHIC

major uplift, which is here named La Casita uplift. This uplift has been cut deeply by three northward-trending cross-canyons—namely, Cañón de la Casita on the east, Cañón Tanque Verde on the west, and Cañón de los Lobos near the western end. The ridges are separated near the middle of the uplift by anticlinal valleys and toward the margin of the uplift by synclinal valleys.

The Sierras Potrillo, del Organo, and the southwestern extension of Sierra Cupido form a nearly continuous ridge on the south margin of La Casita uplift. The Sierra Potrillo rises about 1000 feet above Cañón Panocha, and the Sierra del Organo rises about 1800 feet above Cañón Victoria. Sierra Chileverde, lying north of Sierra Potrillo, is low at its west end but rises sharply near its east end (Pl. 6, fig. 1) into a peak about 2400 feet higher than Cañón Tanque Verde. Sierra de la Gloria, east of Cañón Tanque Verde, has three lofty peaks. The western peak rises about 9900 feet above sea level or 3300 feet above Cañón Tanque Verde; the eastern peak rises about 100 feet higher. Sierra de la Gloria is partly connected with the Sierra del Organo by a high ridge at the head of Cañones Mimbre and del Organo. The Sierra Escondida at its eastern end is nearly as high as Sierra Chileverde but is much narrower. The Sierras de los Patos and Boca de Domingo are separated from the sierras to the south by minor east-west-trending depressions. Viewed from the north, these ranges are the most rugged and picturesque in the area mapped (Pl. 4).

The Sierra Cupido (Pl. 2) is the name applied by the natives to the lofty mountain mass east and southeast of La Casita. Its highest peak rises about 11,000 feet above sea level and 4000 feet above Cañón de la Casita. On Abbot's map of Coahuila, the mountain front from Cañón de la Casita eastward 20 miles to Carneros is named Sierra de la Concordia. Whether or not this is topographically distinct from the Sierra Cupido is unknown.

Sierra Conejo rises 1000 to 1200 feet above Cañón de los Lobos and terminates abruptly at its western end as an anticlinal mountain. Cerro Zapatero (Pl. 5, fig. 1) rises at its east end into a peak about 1600 feet higher than the plain at Tanque Nuevo.

The valleys of the Sierra de Parras may be classified, according to their relations to the major folds, as anticlinal valleys, synclinal valleys, and cross-canyons. All valleys within the Sierra de Parras are called "cañones" by the natives. Anticlinal valleys include Cañones de la Leona, del Buey, Cupido, del Organo, Mimbre, Potrillo, and Sombrero, all related to La Casita uplift. All the rounded anticlinal mountains are separated by synclinal valleys, of which many are unnamed. The principal ones are Cañones de Arroyo Seco, de Potrerillos, de Arroyo Gurustola, Yeguales,

del Bolsón, Mesquite, del Conejo, Chileverde, Panocha, Victoria, San Angel, and Garambullo. Cañón Garambullo has been widened considerably by erosion of the adjacent anticlines. The many cross-canyons are called locally either cañones or puertos. Many of them are probably due to superposition (e.g., Puerto Gurustola, San Angel, and Cañones Salsipuedes, Tunal, Berrendo, Zapatero, Sabinilla, Caracol). Some owe their position to zones of fracturing or faulting. Cañón Tappon del Toro, 3 miles northwest of Garambullo, probably follows a fault zone. Cañones del Rincón, de la Casita, Tanque Verde, and de los Lobos, probably follow zones of fracturing.

The valleys may be classified physiographically as high-level valleys and low-level valleys: the latter lie mainly in the southern part of the sierra, range in altitude roughly from 5000 to 6200 feet, and are undergoing rapid erosion (e.g., Cañones Mesquite and Garambullo); the former lie mainly in the northern part of the sierra, range in altitude roughly from 6200 to 7800 feet, and are undergoing relatively little erosion except near their margins, where short canyons drain north or south. They are represented typically by Cañón Victoria, Cañón Potrillo, and poorly drained basins at La Hoya (head of Cañón Tunal) and east of Cerro Zapatero. Their floors are a gently undulating old erosion surface, which was probably developed coincident with the Mayrán conglomerates and tufas on the Mesa de San José and other places, during a humid erosion cycle. The contrast between the old erosion surface and the present one is well shown in the valleys flanking the western part of the Sierra Astillero. To the north, at Las Playas (Pl. 6, fig. 2) is a fairly flat valley floor from which the bordering sierras rise 500 to 600 feet. It is cut on the west by Cañón San Angel. Remnants of the old valley floor are preserved on the sides of Cañón San Angel and can be traced as a gentle slope westward for 8 miles. At the west end of the Sierra San Angel the highest outcrops of the Indidura formation are beveled to a flat plain, which rises about 150 feet above the present plain, and which is strewn with gravels and large irregular blocks of conglomerate. South of Sierra Astillero, and 1400 to 1600 feet lower, is the more recently eroded floor of Cañón Garambullo (Pl. 7, fig. 1).

The preservation of the old erosion surface in the high-level valleys is ascribed to: (1) insufficient time since the beginning of the last arid cycle for headward-gulleying to destroy them completely and (2) sufficient rainfall in the higher parts of the sierra to nourish a type of vegetation that holds the soil in place.

### CULTURE

Numerous ranches have been built up in the middle part of the Sierra de Parras or along its base. Of 25 ranches, varying in approximate popu-

FIGURE 1. East end of Sierra Chileverde (left) and Sierra Escondida. Mountains rise about 2400 feet above Cañón Tanque Verde. (a) crest of La Gloria Anticline; Ka, Aurora limestone; Klp, La Peña formation.

FIGURE 2. LAS PLAYAS AND SIERRA ASTILLERO
Viewed from Cuesta San Isabel. Headward gulleying of Cañón San Angel (right). Kc, Cuesta del Cura limestone; Ka, Aurora limestone; Klp, La Peña formation.

FIGURE 1. SOUTH SIDE OF SIERRA ASTILLERO
Looking northeast from Rancho Sabinilla across Cañón Garambullo. (a) Puerto San Angel; (b) Sierra de La Tinaja. Axis of Prieta Anticline follows base of Sierra Astillero.

FIGURE 2. CREST AND NORTH FLANK OF PATAGALANA ANTICLINE ON EAST SIDE OF CERRO CAMPANA
Relief about 1000 feet. Mountain composed of thick-bedded Aurora limestone.

lation from 10 to 300 persons, 21 are engaged in stock raising, 22 in farming, 11 in rope making and 2 in wine making.

### WATER SUPPLY

Good drinking-water can be obtained from springs at Parras, Patagalana, and La Casita, and from a well at San Marcos in Cañón Tanque Verde. Springs are found at Huarichic and San Angel, but they are highly alkaline. All the other ranches depend on rain water, trapped by low earthen dams across small drainage channels. Such dams are called tanques, and the water impounded in them is more or less alkaline. The water in the tanques at Victoria and Garambullo is cleaner and less alkaline than at most of the other ranches.

## SEDIMENTARY ROCKS

The sedimentary rocks of the middle part of the Sierra de Parras, with the exception of about 200 feet of Pleistocene gravels and tufas, are of Upper Jurassic and Cretaceous age. Upper Jurassic strata crop out in La Casita uplift, and in the Sierras San Angel, Astillero, and Garambullo. Lower Cretaceous strata constitute the bulk of the mountains. Upper Cretaceous strata crop out along the northern side of the range and in the synclinal valleys in the range. The formations and their approximate thicknesses are as follows:

*Formations in the Middle Part of the Sierra de Parras and in the Parras Basin, Coahuila, Mexico*

| | Feet |
|---|---|
| QUATERNARY: | |
| Mayrán formation | 200 |
| UPPER CRETACEOUS: | |
| Difunta formation (in El Pozo-Boquillas region) | 12,000+ |
| Parras shale | 5,000+,— |
| Caracol formation | 905 |
| Indidura formation | 895 |
| LOWER CRETACEOUS: | |
| Cuesta del Cura limestone | 240 to 1,000 |
| Aurora limestone | 600 to 2,335 |
| La Peña formation | 1,000 to 1,270 |
| Cupido limestone | 1,135 to 1,640 |
| Taraises formation | 230 to 335 |
| UPPER JURASSIC: | |
| La Casita formation | 240 to 330 |
| La Gloria formation | 2,072 |
| Total | 24,517 to 27,982 |

TABLE 2.—*Correlation of the Jurassic and Cretaceous Deposits of the Middle Part of the Sierra de Parras*

| European Equivalents | | | Texas Groups | Northeastern Mexico | Middle part of Sierra de Parras |
|---|---|---|---|---|---|
| UPPER CRETACEOUS | Senonian | Maestrichtian | Navarro | | |
| | | Campanian | Taylor | Mendez shale | Difunta formation |
| | | | | | ——?—— |
| | | Santonian | | | Parras shale |
| | | | | San Felipe limestone | ——?—— |
| | | Coniacian | Austin | | Caracol formation |
| | Turonian | | Eagle Ford | Agua Nueva formation | Indidura formation |
| | Cenomanian | | Woodbine | El Abra and Upper Tamaulipas limestone | |
| | | | Washita | | |
| LOWER CRETACEOUS | Albian | | | | Cuesta del Cura |
| | | | Fredericksburg | | Aurora limestone |
| | | | Trinity | | |
| | Aptian | | —— ——?—— —— | | La Peña formation |
| | | | | | ——?—— |
| | Neocomian | Barremian | | Lower Tamaulipas limestone | Cupido limestone |
| | | Hauterivian | | | |
| | | Valanginian | | | Taraises formation |
| | | Berriasian | | | ——?—— |
| JURASSIC | Tithonian | | | | Hiatus |
| | Portlandian | | | | |
| | Kimmeridgian | | | | La Casita formation |
| | Oxfordian | | | | La Gloria formation |

## JURASSIC SYSTEM

### LA GLORIA FORMATION

*Areal extent.*—La Gloria [8] formation crops out as rounded anticlinal ridges in La Casita uplift, in the eastern end of the Sierra San Angel, and in the Sierra de Garambullo. Large and thick exposures are found along the Organo Anticline, immediately north of the bottoms of Cañones Mimbre and del Organo (Pl. 3, fig. 2). There are excellent exposures of the

[8] Defined by R. W. Imlay: *Geology of the western part of the Sierra de Parras*, Geol. Soc. Am., Bull., vol. 47 (1936) p. 1105.

upper limestone beds along the crests of the Cupido and La Gloria anticlines in Cañón de la Casita.

*Stratigraphic and lithologic features.*—La Gloria formation consists predominantly of thick- to medium-bedded gray limestone. Yellowish sandstone with subordinate amounts of conglomerate constitutes slightly more than a quarter of the total exposed section in La Casita uplift, but it does not crop out in the mountains toward the south. Most of the sandstone is in thin units interbedded with limestone, near the middle of the section. There are no shales. The highest limestone unit directly underlying the sandstones of La Casita formation is dark-gray to black, thick-bedded, and contains a few thin bands of dark-brown chert and some nodules of black chert. In some places the surface of the uppermost beds contains bivalves and high-spired gastropods, which are probably *Nerineas*. Localities where these fossils may be observed are: (1) in Cañón del Organo, about 1½ miles from its mouth; (2) on a small ridge in Cañón del Buey, about half a mile east of Cañón de la Casita; and (3) on a ridge three-quarters of a mile northwest of Rancho La Casita and half a mile west of the bottom of Cañón de la Casita.

The section on the north wall of Cañón Mimbre, measured from top to bottom, is as follows:

| Unit | Feet |
|---|---|
| 1. Limestone, thick-bedded (beds 1 to 6 feet thick) dark-gray, a few beds of dark-brown chert about one inch thick. Contains a 10-inch bed of dark-gray sandstone 36 feet from top and an 8-inch bed of gray sandstone 20 feet from top | 247 |
| 2. Limestone, thick- to medium-bedded, medium-gray to dark-gray | 270 |
| 3. Limestone, thick- to medium-bedded, gray to yellowish gray, contains scattered fragments of pelecypod shells | 202 |
| 4. Limestone, siliceous, gray | 20 |
| 5. Sandstone, light-yellow, thin- to thick-bedded (beds range from 2 inches to 2 feet in thickness); thicker beds contain lenses of conglomerate | 77 |
| 6. Limestone, thin-bedded, gray | 7 |
| 7. Sandstone, yellow; several beds of yellowish limestone near top | 82 |
| 8. Limestone, thick-bedded, yellow to grayish yellow, weathers grayish yellow | 13 |
| 9. Limestone, thin-bedded, nodular, yellow, contains several thin beds of light-yellow sandstone | 39 |
| 10. Sandstone, brilliant, light-yellow, calcareous, weathers brilliant reddish brown | 33 |
| 11. Limestone, thin- to medium-bedded, yellow and gray. Surfaces much pitted by weathering | 86 |
| 12. Sandstone, yellow, thin- to medium-bedded | 20 |
| 13. Limestone, thin-bedded, grayish yellow, contains fragments of pelecypod shells | 20 |
| 14. Sandstone, thin- to thick-bedded, yellow; thicker beds conglomeratic and cross-bedded | 85 |

| Unit | Feet |
|---|---|
| 15. Limestone, thick-bedded, dark- to light-gray, compact, some beds with shell fragments | 264 |
| 16. Limestone, medium-bedded, yellow to gray | 290 |
| 17. Sandstone, yellow | 20 |
| 18. Sandstone, yellow, interbedded with thin beds of grayish yellow limestone. | 85 |
| | 1860 |

Microscopic examination was made of thin-sections of sandstones from the above section. A thin-section of the light-yellow conglomeratic sandstone from unit 14 contains about 40 per cent calcite. The sand grains are large to medium in size and subangular. They consist mainly of quartz and chert, but some are of feldspar, and others are of rhyolite. Some quartz grains show undulatory extinction. There is a little limonite derived from pyrite.

A thin-section of sandstone from unit 10 was examined. The sand grains are mainly quartz, but a few are chert; they are angular to subangular, and most of them are small. The quartz grains contain inclusions of apatite. The cementing material consists, in part, of calcite and, in part, of small interlocking granules of quartz, which is possibly secondary. Many small particles of limonite and organic material are scattered throughout the section.

A thin-section of fine-grained sandstone from unit 5 consists mainly of calcite. Small angular to subangular grains of quartz and feldspar constitute about 20 per cent. The quartz contains apatite, and the feldspar is somewhat altered to kaolin. There are scattered bits of limonite derived from pyrite.

A thin-section of the dark-gray, medium-grained sandstone from unit 1 was examined. Most of the grains are quartz; some are chert, and a few are plagioclase. They are medium in size and angular to well-rounded. Calcite forms about 50 per cent of the section. It consists, in part, of fine interstitial particles but mainly of fairly large concentric bodies (oölites?) of which some consist of concentric layers and a few enclose nuclei of small angular quartz particles. Finely disseminated organic material and some limonite is associated with the oölitic (?) calcite.

*Correlation.*—La Gloria formation of the Sierra de Parras is of Upper Jurassic age and probably belongs in the Oxfordian. It is correlated with the *Nerinea*-bearing limestones [4] near Mazapil, Zacatecas.

### LA CASITA FORMATION

*Areal extent.*—La Casita formation [5] is mainly a narrow strip around

[4] Carlos Burckhardt: *Géologie de la Sierra de Mazapil et Santa Rosa (Mexico)*, 10th Intern. Geol. Cong., Mexico, Guidebook 26 (1906) p. 4-5.

[5] Defined by R. W. Imlay: *Geology of the western part of the Sierra de Parras*, Geol. Soc. Am., Bull., vol. 47 (1936) p. 1110.

the outcrops of La Gloria formation. It is easily eroded and in many places marks the deepest parts of canyons. The best exposures are in Cañón de la Casita and on the divide between Cañones del Organo and Mimbre. Small outcrops are found at the eastern ends of Sierras San Angel, Astillero, and Garambullo.

*Stratigraphic and lithologic features.*—In La Casita uplift, La Casita formation is divisible into two members. The lower member consists of gray conglomeratic sandstone and ranges in thickness from about 20 to 75 feet or more. At the top, in most sections, are a few inches of friable sandstone, which contains brachiopods, bivalves, and belemnites. The upper member consists principally of black shales but includes some buff or gray sandy shales, short lenses of sandstone and arenaceous limestone, and lenticular limestone nodules. Some of the nodules contain well-preserved mollusks. The gray and buff sandy shales contain belemnites that lie at all angles to the bedding. Small fragments of wood were found in the arenaceous limestones. The base of La Casita formation is placed at the contact of the conglomeratic sandstone with the underlying thick-bedded, dark-gray to black, *Nerinea*-bearing limestones, here placed in La Gloria formation. In most sections, however, one or more thin lenses of non-conglomeratic gray sandstone are found in the upper 60 feet of the limestone. The top of La Casita formation is marked by a sharp contact with the basal medium- to thin-bedded, compact, gray limestones of the Taraises formation.

South of La Casita uplift, no sandy facies exists at the base of La Casita formation. The lower part of the formation is characterized by black shale and the upper part by limestone, but limestone, marl, and shale are interbedded throughout.

A section a mile northwest of Rancho La Casita and half a mile west of the bottom of Cañón de la Casita is as follows:

| Unit | Feet | Inches |
|---|---|---|
| 1. Shales, papery to fissile, mainly black, some gray, weather buff to gray; contain lenticular concretions of yellowish gray limestone, of which some are septaria and a few enclose ammonites. (Collection 51) from near top | 226 | |
| 2. Lustrous black calcite resembling anthraconite but not petroliferous | | 4 |
| 3. Sandstone, dark-gray, friable, contains numerous brachiopods, pelecypods, and belemnites (Collection 53) | | 6 |
| 4. Sandstone, conglomeratic, dark-gray, weathers reddish brown. Pebbles consist of chert and quartzite, average a quarter of an inch in diameter, but some are as large as 4 inches, subangular to well-rounded | 38 | |
| | 265 ± | |

A section measured at the head of a small canyon about four-fifths of a mile west-southwest of Rancho La Casita consists of about 25 feet of

conglomeratic dark-gray sandstone, overlain by about 215 feet of black and gray, papery to fissile shales. Limestone nodules in the shale enclose ammonites (Collection 48).

A section on the north wall of Cañón Mimbre, about 1 1/5 miles southeast of Rancho San Marcos, is as follows:

| Unit | Feet |
|---|---|
| 1. Shales, black to gray, fissile to papery, contain some belemnites | 184 |
| 2. Sandstone, shaly, dark yellowish gray, several beds of fine conglomerate in the upper 5 feet | 55 |
| 3. Sandstone, dark-gray, beds range from 1 to 20 inches in thickness | 24 |
| | 263 |

A nearly complete section in the bottom of Cañón de la Casita, about three-quarters of a mile north of the houses, is as follows:

| Unit | Feet | Inches |
|---|---|---|
| 1. Shales, black, papery to fissile, including many short lenses of black limestone and dark-gray arenaceous limestone ranging from 1 to 18 inches in thickness. Some thin beds of friable gray sandstone are found in the lower 10 feet of unit. Lenticular concretions of yellowish gray limestone are seen throughout, are most common near the top, and range in diameter from several inches to several feet. Some are septaria. Some contain well-preserved mollusks (Collection 43) | 83 | |
| 2. Shales, mainly black but some gray, with belemnites, weather buff to gray | 171 | |
| 3. Lustrous black calcite resembling anthraconite | | 4 |
| 4. Sandstone, dark-gray, friable, contains some brachiopods, pelecypods, and belemnites | | 8 |
| 5. Sandstone, conglomeratic, dark-gray, weathers reddish brown. Pebbles consist of chert and quartzite, are subangular, and average about one-quarter of an inch in diameter | 30 | |
| | 285 | |

*Fossils.*—La Casita formation of the middle part of the Sierra de Parras contains a large fauna of ammonites, belemnites, brachiopods, pelecypods, and gastropods. Some of these fossils have been identified as follows:

LOCALITY 57

(Locality numbers indicated on Figure 2)

(Fossils are found in lenticular concretions of limestone about 50 feet below the top of the formation, about 450 yards east of Cañón de la Casita near Cañón del Buey.)

| | Univ. Mich. No. |
|---|---|
| *Aspidoceras* sp. | 12169, 16983 |
| *Aulacosphinctoides* sp. | 16982 |
| *Glochiceras* sp. | 16974 |
| *Katroliceras* ? aff. *pervinquiri* (Burckhardt) | 16980 |
| *Lucina potosina* Castillo and Aquillera | 15418 |
| *Nucula* sp. | 16970 |
| *Parallelodon* sp. | 16973 |

Univ. Mich. No.

*Pleuromya* ? sp. ..... 16984
*Posidonomya* ? sp. ..... 16989
*Rhynchonella* sp. ..... 16992
*Subdichotomoceras* sp. ..... 16975, 16977, 16978, 16979
*Torquatisphinctes kokeni* Burckhardt (non Behrendsen) ..... 16981

LOCALITY 46

*Torquatisphinctes* sp. ..... 15331
Many small gastropods and pelecypods.

LOCALITY 51

(Fossils are found in limestone concretions near the top of the formation, about a quarter of a mile west of Cañón de la Casita and 400 yards west of a big spring.)

Univ. Mich. No.

*Glochiceras* sp. ..... 15332
*Subplanites* sp. ..... 15333

LOCALITY 43

(Right bank of Cañón de la Casita, about three-quarters of a mile north of Rancho La Casita.)

Univ. Mich. No.

*Aptychus* ..... 17618
*Aspidoceras* sp. ..... 17623
*Astarte* sp. ..... 17621
Fragments of belemnites ..... 17620
*Subdichotomoceras* sp. ..... 17745
*Glochiceras* sp. ..... 17617
*Torquatisphinctes* sp. ..... 17622

LOCALITY 34

(About 1½ miles southwest of Rancho Astillero, on trail to La Unión. Fossils are found in a thin lens of nodular dark-gray limestone enclosed in gray and pinkish shale.)

Univ. Mich. No.

*Durangites* sp. ..... 17706, 17707, 17708
*Ochetoceras* sp. ..... 17705
*Taramelliceras* sp. ..... 17709

LOCALITY 46

(On trail, 3½ miles up Cañón del Organo)

Univ. Mich. No.

*Mazapilites* sp. ..... 17643
*Mazapilites* cf. *zitteli* Burckhardt ..... 17641
*Katroliceras* sp. ..... 17637
*Idoceras* ? sp. ..... 17635
*Belemnopsis* sp. ..... 17639
Many small pelecypods and gastropods.

*Correlation.*—The correlation of the Upper Jurassic sequence of north-central Mexico with the European stages, as given by Burckhardt,[6] was

[6] Carlos Burckhardt: *Etude synthétique sur le Mésozoique mexicain*, Soc. Paléont. Suisse, Mém., vol. XL (1930) tables 4, 5, and 6.

revised in 1931 by Spath.[7] On the basis of Spath's work, La Casita formation of the middle part of the Sierra de Parras is mainly of Kimmeridgian and Portlandian age. The basal sandstones may be of Oxfordian age. The Portlandian has been definitely identified only at the eastern end of the Sierra Astillero and may not be completely represented in La Casita uplift. The faunal relations of La Casita formation to the Mexican faunal zones cited by Burckhardt[8] and emended by Spath are shown on the accompanying table.

TABLE 3.—*Faunal relations of La Casita formation*

| | Subdivisions after Burckhardt | La Casita Uplift | Eastern End of Sierra Astillero |
|---|---|---|---|
| PORTLANDIAN | *Kossmatia* beds | | *Durangites* sp.<br>*Ochetoceras* sp.<br>*Taramelliceras* sp. |
| | *Proniceras* beds | | |
| KIMMERIDGIAN | *Aulacosphinctoides* beds | (Localities 43, 46, 51, and 57)<br>*Torquatisphinctes kokeni* Burckhardt (non Behrendsen)<br>*Subdichotomoceras*<br>*Katroliceras* ? aff. *pervinquiri* Burckhardt<br>*Aspidoceras*<br>*Subplanites*<br>*Glochiceras*<br>*Lucina potosina* Castillo and Aquillera<br>*Aulacosphinctoides* sp. | |
| | *Mazapilites* beds | *Mazapilites* cf. *zitteli* Burckhardt<br>*Mazapilites* sp.<br>*Katroliceras* sp.<br>*Idoceras* ? sp.<br>*Belemnopsis* sp. | |
| | *Waagenia* beds | | |
| | *Glochiceras fialar* beds | (Following fossils determined by Burckhardt)<br>*Glochiceras fialar* Oppel<br>*Glochiceras zacatecanum* Burckhardt<br>*Glochiceras* aff. *costatum* Burckhardt<br>*Perisphinctes* sp.<br>*Inoceramus* sp. | |
| | *Idoceras* beds | Belemnites, brachiopods, and pelecypods | |
| | *Sutneria* beds | | |
| UPPER OXFORDIAN | *Ochetoceras* beds | | |
| | *Perisphinctes* beds | | |

[7] L. F. Spath: *Revision of the Jurassic cephalopod fauna of Kachh (Cutch)*, Palaeontolog. Indica, n. s., vol. IX, Mem. 2, pt. V (1931) tables I and II on p. 864-865, 872-873.

[8] Carlos Burckhardt: *op. cit.*, p. 76.

## CRETACEOUS SYSTEM

### TARAISES FORMATION

*Areal extent.*—The Taraises formation [9] crops out extensively in La Casita uplift, along Cañones Mimbre, del Organo, and de la Casita. It also is found in the eastern parts of Sierras San Angel, Astillero, and Garambullo. It is only slightly less resistant to erosion than is La Casita formation, and forms the lower parts of the canyon walls or the canyon bed.

*Stratigraphic and lithologic features.*—Exposures of the Taraises formation in the middle and western parts of the Sierra de Parras are almost identical lithologically, and they carry the same fossils. In both parts of the range the compact gray limestones of the lower member rest on the black shales and shaly sandstones of La Casita formation. In the middle part of the range, the upper member is not overlain by sandstone, as in the western part, but by medium-bedded gray limestones containing pyrite concretions. On the north wall of Cañón del Organo, the section, measured from top to bottom, is as follows:

| Unit | Feet |
|---|---|
| 1. Limestones, medium- to thin-bedded, and shaly, dark- to light-gray, weathers deep yellow to cream-colored or pinkish in spots. In lower part, *Olcostephanus* sp., *Bochianites* sp., and *Kilianella* sp. are found | 130 |
| 2. Limestone, medium- to thin-bedded, medium- to dark-gray, brittle, compact, weathers light-gray. *Olcostephanus* sp. found at top | 100 |

On the north wall of Cañón Mimbre the section, measured from top to bottom, is as follows:

| Unit | Feet |
|---|---|
| 1. Limestone, thin-bedded to shaly, nodular to splintery, medium- to dark-gray, weathers light yellowish gray. Contains many fossils, preserved mainly as pyrite partially altered to limonite (Collection 18) | 175 |
| 2. Limestone, medium- to thin-bedded, some beds nodular, dark- to medium-gray. Contains traces of ammonites | 160 |
| | 335 |

*Fossils and correlation.*—Fossils are scarce in the lower member of the Taraises formation of the Sierra de Parras. The presence of *Olcostephanus* in the lowest beds suggests an age not older than the Valanginian.

Fossils are plentiful in the upper member of the Taraises formation. The lower part of the upper member contains many species belonging, in part, to the genera *Acanthodiscus, Distoloceras, Neocomites, Thurmannites, Kilianella, Olcostephanus,* and *Bochianites.* The highest beds contain fragments of *Olcostephanus.* This faunal assemblage shows that the upper member is of lower Hauterivian age.

[9] Defined by R. W. Imlay: *Geology of the western part of the Sierra de Parras,* Geol. Soc. Am., Bull., vol. 47 (1936) p. 1111.

### CUPIDO LIMESTONE

*Definition.*—The Cupido limestone includes the thick- , medium- , and thin-bedded gray limestones above the Taraises formation and below La Peña formation. Medium-bedded dark-gray limestones predominate. Many beds contain pyrite concretions, and a few beds contain small, cylindrical, light-gray chert concretions. The Cupido limestone is transitional into the overlying La Peña formation. The contact between them is drawn where thin-bedded and platy limestones become abundant. The type locality is here designated as the north wall of Cañón Mimbre.

*Areal extent.*—The Cupido limestone crops out widely in the eastern part of the area mapped, forming the lower walls of Cañones Mimbre, del Organo, La Casita, Cupido, La Leona, and del Buey, the crests of Sierras Astillero and San Angel, the flanks of Sierra Garambullo, and some of the low ridges west and northwest of Rancho Sabinilla.

*Stratigraphic and lithologic features.*—The section on the north wall of Cañón Mimbre, measured from top to bottom, is as follows:

| Unit | Feet |
|---|---|
| 1. Limestone bed, grayish yellow, weathers yellowish | 4 |
| 2. Limestone, medium-bedded, dark-gray, becomes somewhat thicker-bedded toward top of unit, weathers medium-gray, contains scattered pyrite concretions | 925 |
| 3. Limestone, medium-bedded, light-gray, weathers light-gray to nearly cream-color. Contains many pyrite concretions. Beds range from 2 inches to 2 feet thick but average 8 to 10 inches | 229 |
| 4. Limestone, medium- to thin-bedded, dark-gray, weathers medium-gray | 257 |
| | 1,415 |

The section on the north wall of Cañón del Organo, measured from top to bottom, is as follows:

| Unit | Feet |
|---|---|
| 1. Limestone, medium-bedded, dark-gray | 319 |
| 2. Limestone, medium- to thin-bedded, dark-gray, contains numerous veinlets of calcite | 139 |
| 3. Limestone, medium-bedded, light- to medium-gray, weathers light-gray, contains some pyrite concretions | 677 |
| | 1,135 |

The section on the south flank of Sierra Astillero, north of Garambullo, is as follows:

| Unit | Feet |
|---|---|
| 1. Limestone, medium-bedded, dark-gray to black; some beds contain pyrite concretions, others chert concretions; becomes thicker-bedded toward base | 96 |
| 2. Limestone, thick-bedded (some beds 3 feet thick), dark-gray, weathers light-gray, contains small light-gray chert nodules | 171 |
| 3. Limestone, thin-bedded, dark-gray | 17 |

| Unit | Feet |
|---|---|
| 4. Limestone, medium-bedded, dark-gray | 540 |
| 5. Limestone, thin-bedded, dark-gray, contains fragments of echinoids | 15 |
| 6. Limestone, thin- and medium-bedded alternating, dark-gray | 52 |
| 7. Limestone, medium-bedded, dark-gray | 253 |
| 8. Limestone, medium- to thick-bedded, light-gray | 498 |
| | 1,642 |

*Correlation.*—No fossils have been found in the Cupido limestone, but it is doubtless of upper Hauterivian and Barremian age, judging from the fossils contained in the adjoining formations. It is probably equivalent to Las Vigas and the Parritas formations of the western part of the Sierra de Parras.

### LA PEÑA FORMATION

*Areal extent.*—La Peña formation crops out widely in the eastern and southern parts of the sierra. Failure to crop out in the region north of Cañones Mesquite and Yeguales is due to less intense folding there than in the adjoining region, and to the great thickness of the Aurora limestone. In most places, La Peña formation forms the middle or upper slopes of mountains or canyons.

*Stratigraphic and lithologic features.*—La Peña formation ranges from about 1000 to 1270 feet in thickness. Units of medium- or thick-bedded limestone alternate with thin-bedded limestones. The latter are fossiliferous, are of smaller aggregate thickness, but increase toward the south to nearly half the total thickness, and especially distinguish La Peña formation from the contiguous Aurora and Cupido limestones. The top of the formation in all sections is distinguished by a unit of fossiliferous thin-bedded limestone, which is about 80 feet thick along the northern side of the range and thickens southward to about 300 feet. The medium- and thick-bedded limestones in the southern part of the range contain some pyrite concretions and brownish gray chert concretions, which weather reddish brown and light-gray.

The section on the north wall of Cañón Mimbre, from top to bottom, is as follows:

| Unit | Feet |
|---|---|
| 1. Limestone, medium-bedded alternating with nodular thin-bedded, dark-gray. Collection 19 taken 20 feet from base | 81 |
| 2. Limestone, thick-bedded, black to dark-gray | 210 |
| 3. Limestone, thin-bedded, nodular, gray | 64 |
| 4. Limestone, thick-bedded, gray | 6 |
| 5. Limestone, thin-bedded, nodular to splintery, dark-gray, weathers medium-gray | 160 |
| 6. Limestone, thick- to medium-bedded, medium-gray | 358 |
| 7. Limestone, medium- to thin-bedded, dark-gray | 152 |
| | 1,031 |

The section on the north wall of Cañón del Organo, from top to bottom, is as follows:

| Unit | Feet |
|---|---|
| 1. Limestone, thin-bedded, nodular, some medium-bedded, dark-gray to yellowish gray | 86 |
| 2. Limestone, medium-bedded, most beds dark-gray, some beds yellowish gray, weathers yellowish gray | 342 |
| 3. Limestone, thick- to medium-bedded, beds average about one foot in thickness, some beds 3 feet thick, dark-gray, weathers medium- to light-gray | 276 |
| 4. Limestone, medium-bedded, dark-gray | 147 |
| 5. Limestone, thin-bedded, dark-gray | 12 |
| 6. Limestone, thick-bedded, dark-gray | 8 |
| 7. Limestone, medium-bedded, dark-gray | 66 |
| 8. Limestone, thin-bedded, medium-gray | 16 |
| 9. Limestone, medium-bedded, medium-gray | 25 |
| 10. Limestone, shaly, gray | 32 |
| | 1,010 |

The section on the south side of Sierra Astillero, north of Garambullo, measured from top to bottom, is as follows:

| Unit | Feet |
|---|---|
| 1. Limestone, thin-bedded, nodular, medium-gray to black, contains numerous upper Aptian ammonites (Collection 36) | 78 |
| 2. Limestone, thin-bedded, platy, medium-gray | 46 |
| 3. Limestone, thin-bedded, platy, including numerous thin bands of black chert | 79 |
| 4. Limestone, thick-bedded, yellowish gray, contains numerous poorly preserved silicified ammonites, gastropods, and corals, weathers yellow to yellowish gray | 25 |
| 5. Limestone, thick-bedded, dark-gray; contains dark brownish gray chert concretions and chert lenses up to 4 inches thick, which weather reddish brown; some chert concretions have elliptical dark and light bands | 95 |
| 6. Limestone, thick-bedded, dark-gray, contains scattered chert nodules, which are small, elongate, and range from 1 to 1½ inches in length | 480 |
| 7. Limestone, thin-bedded, dark-gray, contains echinoids (Collection 37) | 58 |
| 8. Limestone, thin- and medium-bedded alternating, light-gray; thin-bedded limestone forms about two-thirds of the unit and contains nodules of pyrite more or less altered to limonite. One 3-foot layer of dark-gray limestone, 110 feet below top of unit, contains nodules of dark-gray chert | 280 |
| 9. Limestone, thin-bedded mainly, but thick beds every 8 or 10 feet; dark-gray chert concretions in thick beds and pyrite nodules in thin beds; contains some poorly preserved pyritized ammonites and belemnites | 47 |
| 10. Limestone, thin-bedded, nodular, medium-gray, contains ammonites (of the Ancyloceratidae) and echinoids. (Collection 38) | 31 |
| 11. Limestone, thin-bedded mainly, but includes several thick beds, dark-gray to black | 48 |
| | 1,267 |

The section across the east end of Sierra Yeso, from top to bottom, is as follows:

| Unit | Feet |
|---|---|
| 1. Limestone, thin-bedded, nodular, light-gray to yellowish gray | 90 |
| 2. Limestone, thin-bedded, platy, gray | 32 |
| 3. Limestone, thin-bedded, contains some bands of black chert, medium-gray tinged with yellow | 58 |
| 4. Limestone, thick-bedded, medium-gray, contains some nodules of dark yellowish gray chert | 220 |
| 5. Limestone, thick-bedded, alternating in lower 15 feet with nodular thin beds, medium-gray | 73 |
| 6. Limestone, thin-bedded, grading downward into shaly limestone | 48 |
| 7. Limestone, medium-bedded, dark-gray, contains nodules of yellowish gray chert | 8 |
| 8. Limestone, thin- to medium-bedded, medium-gray | 216 |
| 9. Limestone, thick- to medium-bedded, medium- to dark-gray, weathers dark yellowish gray | 8 |
| 10. Limestone, thin-bedded, nodular, gray | 38 |
| 11. Limestone, medium-bedded, gray | 20 |
| 12. Limestone, thin-bedded, nodular, gray | 24 |
| 13. Limestone, medium- to thin-bedded, gray | 33 |
| 14. Limestone, thick-bedded, dark-gray, weathers yellowish gray | 25 |
| 15. Limestone, thin-bedded to shaly, dark-gray | 37 |
| 16. Limestone, thick-bedded, dark-gray | 11 |
| 17. Limestone, medium- and thin-bedded, dark-gray | 93 |
| | 1,034 |

The section across Sierra Mesquite del Sur, south of El Angel, measured from top to bottom, is as follows:

| Unit | Feet |
|---|---|
| 1. Limestone, thin-bedded, dark-gray, contains limonite concretions derived from pyrite. Some beds near top contain numerous upper Aptian ammonites (Collection 33) | 69 |
| 2. Limestone, thin-bedded, dark-gray and pinkish | 71 |
| 3. Limestone, thin-bedded, dark-gray, contains some thin bands of black chert | 160 |
| 4. Limestone, thick-bedded, compact, siliceous, medium-gray, weathers grayish brown | 6 |
| 5. Limestone, medium-bedded at top but becoming thick-bedded toward base. Nodules of brownish gray chert are abundant near top and scarce near base | 69 |
| 6. Limestone, thick- and medium-bedded, medium-gray, contains pyrite concretions toward base | 93 |
| 7. Limestone and shales, yellowish gray. At top, 10 feet of thin-bedded nodular limestone grades downward into nodular shales, which grade downward into platy shales. Contains a few ammonites and echinoids (Collection 31) | 84 |
| 8. Limestone, thick-bedded, dark-gray | 76 |
| 9. Limestone, thin-bedded, nodular, gray | 13 |
| 10. Limestone, thick-bedded, dark-gray, some yellowish gray chert | 26 |

| Unit | Feet |
|---|---|
| 11. Limestone, medium-bedded, siliceous, medium-gray, weathers grayish brown. Contains many poorly preserved corals, and mollusks | 44 |
| 12. Limestone, medium-bedded, medium-gray, contains yellowish brown chert nodules | 64 |
| 13. Concealed by débris | 48 |
| 14. Limestone, medium-bedded, dark-gray, weathers yellowish gray | 181 |
| 15. Limestone, thin-bedded, medium-gray. Contains ammonites (mostly of the Ancyloceratidae), echinoids, and pelecypods (Collection 32) | 10 |
| 16. Limestone, alternating medium- and thin-bedded, medium-gray; nodules of brownish chert in lower part | 100 |
| | 1,114 |

*Fossils and correlation.*—The fossils of La Peña formation show that it represents the entire Aptian. The highest beds are fossiliferous in nearly all sections and belong in the highest Aptian. Some of the fossils from these beds have been partly identified as follows:

| | Univ. Mich. No. |
|---|---|
| **Locality 36 on south side of Sierra Astillero** | |
| *Dufrenoya* sp. | 17644 |
| *Hypacanthoplites* sp. | 17675, 17676, 17656, 17669, 17671, 17657 |
| *Parahoplites* sp. | 17653, 17677 |
| *Uhligella* sp. | 17673 |
| **Locality 33 on Sierra Mesquite del Sur** | |
| *Hypacanthoplites* sp. | 17648, 17647, 17665, 17649, 17645 |
| *Uhligella* sp. | 17645 |
| **Locality 54 on Sierra Cupido** | |
| *Plicatula* sp. | 9984 |
| Echinoids | 15424 |
| **Locality 15 on Sierra San Angel** | |
| *Plicatula* sp. | 15423 |
| *Exogyra* sp. | 15421 |
| Echinoids | 15337 |
| Brachiopods | 15422 |

At locality 39, on the north slope of Sierra Astillero, a lens of black limestone enclosed in gray platy and thin-bedded limestones, near the top of La Peña formation, has furnished some belemnites, brachiopods, numerous pelecypods, and one ammonite. The ammonite (Univ. Mich. No. 17698) belongs to the genus *Aioloceras*, which resembles *Cleoniceras* and has been recorded from the Aptian of Australia and South America.[10]

Beds that probably represent the lower part of the upper Aptian are represented by fossils from localities 31, 37, and 40. Most of the fossils are echinoids and have not been studied.

[10] F. W. Whitehouse: *The Cretaceous ammonoidea of eastern Australia*, Queensland Mus., Mem., vol. VIII, pt. III (1926) p. 206-207.

FIGURE 1. UPPER PART OF LA CASITA FORMATION IN CAÑÓN LA CASITA
East wall of canyon about half a mile north of houses.

FIGURE 2. UPPER LIMESTONES OF LA GLORIA FORMATION IN CAÑÓN LA CASITA
East wall of canyon about a quarter of a mile north of houses.

JURASSIC FORMATIONS

FIGURE 1. AURORA LIMESTONE ON NORTH WALL OF CAÑÓN DEL ÓRGANO
Thick beds form sheer cliffs as much as 30 feet high.

FIGURE 2. AURORA LIMESTONE IN CAÑÓN TANQUE VERDE

AURORA LIMESTONE

Fossils of lower Aptian (Bedoulian) age were found near or at the base of La Peña formation at localities 32 and 38. Some of the fossils have been tentatively identified as follows:

LOCALITY 32 ON SIERRA MESQUITE DEL SUR

| | Univ. Mich. No. |
|---|---|
| *Parancyloceras* sp. | 17722 |
| *Parancyloceras* ? sp. | 17714, 17724 |
| *Hemicrioceras* ? sp. | 17720 |
| *Tonohamites* ? sp. | 17713 |
| *Saynoceras* ? sp. | 17715 |
| *Plicatula* sp. | 17711 |
| Echinoids | 17716, 17710 |

AURORA LIMESTONE

*Areal extent.*—In the northern part of the area mapped, the Aurora limestone [11] crops out extensively and is the main mountain-forming limestone. In the southern part, it is less important as a ridge-former and does not crop out nearly so extensively. This difference is due principally to a marked diminution in thickness toward the south.

*Stratigraphic and lithologic features.*—The Aurora limestone exists in two facies, which are transitional into each other within short distances along a zone marked by Cañones Mesquite and Victoria. In the northern part of the range is a thick-bedded facies of variable thickness, which attains a thickness of 2300 feet on Sierra Cupido. In this facies, most beds contain many rudistids, caprinids, or other pelecypods, the genus *Requienia* being most common, whereas other beds near the top contain yellowish gray chert concretions. A few beds of brown, sugary-grained, dolomite interfinger from the north, having been found in Sierra de la Gloria, Sierra Cupido, Cañón Salsipuedes and Cañón Gurostola. In the southern part of the range, the Aurora limestone is about 600 feet thick and consists of units of thick- and medium-bedded limestone alternating with units of thin-bedded platy limestone containing many thin layers of black chert. Some of the latter units resemble the Cuesta del Cura limestone but can be distinguished by the lack of undulatory bedding and the platy character of the limestones.

The incomplete section on the north side of Cañón del Organo, measured from top to bottom, is as follows:

| Unit | Feet | Inches |
|---|---|---|
| 1. Limestone thick-bedded, dark-gray to medium-gray, weathered surfaces of some beds much pitted; many beds bear rudistids | 456 | |
| 2. Dolomite, dark grayish brown, sugary texture | | 20 |
| 3. Limestone, thick-bedded, light-gray | 5 | |

[11] Defined by R. H. Burrows: *Geology of northern Mexico*, Soc. Geol. Mex., Bol., tomo VII, 1era parte (1910) p. 96-97.

| Unit | Feet | Inches |
|---|---|---|
| 4. Limestone, thick-bedded, light-gray, contains numerous rudistids | 9 | |
| 5. Limestones, thick-bedded, light-gray | 338 | |
| 6. Limestone, thick-bedded, light-yellow | 10 | |
| 7. Limestone, thick-bedded, light-gray to yellowish gray, some beds contain rudistids | 118 | |
| 8. Limestone, thick-bedded, medium- to light-gray, contains shells of rudistids and other pelecypods in the lower 66 feet. One bed 150 feet from the base of the unit contains small, long-spired gastropods. | 178 | |
| 9. Limestone, medium-bedded, yellowish gray, weathers grayish yellow. Some beds contain small oysters | 32 | |
| 10. Dolomite, calcareous, thick-bedded (beds range from 1 to 10 feet in thickness), light-gray, weathers light-gray, texture sugary (a thin-section contains about 40 per cent calcite). Some beds in the upper 110 feet bear rudistids | 263 | |
| 11. Dolomite, dark-brown, sugary | 15 | |
| 12. Limestone, thick- and medium-bedded, medium-gray, contains large oysters (some 8 inches in length) | 81 | |
| | 1,507± | |

The section on the south side of Sierra Cupido, measured from top to bottom, is as follows:

| Unit | Feet |
|---|---|
| 1. Limestone, thick-bedded (beds 1 to 4 feet thick), medium-gray, most beds contain many nodules of dark-gray chert, which weather reddish and light-gray, some beds contain fragments of bivalves. Directly underlies the Cuesta del Cura limestone | 181 |
| 2. Limestone, thick-bedded, light-gray. Some beds carry scattered nodules of dark-gray chert. Some other beds in the lower part of the unit contain rudistids | 241 |
| 3. Limestone, medium-bedded, yellowish gray, weathers yellowish gray, weathered surfaces much pitted | 161 |
| 4. Limestone, medium-bedded, dark-gray, weathered surfaces somewhat pitted | 157 |
| 5. Limestone, thick-bedded, dark-gray, most beds contain numerous traces of bivalve shells | 154 |
| 6. Shale, gray | 2 |
| 7. Limestone, medium-bedded, dark-gray, contains numerous traces of bivalve shells | 165 |
| 8. Limestone, thick-bedded, light-gray and yellowish gray; some beds bear rudistids | 397 |
| 9. Limestone, thick-bedded, light-gray, no rudistids | 85 |
| 10. Limestone, thick-bedded, light-gray, most beds contain rudistids in abundance. About 80 feet from top of unit are several thin beds of sugary brown dolomite | 571 |
| 11. Limestone, thick-bedded, light-gray, no rudistids. Directly overlies La Peña formation, which carries upper Aptian fossils | 220 |
| | 2,334 |

The complete section on Sierra Mesquite del Sur south of Rancho El Angel, measured from top to bottom, is as follows:

| Unit | Feet |
|---|---|
| 1. Limestone, thick- and medium-bedded, dark-gray, contains bands of black chert and nodules of brownish gray chert. Directly underlies the Cuesta del Cura limestone | 95 |
| 2. Limestone, thick-bedded, dark-gray | 168 |
| 3. Limestone, thin-bedded, platy, medium- to dark-gray, contains many thin bands of black chert | 20 |
| 4. Limestone, medium-bedded, contains some bands of black chert | 37 |
| 5. Limestone, thick-bedded, medium-gray, contains nodules of brownish gray chert | 20 |
| 6. Limestone, thin- to medium-bedded, dark-gray, contains some bands of black chert, contains some shaly partings. Beds range from 2 to 10 inches in thickness. Directly overlies La Peña formation, which carries upper Aptian fossils | 253 |
| | 593 |

The complete section on the south side of Sierra Astillero, measured from top to bottom, is as follows:

| Unit | Feet |
|---|---|
| 1. Limestone, thick-bedded, medium-gray, some bands of black chert in the upper 40 feet, some nodules and lenticular bodies of dark brownish gray chert throughout the remainder of the unit. Directly underlies Cuesta del Cura limestone | 290 |
| 2. Limestone, thick-bedded, medium-gray, some thin bands of black chert, which are more abundant toward the base | 62 |
| 3. Limestone, medium- and thin-bedded, contains thin bands of black chert | 51 |
| 4. Limestone, thick-bedded, medium-gray, contains nodules of light-gray chert | 58 |
| 5. Limestone, thin-bedded, medium-gray, contains thin bands of black chert | 37 |
| 6. Limestone, thin- and medium-bedded, light-gray and yellowish gray, weathers yellowish gray, contains bands and nodules of gray chert. Directly overlies La Peña formation, which carries upper Aptian fossils | 97 |
| | 595 |

*Origin and correlation.*—The Aurora limestone of the northern part of the Sierra de Parras is a rudistid reef facies, probably of lower and middle Albian age, which interfingers toward the south, along a rather narrow zone, with a deeper-water facies formed along the oceanward margin of the reefs. The presence of some dolomite beds in the reef facies suggests interfingering toward the north with a lagoonal facies such as is known in Las Delicias region.[12]

### CUESTA DEL CURA LIMESTONE

*Areal extent.*—In the northern part of the Sierra de Parras the Cuesta del Cura limestone [13] crops out to a limited extent, being preserved from erosion only in the synclines. In the southern part of the range the forma-

[12] W. A. Kelly: *Geology of the mountains bordering the valleys of Acatita and Las Delicias*, Geol. Soc. Am., Bull., vol. 47 (1936) p. 1009-1038.

[13] Defined by R. W. Imlay: *Geology of the western part of the Sierra de Parras*, Geol. Soc. Am., Bull., vol. 47 (1936) p. 1125.

tion crops out more widely along the bases of the mountains and around the plunging noses of anticlines. Its upper boundary in many places marks the margins of the mountains and the valley floors. The best exposed section is on the south slope of Sierra Cupido, north of Rancho Concordia.

*Stratigraphic and lithologic features.*—The upper and lower limits of the Cuesta del Cura limestone are sharply differentiated from the contiguous formations at all localities. As deposition was apparently continuous, the striking lithologic changes were probably due to rather abrupt facies changes in space or time.

The Cuesta del Cura limestone thickens southward, generally from about 250 feet along the northern front of the range to about 1000 feet along the southern side of Sierra Garambullo. Most of the thickening takes place south of the line passing along Sierra Mesquite del Norte and Sierra del Organo, corresponding, in general, with the southern limit of the thick rudistid-bearing Aurora limestone. From east to west the thickness seems to vary considerably within short distances, as judged by the width of the outcrops. However, the true thickness is difficult to determine in most sections, owing to knee-like crumpling (Pl. 10, fig. 2), which is characteristic of the formation.

The section at the mouth of Cañón de la Casita is about 240 feet thick and consists of thin-bedded limestones that are wavy-bedded, dark-gray to brownish black, and contain numerous bands of black chert.

On the south flank of Sierra Cupido, north of Rancho Concordia, the section, from top to bottom, is as follows:

| Unit | Feet |
|---|---|
| 1. Limestone, wavy-bedded, mostly thin-bedded (beds range from 2 to 14 inches in thickness) dark-gray to brownish black; some beds with fine dark-gray and brown lamellae; some thin layers of platy limestone. Considerable black chert as thin lenticular layers | 206 |
| 2. Limestone, wavy-bedded, most beds range from 4 to 8 inches in thickness, dark-gray; includes some lenticular layers of black chert | 141 |
| 3. Limestone, medium-bedded, dark-gray, a little black chert | 45 |
| 4. Limestone, thin- to medium-bedded, wavy-bedded, dark-gray, includes numerous lenticular layers of black chert and some shaly partings | 283 |
| | 675 |

The Cuesta del Cura limestone is about 800 feet thick at the east end of Sierra Yeso, about 760 feet thick at the west end of Sierra San Angel, and about 670 feet thick on the north side of Sierra Mesquite south of Rancho El Angel. The width of the outcrops along the Sierra Garambullo and the east end of Sierra San Francisco indicates a thickness of at least 1000 feet. At all these localities the formation is remarkably similar

FIGURE 1. CONTACT OF PARRAS SHALE (LEFT) AND CARACOL FORMATION
Near west end of Sierra San Angel.

FIGURE 2. CUESTA DEL CURA LIMESTONES IN CAÑÓN BLANCO
Near east end of Sierra Mesquite del Norte.
Sharp knee-fold (right) is characteristic.

CRETACEOUS FORMATIONS

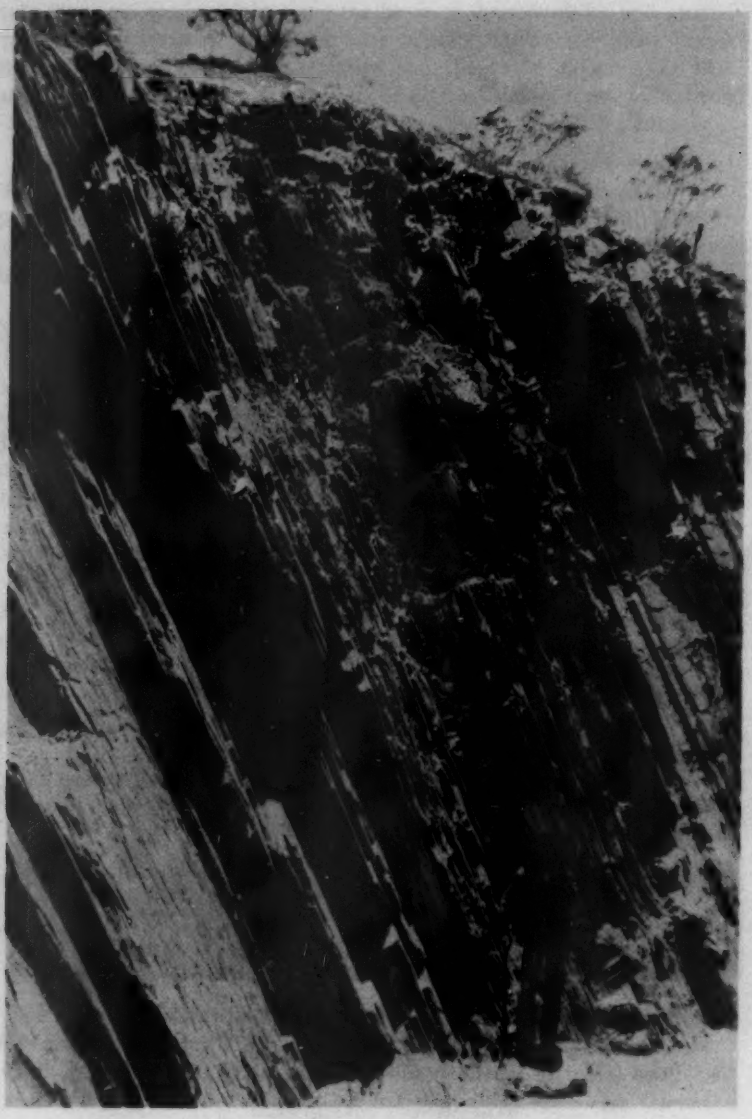

INDIDURA FORMATION

Thin-bedded to shaly limestone in Cañón San Angel.

lithologically. The upper part consists of wavy-bedded, thin-bedded, medium- to dark-gray or brownish black limestones. Some beds are thinly laminated, and some are separated by thinly laminated shaly partings. Many lenticular layers of black chert are found throughout. The beds range from 1 to 8 inches in thickness but average about 3 or 4 inches. The lower part of the formation differs only in being slightly thicker-bedded. Some beds are as much as 14 inches thick, but most beds fall in a range of 4 to 8 inches.

*Correlation.*—The Cuesta del Cura limestone is probably of upper Albian age. Its thickening toward the south coincident with thinning of the underlying Aurora limestone suggests that the lowest beds become older toward the south and are equivalent to the highest beds of the Aurora limestone along the northern side of the Sierra de Parras. This suggestion is partly discounted by the fairly thick section of Cuesta del Cura limestone overlying a thick section of Aurora limestone on the south flank of Sierra Cupido.

### INDIDURA FORMATION

*Areal extent.*—The Indidura formation crops out extensively in many synclinal valleys and depressions west and south of La Casita uplift, but, in most places, it is covered with alluvium. Well-exposed complete sections can be found only along Arroyo Caracol at the east end of Cañón Mesquite, along the northern base of the range east of Cañón de los Lobos, and along the southern base of Sierra Garambullo.

*Stratigraphic and lithologic features.*—The complete section of the Indidura formation along the west bank of Arroyo Caracol, measured from top to bottom, is as follows:

| Unit | Feet |
|---|---|
| 1. Limestone, thin-bedded and shaly, interbedded in about equal proportions, brownish black, weathers light-yellow | 176 |
| 2. Limestone, predominantly shaly but some beds ranging from 3 to 8 inches in thickness, brownish black, weathers grayish yellow | 92 |
| 3. Limestone, predominantly shaly, some thin-bedded, brown to brownish black. In upper 100 feet, several beds of calcareous black shale range from 1½ to 10 feet in thickness. *Inoceramus* cf. *labiatus* Schlotheim found near top (Collection 26) | 234 |
| 4. Limestone, platy, thin-bedded to shaly, brownish black, weathers light-yellow | 234 |
| 5. Limestone, thin-bedded to shaly, interbedded with calcareous shales, brown to brownish black, weathers light-yellow | 160 |
| | 896 |

The Indidura formation at the mouth of Cañón de la Casita is not more than 170 feet thick, if the upper contact is drawn at the base of the devitrified tuffs characterizing the Caracol formation. This diminished thickness

might be explained by: (1) a thrust fault cutting out part of the beds, or (2) a smaller amount of deposition than in the regions to the south and west, or (3) deposition of the tuffs of the Caracol formation beginning here earlier than farther west. The latter explanation is favored, but all three processes may have taken place. No positive evidence of thrust faulting was observed.

*Correlation.*—The Indidura formation along Arroyo Caracol is correlated with members 1, 2, and 3 of the Indidura formation near Parras. The middle and upper beds are of Turonian age, as shown by the presence of *Inoceramus* cf. *labiatus* Schlotheim. The lower beds may be of Cenomanian age.

### CARACOL FORMATION

*Definition.*—The name Caracol is here applied to a series of devitrified tuffs and shales with subordinate amounts of limestones, directly overlying the Indidura formation in the middle part of the Sierra de Parras. It is distinguished from the Indidura formation by the presence of tuffs, and, with the disappearance of the tuffs, it grades westward into a shale and limestone facies, typical of the Indidura formation. The overlying Parras shale is distinguished by the predominance of black shale. The type locality is here designated as the western side of Arroyo Caracol, near the western end of Sierra San Angel.

*Areal extent.*—The most western outcrop of the Caracol formation in the middle part of the Sierra de Parras is 20 miles southeast of Parras, where it is seen in some low sandstone-capped ridges at the eastern end of Cañón Mesquite (Pl. 3, fig. 1). From this locality, it extends eastward along the synclinal depression directly south of Sierra San Angel. It crops out along the northern base of the range, from the mouth of Cañón de los Lobos eastward. Large exposures are seen along the south side of Sierra Garambullo and on some hills rising from the plain, about 5 miles south of Sabinilla.

*Stratigraphic and lithologic features.*—The section on the west side of Arroyo Caracol, measured from top to bottom, is as follows:

| Unit | Feet | Inches |
|---|---|---|
| 1. Tuff, medium-bedded, micaceous, fine-grained, compact, brittle, yellowish white to yellowish brown, weathers cream-colored to reddish yellow | 25 | |
| 2. Tuffaceous shale interbedded with thin-bedded tuff, gray to yellowish gray | 107 | |
| 3. Shale, tuffaceous, yellowish gray | 62 | |
| 4. Novaculite like unit 14 | 2 | |
| 5. Shale and tuff, interbedded. Gray fissile shale, yellowish gray tuffaceous shale, and grayish yellow shaly tuff. *Inoceramus* cf. *convexus* Meek from base | 27 | |

FIGURE 1. PARRAS SHALE AT EAST END OF CAÑÓN MESQUITE

FIGURE 2. CARACOL SHALE AND TUFF IN CAÑÓN DE LA CASITA

CRETACEOUS FORMATION

| Unit | Feet | Inches |
|---|---|---|
| 6. Novaculite like unit 14 | 3 | |
| 7. Shale and tuff interbedded like unit 5. Gray fissile shale predominates, but shaly tuff becomes more abundant toward the top | 136 | |
| 8. Novaculite like unit 14 | | 6 |
| 9. Shale, dark-gray, papery to fissile, predominant; a few short lenticular beds of black limestone not exceeding 6 inches in thickness; two very thin beds of fine-grained yellow tuff about 8 feet from top | 88 | |
| 10. Novaculite like unit 14. Beds ⅛ to 2 inches thick | 10 | |
| 11. Limestone, fissile, brownish black | | 16 |
| 12. Shale, dark-gray, papery, predominant; some interbedded yellow tuffaceous shale and a few thin beds of yellow tuff | 53 | |
| 13. Shale, tuffaceous, gray, in places almost papery, weathers grayish yellow; some beds of yellow tuff about half an inch thick near top | 68 | |
| 14. Novaculite, greenish yellow, brittle, much broken into rectangular pieces but fractures cemented with calcite, weathers yellow to red | 5 | |
| 15. Shale, papery, gray, predominant; some layers of yellowish tuffaceous shale; one thin layer of brownish black shaly limestone bearing many algal (?) markings, 25 feet from base; a few thin beds of grayish yellow, fine-grained tuff | 180 | |
| 16. Thin-bedded tuff and tuffaceous shale, interbedded, grayish yellow | 18 | |
| 17. Shale, papery, gray, contains thin beds of yellowish gray tuff | 8 | |
| 18. Tuff, thin-bedded to shaly, fine-grained, grayish yellow, weathers yellowish red to brownish red; some beds of yellowish tuffaceous shale in upper part | 80 | |
| 19. Limestone, thin-bedded, nodular, brownish black to black, weathers yellowish to cream-colored, contains markings probably of algal origin | 7 | |
| 20. Tuff, yellowish gray, calcareous, weathers yellow to yellowish red | 24 | |
| | 925 | |

Microscopic examination was made of a thin-section of dark yellowish brown tuff from unit 1. The groundmass consists of cryptocrystalline chalcedony, in which are embedded sharply angular grains of quartz and feldspar of various sizes. There are a few grains of rutile, and some limonite, calcite, and organic material. A thin-section of tuff from unit 18 differs from the one just described in containing about 50 per cent calcite and little chalcedony. A thin-section of the novaculite from unit 14 consists mainly of cryptocrystalline quartz, shot through with many threads of sericitic material. At a magnification of about 450, only a few of the quartz particles could be distinguished. Scattered throughout the section are a few small angular quartz grains of sand size. There is some limonite, probably derived from pyrite. Small amounts of secondary calcite form veinlets and rounded radiating masses.

The Caracol formation is well exposed at the mouth of Cañón de la Casita. The following section was determined roughly by pace traverse:

| Unit | Feet |
|---|---|
| 1. Thin beds of gray, green, and black tuff interbedded with greenish gray and green shale | 12 |
| 2. Thin beds of yellow, black, and brown tuff alternating with dark-gray and greenish gray shale | 70 |
| 3. Shale, dark-gray to greenish gray | 85 |
| 4. Tuff, dark-gray | 2½ |
| 5. Shaly limestone and shale, dark-gray | 260 |
| 6. Shale and limestone, dark-gray, interbedded with some tuff | 74 |
| 7. Novaculite and shale interbedded | 5 |
| 8. Shaly limestone and shale, dark-gray, with interbedded yellowish tuff, at intervals ranging from 3 to 10 feet | 184 |
| 9. Tuff, brownish gray | 3 |
| 10. Shale, dark-gray, some thin-bedded limestone | 290 |
| 11. Tuff, yellowish white, two beds separated by 6 inches of dark-gray shaly limestone | 3½ |
| | 989 |

Microscopic examination of a thin-section of the tuff of unit 11 showed many angular fragments of quartz and feldspar of various sizes, in a groundmass of chalcedony and some calcite. There are shreds of biotite and a few grains of rutile. A thin-section of tuff from unit 9 has a matrix of chalcedony and calcite in about equal amounts, in which are scattered splinters of quartz and feldspar of various sizes. There are shreds of biotite, some limonite, and considerable organic material scattered throughout the section. Thin-sections from unit 1 show essentially the same minerals with the same characteristics. The black material is organic, and the green is probably biotite. Chalcedony is more abundant than is calcite in most specimens examined.

*Origin.*—The tuffaceous material of the Caracol formation came from a volcano. A rising landmass must have existed in central Mexico during lower Upper Cretaceous time in order to account for the much greater thickness and coarser texture of sediments of that age in the Parras Basin than exists in those to the north. The volcano was probably associated with the rising landmass.

The distribution of the Caracol formation shows that the source of the tuffaceous material lay to the southeast rather than to the south. The tuff-capped ridges along the east side of Cañón Mesquite dwindle toward the western end of the canyon, apparently due to the pinching out of the tuff. Disappearance of the tuffaceous material toward the west is shown also by its absence along the northern front of the Sierra de Parras, near Parras, and its presence at the mouth of Cañón de la Casita. Search for the source of the tuff should be made in southeastern Zacatecas or southwestern San Luis Potosí.

*Correlation.*—The Caracol formation is equivalent to Members 4 and 5 of the Indidura formation near Parras but is distinguished from them by the presence of tuff. It is probably Coniacian in age and equivalent to the lower part of the Austin Chalk of Texas.

PARRAS SHALE

*Areal extent.*—The Parras shale [14] crops out in several small areas at the eastern end of Cañón Mesquite and in a belt, about a mile wide, along the northern base of the Sierra de Parras.

*Stratigraphic and lithologic features.*—The incomplete section at the east end of Cañón Mesquite, from top to bottom, is as follows:

| Unit | Feet |
|---|---|
| 1. Shale, fissile to splintery, black | 270 |
| 2. Novaculite, greenish yellow, brittle, weathers yellow to red | 2 |
| 3. Shale, fissile to splintery, black. Lower 80 feet contains several thin beds of yellow novaculite | 285 |
| 4. Shale, fissile to splintery, dark-gray to black | 93 |
| | 650 |

A complete section of the Parras shale is exposed along Arroyo de la Casita, between the mountain front and Rancho Paraje (Pl. 4, fig. 1). Exposures are continuous in the upper half mile and are nearly continuous in the lower half mile. Throughout this distance the beds are overturned, dipping about 65 degrees south at the lower contact near the mountain and 80 degrees south at the contact with the Difunta formation. If the width of the outcrop has not been increased by isoclinal folding, the thickness of the formation, as determined by pacing, is about 5000 feet. Perhaps, part of the section is repeated by folding, although no evidence of such was noted.

The Parras shale along Arroyo La Casita consists predominantly of calcareous, nodular to fissile, black shale. At the base are 85 feet of black shale, which are overlain by 40 inches of dark-gray, calcareous, fine-grained sandstone. Overlying this series is about 1950 feet of black shale, which contains many thin beds of fine-grained, dark-gray sandstone. This is overlain, in turn, by about 2000 feet of black shale. The contact with the yellowish gray, fine-grained sandstones of the Difunta formation is definite, although the lower 300 feet of the Difunta formation contains several units of gray and yellowish gray shale, intercalated with units of sandstone.

*Source of sediment.*—The Parras shale near Parras contains few beds of sandstone. The lower part of the formation, near the mouth of Cañón

[14] Defined by R. W. Imlay: *Geology of the western part of the Sierra de Parras*, Geol. Soc. Am., Bull., vol. 47 (1936) p. 1133.

Tanque Verde, contains a number of sandstone beds, and, near the mouth of Cañón de la Casita it contains many thin sandstone beds. This increasing coarseness toward the east indicates that the main source of the sediments was to the southeast.

*Correlation.*—No fossils have been found in the Parras shale, but, judging from its stratigraphic position, it must be equivalent to the upper part of the Austin Chalk and perhaps to the lower part of the Taylor Marl.

## QUATERNARY SYSTEM

### MAYRÁN FORMATION

Conglomerates and tufa deposits cover a large area along the northern part of the Sierra de Parras, between the Lomas de San Pablo and the mouth of Cañón de los Lobos. Isolated remnants are found at the mouth of Cañón Tanque Verde and at the lower end of Cañón Yeguales.

### ALLUVIUM

A thin veneer of alluvium blankets the floors of most of the synclinal valleys in the middle part of the Sierra de Parras. The alluvium of the higher-level valleys is mainly held *in situ* by a mat of grass and herbage and contains considerable humic material. The alluvium in the low-level valleys is mainly in transit, nourishes a scanty desert type of vegetation, is light-colored, and contains much coarse material.

## IGNEOUS ROCKS

### DISTRIBUTION AND STRUCTURAL RELATIONS

Igneous rocks in the middle part of the Sierra de Parras are of limited extent and have been observed only on the south side, in the west-central part of the area mapped. Monzonite porphyry and medium-fine-textured granite are found only at, or near, the western end of the Sierra Mesquite del Sur, associated with Lower Cretaceous limestones. Monzonite porphyry, the predominant type, is found mainly on the crest and overturned north flank of the Juan Perez Anticline. One 3½-foot sill is seen about a mile south of Rancho Mesquite, on a small hill near a tanque. Where associated with the thick-bedded limestones of the Aurora and La Peña formations, the outcrops of monzonite porphyry are restricted to the deepest parts of the canyons or to the truncated bases of the mountains. Where associated with thin-bedded limestones, especially the Cuesta del Cura limestone, the monzonite porphyry is found as sills at various elevations. Some veins of calcite, bearing pyrite, are found in the porphyry. Metamorphic effects are conspicuous only in thin-bedded limestones. Locally, the Cuesta del Cura limestone and chert have been bleached white, and the limestone has acquired a granular texture.

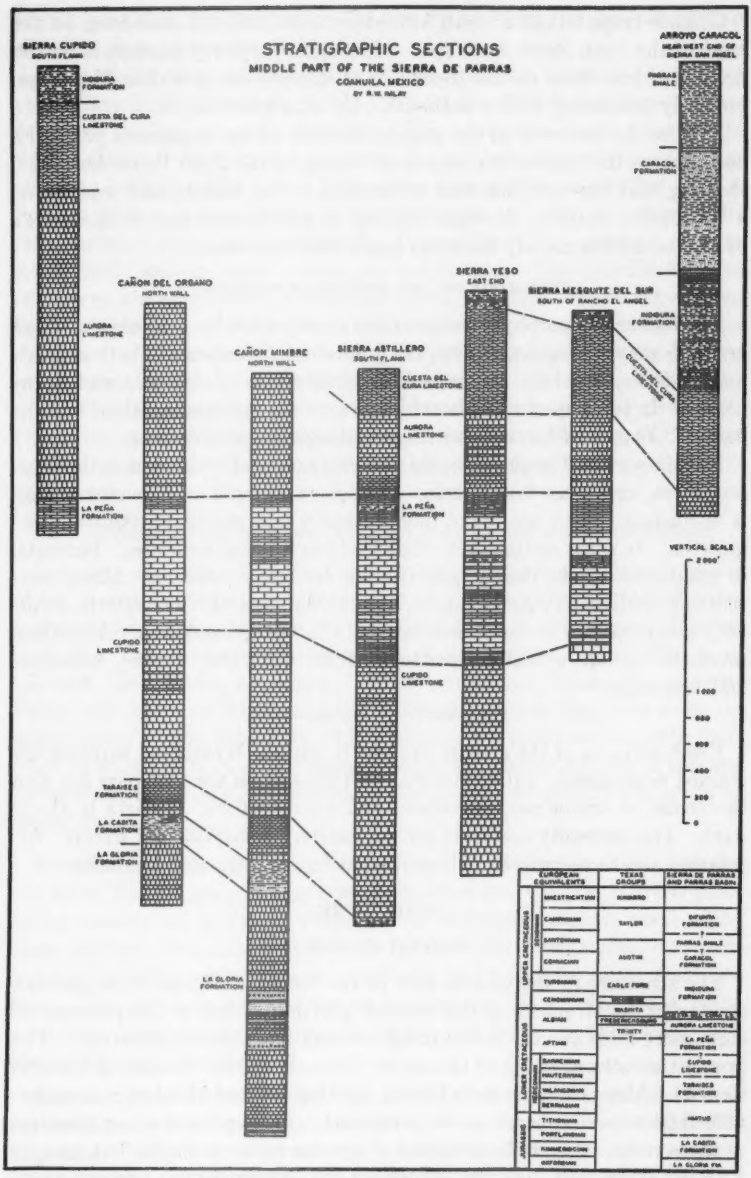


FIGURE 2.—*Stratigraphic sections of the middle part of the Sierra de Parras*

Granite crops out as a small hill, about one-fifth of a mile long, at the crest of the Juan Perez Anticline. Monzonite porphyry borders it on the north and limestone on the south. It is interpreted as a dike-like mass, probably connected with a batholith only at a great depth.

Neither the intrusion of the granite nor that of the monzonite porphyry has affected the kind or the degree of folding of the Juan Perez Anticline, showing that the intrusion was subsequent to the folding and was not of a batholithic nature. A slight doming of the western end of the Sierra Mesquite del Sur merely indicates laccolithic intrusion.

#### PETROLOGY OF THE MONZONITE PORPHYRY

The monzonite porphyry ranges from nearly white to medium-gray and greenish gray. Megascopically, the groundmass consists of finely crystalline feldspar, in which are embedded phenocrysts of feldspar and hornblende. In some specimens, hornblende crystals attain a length of 8 millimeters. Flakes of biotite and masses of epidote are common.

In thin-section the phenocrysts are common and consist of orthoclase, oligoclase, and green hornblende. Oligoclase is much more common than is orthoclase. Both are found independently and as microperthitic intergrowths. In some sections the oligoclase has a zonal structure. Ilmenite, or magnetite, brown biotite, and titanite are fairly common. Minor constituents include pale green augite, apatite, and quartz. The quartz, probably secondary, is in small amounts only in the groundmass. Alteration products include epidote, chlorite, sericite, kaolinite, calcite, hematite, and leucoxene.

#### PETROLOGY OF THE GRANITE

Fresh surfaces of the granite are nearly white. Weathered surfaces are stained considerably with limonite. In thin-section the feldspars are seen to consist of orthoclase, oligoclase, and microperthite. Quartz is abundant. The accessory minerals are magnetite, muscovite, and zircon. Alteration products include calcite, hematite, sericite, and kaolinite.

## STRUCTURE

### GENERAL FEATURES

The structure of the middle part of the Sierra de Parras is, in general, similar to the structure of the western part but differs in the presence of eight more folds and the overturning of many folds toward the south. The greatest structural uplift of the entire Sierra de Parras is south of General Cepeda. Along Cañones de la Casita, del Organo, and Mimbre, a considerable thickness of Jurassic rocks is exposed. The lead and silver minerals in these rocks suggest the presence of igneous rocks at depth, but igneous activity apparently has not influenced the deformation. Igneous rocks

crop out only in the western end of the Sierra Mesquite del Sur and are clearly subsequent to the folding.

Some of the eastward extensions of five anticlines noted in the western part of the Sierra terminate within the area investigated; others continue eastward for an unknown distance. The terminations are characteristically abrupt. New folds arise along the northern side of the sierra and trend at a slight angle to it. New folds arise within the folded area as flexures on the longest flanks of the anticlines or in the synclines. The northernmost anticlines fronting the Parras Basin are steepest on their north limbs and in many places are overturned. The anticlines within the sierra are overturned toward the north, or south, or are fan-shaped, there being no apparent system as regards direction of overturning. Along the trend of some anticlines (e.g., Taraises Anticline) the direction of overturning changes at intervals of 5 to 10 miles. In cross-section, some of the folds are flexed gently and rather uniformly (e.g., the Parras Anticline), but most of them are flexed along narrow zones, forming angles that, in some, exceed 90 degrees (e.g., Patagalana Anticline, Pl. 5, fig. 2; Pl. 13, Sec. A-A').

#### FOLDS CONTINUOUS FROM THE WESTERN PART OF THE SIERRA DE PARRAS

*Santiago Anticline.*—The Santiago Anticline forms the northernmost fold of the Sierra de Parras from the region of Parras southeastward 9 miles, to Puerto Gurostola. At this place the axis turns east-southeast 10 miles, to Cañón Tunal, passes slightly south of the highest ridge of Sierra de Cabrera, then trends southeast 7 miles, across the south side of Cerro Prieto and Sierra de los Pinos, and finally plunges into the plain along the north side of Cañón Piloncillo. The anticline is steepest on its north flank from its west end to near the eastern end of Sierra de Cabrera, is steepest on its south flank on Cerro Prieto, and is overturned toward the south on Sierra de los Pinos.

*Parras Anticline.*—The Parras Anticline trends east-southeast as far as Cañón Blanco, then swings east for 3 miles and plunges into the plain at the western end of Cañón Victoria. Its axis passes slightly north of the crest of Sierra Mesquite del Norte, as far as Cañón Salsipuedes, but, eastward it coincides with the crest. Both the north and the south limbs are steep. The north limb is steepest as far east as Cañón Salsipuedes, being vertical in the vicinity of Puerto del Indio, and the south flank is steepest and overturned farther east.

*Taraises Anticline.*—The Taraises Anticline persists as a small fold in the Indidura formation through the center of the synclinal valley of Cañón Yeguales. It is covered by alluvium in Cañón Mesquite but reappears farther east in the Sierra San Angel. West of Cuesta San Angel the fold

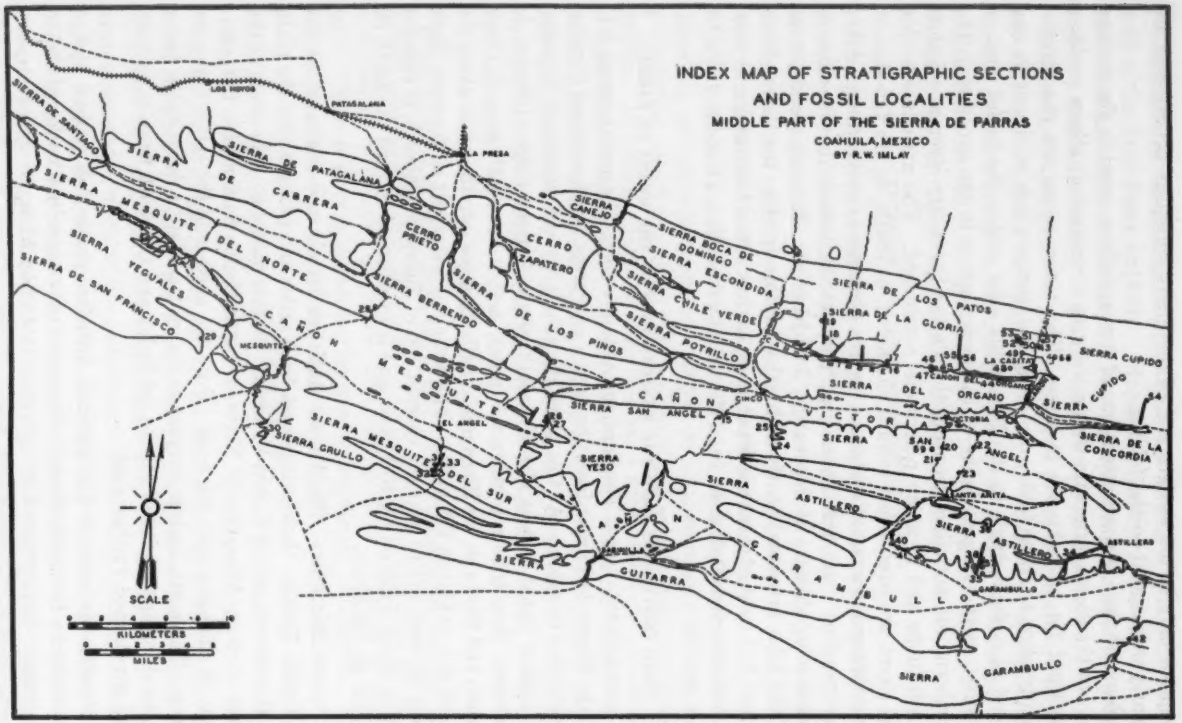


FIGURE 3.—*Index map of stratigraphic sections and fossil localities in the middle part of the Sierra de Parras*

is reflected by a rounded anticlinal mountain, but, eastward, its crest becomes dissected. The trend of the axis in Cañón Yeguales is east-southeast to southeast. Along the Sierra San Angel the axis trends almost due east as far as the head of Cañón Sombrero and then swings east-southeast. It is likely that the fold ends, or perhaps merges with the Prieta Anticline, several miles southeast of Palmas Altas.

The Taraises Anticline is overturned toward the south at the west end of Cañón Yeguales and overturned toward the north at the east end of the canyon. Along the western part of the Sierra San Angel the fold is overturned toward the north; along the middle part, it is overturned toward the south; and along the eastern part, toward the north. At all localities the overturning becomes progressively greater toward the synclines.

*Prieta Anticline.*—The Prieta Anticline trends southeast from Picacho Yeguales, and plunges into the plain about 2 miles southeast of Mesquite. Its persistence across the southern end of Cañón Mesquite is shown by the attitude of the Caracol formation. It rises abruptly, at the west end of Sierra Yeso, and continues eastward for an unknown distance as a major fold, being reflected topographically by the hogback ridges of Sierras Yeso and Astillero. From Sierra Astillero eastward for 4 or 5 miles the anticline has been deeply eroded into low hills, but at La Tinajuela, 2 miles north of Fraile, it is expressed by a high ridge, which continues eastward many miles. Along Sierra Yeguales the Prieta Anticline tends to be isoclinal, being overturned toward the south in the region of Picacho Yeguales and toward the north from Cañón del Rincón eastward. Along Sierras Yeso and Astillero the fold is more or less strongly overturned toward the north.

*Juan Perez Anticline.*—The Juan Perez Anticline trends from east-southeast to southeast and is strongly overturned toward the north throughout its extent. Its nearly recumbent north limb is represented topographically at the west by Sierra de San Francisco and at the east by Sierra Mesquite del Sur. Its crest and south limb are poorly exposed, and can be seen best in Sierra Grullo, south of Mesquite. East of Sierra Mesquite del Sur the anticline either terminates gradually within several miles or merges with the axis of the Sabinilla Anticline.

#### FOLDS BEGINNING IN THE MIDDLE PART OF THE SIERRA DE PARRAS

*Conejo Anticline.*—The Conejo Anticline is the northernmost major fold of the Sierra de Parras, from the west end of Sierra Conejo eastward to the mouth of Cañón Meco. North of the main axis of the Conejo Anticline, near the mouth of Cañón de los Lobos, is a minor flexure about 4 miles long. The crest of the Conejo Anticline lies slightly south of the highest parts of Sierras Conejo, Boca de Domingo, and Los Patos. Its

north limb is strongly overturned. Its south limb dips gently southward from the crest and then dips downward abruptly into a narrow syncline.

*La Gloria Anticline.*—La Gloria Anticline, first evident to the west in a small hill directly south of Sierra Conejo, rises out of the center of a syncline. The axis trends east-southeast, somewhat south of the crest of Sierra Escondida to Cañón Tanque Verde, and then trends eastward out of the region, passing north of the crests of Sierra de la Gloria and Sierra Cupido. Its position is marked throughout most of its extent by topographic depressions. North of Cañón Chileverde the south limb is steepest; the north limb dips gently north for half a mile from the axis and then dips steeply into a narrow syncline. East of the region of Cañón Chileverde the anticline is strongly overturned toward the north (Pl. 6, fig. 1), and east of Cañón Meco, it constitutes the northernmost fold of the Sierra de Parras.

*Patagalana Anticline.*—In the western part of the area the Patagalana Anticline forms the northernmost fold of the Sierra de Parras south of Los Hoyos and La Presa. Its axis trends east-southeast for 13 miles, coinciding with the crests of Sierra de Patagalana and Cerro Campana, but it is low on the north limb of Cerro Zapatero. On Sierra Patagalana the south limb dips about 40 degrees south, and the north limb is vertical. On Cerro Campana the north limb is nearly vertical, and on Cerro Zapatero, it is overturned. The Patagalana Anticline, as well as the syncline to the south, terminates gradually to the east of Cerro Zapatero.

*Organo Anticline.*—The Organo Anticline begins at the west in some low hills lying immediately north of Cerro Prieto, about 2½ miles southwest of La Presa. Its axis trends generally east-southeast along the following topographic features: a ridge between Cerro Campana and Sierra de los Pinos, the south flank of Cerro Zapatero (Pl. 5, fig. 1), the canyons between Sierra Chileverde and Sierra Potrillo, a ridge of Jurassic rocks directly north of the bottom of Cañones Mimbre and that of del Organo, through the center of Cañón Cupido, and then along the upper part of the south flank of Sierra Cupido. The anticline rises into a "high" at the east end of Cerro Zapatero and into the greatest "high" in the range near the head of Cañón Mimbre. Its south limb is overturned from Cerro Zapatero eastward. On Cerro Zapatero and Sierra Chileverde the north limb is broad and gently inclined. From Cañón Tanque Verde eastward the north limb dips steeply northward from the crest for a short distance and then flattens out into a broad flat syncline whose axis is marked by the highest peaks of Sierra de la Gloria and Sierra Cupido.

*Concordia Anticline.*—The Concordia Anticline extends across nearly the entire area. It begins on the west at the Rincón de Dolores, about

2½ miles southwest of Los Hoyos, and trends sinuously east-southeast, passing along the north flanks of the Sierra de Cabrera, Cerro Prieto, and Sierra de los Pinos, and along the crests of Sierra Panocha, Sierra Sitio, the hills north of Rancho Victoria, and Sierra de la Concordia. The fold rises gradually to a "high" in the vicinity of Cañón Tunal, then declines gradually to the east end of Sierra Panocha. Minor "highs" are at Sierra Sitio and at the hills north of Rancho Victoria. At the west end of the Sierra de la Concordia the fold rises rather abruptly into a large "high," which culminates half a mile east of the area mapped.

The fold is overturned toward the north, from its first appearance on the west to a point near the east end of Sierra de los Pinos, and then becomes overturned toward the south. Along Sierras Panocha and Sitio the south limb is vertical or overturned. Along the western 2 miles of Sierra de la Concordia the south limb is overturned, and the north limb is steep. Eastward, the north limb becomes overturned, and the south limb dips from 20 to 40 degrees south.

*Berrendo Anticline.*—In the west-central part of the area, a small but conspicuous fold parallels the eastern end of the Parras Anticline on the north. It begins in the low mountains west of La Hoya basin and extends southeastward for 8 miles, its axis following the crest of Sierra Berrendo. Near La Hoya the south limb is overturned, and the north limb slopes gently northward to a narrow vertical downfold. Along the eastern part of Sierra Berrendo the north limb is overturned, and the south limb dips steeply southward.

*Sabinilla Anticline.*—The Sabinilla Anticline extends sinuously along the southern margin of the Sierra de Parras, as one of the largest folds. Possibly, it is along the same line of folding as the Capadero Anticline of the western part of the Sierra de Parras, but, as the surface exposures are separated by many miles of alluvium, a new name seems advisable. On the west, in the vicinity of Rancho Sabinilla, the anticline has been deeply eroded into low ridges. Sierra Guitarra is on the south flank. The axis can be traced with difficulty through the series of ridges composed of the Cupido limestone. To the east, along the Sierra Garambullo, the axis follows the topographic crest. East of Fraile, beyond the area mapped, the fold is represented topographically by the Sierra del Fraile and continues eastward many miles.

The western part of the Sabinilla Anticline is strongly overturned toward the south, but, toward the east, the fold becomes gradually less overturned until, south of La Unión, it is symmetrical, and, at Puerto del Indio, it is somewhat overturned toward the north.

### FAULTS

Faults are found at many places, but, on the whole, they are of minor importance compared with the intense folding, suggesting that Lower Cretaceous rocks, which at present constitute the bulk of the mountains, were overlain at the time of deformation by a great thickness of Upper Cretaceous sediments, comparable to those which now crop out along the northern base of the range.

Several cross-faults with displacements less than 100 feet are present in the Upper Cretaceous strata at the east end of Cañón Mesquite. Cañón Tappon del Toro, northwest of Garambullo, probably follows a cross-fault. A cross-fault probably exists at the east end of the Sierra de San Francisco. Some of the cross-canyons, especially Cañón de los Lobos, Cañón Tanque Verde, Cañón de la Casita, and Puerto El Angel, probably follow fracture zones.

Bedding faults are common in the soft limestone and shales of the Upper Cretaceous formations and in the shales of the Upper Jurassic. The axial planes of many anticlines mark zones of brecciation, which are especially well shown on Sierras Astillero, Garambullo, and on the ridges of Jurassic strata near the bottom of Cañones Mimbre and that of del Organo. The structure of the Sabinilla, the Prieto, and the Taraises anticlines shows that there must have been considerable readjustment of the beds along the axial planes, and it seems likely that most of this readjustment has taken place in the relatively soft beds of the Taraises and La Casita formations.

## MINERAL DEPOSITS

Prospectors' pits are seen at many places in the Sierra de Parras, but the only pits containing traces of lead minerals are those in the ridge of La Gloria limestone directly north of the bottom of Cañón Mimbre. One pit at the western end of the ridge had been worked, during the spring of 1935, to a depth of about 30 feet. Several tons of high-grade ore still lay at the mouth of the pit. The ore minerals consist of calamine, cerussite, and galena. The gangue consists of calcite, limonite, and ferruginous clay. There are traces of drusy quartz. Calamine (hemimorphite) is found in massive and granular forms and also in radiating crystal groups of striated prisms, which are singly terminated. Calcite is seen as ordinary rhombohedrons and also as flattened, interpenetrating, simple rhombohedrons in parallel groupings.

## SUMMARY OF GEOLOGIC EVENTS

Figure 4 briefly summarizes the geologic events in the region.

# GEOLOGIC CROSS
## MIDDLE PART OF THE SI
COAHUILA, MEX
BY R.W. IMLAY

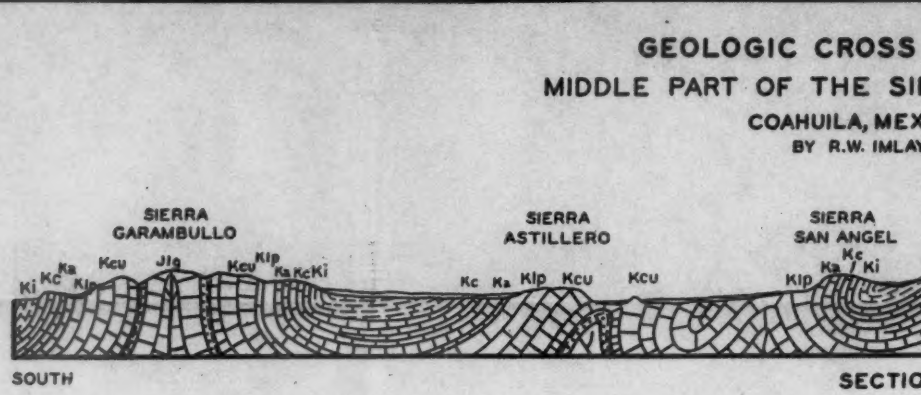


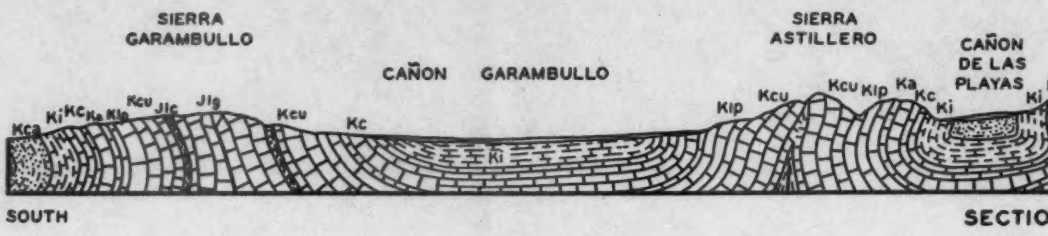


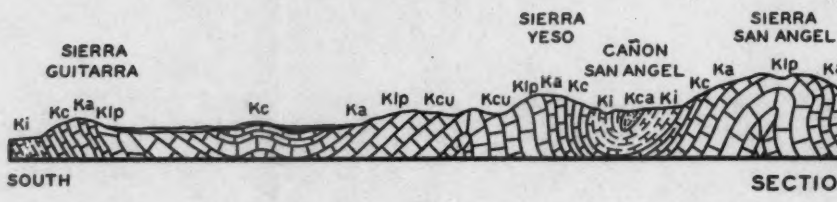


## LEGEND

### SEDIMENTARY ROCKS

| | | |
|---|---|---|
| RECENT | Qa | ALLUVIUM |
| PLEISTOCENE | Qm | MAYRAN CONGLOMERATES AND TUFA |
| UPPER CRETACEOUS — CAMPANIAN SANTONIAN ? | Kd | DIFUNTA FORMATION |
| UPPER CRETACEOUS — SANTONIAN | Kp | PARRAS SHALES |
| UPPER CRETACEOUS — CONIACIAN | Kc | CARACOL FORMATION |
| UPPER CRETACEOUS — TURONIAN CENOMANIAN | Ki | INDIDURA FORMATION |
| LOWER CRETACEOUS — ALBIAN | Kcu | CUESTA DEL CURA LIMESTONE |
| LOWER CRETACEOUS — ALBIAN | Ka | AURORA LIMESTONE |
| LOWER CRETACEOUS — APTIAN | Klp | LA PEÑA FORMATION |
| LOWER CRETACEOUS — BARREMIAN HAUTERIVIAN ? | Kcu | CUPIDO LIMESTONE |
| LOWER CRETACEOUS — HAUTERIVIAN VALANGINIAN | | TARAISES FORMATION |
| JURASSIC — PORTLANDIAN KIMMERIDGIAN | Jlc | LA CASITA FORMATION |
| JURASSIC — OXFORDIAN | | LA GLORIA FORMATION |

### IGNEOUS ROCKS

| | | |
|---|---|---|
| CENOZOIC ? | | PORPHYRY AND GRANITE |

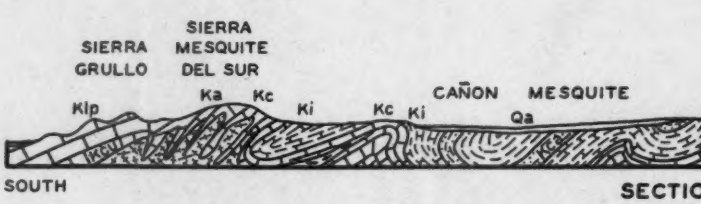


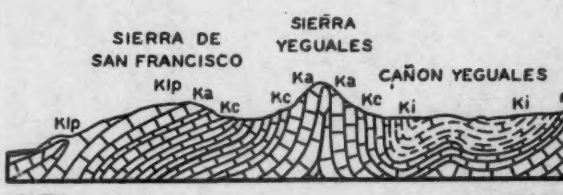

# CROSS SECTIONS
## THE SIERRA DE PARRAS
## HUILA, MEXICO
BY R.W. IMLAY

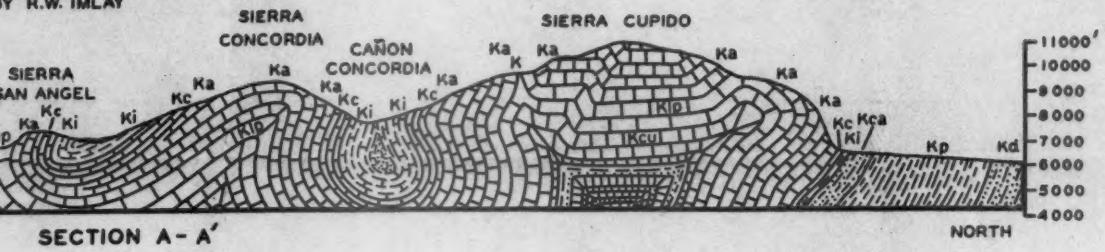


SECTION A-A′

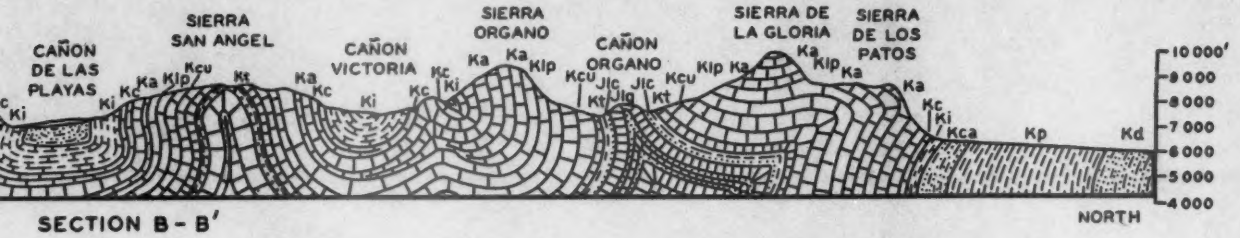


SECTION B-B′

SECTION C-C′

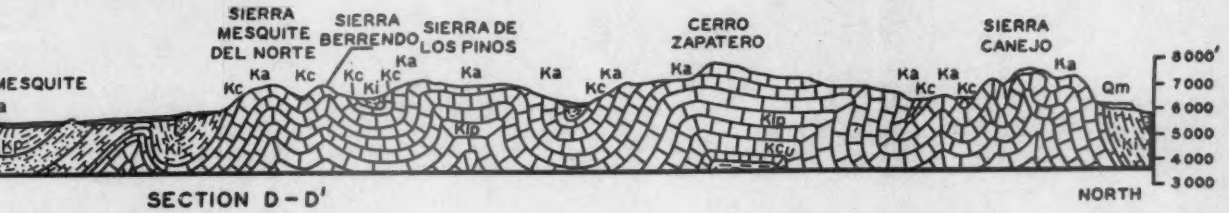


SECTION D-D′

SECTION E-E′

VERTICAL AND HORIZONTAL SCALES IDENTICAL

SECTION F-F′

ELEVATION ABOVE MEAN SEA LEVEL IN FEET

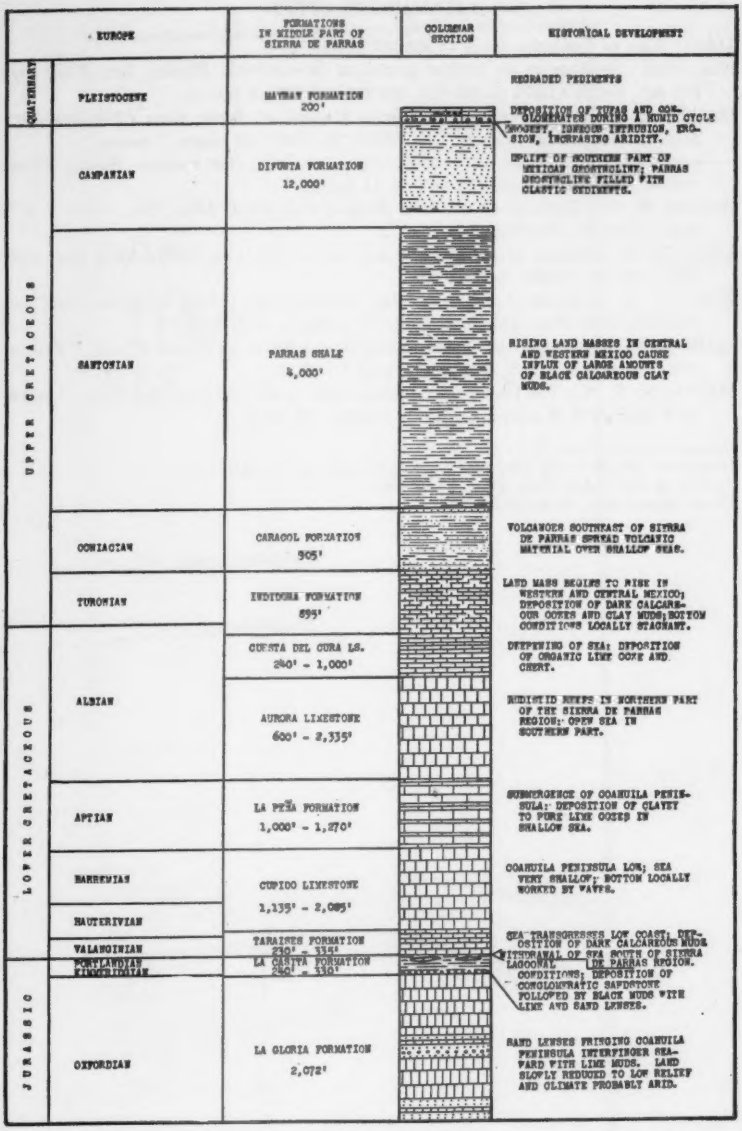
EUROPE
FORMATIONS IN MIDDLE PART OF SIERRA DE PARRAS
COLUMNAR SECTION
HISTORICAL DEVELOPMENT
QUATERNARY
PLEISTOCENE
MAYRAN FORMATION 200'
DEGRADED PEDIMENTS
DEPOSITION OF TUFAS AND CONGLOMERATES DURING A HUMID CYCLE FOLLOWED, IGNEOUS INTRUSION, EROSION, INCREASING ARIDITY.
UPPER CRETACEOUS
CAMPANIAN
DIFUNTA FORMATION 12,000'
UPLIFT OF SOUTHERN PART OF MEXICAN GEOSYNCLINE; PARRAS GEOSYNCLINE FILLED WITH CLASTIC SEDIMENTS.
SANTONIAN
PARRAS SHALE 4,000'
RISING LAND MASSES IN CENTRAL AND WESTERN MEXICO CAUSE INFLUX OF LARGE AMOUNTS OF BLACK CALCAREOUS CLAY MUDS.
CONIACIAN
CARACOL FORMATION 505'
VOLCANOES SOUTHEAST OF SIERRA DE PARRAS SPREAD VOLCANIC MATERIAL OVER SHALLOW SEAS.
TURONIAN
INDIDURA FORMATION 895'
LAND MASS BEGINS TO RISE IN WESTERN AND CENTRAL MEXICO; DEPOSITION OF DARK CALCAREOUS OOZES AND CLAY MUDS; BOTTOM CONDITIONS LOCALLY STAGNANT.
LOWER CRETACEOUS
ALBIAN
CUESTA DEL CURA LS. 280' - 1,000'
DEEPENING OF SEA; DEPOSITION OF ORGANIC LIME OOZE AND CHERT.
AURORA LIMESTONE 600' - 2,335'
RUDISTID REEFS IN NORTHERN PART OF THE SIERRA DE PARRAS REGION; OPEN SEA IN SOUTHERN PART.
APTIAN
LA PEÑA FORMATION 1,000' - 1,270'
SUBMERGENCE OF COAHUILA PENINSULA; DEPOSITION OF CLAYEY TO PURE LIME OOZES IN SHALLOW SEA.
BARREMIAN
CUPIDO LIMESTONE 1,135' - 2,085'
COAHUILA PENINSULA LOW; SEA VERY SHALLOW; BOTTOM LOCALLY WORKED BY WAVES.
HAUTERIVIAN
VALANGINIAN
TARAISES FORMATION 230' - 335'
SEA TRANSGRESSES LOW COAST; DEPOSITION OF DARK CALCAREOUS MUDS
PORTLANDIAN
KIMMERIDGIAN
LA CASITA FORMATION 280' - 330'
WITHDRAWAL OF SEA SOUTH OF SIERRA LAGOONAL LIME PARRAS REGION. CONDITIONS; DEPOSITION OF CONGLOMERATIC SANDSTONE FOLLOWED BY BLACK MUDS WITH LIME AND SAND LENSES.
JURASSIC
OXFORDIAN
LA GLORIA FORMATION 2,072'
SAND LENSES FRINGING COAHUILA PENINSULA INTERFINGER SEAWARD WITH LIME MUDS. LAND SLOWLY REDUCED TO LOW RELIEF AND CLIMATE PROBABLY ARID.

FIGURE 4.—*Summary of geologic events in the middle part of the Sierra de Parras*

## LITERATURE CITED

Abbot: Map of Coahuila, scale 1: 500,000 (1905).

Böse, Emil: *Vestiges of an ancient continent in northeast Mexico,* Am. Jour. Sci., 5th ser., vol. 6 (1923) p. 127-136, 196-214, 310-337, 4 figures.

Burckhardt, Carlos: *Géologie de la Sierra Mazapil et Santa Rosa (Mexico),* 10th Intern. Geol. Cong., Mexico, Guidebook 26 (1906) 40 pages, 2 maps.

———: *Etude synthétique sur le Mésozoïque mexicain,* Soc. Paléont. Suisse, Mém., vol. 40 (1930) 280 pages, 32 figures, 11 tables.

Burrows, R. H.: *Geology of northern Mexico,* Soc. Geol. Mex., Bol., tomo 7, I$^{era}$ parte (1910) p. 85-103, map.

Imlay, R. W.: *Geology of the western part of the Sierra de Parras,* Geol. Soc. Am., Bull., vol. 47 (1936) p. 1091-1152.

Kelly, W. A.: *Geology of the mountains bordering the valleys of Acatita and Las Delicias,* Geol. Soc. Am., Bull., vol. 47 (1936) p. 1009-1032.

Spath, L. F.: *Revision of the Jurassic cephalopod fauna of Kachh (Cutch),* Paleontolog. Indica, n. s., vol. 9, Mem. 2, part 5 (1931).

Whitehouse, F. W.: *The Cretaceous Ammonoidea of eastern Australia,* Mem. Queensland Mus., vol. 8, part 3 (1926) p. 195-242, pls. 34-41.

University of Michigan, Ann Arbor, Michigan.
Manuscript received by the Secretary of the Society, August 10, 1936.
Accepted by the Committee on Publications, 1936.
Project Grants 16-33, 78-34, 126-35, 167-36.

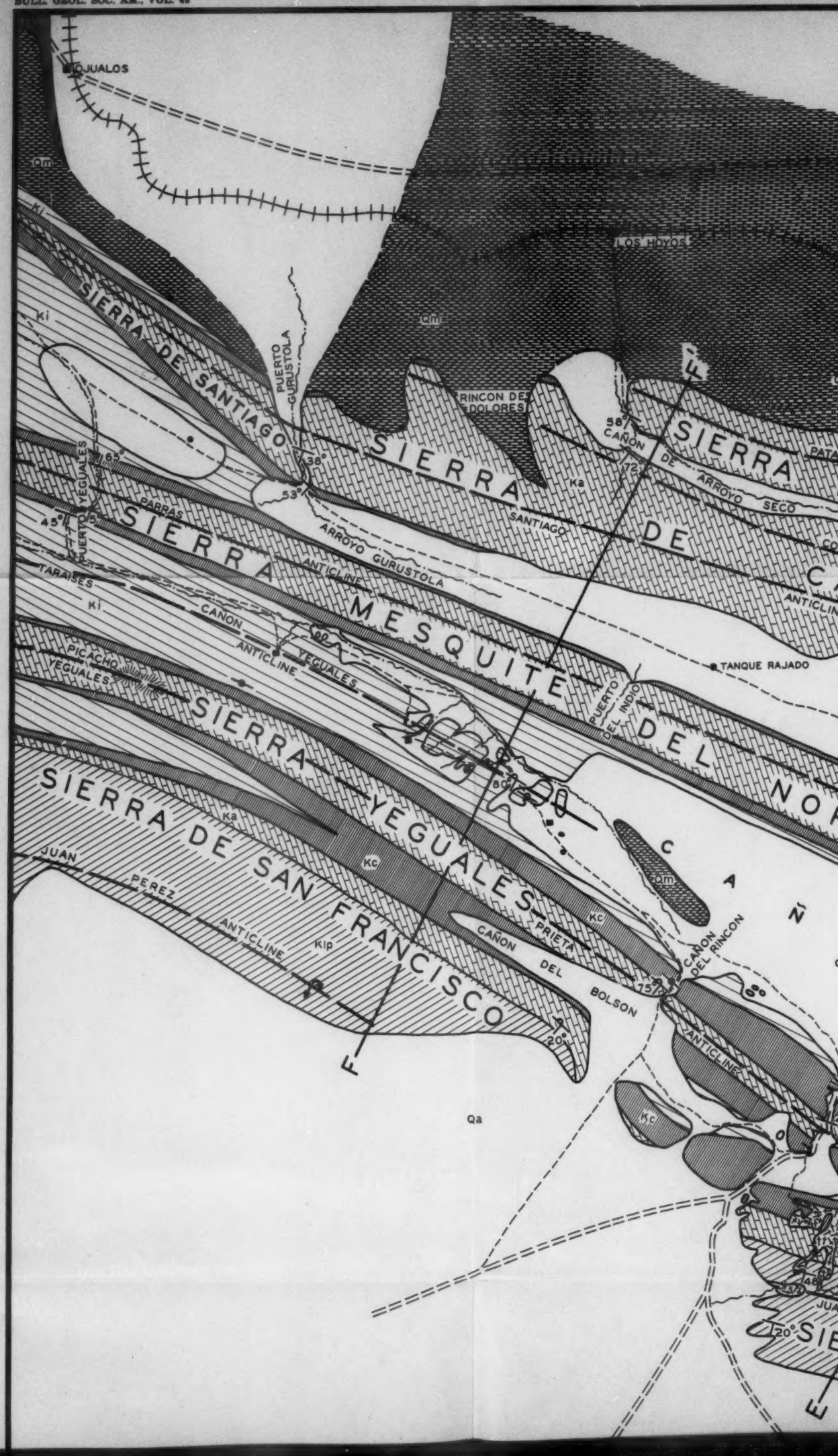
HIJUALOS
Qm
Ki
SIERRA DE SANTIAGO
PUERTO GURUSTOLA
LOS HOYOS
Qmi
RINCON DE DOLORES
SIERRA DE SANTIAGO
ARROYO SECO
ANTICLINE
Ka
PARRAS
ARROYO GURUSTOLA
TARAISES
CANON
PICACHO
YEGUALES
SIERRA MESQUITE
TANQUE RAJADO
PUERTO DEL INDIO
SIERRA DE YEGUALES
SIERRA DE SAN FRANCISCO
JUAN PEREZ
Kc
Klp
PRIETA
CAÑON DEL BOLSON
CAÑON DEL RINCON
Qa
F
65°
38°
53°
45°
58°
72°
89°
75°
20°

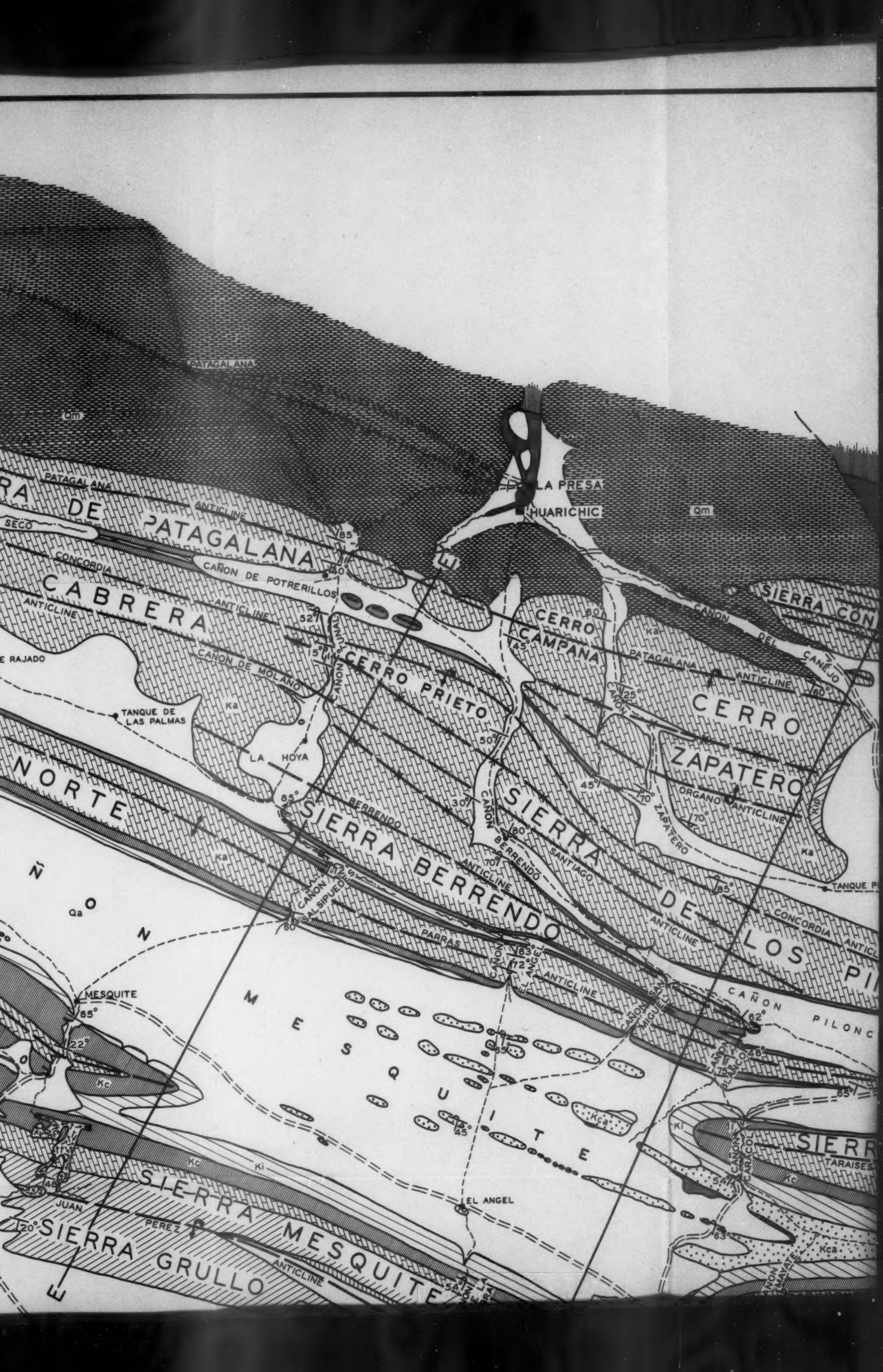
PATAGALANA
Qm
LA PRESA
HUARICHIC
Qm
SIERRA CON
RA DE PATAGALANA
PATAGALANA ANTICLINE
SECO
CONCORDIA ANTICLINE
CAÑON DE POTRERILLOS
CABRERA
ANTICLINE
ANTICLINE
CAÑON DEL CANEJO
CERRO CAMPANA
CERRO PRIETO
CAÑON DE MOLANO
TANQUE DE LAS PALMAS
LA HOYA
PATAGALANA ANTICLINE
CERRO ZAPATERO
ORGANO ANTICLINE
ZAPATERO
SIERRA DE LOS PI
CONCORDIA ANTICL
NORTE
SIERRA BERRENDO
BERRENDO ANTICLINE
CAÑON BERRENDO
SANTIAGO
CAÑON ALSIPUEDES
PARRAS ANTICLINE
ANTICLINE
CAÑON
PILONC
MESQUITE
MESQUITE
SQUITE
SIERR
TARAISES
EL ANGEL
SIERRA MESQUITE
SIERRA GRULLO
ANTICLINE
JUAN PEREZ
Kca
Ki
Kc
Ka
Qa

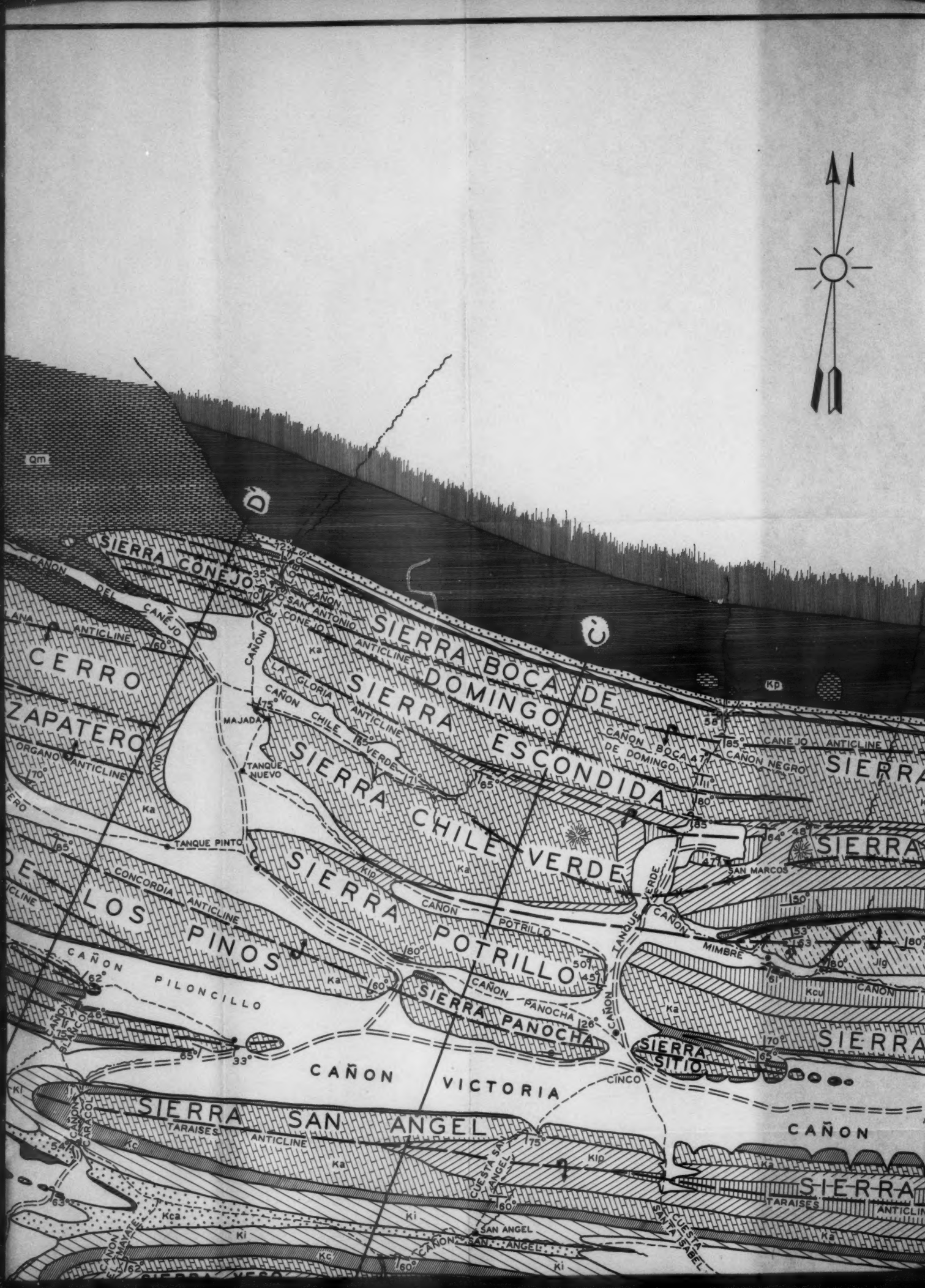
SIERRA CONEJO
CAÑON DEL CANEJO
CAÑON SAN ANTONIO
CONEJO ANTICLINE
SIERRA BOCA DE DOMINGO
SIERRA ESCONDIDA
CERRO ZAPATERO
ANTICLINE
LA GLORIA ANTICLINE
CAÑON CHILE VERDE
CAÑON BOCA DE DOMINGO
CAÑON NEGRO
CANEJO ANTICLINE
MAJADA
TANQUE NUEVO
TANQUE PINTO
SIERRA CHILE VERDE
SAN MARCOS
CONCORDIA ANTICLINE
SIERRA DE LOS PINOS
CAÑON POTRILLO
TANQUE VERDE CAÑON
MIMBRE
SIERRA POTRILLO
CAÑON PILONCILLO
CAÑON PANOCHA
SIERRA PANOCHA
SIERRA SITIO
CINCO
CAÑON VICTORIA
SIERRA SAN ANGEL
TARAISES ANTICLINE
CUESTA SAN ANGEL
SAN ANGEL
CAÑON SAN ANGEL
CUESTA SABEL
Qm
Kp
Ka
Kcu
Kca
Kc
Ki
Kip
Jlg

# GEOLOGIC MAP
## MIDDLE PART OF THE SIERRA DE PARRAS
COAHUILA, MEXICO

BY R.W. IMLAY

SCALE

0 1 2 4 6 8 10
KILOMETERS

0 1 2 3 4 5 6
MILES

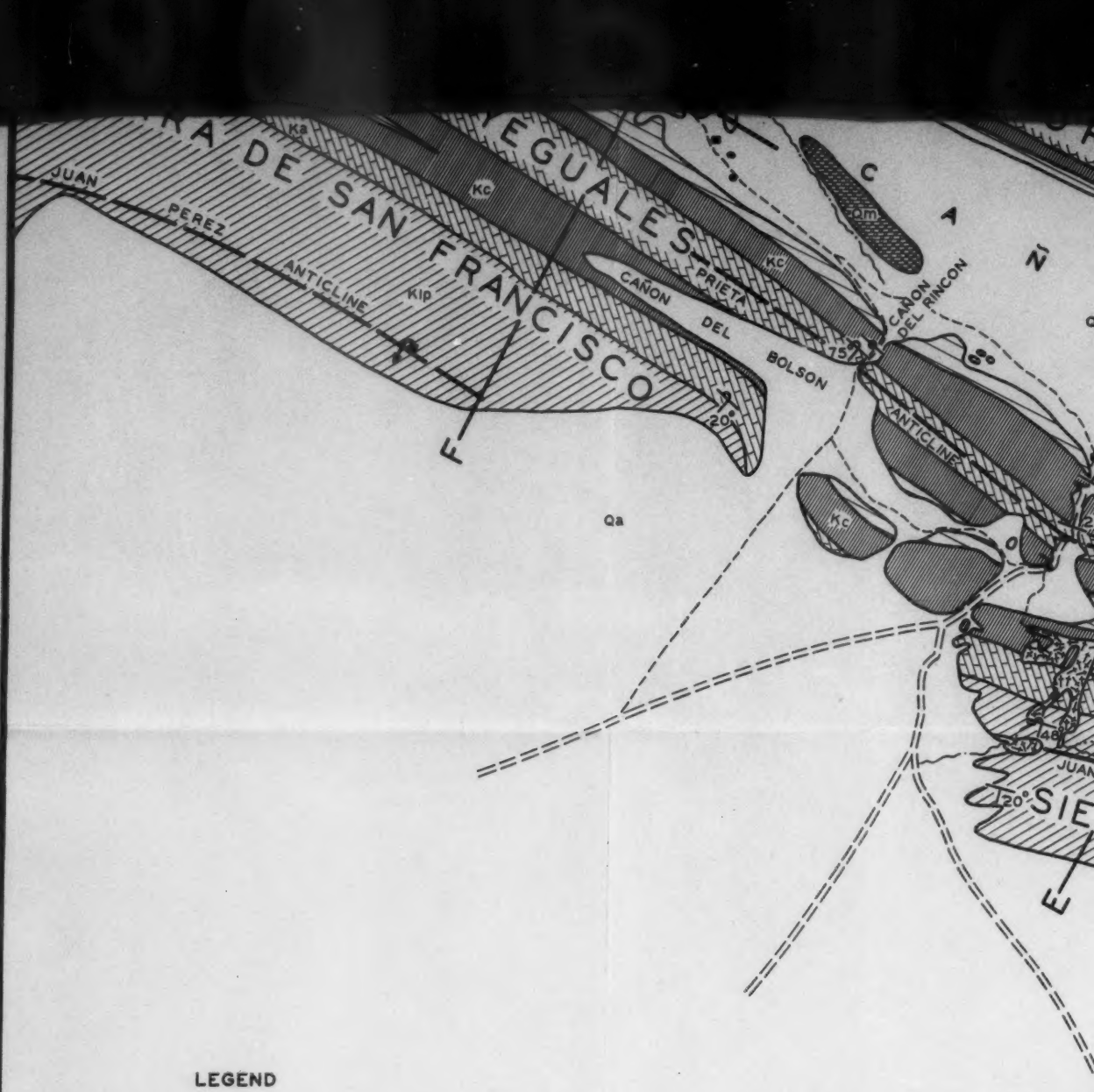


## LEGEND

### SEDIMENTARY ROCKS

| | | | |
|---|---|---|---|
| | RECENT | Qa | ALLUVIUM |
| | PLEISTOCENE | Qm | MAYRAN CONGLOMERATES AND TUFA |
| UPPER CRETACEOUS | CAMPANIAN SANTONIAN ? | Kd | DIFUNTA FORMATION |
| | SANTONIAN | Kp | PARRAS SHALES |
| | CONIACIAN | Kca | CARACOL FORMATION |
| | TURONIAN CENOMANIAN | Ki | INDIDURA FORMATION |
| LOWER CRETACEOUS | ALBIAN | Kc | CUESTA DEL CURA LIMESTONE |
| | ALBIAN | Ka | AURORA LIMESTONE |
| | APTIAN | Kip | LA PEÑA FORMATION |
| | BARREMIAN HAUTERIVIAN ? | Kcu | CUPIDO LIMESTONE |
| | HAUTERIVIAN VALANGINIAN | Kt | TARAISES FORMATION |
| JURASSIC | PORTLANDIAN KIMMERIDGIAN | Jlc | LA CASITA FORMATION |
| | OXFORDIAN | Jlg | LA GLORIA FORMATION |

### IGNEOUS ROCKS

| | | | |
|---|---|---|---|
| | CENOZOIC ? | | PORPHYRY AND GRANITE |

### SYMBOLS

- AXIS OF ANTICLINE
- AXIS OF OVERTURNED ANTICLINE
- AXIS OF SYNCLINE
- FORMATION BOUNDRY
- PROBABLE FORMATION BOUNDRY
- 45° STRIKE AND DIP
- 60° STRIKE AND DIP OF OVERTURNED STRATA
- MINE

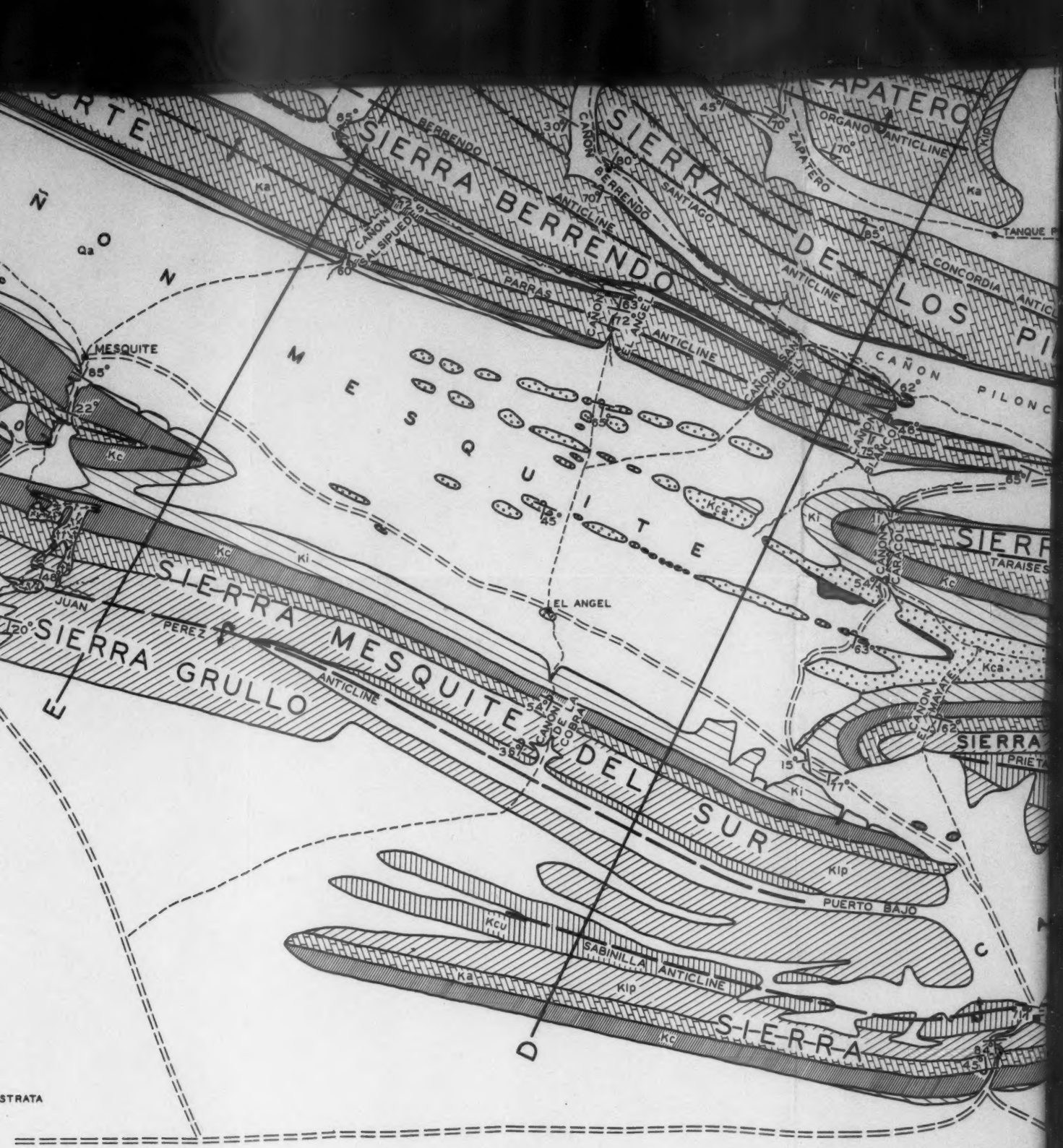


STRATA

GEOLOGIC MAP OF MIDDLE PART OF THE SIER

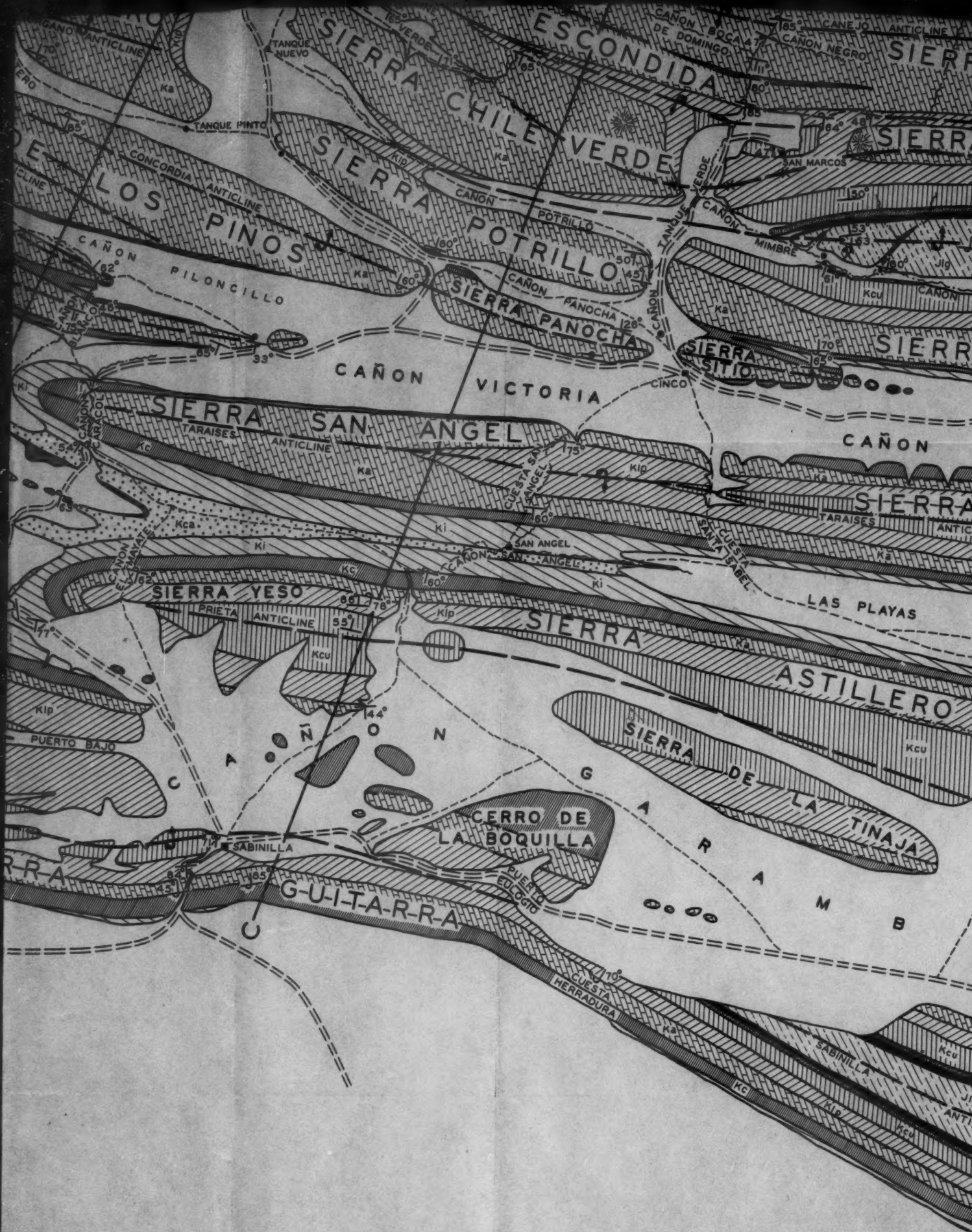


P OF MIDDLE PART OF THE SIERRA DE PARRAS, COAHUILA, MEXICO

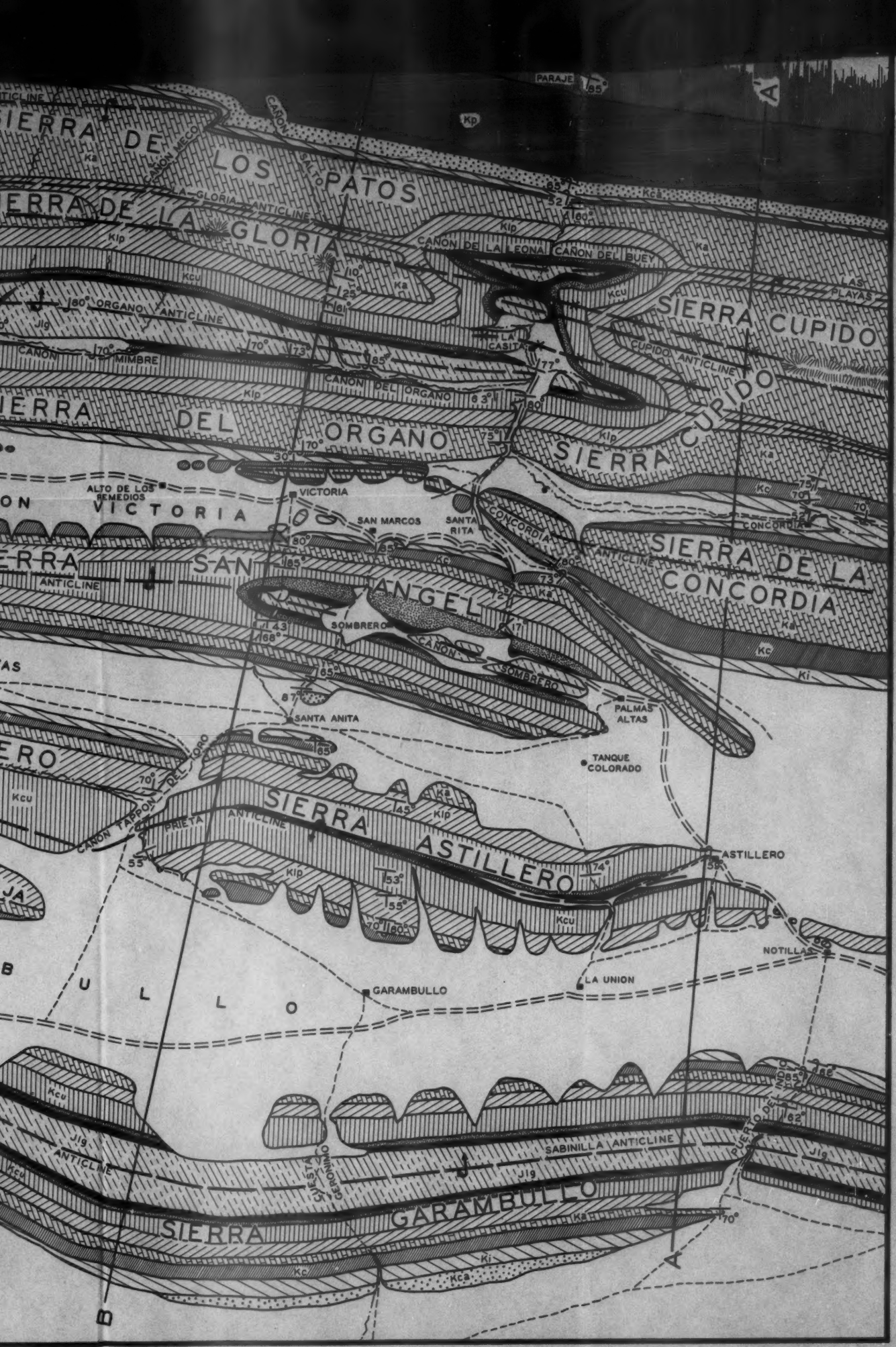
SIERRA DE LOS PATOS
SIERRA DE LA GLORIA
LA GLORIA ANTICLINE
ORGANO ANTICLINE
SIERRA DEL ORGANO
SIERRA CUPIDO
CUPIDO ANTICLINE
CONCORDIA ANTICLINE
SIERRA DE LA CONCORDIA
SIERRA SAN ANGEL
SIERRA ASTILLERO
SABINILLA ANTICLINE
SIERRA GARAMBULLO
CAÑON DEL MIMBRE
CAÑON DEL ORGANO
CAÑON DE LA LEONA
CAÑON DEL BUEY
CAÑON DEL SOMBRERO
CAÑON TAPON DEL ORO
LAS PLAYAS
LA CASITA
VICTORIA
ALTO DE LOS REMEDIOS
SAN MARCOS
SANTA RITA
CONCORDIA
SOMBRERO
SANTA ANITA
PALMAS ALTAS
TANQUE COLORADO
ASTILLERO
NOTILLAS
LA UNION
GARAMBULLO
PARAJE
Kp
Ka
Kip
Kcu
Kc
Ki
Kca
Jlg
A
B

BULLETIN OF THE GEOLOGICAL SOCIETY OF AMERICA
VOL. 48, PP. 631-666, 4 PLS., 1 FIG. MAY 1, 1937

# STRUCTURE OF THE UINTA MOUNTAINS

BY J. DONALD FORRESTER

## CONTENTS

Page

Introduction ..... 632
Acknowledgments ..... 633
Topographic features ..... 633
Geosyncline of deposition ..... 634
Relation of Uinta geosynclinal sediments to Rocky Mountain sediments ..... 634
Trend of Uinta Mountain trough relative to the Rocky Mountain geosyncline and the Wasatch Mountain trough ..... 636
Lithology of the region ..... 637
Structural features ..... 642
Folding ..... 642
Faulting ..... 644
South Flank Fault ..... 644
Brush Creek Zone ..... 645
Yampa Fault ..... 645
Uinta or Crest Fault ..... 645
North Flank Fault ..... 646
Faulting adjacent to the Uintas ..... 647
Jointing ..... 648
Diastrophism ..... 648
General statement ..... 648
Deformation of Uinta and Wasatch geosynclines during the Laramide Revolution ..... 649
Folding of the Wasatch and other northward-trending ranges ..... 649
Folding of the Uinta Mountains ..... 650
General symmetry of the Uinta Fold ..... 650
Minor folds adjacent to the Uinta Range ..... 651
Detailed consideration of Uinta Mountain structure ..... 652
Western portion ..... 652
Eastern portion ..... 652
Faulting ..... 653
Time of folding ..... 654
Post-folding erosional history ..... 655
Vertical uplift and large-scale faulting ..... 656
General statement ..... 656
Extent and intensity of uplift ..... 657
Uinta Mountain area ..... 657
Wasatch Mountain area ..... 658
Coalville-Weber River and Daniels Canyon-Strawberry areas ..... 659
Axial Basin region ..... 659
Rock Springs area ..... 659
Time of vertical uplift ..... 659
Theory as to cause of vertical uplift ..... 660

Page

Post-vertical uplift erosional history ..... 661
Continental uplift in late Pliocene or early Pleistocene ..... 663
General Plateau area ..... 663
Time of continental uplift ..... 663
Bibliography ..... 664

## ILLUSTRATIONS

Figure Page

1. Isopach map ..... 635

Plate Facing page

1. Index map of the Uinta Mountains ..... 632
2. Composite geologic columnar sections of the Uinta Mountains ..... 636
3. Areal geology and structure sections of the Uinta Mountains ..... 640
4. Regional structural relationships in the Uinta Mountains ..... 644

## INTRODUCTION

Geologists have long been interested in the Uinta Mountains, partly because of the unusual erosional features, but chiefly, perhaps, because of the orientation with respect to most mountain ranges of the Cordilleran region. These mountains, which form the largest east-west-trending range in the western hemisphere, are in northeastern Utah and northwestern Colorado, just south of the Utah-Wyoming and Colorado-Wyoming boundary. They extend as a physiographic unit from Kamas, Utah, on the west, to Cross or Junction Mountain, Colorado, on the east, a distance of approximately 160 miles. The width of the range, averaging about 45 miles, varies considerably, and, because of certain structural features, is somewhat greater toward the eastern end.

As a structural element, the Uinta Range is a prominent feature of the Rocky Mountain system and extends into the north-south-trending Wasatch Range and possibly even into the Oquirrh Range, still farther west. Eastward, its anticlinal axis extends through the Axial Basin uplift into the Grand Hogback, which has a north-south trend.

The Uinta Mountains have been the subject of study and discussion since the time of the earliest exploratory surveys of the West. Indeed, some of the classics of geological literature deal, to a greater or lesser extent, with this interesting feature of the central Cordilleran region. Of these earlier papers, with the exception of the Fortieth Parallel reports of the King Survey, none has covered the entire range as a structural unit.

The primary purpose of this paper is to consider, from field evidence, the Uinta Range as a structural unit, in an attempt to find a satisfactory explanation of the origin and peculiar orientation of this range with respect to neighboring Rocky Mountain ranges.

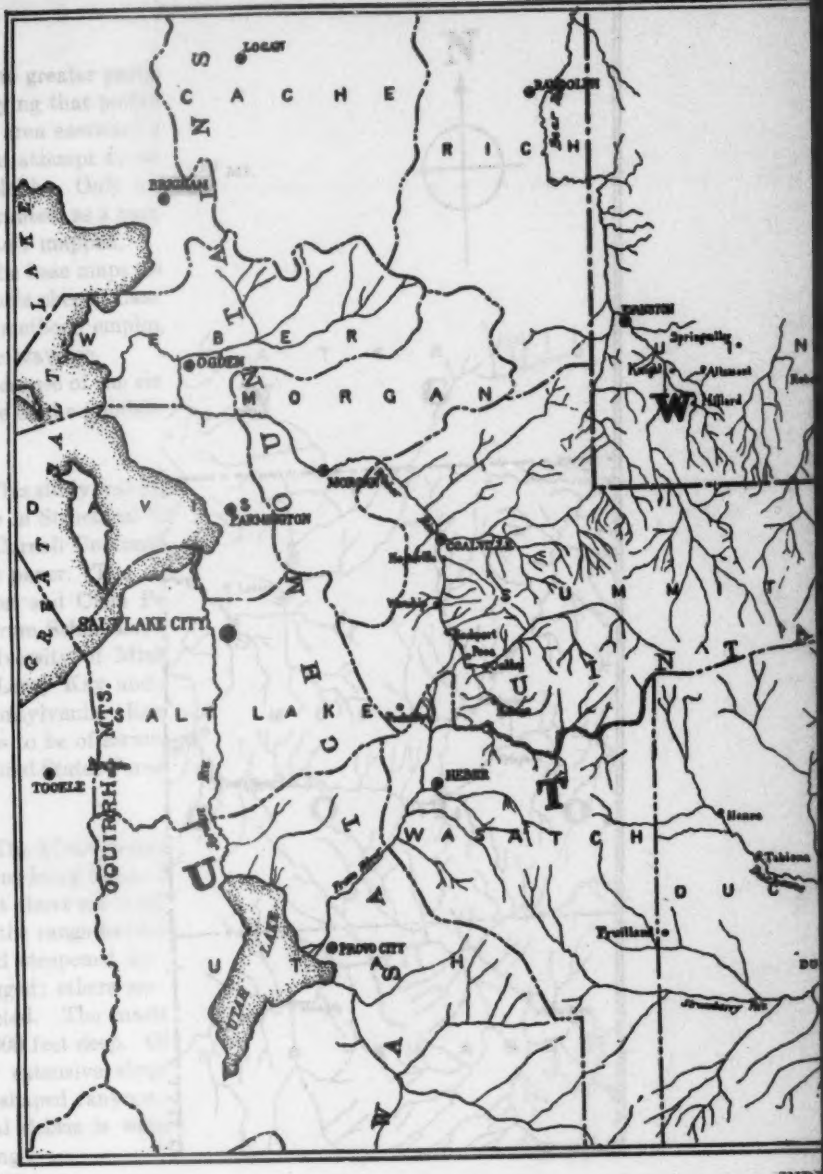
LOGAN
CACHE
RICH
BRIGHAM
GREAT SALT LAKE
WEBER
OGDEN
MORGAN
DAVIS
FARMINGTON
MORGAN
COALVILLE
SUMMIT
SALT LAKE CITY
SALT LAKE
TOOELE
SOUTH MTS.
UTAH LAKE
PROVO CITY
HEBER
WASATCH
DUC
Tabiona
Hanna
Duchesne

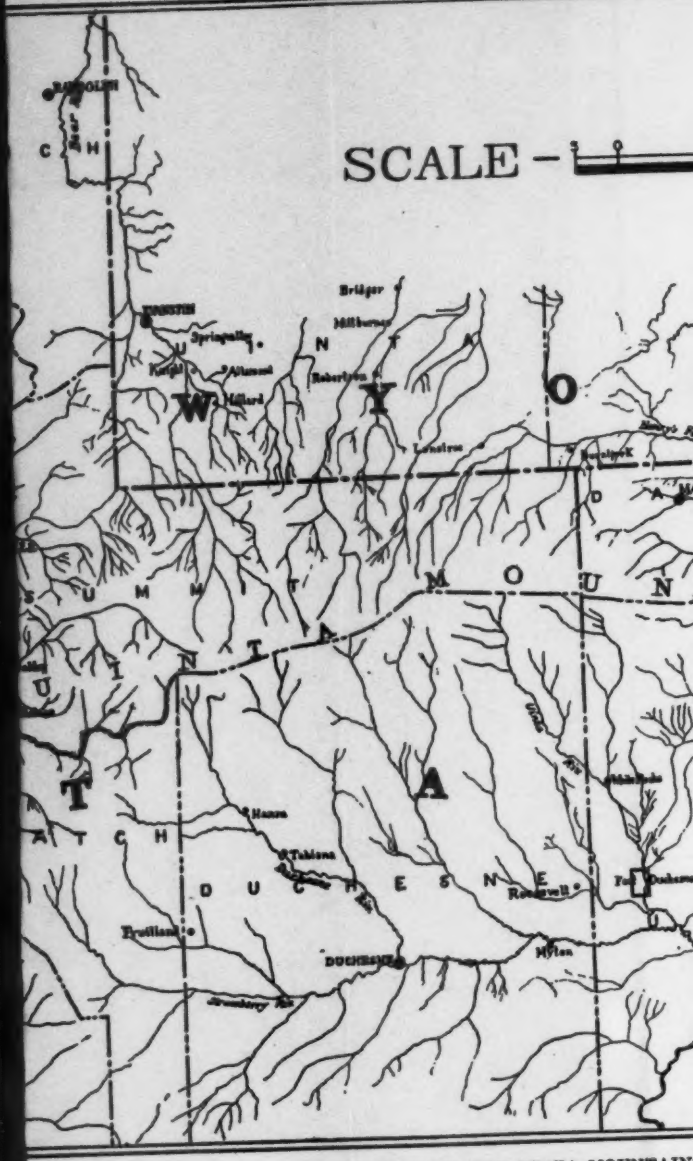


INDEX MAP OF THE UINTA MOUNTAIN

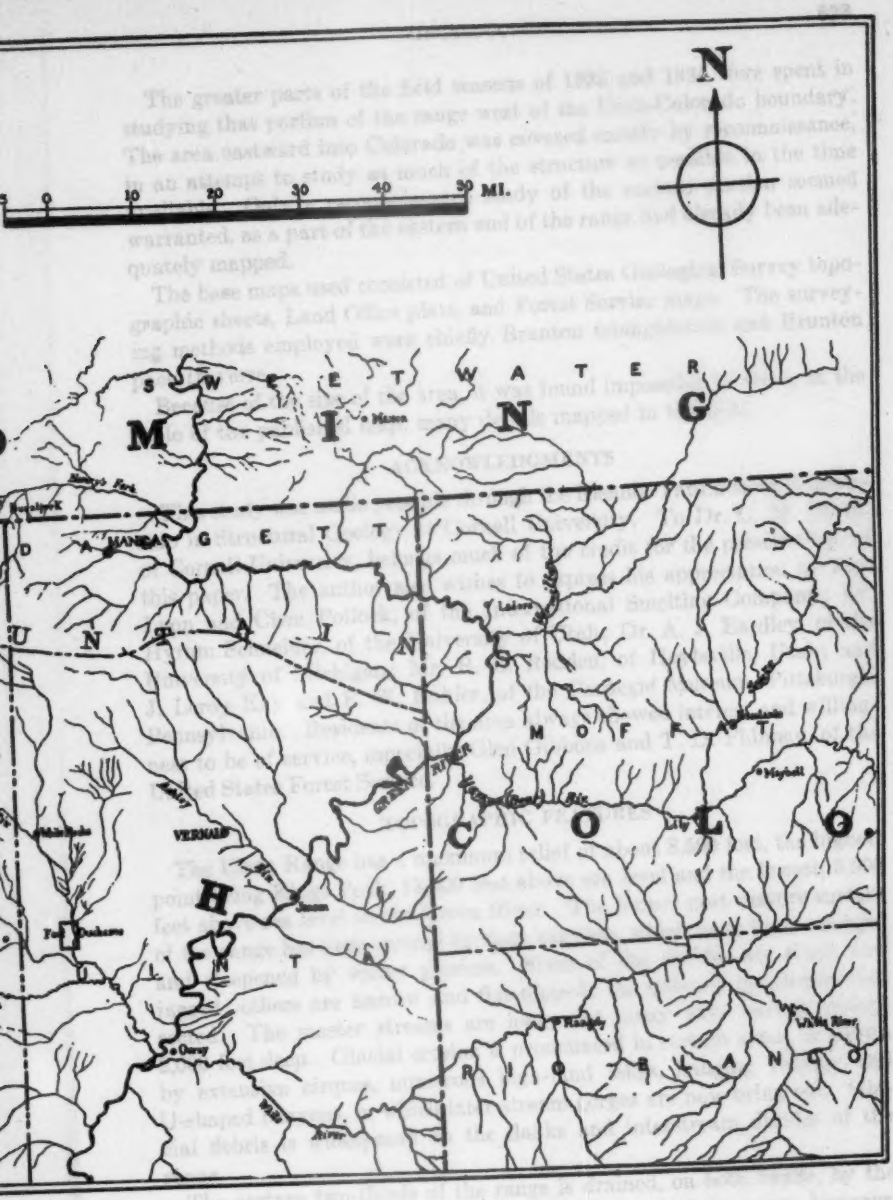
N
0 10 20 30 40 50 MI.
SWEETWATER
MANILA
UINTA
MOFFAT
COLORADO
VERNAL
RIO BLANCO

A MOUNTAINS

The greater parts of the field seasons of 1933 and 1934 were spent in studying that portion of the range west of the Utah-Colorado boundary. The area eastward into Colorado was covered mostly by reconnaissance, in an attempt to study as much of the structure as possible in the time available. Only a reconnaissance study of the eastern portion seemed warranted, as a part of the eastern end of the range had already been adequately mapped.

The base maps used consisted of United States Geological Survey topographic sheets, Land Office plats, and Forest Service maps. The surveying methods employed were chiefly Brunton triangulation and Brunton pace traverse.

Because of the size of the area, it was found impossible to show, on the scale of the published map, many details mapped in the field.

## ACKNOWLEDGMENTS

This study was made possible through the Eleanor Tatum Long Scholarship in Structural Geology at Cornell University. To Dr. C. M. Nevin, of Cornell University, belongs much of the credit for the presentation of this paper. The author also wishes to express his appreciation to Tom Lyon and Clem Pollock, of the International Smelting Company; Dr. Hyrum Schneider, of the University of Utah; Dr. A. J. Eardley, of the University of Michigan; Mr. R. E. Redden, of Hoytsville, Utah; and J. Leroy Kay and F. W. Kohler, of the Carnegie Museum, Pittsburgh, Pennsylvania. Residents of the area always showed interest and willingness to be of service, especially Glen Gibbons and T. D. Phinney, of the United States Forest Service.

## TOPOGRAPHIC FEATURES

The Uinta Range has a maximum relief of about 8,500 feet, the highest point being Kings Peak, 13,500 feet above sea level and the lowest, 5,000 feet above sea level on the Green River. The former post-mature surface of the range has been incised by deep canyons, which have been enlarged and steepened by valley glaciers. Some of the divides are sharp and jagged; others are narrow and flat-topped; the uplands are deeply dissected. The master streams are long, and many have carved valleys 2,000 feet deep. Glacial erosion is pronounced in certain areas, as shown by extensive cirques, numerous high-land lakes, hanging valleys, and U-shaped canyons, in which later stream gorges are now being cut. Glacial debris is widespread on the flanks and interstream divides of the range.

The eastern two-thirds of the range is drained, on both flanks, by the Green River and its tributaries. The western end of the range, however, drains into the Great Basin.

In general, the main divide is slightly north of the center of the range. This divide consists of a broad plateau-like summit area, deeply incised by cirques and steep canyons, with many peaks that rise above the general plateau level. Both north and south of the higher areas the land surface steadily drops off into broad basins of generally low relief. At the western end of the range the hills slope off more steeply into the Kamas Valley. In the eastern portion, there is no well-defined line of high peaks, because the axial portion has been deeply dissected.

## GEOSYNCLINE OF DEPOSITION

### RELATION OF UINTA GEOSYNCLINAL SEDIMENTS TO ROCKY MOUNTAIN SEDIMENTS

Because it has been recognized that mountain-building is generally localized along geosynclinal belts, discussion of orogeny may profitably begin with a consideration of the trough of deposition.

That the Uinta trough, or zone of deposition, was an integral part of the Rocky Mountain geosyncline is shown by the following facts:

(1) The Rocky Mountain area, including the Uinta Mountain region, began receiving sediments at least as early as Algonkian time. These deposits now constitute the widespread, thick Belt Series or its probable equivalents.

(2) The sequence and characteristics of the sedimentary rocks in the Uinta Mountain region are similar to the sedimentary sequence throughout the Rocky Mountain region, and, more significantly, show close similarity to those deposited in the Wasatch Mountain area.

(3) The fact that the Rocky Mountain geosyncline received sediments undisturbed by marked deformation, from the beginning of the Algonkian up to Laramide time, has been well established. Similarly, the Uinta Mountain region was receiving sediments until the end of Cretaceous time. Moreover, the position and magnitude of the unconformities are essentially the same, particularly in Wasatch and Uinta Mountain sections. For instance, the Wasatch Mountain stratigraphy shows an unconformity from Cambrian to Devonian or Mississippian, and the Uinta Mountain section shows a similar break. Field evidence does not agree with Ver Wiebe's [1] suggestion that the Uinta Mountain area was a tectonic high during Cambrian, Pennsylvanian, and Permian times, because formations of these periods have been found.

(4) The Uinta Mountain region is within the borders of the Rocky Mountain trough. Over such a broad area as that encompassed by the Rocky Mountain geosyncline, there must have been variations in sedimentation from time to time. Thus, necessarily, were developed excep-

[1] W. A. Ver Wiebe: *Present distribution and thickness of Paleozoic systems*, Geol. Soc. Am., Bull., vol. 43 (1932) p. 497; maps.

tionally great local thicknesses of sediments or "deeps", which would be defined as troughs, although the adjacent regions may also have been sites of considerable deposition. As illustrated in Figure 1 the Uinta Moun-

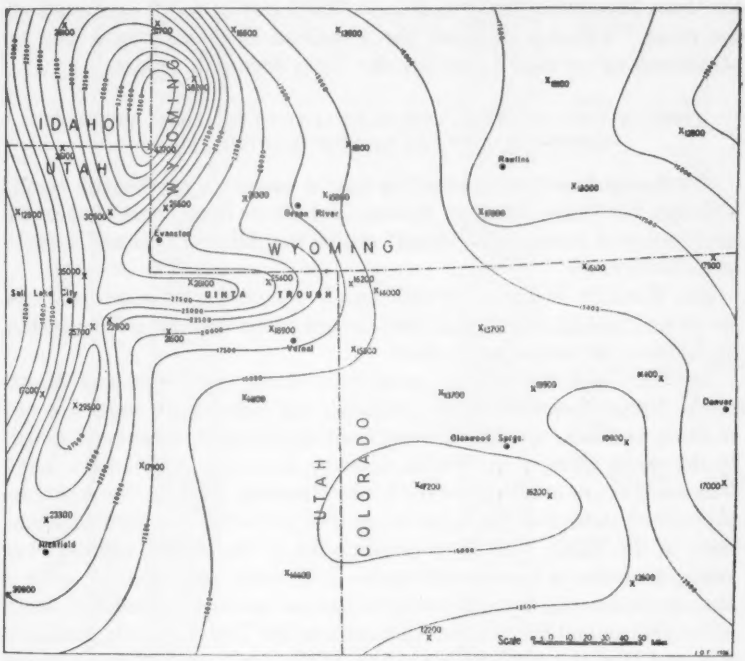


FIGURE 1.—*Isopach map*

Showing thickness of combined Paleozoic and Mesozoic sedimentary sections.

tain area was such a trough within the Rocky Mountain geosyncline at the end of the Cretaceous period. The data used in compiling Figure 1 are based on field work, Ver Wiebe's maps,[2] and United States Geological Survey publications. Although the total sedimentary section involved in the Uinta Mountain folding includes a considerable additional thickness of Algonkian strata, the use of only the Paleozoic and Mesozoic sections in establishing the Uinta Mountain trough is justifiable for the following reasons: (1) The Cordilleran geosyncline was probably in existence during the Proterozoic era and probably in the same position as during Paleozoic time. Therefore, it may here be assumed that the Proterozoic sediments

[2] *Ibid.: Present distribution and thickness of Mesozoic systems*, Geol. Soc. Am., Bull., vol. 44 (1933) p. 827-864.

had essentially the same general distribution as the Paleozoic and thus, if omitted, would not change the present geosynclinal picture. (2) According to most geologists, the thickness of the Algonkian series throughout the central Rocky Mountain region is approximately 12,000 feet. In the Uinta Mountains, however, at least 15,000 feet is present over much of the range. Therefore, if used, the Algonkian thickness would tend to accentuate rather than to shallow the Uinta Mountain trough.

### TREND OF UINTA MOUNTAIN TROUGH RELATIVE TO THE ROCKY MOUNTAIN GEOSYNCLINE AND THE WASATCH MOUNTAIN TROUGH

The Rocky Mountain geosyncline has, in general, a north-south trend, although Ver Wiebe, Lawson, Heaton, and others have noted changes in the position of many of its "deeps" during the different eras and periods of its history.

The Wasatch Mountain trough trends roughly north-south and, as shown by Figure 1, represents a well-defined "deep" in total section within the limits of the major geosyncline.

The Uinta Mountain "deep", on the other hand, trends east-west. North of the Uinta Mountain trough, although the sedimentary units are not so thick, the same general lithology and stratigraphic breaks are noted. In the region south of the Uintas, however, several geologists have noted features that are not found in the Uinta Mountain section. For example, Schneider [3] states that the log of an oil well, drilled by the Utah Oil Company in the Moab, Utah, region (125 miles to the south), showed Mississippian rocks in contact with rocks of Archean age. Butler [4] notes a stratigraphic break from Mesozoic formations to the pre-Cambrian, south of the Denver and Rio Grande Railroad near the Utah-Colorado boundary line, and Heaton postulates land areas to the south and southeast during much of the Paleozoic. These statements clearly establish a high land area south of the Uinta Mountain region during much of the time when the Uinta Mountain trough was receiving sediments.

The fact that the Uinta trough is really an arm of the Wasatch trough is demonstrated by the following facts, especially if taken in conjunction with thickness relationships as shown in Figure 1:

(1) Sediments of the Uinta and the Wasatch mountain areas, where the two regions join, are individually, and as a group, lithologically similar.

(2) The stratigraphic section in the Wasatch Mountain region thins rapidly eastward both north and south of the Uinta Range, but, where the Wasatch and the Uinta troughs join, this rate of eastward thinning is much lessened.

---

[3] Hyrum Schneider: *Personal communication* (1933).

[4] B. S. Butler, *et al.: The ore deposits of Utah*, U. S. Geol. Surv., Prof. Paper 111 (1920) p. 80.

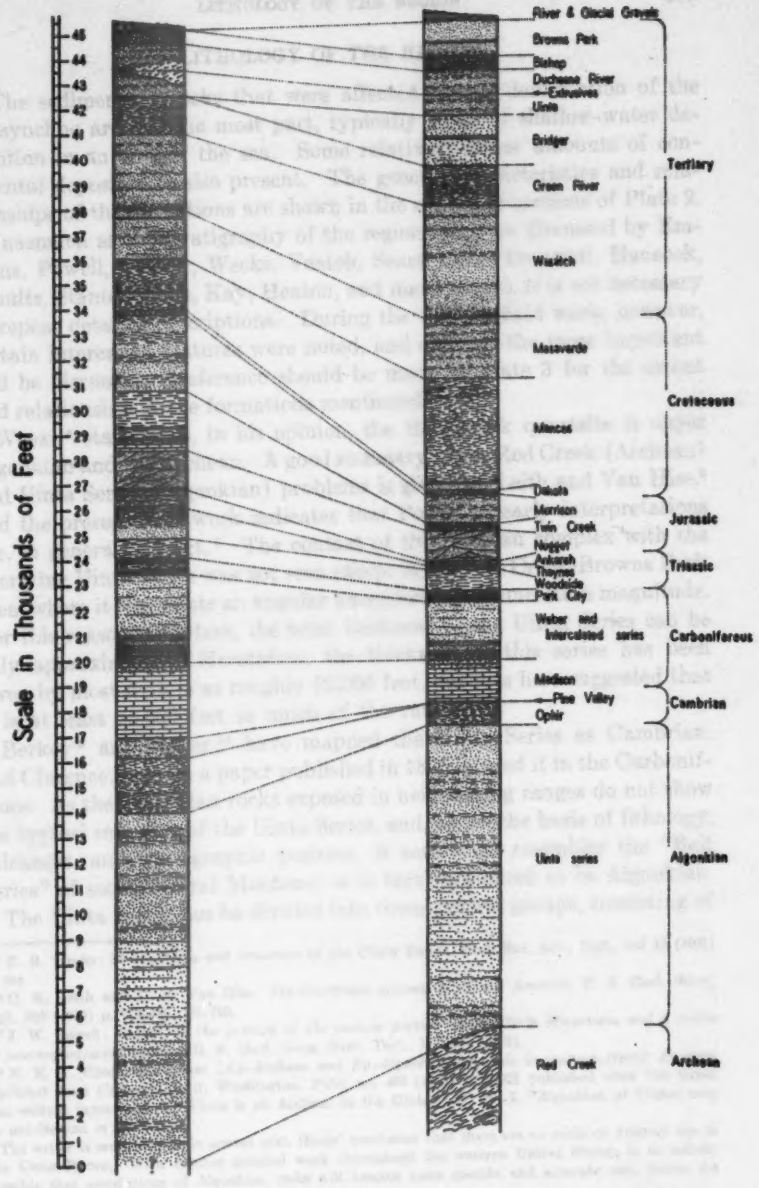


COMPOSITE GEOLOGIC COLUMNAR SECTIONS OF THE UINTA MOUNTAINS

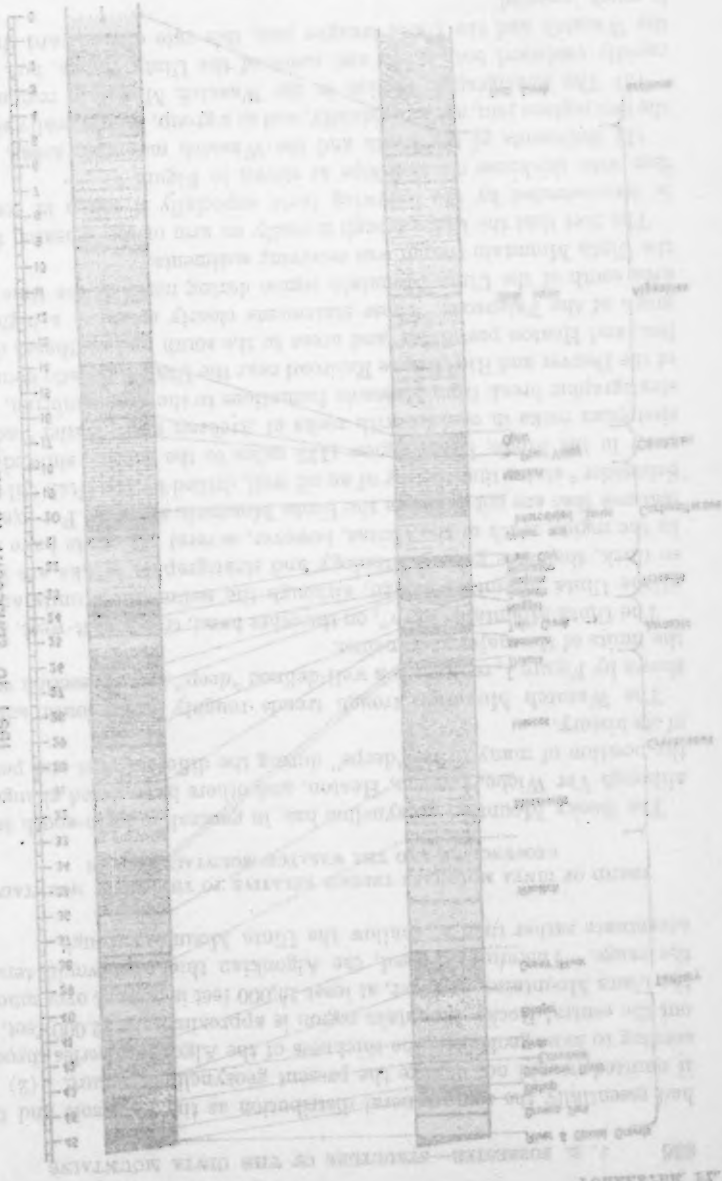
scale in thousands of feet

## LITHOLOGY OF THE REGION

The sedimentary rocks that were affected by the deformation of the geosyncline are, for the most part, typically those of shallow-water deposition in an arm of the sea. Some relatively minor amounts of continental deposits are also present. The general characteristics and relationships of the formations are shown in the columnar sections of Plate 2.

Inasmuch as the stratigraphy of the region has been discussed by Emmons, Powell, Berkey, Weeks, Veatch, Sears, Gale, Boutwell, Hancock, Schultz, Stanton, Rich, Kay, Heaton, and many others, it is not necessary to repeat detailed descriptions. During the writer's field work, however, certain interesting features were noted, and of these the more important will be discussed. Reference should be made to Plate 3 for the extent and relationship of the formations mentioned.

Weeks [5] states that, in his opinion, the Red Creek quartzite is upper Algonkian and not Archean. A good summary of the Red Creek (Archean) and Uinta Series (Algonkian) problems is given by Leith and Van Hise,[6] and the present field work indicates that Powell's [7] early interpretations are, in general, correct. [8] The contact of the Archean complex with the overlying Uinta Series was not seen except in the Red Creek-Browns Park area, where it represents an angular unconformity of uncertain magnitude. For this reason, therefore, the total thickness of the Uinta Series can be only approximated. Heretofore, the thickness of this series has been given by most writers as roughly 12,000 feet, but it is here suggested that it is at least 15,000 feet in much of the range.

Berkey [9] and Butler [10] have mapped the Uinta Series as Cambrian, and Clarence King, in a paper published in 1876, placed it in the Carboniferous. As the Cambrian rocks exposed in neighboring ranges do not show the typical red color of the Uinta Series, and, as, on the basis of lithology, thickness, and stratigraphic position, it somewhat resembles the "Belt Series" of south-central Montana; it is here considered to be Algonkian.

The Uinta Series can be divided into three general groups, consisting of

---

[5] F. B. Weeks: *Stratigraphy and structure of the Uinta Range*, Geol. Soc. Am., Bull., vol 18 (1907) p. 444.

[6] C. K. Leith and C. R. Van Hise: *Pre-Cambrian geology of North America*, U. S. Geol. Surv., Bull. 360 (1909) p. 779-780, 789-790.

[7] J. W. Powell: *Report on the geology of the eastern portion of the Uinta Mountains and a region of country adjacent thereto*, U. S. Geol. Geog. Surv. Terr., II Div. (1876).

[8] N. E. A. Hinds in a paper [*Ep-Archean and Ep-Algonkian intervals in western North America*, reprinted from Carnegie Instit. Washington, Publ. no. 463 (1935) p. 1-52] published since this paper was written notes that, 1. "There is no Archean in the Uintas", p. 13; 2. "Algonkian of Uintas may be pre-Beltian in age", p. 7.

The writer is certainly not in accord with Hinds' conclusion that there are no rocks of Archean age in the Uinta Range. With further detailed work throughout the western United States, it is entirely possible that correlations of Algonkian rocks will become more specific and accurate and, hence, the Uinta Series may indeed be found to be pre-Beltian.

[9] C. P. Berkey: *Stratigraphy of the Uinta Mountains*, Geol. Soc. Am., Bull., vol. 18 (1907) p. 529-530.

[10] B. S. Butler: *op. cit.*, pl. iv.

lower and upper red units, separated by a relatively light, buff zone. This sequence shows to best advantage on the divide area in the vicinity of Mount Lovenia and Hayden Peak. Numerous beds of black, carbonaceous shale are intercalated in the series and thus give evidence of the presence of vegetation at the time of deposition. Gradations from true quartzite to sandstone may be seen throughout the range, and in many places the quartzitic beds directly overlie the sandstone layers. Probably, these variations are the result of changes in the degree and type of cementation. Near the top of these Algonkian sediments the beds become arkosic.

Powell [11] reported an unconformity between the Uinta Series and his Lodore group in the eastern part of the range. If such an unconformity is present, it must be small, for it was not noted in the western portion. Hintze [12] suggests an unconformity between the Cambrian and the pre-Cambrian; he places approximately 1,000 feet of the upper Uinta Series in the Cambrian. If such a division were followed, it would tend to give a greater thickness to the Paleozoic sediments than is used in this discussion.

The Lodore shale of Powell is here tentatively correlated with the Ophir shale of the Oquirrh Mountains, to which it is lithologically similar. It ranges up to 3,000 feet in thickness. Berkey's [13] measurement of 3,000 feet at Iron Creek on the North Fork of the Duchesne River was substantiated by present field work; whereas, the thickness given by Weeks [14] for the same locality is far too small.

Conformably overlying the Ophir shale is the so-called Ogden (Ordovician) quartzite of Weeks. The type Ogden is now known to be older rocks repeated by faulting. Although no fossils were found in this formation, it is thought to be of Cambrian age. Because of its good exposure in Pine Valley near Stewart's Ranch on the Provo River, the name Pine Valley quartzite is here proposed. Weeks [15] has given a description of it. The formation varies in thickness up to approximately 1,200 feet, and, in general, it tends to pinch out gradually to the eastward. Weeks stated that it is absent on the north flank of the range, but the writer found it well developed there in several places. It was seen in discontinuous exposures as far east as Blacks Fork of the Green River.

Between the Cambrian formations just described and the Mississippian limestones, with which they are in contact, there is a well-defined angular unconformity, which may be seen in several places throughout the range and to especially good advantage in Pine Valley near Stewart's Ranch

[11] J. W. Powell: *op. cit.*, p. 144.
[12] F. F. Hintze: *The Proterozoic-Paleozoic contact in the western Uinta and central Wasatch Mountains, Utah*, Utah Acad. Sci., Pr., vol. 11 (1934) p. 166.
[13] C. P. Berkey: *op. cit.*, p. 521.
[14] F. B. Weeks: *op. cit.* p. 436.
[15] *Op. cit.*, p. 437.

and in Whiterocks Canyon, north of Whiterocks Point. This unconformity, representing an extensive erosional interval, explains the marked thinning or absence of Cambrian formations in many places, particularly in the eastern portion of the range. Indeed, in some places, Mississippian limestone is in contact with the Uinta Series (pre-Cambrian). The marked unconformity may possibly be correlated with the late Canadian stratigraphic break mentioned by Ver Wiebe.[16]

The Mississippian formations, because of their lithologic and stratigraphic characteristics, are here considered as the equivalent of the Madison limestones of the Wasatch Range. Berkey [17] mentions an unconformity between the Madison limestone and the Pennsylvanian sediments. Although the writer made a careful search, he found no evidence in the field to support this suggestion, and other writers [18] have also failed to find it.

The sediments overlying the Mississippian limestones are Pennsylvanian in age, and although Fenneman [19] speaks of Mississippian quartzites, he surely must have meant Pennsylvanian, inasmuch as there are no Mississippian quartzites in the Uintas. Pennsylvanian formations are exposed in the Daniels Canyon-Strawberry area and, indeed, can be traced over much of the range.

No unconformities either above or below the Park City (Permian) formation were found. Schultz [20] gives a good description of this formation.

Next in stratigraphic sequence are the Woodside shale, the Thaynes formation, and the Ankareh shale. These formations are all included in the Triassic and, because of a marked thinning eastward, have been grouped as one unit on the areal map and in some of the cross sections.

Separating the Ankareh and the Nugget (Jurassic) formations is a light-gray sandstone of varying thickness. This member has evidently been noted by Boutwell [21] in the Park City district of the Wasatch Range. In the Uinta Mountain area, it is best exposed in the western portion.

Wherever it is exposed, the cross-bedded, wind-laid Nugget sandstone is an excellent horizon marker throughout the Uinta Range. The formation thins eastward and gradually changes from a marked red in the western area to a buff or cream-color farther east.

Conformably overlying the Nugget sandstone is the Twin Creek (Juras-

[16] W. A. Ver Wiebe: *Oil fields in the United States*, 1st ed. (1930) p. 443, McGraw-Hill Co.
[17] C. P. Berkey: *op. cit.*, p. 524.
[18] S. F. Emmons: *Uinta Mountains*, Geol. Soc. Am., Bull., vol. 18 (1907).
F. B. Weeks: *op. cit.*, p. 442.
A. R. Schultz: *A geologic reconnaissance of the Uinta Mountains, northern Utah, with special reference to phosphate*, U. S. Geol. Surv., Bull. 690-C (1918) p. 46.
[19] N. M. Fenneman: *Physiography of western United States* (1931) p. 178. McGraw-Hill.
[20] A. R. Schultz: *op. cit.*, p. 46-54.
[21] J. M. Boutwell: *Geology and ore deposits of the Park City district, Utah*, U. S. Geol. Surv., Prof. Paper 77 (1912) p. 58.

sic) formation. Because of thinning to the eastward, identification of this series becomes difficult.

The Morrison formation, tentatively placed in the upper Jurassic, is well exposed along the flanks of the range.

At the base of the Cretaceous formations is the persistent Dakota conglomerate. As determined by Boutwell [22] on the Weber River north of Peoa, the Dakota represents a conglomeratic member of the Morrison formation.

In the Aspen or Mowry shale, Cycloid scales of Teleost fishes have been observed by several writers.[23] These good index fossils were used in the course of this field work for purposes of correlation. The sediments overlying the fish-scale horizon have been described under the names of Frontier and Mancos formations.

That the Frontier of the western part of the area and the Mancos of the eastern part are equivalent deposits and merely represent different facies is substantiated by: (1) Their stratigraphic position above the Aspen or Mowry fish-scale horizon, and, (2) the fact that, inasmuch as the Cretaceous sediments of this region were all brought in from the west, it is to be expected that the sandy Frontier would be the western equivalent of the more shaly Mancos. In fact, the sandy Mesaverde formation, which immediately overlies the Mancos on the east, grades imperceptibly, to the west, into the upper part of the Frontier. On the other hand, as these formations are traced farther southeastward, the Mesaverde thins as the underlying shaly Mancos thickens.

The Mesaverde represents the uppermost Cretaceous deposits outcropping in the Uinta Mountain region, whereas, according to Sears,[24] still younger sediments (Laramie) are found in the Axial Basin.

In the Coalville area, on all relatively recent maps, no sediments older than the Frontier are shown. However, the index fish-scales of the Aspen were found in section 7, T. 2 N, R. 6 E, overlying the Dakota and the "terra cotta" beds of the misnamed Frontier (Pl. 3). This indicates that these "terra cotta" beds are, in reality, a part of the Morrison formation; in fact, beds of this character are rather common in typical Morrison of the Uinta Mountain region. Stanton [25] evidently reached a similar

[22] J. M. Boutwell: *The Salt Lake region*, 16th Internat. Geol. Congr., Guidebook 17, Exc. C-1, (1933) p. 62.

[23] T. W. Stanton: *Colorado formation and its invertebrate fauna*, U. S. Geol. Surv., Bull. 106 (1893) p. 44.

A. C. Veatch: *Geography and geology of a portion of southwestern Wyoming, with special reference to coal and oil*, U. S. Geol. Surv., Prof. Paper 56 (1907) p. 64.

J. D. Sears: *Geology and oil and gas prospects of part of Moffat county, Colorado, and southern Sweetwater county, Wyoming*, U. S. Geol. Surv., Bull. 751-G (1924) p. 286.

C. T. Lupton: *The Deep Creek district of the Vernal coal field, Uinta county, Utah*, U. S. Geol. Surv., Bull 471 (1912) p. 585.

[24] J. D. Sears: *op. cit.*, p. 291-292.

[25] T. W. Stanton: *op. cit.*, p. 38, 44.

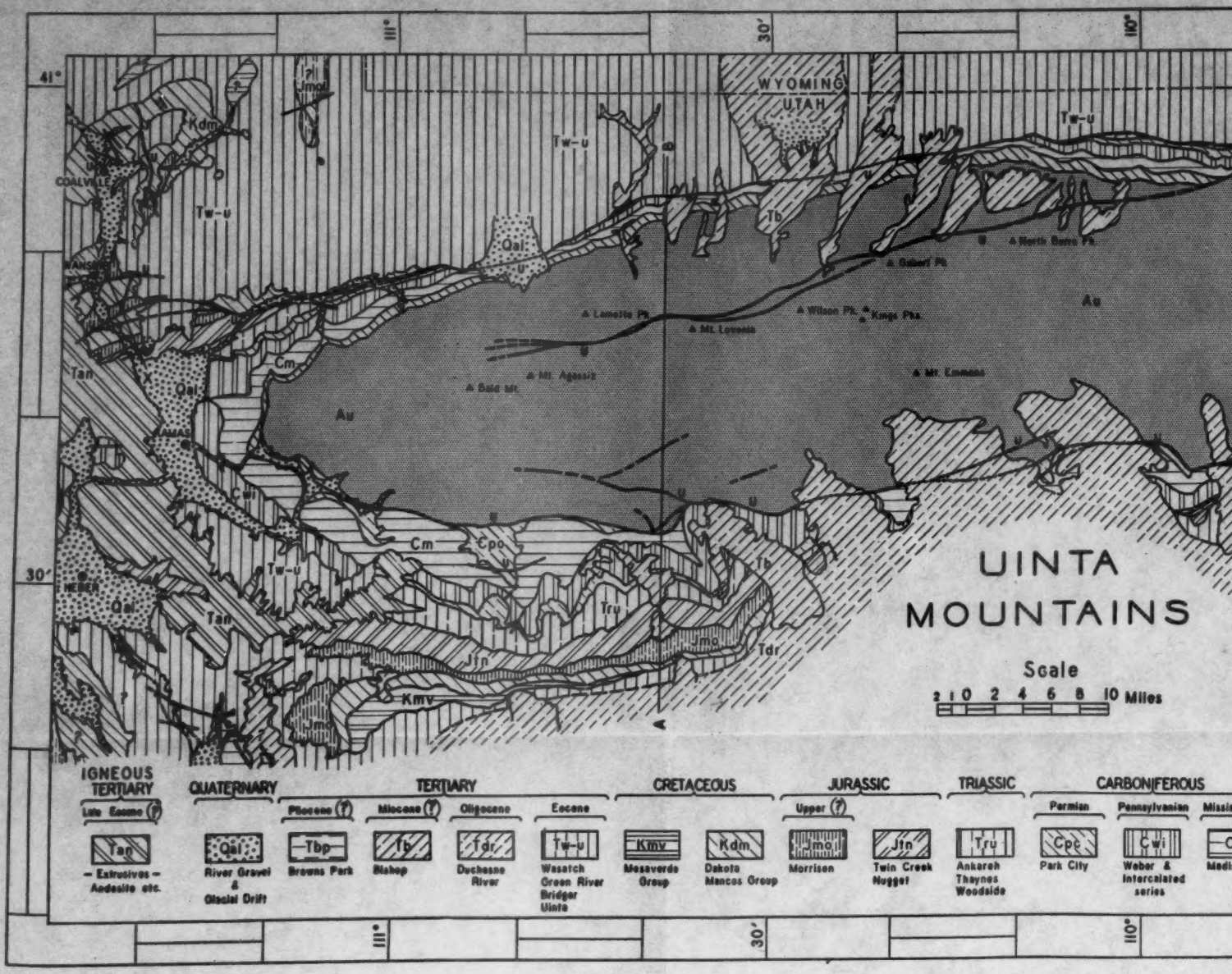


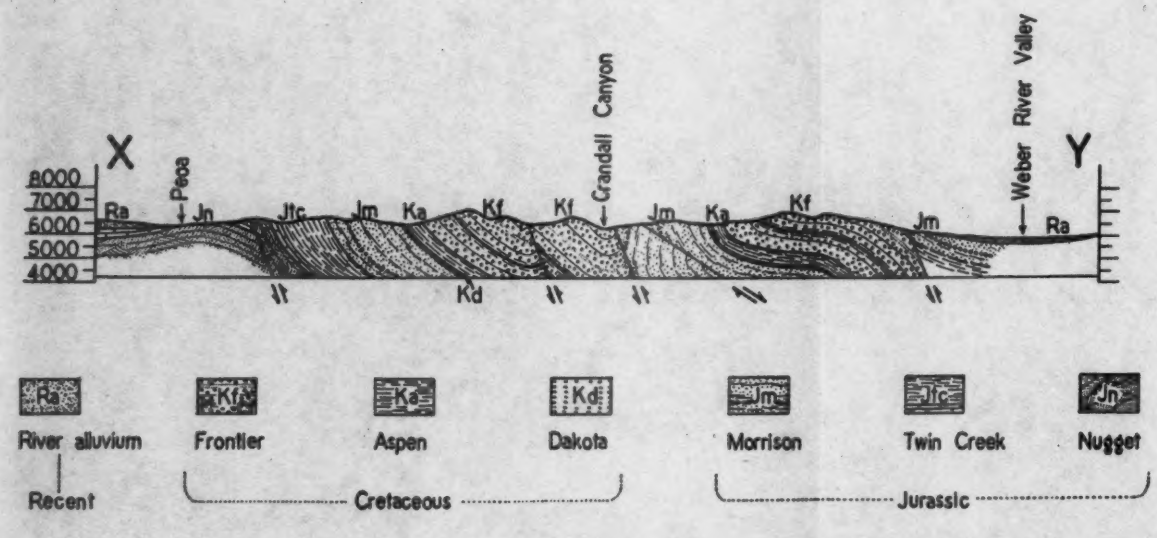


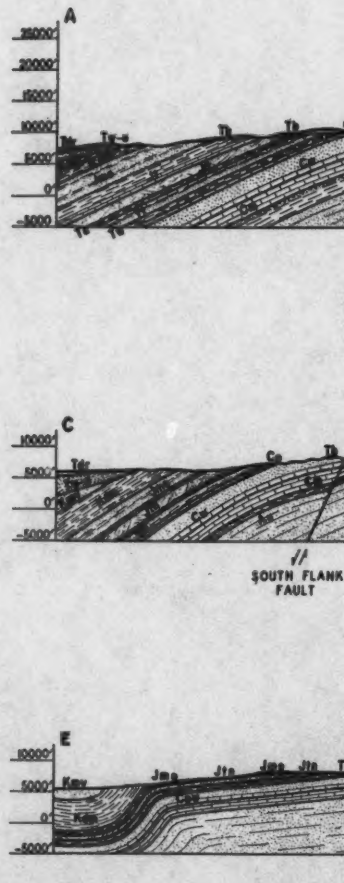


AREAL GEOLOGY AND STRUCTURE SE

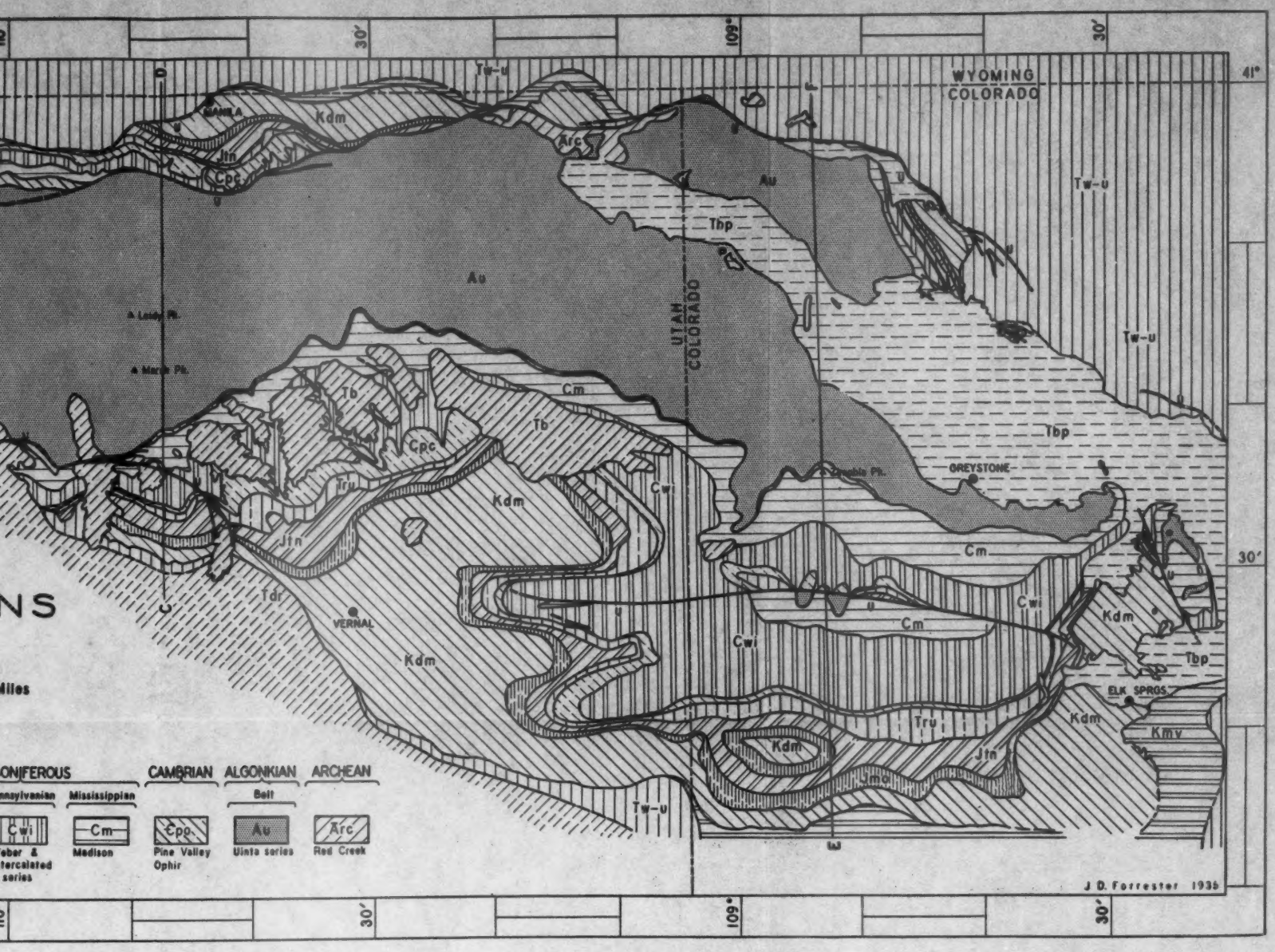


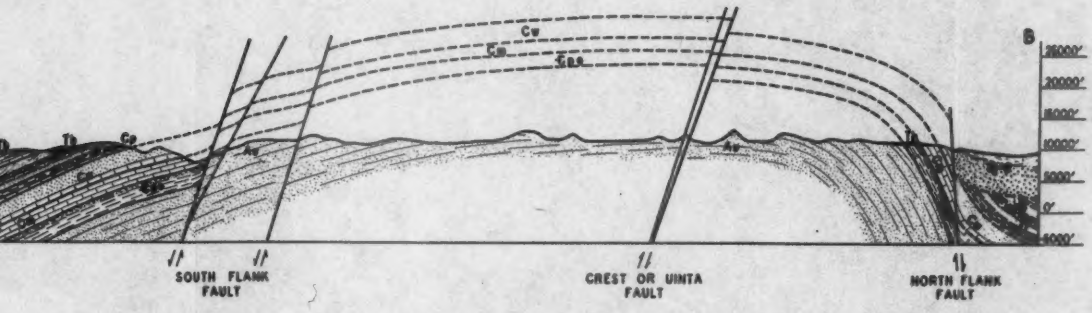


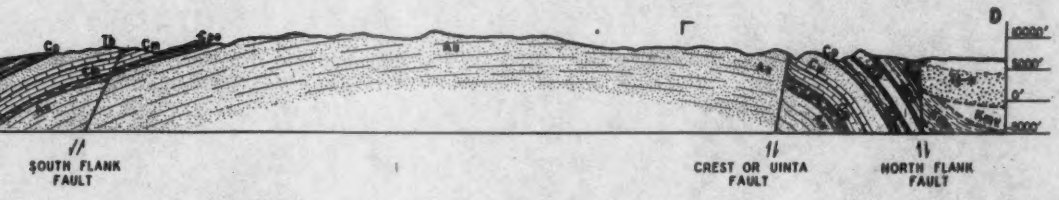


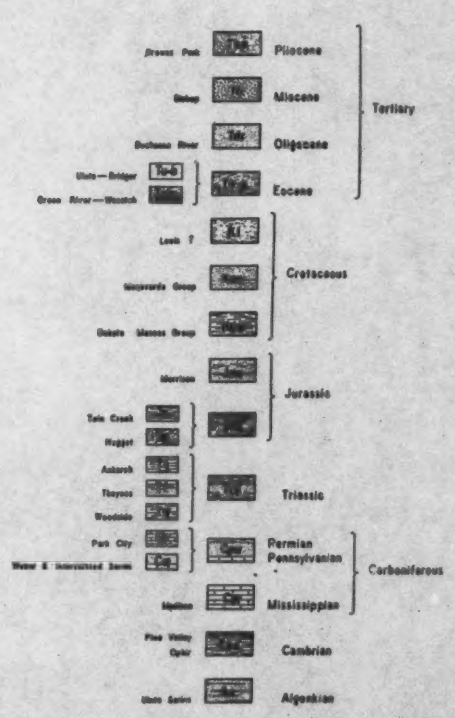


Scale — Feet

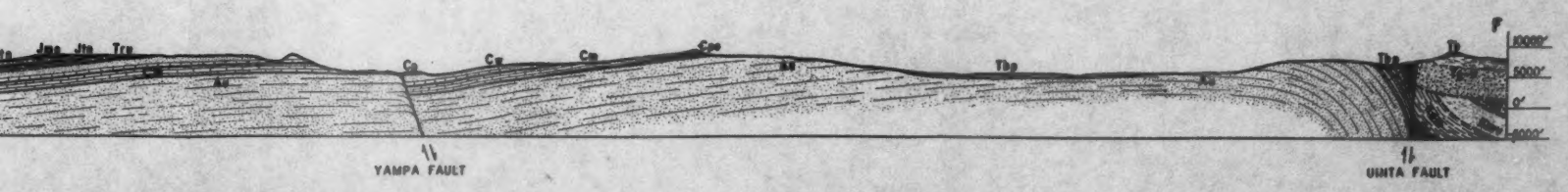


RUCTURE SECTIONS OF THE UINTA MOUNTAINS

conclusion in 1893. Because of these apparently incorrect interpretations of the stratigraphy, too great a thickness has previously been assigned to the Frontier in the Coalville area and along the Weber River from Peoa to Wanship, Utah.

Wasatch (Eocene) sediments, wherever exposed, are unconformable on Mesaverde and older formations in the Uinta Range. In the Axial Basin region, however, Eocene sediments older than Wasatch have been mapped by Sears.[26] Interpretations of the relations between the Tertiary formations have varied considerably. For instance, Lupton [27] reported 10,000 feet of Wasatch overlying Cretaceous beds on the North Fork of the Duchesne River, whereas Kay [28] concludes that the thickness is much less. In this paper, Kay's interpretations of the Tertiary rocks along the south flank have been followed. Along much of the north flank of the range, the Green River and the Bridger formations of the Eocene are the lowest Tertiary sediments exposed. Duchesne River (Oligocene) sediments were not found on the north flank of the range. Where the Duchesne River sediments extend farthest north, across the older rocks along the south flank, the sediments were evidently deposited in an old drainage channel coursing at right angles to the axis of the range. This valley was previously developed between the lateral limits of Rock Creek on the west and Whiterocks Creek on the east. The source of these Oligocene beds was from the central portion of the Uinta uplift, inasmuch as the sediments were derived from formations younger than those now exposed along the crest.

There has been considerable speculation concerning the origin and relationship of the Bishop conglomerate and the Browns Park formation. Powell [29] placed the Browns Park sediments stratigraphically below the Bishop conglomerate. Sears [30] states that they represent similar time deposition, but later field work by Bradley [31] indicates that the Bishop conglomerate is considerably older than the Browns Park beds. Bradley's interpretation has been accepted in this mapping. Schultz [32] maps Bishop conglomerate on Phil Pico Mountain, which is near Manila, Utah, but the writer's field work shows that this mountain is chiefly made up of conglomeratic facies of the Green River and the Bridger formations.

Extrusive igneous rocks, chiefly andesites and agglomerates, are found

[26] J. D. Sears: *op. cit.*, p. 292.

[27] C. T. Lupton: *The Blacktail (Tabby) Mountain coal field, Wasatch county, Utah*, U. S: Geol. Surv., Bull. 471 (1912) p. 607.

[28] J. L. Kay: *The Tertiary formations of the Uinta Basin, Utah*, Carnegie Mus., Ann., vol. 23 (1934) p. 359.

[29] J. W. Powell: *Report on the geology of the eastern portion of the Uinta Mountains and a region of country adjacent thereto*, U. S. Geol. Geog. Surv. Terr., II Div. (1876) p. 168-169.

[30] J. D. Sears: *Relations of the Browns Park formation and the Bishop conglomerate, and their rôle in the origin of Green and Yampa rivers*, Geol. Soc. Am., Bull., vol. 35 (1924) p. 284.

[31] W. H. Bradley: *oral communication* (1934).

[32] A. R. Schultz: *A geologic reconnaissance of the Uinta Mountains, northern Utah, with special reference to phosphate*, U. S. Geol. Surv., Bull. 690-C (1918) pl. v.

in the extreme western end of the Uinta Mountain region. That these extrusions covered a somewhat irregularly eroded surface can be seen in the Weber River area near Peoa, Utah, and on Lake Fork Creek fork of the Provo River southeast of Heber City, Utah. Formations mapped as Bishop conglomerate by Schultz on Wolf Creek Peak are definitely extrusive materials.

The flows cover lower Eocene sediments and are older than Miocene. They are, therefore, placed in late Eocene and early Oligocene time, which is essentially in accord with conclusions reached by Dutton,[33] Butler,[34] and Boutwell.[35] From the nature of the extrusives, they appear to be genetically related to the intrusive rocks of the central Wasatch Mountain region, with which they are essentially contemporaneous.

No intrusive rocks were found in the Uinta Range, although Beeson [36] reports an outcrop of intrusive rock near the headwaters of the South Fork of the Weber River. Unfortunately, deep snow made this area inaccessible at the time the writer was in that vicinity.

Pleistocene glacial drift and debris mask much of the underlying structure in the Uinta Range, and it is often difficult to separate later deposits from the older Tertiary sediments. River gravels and valley alluvium, which cover wide areas, have been only locally mapped.

## STRUCTURAL FEATURES

### FOLDING

As structural relationships of the Uintas and adjacent areas may be obtained from the maps and sections accompanying this paper, only the outstanding features will be considered in detail.

The Uinta Mountain structure is, in general, a broad, open anticline, somewhat overturned and arcuate to the north. The axis trends roughly east-west over much of the range, and pitches to the southeast toward Cross Mountain and to the west southwest into Kamas Valley, and continues under the extrusive flows of the West Hills, which separate the Uinta and the Wasatch ranges. The exact point of reversal in the pitch is indefinite, inasmuch as there are many minor warps along the axis, but it is certain that this point lies much nearer the western end of the range. Considering the length of the Uinta Mountains as extending from Kamas, Utah, to Cross Mountain, Colorado, the reversal is at a point approximately a third of the length from the western end.

---

[33] C. E. Dutton: *Report on the geology of the high plateaus of Utah*, U. S. Geol. Geog. Surv. Rocky Mtn. Reg. (1880) p. 55.

[34] B. S. Butler, *et al.: The ore deposits of Utah*, U. S. Geol. Surv., Prof. Paper 111 (1920) p. 99.

[35] J. M. Boutwell: *Geology and ore deposits of the Park City district, Utah*, U. S. Geol. Surv., Prof. Paper 77 (1912) p. 70, 93-94.

[36] J. J. Beeson: *personal communication* (1934).

A notable re-entrant of the Paleozoic formations into the axial region north of Vernal, Utah, results from a lessening pitch and the low dips of the rocks in that locality.

Throughout the range, there are many minor folds, which are, as a rule, numerous and particularly well developed along the flanking portions. On the flanks, these minor folds, in general, tend to lie parallel to the major axis of the range. In the vicinity of Manila, Utah, there are several folds that change their trend from northwest to northeast and back to northwest again. Where the formations strike northwest, the dip is usually steep to the northeast, but where they strike northeast the dip is gentle to the northwest.

West of the Uintas, the major axis can be traced into the Wasatch Range, although the direction of pitch reverses, and a syncline lies between the two ranges. At the junction of the Uinta and the Wasatch ranges the usual north-south-striking formations of the Wasatch Mountains swing to a more or less east-west strike. The structure in the Wasatch Range where the Uinta Range axis crosses it is, therefore, unusual and quite complex.

In the Daniels Canyon-Strawberry area (5) [87] is a northwestward-trending fold, which is midway between the trend of the Uinta Mountain folds and those in the Wasatch Mountains. The formations may be readily traced along the strike, from a place where they exhibit the typical east-west Uinta trend to the point where they take this resultant northwest trend. West of this area, within the Wasatch Range, the strikes of the folds gradually swing into the normal north-south Wasatch Mountain type.

The Split Mountain-Yampa Plateau area (6) shows true Uinta Mountain structural trends, and represents supplementary anticlinal structures on the major Uinta Mountain fold. In the vicinity of Jensen, Utah, they appear as two noses pitching rather abruptly westward into the Ashley or Vernal Valley.

In the Coalville-Weber River region (3), on the north flank of the Uintas, the structure is a trend type similar to that in the Strawberry-Daniels Canyon area on the south flank of the range. The Weber River section from Peoa to Wanship shows distinct east-west Uinta Mountain type folding trends, which swing rather sharply, as the Coalville section is approached, to Wasatch Mountain north-south trends. The anticlinal folding was intense at Coalville, and the Morrison formation is exposed along the axis of the major fold.

In the Porcupine Mountain area (2), the formations trend generally north-south. This region is too far north of the Uinta Mountain struc-

[87] These numbers refer to the locality index of Plate 4.

ture for east-west trends. Although no closer to the Wasatch Range, the trend is that of the Wasatch Mountain type, which is predominant in this part of the Rocky Mountains.

The Rock Springs (12) uplift, for the most part, has a similar north-south trend. Southward, toward the Uinta Range, however, there is a tendency for the axes of the folds to swing eastward, and thus take a Uinta Mountain trend.

Cross Mountain (11) is an elongated dome at the extreme eastern end of the Uinta Range and evidently represents a Uinta Mountain structural type, for its axis is practically coincident with the Uinta Mountain axis.

### FAULTING

*South Flank Fault.*—The Uinta Range is cut by many major strike fault zones. As a rule, the faults in these zones dip steeply and in some places resemble *en echelon* fractures. Within the faulted areas, the beds adjacent to the faults have been dragged so that the dips are abnormally steep.

The South Flank Fault (Pl. 4, c) is, in reality, a fault zone with numerous splits. It was first reported by Berkey [38] at Iron Creek on the North Fork of the Duchesne River and was named by him the Iron Creek Fault. Berkey traced it approximately 14 miles and regarded it as a normal fault, with the south block downthrown. On Rock Creek, east of the North Fork of the Duchesne River, Weeks [39] observed this fault and described it as a thrust fault. Other writers [40] have observed faults along the south flank of the range in this same general zone; Emmons [41] suggests that it is not so important as Berkey thought.

Although the south flank is widely covered by later sediments, the fault zone is traceable in several canyons, from Upper Soapstone Creek on the west to Little Mountain on the east, a distance of approximately 70 miles. The south side is the downthrown side, and, wherever measured, the dip of the fault is steep (55 to 70 degrees) to the south. The sinuosity of the fault trace on the map is not primarily the result of topography but is caused by variations in the strike of the fault. On Whiterocks Creek, the structure is involved, and Schultz,[42] in reconnaissance, evidently misinterpreted it. The fault described by him as striking northeasterly, in reality, strikes northwesterly. To the east, the throw diminishes as the

[38] C. P. Berkey: *Stratigraphy of the Uinta Mountains*, Geol. Soc. Am., Bull., vol. 16 (1905) p. 523.

[39] F. B. Weeks: *Stratigraphy and structure of the Uinta Range*, Geol. Soc. Am., Bull., vol. 18 (1907) p. 443.

[40] S. F. Emmons: *Uinta Mountains*, Geol. Soc. Am., Bull., vol. 18 (1907) p. 297.

A. R. Schultz: *A geologic reconnaissance of the Uinta Mountains, northern Utah, with special reference to phosphate*, U. S. Geol. Surv., Bull. 690-C (1918) p. 66-67.

[41] S. F. Emmons: *op cit.*, p. 297.

[42] A. R. Schultz: *op cit.*, p. 67.

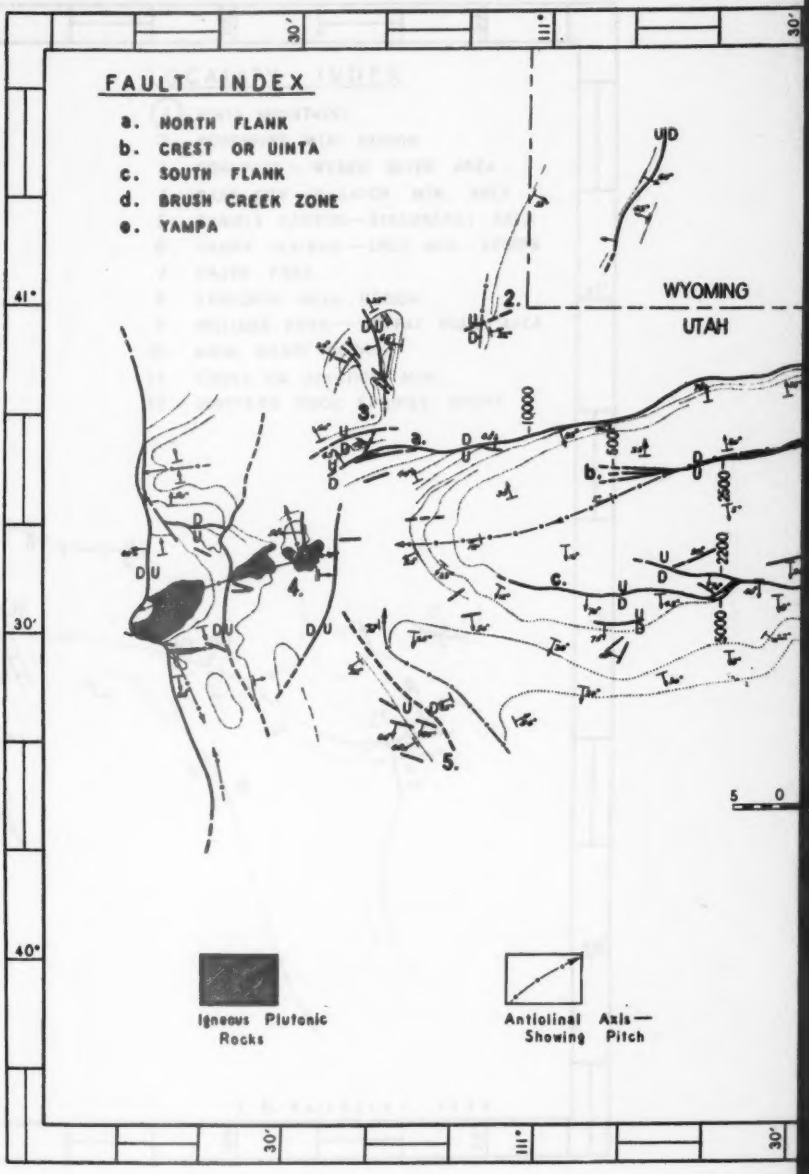
FAULT INDEX
a. NORTH FLANK
b. CREST OR UINTA
c. SOUTH FLANK
d. BRUSH CREEK ZONE
e. YAMPA
WYOMING
UTAH
111°
30'
41°
40°
10000
6000
2500
2200
3000
5 0
Igneous Plutonic Rocks
Anticlinal Axis— Showing Pitch

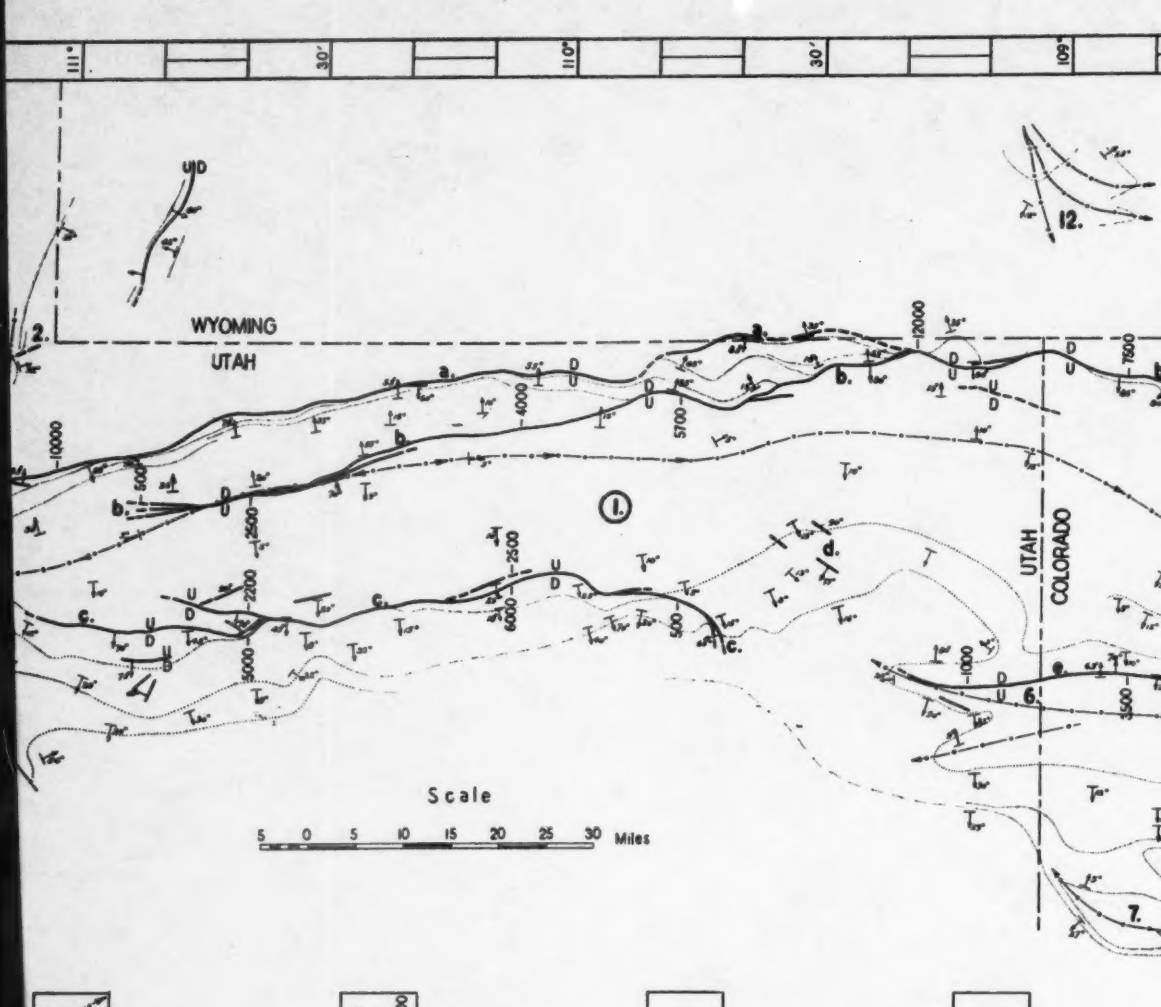


REGIONAL STRUCTURAL RELATIONSHIPS IN THE UINTA MOUNTAINS

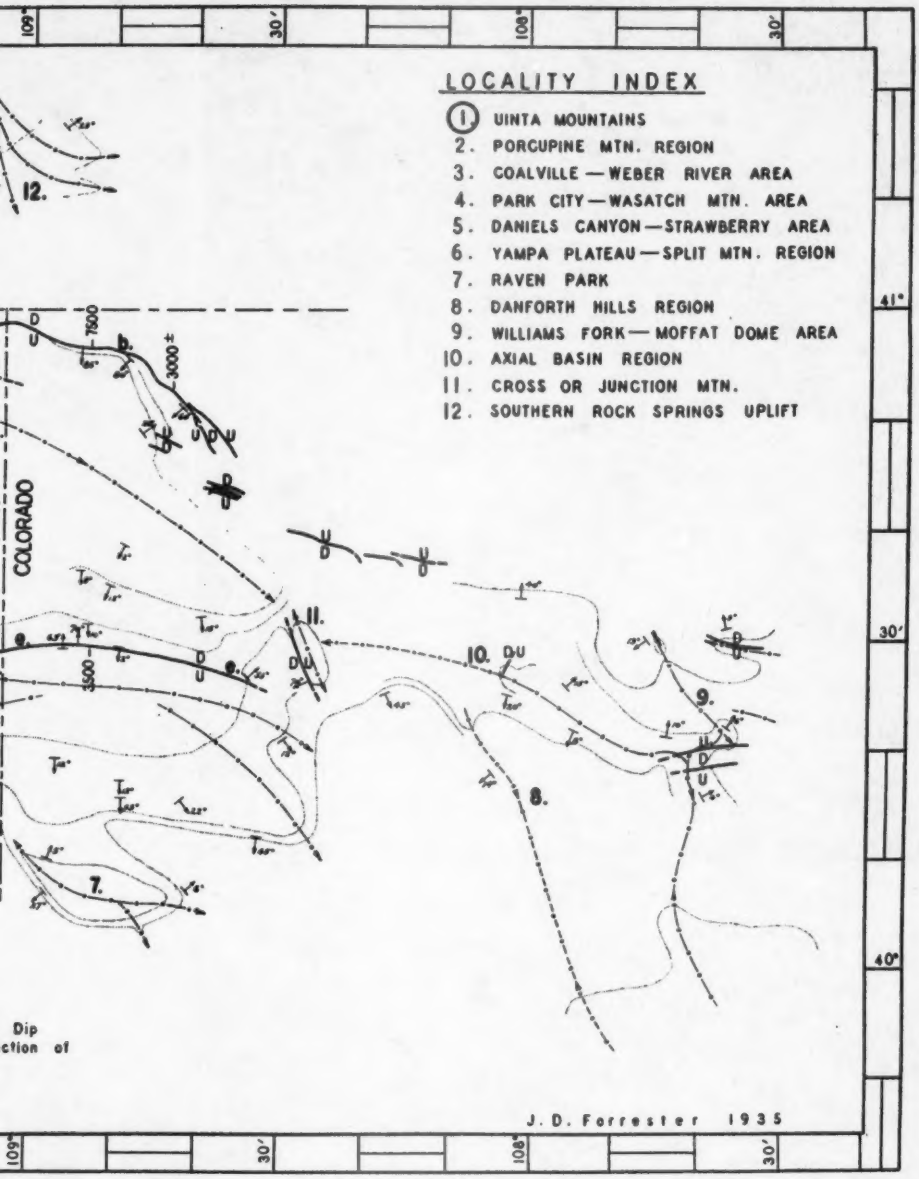


Dip
ction of

AINS

strike swings southeastward, and the fault disappears under Little Mountain. Usually, the stratigraphic throw is somewhat decreased by dragging of the formations on both sides of the fault.

*Brush Creek Zone.*—Shearing was observed in Upper Brush Creek and Ashley Creek areas and, in this paper, has been designated the Brush Creek Shear Zone (d). Displacements appear to be of small magnitude. Schultz [43] reported fracturing in this same general vicinity. Near this zone, many of the streams of the area disappear into solution channels in the Mississippian limestones; these channels are probably localized along fracture zones.

*Yampa Fault.*—The Yampa Fault (e), first described by Powell,[44] may be observed in the gorge of the Yampa River, west of Lily Park, Colorado. The river meanders, apparently without regard to the position of the fault. The fault dips steeply (70 degrees) to the north, and strikes in general east-west, although the trend swings to the northwest as the throw decreases in Split Mountain Canyon. The north block is the side downthrown.

*Uinta or Crest Fault.*—The Uinta or Crest Fault (b), the fault first to be described on the north flank, was traced from a place near Manila, Utah, eastward approximately 60 miles by Powell [45] and later by Schultz [46] and Sears.[47] The fault in this locality will, therefore, not be further discussed.

Schultz [48] mentioned, but did not map, a continuation of this fault as far westward as the Gilbert Peak area, and Emmons [49] mentions a fractured or crushed zone near the divide area in the western portion of the range. The position of this fault has been mapped by the writer; it extends to a point approximately 30 miles westward from Gilbert Peak. As it lies entirely in the thick Uinta Series throughout much of its outcrop west of Manila, and hence is rather obscure, Emmons' difficulties are easily appreciated. However, it is possible to recognize the fault and approximate its throw, inasmuch as the central buff-colored zone of the Uinta Series has been faulted into contact with the lower red phase. The fault termi-

[43] *Ibid.*

[44] J. W. Powell: *Report on the geology of the eastern portion of the Uinta Mountains and a region of the country adjacent thereto*, U. S. Geol. Geog. Surv. Terr., II Div. (1879) p. 202; atlas, map B and pl. I.

[45] *Op cit.*, p. 177; atlas, map B, pl. I.

[46] A. R. Schultz: *op. cit.*, pl. V; *Oil possibilities in and around Baxter Basin, in the Rock Springs uplift, Wyoming*, U. S. Geol. Surv., Bull. 702 (1920) pl. 1.

[47] J. D. Sears: *Geology and oil and gas prospects of part of Moffat County, Colorado, and southern Sweetwater County, Wyoming*, U. S. Geol. Survey, Bull. 751-G (1924) pl. XXXV; *Relations of the Wasatch and Green River formations in northwestern Colorado and southern Wyoming*, U. S. Geol. Surv., Prof. Paper 132-F (1924) pl. XXIV.

[48] A. R. Schultz: *op. cit.*, p. 71.

[49] S. F. Emmons: *op cit.*, p. 299.

nates on Hayden Peak, by splitting into three shear zones. East of Gilbert Peak, because of a swing to the northeast, the trace approaches Paleozoic and Mesozoic sediments along the north flank of the range, and, at a place about 12 miles southwest of Manila, it cuts them.

The fault, whose strike is in many places quite sinuous, has a tendency to split and form offshoots throughout its extent. The dip of the fault is steep (75 degrees) to the south, and not approximately 45 degrees as was suggested by De Lyndon [50] and Ver Wiebe.[51] Throughout the Uinta Range the side south of the fault is upthrown; whereas, along its probable extension into the Axial Basin region (10), the south side, according to Sears,[52] is downthrown. Fault drag, generally marked on both sides of the shear zone, is especially strong on the north side, where its effect is traceable to the adjoining North Flank Fault.

*North Flank Fault.*—The North Flank Fault (a) is represented by a zone of considerable magnitude along the north flank of the range. When one interprets Powell's [53] map and sections, it appears that he suspected faulting in this position near Manila, Utah. Gale [54] speaks of a fault of considerable magnitude, 6 miles east of Manila, which, although the fault trace is obscured by recent alluvium and valley wash, probably ties in with the fault as here mapped.[55] Farther west, in the Weber River vicinity, Schultz [56] observed faulting and says of it:

"The true nature of the fault zone . . . has not been determined. Enough has been seen, however, to warrant the statement that it is not a simple fault but is somewhat complex. . . . The throw increases materially toward the east."

Field work has extended this zone of faulting approximately 65 miles.

This North Flank Fault Zone is of a complex nature. For instance, throughout the greater part of its extent, the north block is downthrown. Near the western end, however, the blocks appear to pivot, and on the Weber River, near Rockport, the south side is downthrown. The point of pivot is in the Big Piney Mountain area, north of the Kamas Valley, and there the formations show little disturbance.

[50] F. De Lyndon: *Discussion of "The isostasy of the Uinta Mountains"* by A. C. Lawson. Jour. Geol., vol. 40, no. 7 (1932) p. 665.

[51] W. A. Ver Wiebe: *Oil fields in the United States*, 1st ed. (1930) p. 487. McGraw-Hill.

[52] J. D. Sears: *Geology and oil and gas prospects of part of Moffat county, Colorado, and southern Sweetwater county, Wyoming*, U. S. Geol. Surv., Bull. 751-G (1924) p. 307, and pl. xxxv.

[53] J. W. Powell: *op. cit.*, atlas, map B, and pl. I.

[54] H. S. Gale: *Coal fields of northwestern Colorado and northeastern Utah*, U. S. Geol. Surv., Bull. 341 (1909) p. 311-312.

[55] Since the field work was completed, the writer has had the opportunity of examining an unpublished map made by Dr. W. H. Bradley of the United States Geological Survey. The map covers several square miles in the Phil Pico Mountain and Manila, Utah region. Dr. Bradley, in his detailed work, has also mapped faults on the north flank of the range but he feels that the fault spoken of by Gale dies out near Phil Pico Mountain, and that the Uinta Fault Zone, in part at least, probably becomes the North Flank Fault west of Phil Pico Mountain.

[56] A. R. Schultz: *op. cit.*, p. 69-70.

Although obscured at many places by later sediments and by the easily weathered portions of the faulted formations, the presence of this fault zone is revealed by: (1) Marked steepening of dips, interpreted as drag; (2) a notably straight contact line of relatively low-dipping Eocene beds with older formations, which in other parts of the Uinta Mountain region is very irregular; (3) total or virtual absence of outcrops of the Wasatch (lower Eocene) sediments along most of the north flank; and (4) definite subsidiary faults observed in older formations, which are downthrown on the north side.

The fault shows characteristics in common with other faults of the region, and it is inferred that it dips steeply, because of its relatively straight trace, and because of the steep dips of the subsidiary faults. There is a marked drag along this zone, the drag on the south side being, in general, greater. This is a reversal of the best-developed drag along the Uinta, or Crest, Fault. The Uinta, or Crest, Fault and the North Flank Fault probably join to the east. These two faults tend to compensate each other; that is, an algebraic summation of the throw on the two faults remains about the same throughout the central portion of the range. On the other hand, a comparison of the combined throws of all the faults on the north flank, with those of the south flank, shows that displacements on the north flank are greater.

*Faulting adjacent to the Uintas.*—In the Weber River section of the Coalville-Weber River area (3), faults have been reported between Peoa and Wanship, but they have never been mapped in detail. This section is important because it shows Wasatch Mountain influences on faults related to those in the Uintas. The faults in the Weber River area generally strike east-west, with the south block downthrown. The dips are generally steep to the north (Pl. 3, B), except on a northeastward-striking cross fault, which dips 45 degrees to the northwest, the north block being downthrown.

The North Flank Fault cuts through this region and shows evidence of some strike slip, probably caused by the pivotal movements previously mentioned. West of the Weber River area, these faults are covered by extrusive andesitic flows. In the Coalville section, where mapping of the faults has been adapted from other sources,[57] they appear to have been influenced by the Wasatch Mountain structural trends.

Schultz [58] mentions faulting in the Daniels Canyon-Strawberry area (5). The faults are generally obscured by thick Tertiary cover. Well-

[57] Unpublished map by Tom Lyon and Paul Billingsley. (Courtesy of Tom Lyon, International Smelting Company, Salt Lake City, Utah).
C. H. Wagemann: *The Coalville coal field, Utah*, U. S. Geol. Surv., Bull. 531 (1915) pl. xi.
A. R. Schultz: *op. cit.*, pl. v.

[58] A. R. Schultz: *op. cit.*, p. 65.

developed shears, striking, in general, northwest and dipping 80 to 85 degrees south, are apparent in several localities, as in Daniels Canyon and Willow Creek of the upper Strawberry River. A major fault is postulated through this region because southwestward-dipping Mississippian limestones are southwest of, and in close proximity to, the younger southwestward-dipping Morrison formation. It is concluded that this faulting and shearing represent resultants of the strains caused by the stresses that produced the Uinta and the Wasatch ranges.

Faults of the Cross Mountain (11), Axial Basin (10), Rock Springs (12), and neighboring areas have been described by Powell, Sears, Schultz, and Hancock; as their work has been adopted, except where noted, no detailed discussion will be presented. The fault on the west flank of Cross Mountain dips about 70 degrees west.

### JOINTING

Joints are well developed throughout the Uinta Range, and most of them are found in one of two master sets. One set roughly parallels the axis of the range; the other set is approximately at right angles to it. These sets appear to be equally developed and are generally within 5 to 10 degrees of vertical. Excellent joints are found in the Uinta Series, which constitutes the core of the range, but in many places the younger formations also show both sets. Generally, the joints cut through all types of beds without change in character.

## DIASTROPHISM

### GENERAL STATEMENT

The writer believes that the unusual orientation of the Uinta Range, with relation to the Rocky Mountain System, is the direct result of peculiarities within the major Rocky Mountain geosyncline. It is well established that the locus of folded mountains is generally along the deepest part of a previous geosynclinal trough, and that, in many mountain ranges, if rotational or "unbalanced" stresses were dominant in producing the folding, the major thrust apparently has been from the direction of the landmass supplying most of the sediments, and toward the trough.[59]

Because of the unusual orientation of the Uinta trough as a spur of the Rocky Mountain trough, the deformation of its sediments was by no means as simple as is usually thought to be the case; but, as will be shown, the region gives evidence of having, in general, followed the rule.

Field data indicate three major periods of diastrophic activity in the Uinta Mountains, and these have been responsible for a maximum vertical uplift of approximately 45,000 feet in the center of the range; that is,

[59] C. M. Nevin: *Principles of structural geology* (1931) p. 283-284. John Wiley and Sons.

the lower beds of the Uinta Series, which were covered by 35,000 feet of shallow-water sediments, now stand 10,000 feet above sea level.

The major diastrophic events that produced the Uinta Mountains will be discussed in the sequence of their effects:

1. Deformation of the Uinta Mountain and Wasatch Mountain geosynclines during the Laramide Revolution.
2. Vertical uplift and large-scale faulting in late Eocene.
3. Continental uplift of the general plateau area in late Pliocene or early Pleistocene.

### DEFORMATION OF UINTA AND WASATCH GEOSYNCLINES DURING THE LARAMIDE REVOLUTION

*Folding of the Wasatch and other northward-trending ranges.*—Major folding and some faulting began the destruction of the geosynclinal troughs. Because the Uinta Mountain and the Wasatch Mountain troughs were so closely related in their depositional history and, as will be shown later, in their deformational history, it is convenient to consider the folding of the Wasatch trough before discussing deformation of the Uinta geosyncline.

Northward-trending folds of the Wasatch Mountain type prevail throughout the central Rocky Mountain region. They are characterized by severe deformation, overturning, and faulting in the Wasatch Range proper and, to a lesser degree, in the foreland folds of the Porcupine (2), Rock Springs (12), Coalville (3), and Daniels Canyon-Strawberry (5) areas. This is illustrated by: (1) Thrust faulting and overturning to the east in the central part of the Wasatch Mountains; (2) folding overturned to the east on the Coalville anticline; (3) shearing and probable reverse faulting, with the fault surfaces dipping to the southwest, in the Daniels Canyon-Strawberry area; and (4) general northward trend and asymmetry of the folds, with the steep limb on the east side in the Porcupine and Rock Springs regions.

Studies of the central Wasatch Range have led many writers [60] to the conclusion that, for the most part, the central Wasatch Range has been subjected to rotational tangential stresses of great magnitude, from the west or southwest. Indeed, this was possibly the prevailing direction of stress over the central Rocky Mountain region. In any case, it is generally accepted that the forces were working in an easterly and westerly direction. That this widespread folding took place in the Laramide near the close of the Cretaceous is well established.

[60] Hyrum Schneider: *A discussion of certain geologic features of the Wasatch Mountains*, Jour. Geol., vol. 33 (1925) p. 39-40.

F. B. Stillman: *A reconnaissance of the Wasatch Front between Alpine and American Fork canyons, Utah*, Jour. Geol., vol. 36, no. 1 (1928) p. 55.

J. D. Forrester: *Structure of the Wasatch Front between Rock canyon and Slate canyon, near Provo City, Utah* (unpublished manuscript).

*Folding of the Uinta Mountains.*—The general east-west trend of the Uinta Mountain and related folds can be traced from the western front of the central Wasatch Range, near Salt Lake City, Utah, as far eastward as Cross Mountain in Colorado. This trend is a direct expression of a zone of weakness inherited from the old east-west Uinta Mountain trough. It gives little information concerning the deforming stresses except insofar as it is possible to postulate that they were working from either a northerly or a southerly direction, or from both.

The major structural axis of the Uinta Range is, as noted, generally arcuate or slightly convex to the north, the point of greatest convexity being approximately equidistant from the eastern and from the western ends of the range. In the western portion, the trend takes a rather gentle curve to the southwest, where its projection can be traced through the Wasatch Mountain region. The eastern half shows a rather abrupt swing to the southeast and projects toward the Cross Mountain area. This arcuacy suggests that the deforming stresses probably acted from a southerly or a southwesterly direction, and, more particularly so, because, as has been shown, a "highland" area supplying sediments lay south of the range during much of the time the trough was being filled.

*General symmetry of the Uinta Fold.*—The Uinta Mountain structure, as a whole, is uniform in trend and attitude and is remarkably simple, when the size of the area involved and the height of the fold are considered. The folding was localized because of the previously well-defined geosyncline.

Although the writer belives that some of the faulting took place during the folding, the major movements on the faults, as will be discussed, were considerably later than the folding. Therefore, it is necessary, for this discussion, to remove the effect of most of the displacements with their accompanying drag and warping, in order to determine the symmetry of the structure immediately after folding. When this procedure is followed, the Uinta Mountain arch becomes a broad, open anticline, with low dips—that is, dips only slightly asymmetrical toward the north. This procedure also brings out the fact that the crustal shortening, caused by folding, is about 2 miles over a span of 50 miles, or as 1 is to 25. This type of structure suggests compressive folding stresses from a southerly or a northerly direction, or from both.

As already stated, the range has undergone a total uplift of about 45,000 feet, but, as the height of the arch produced by folding must have been relatively low, only 10,000 to 12,000 feet of this total uplift can be accounted for by folding. Although the writer does not agree with Lawson's [61] sequence of diastrophic events nor with his estimate of total sedi-

[61] A. C. Lawson: *The isostasy of the Uinta Mountains*, Jour. Geol., vol. 39, no. 3 (1931) p. 271.

mentary thickness, his figures for the percentage of uplift caused by folding are comparable with those presented here. This comparison is based on the total percentage of uplift by folding, as contrasted with the total uplift.

The form, symmetry, and magnitude of the fold indicate that the deforming stress was deep-seated. Such a broad, open anticlinal structure could best be developed in a zone where the axes of relief are almost equal, with the easiest relief vertically being only slightly greater than in other directions; this zone of confining pressures must necessarily be deep-seated. Such deep-seated compressive stress, acting in a southerly or northerly direction, probably from the south and southwest, contrasts markedly with the tangential Wasatch Mountain type of stress from the west or southwest, suggested by many geologists for a majority of the northward-trending ranges of the region.

*Minor folds adjacent to the Uinta Range.*—As previously noted, the Uinta Mountain trough was well developed and deep in an east-west direction, shallowing gradually eastward but rapidly to the north and south throughout the greater part of its extent (Fig. 1).

The appearance of minor folds on the flanks of the Uintas and in adjacent areas may be an expression of the shallowing of this geosyncline. This is illustrated by such folds as those in the Porcupine Mountain (2), Coalville-Weber River (3), and Daniels Canyon-Strawberry (5) areas.

The Coalville-Weber River and Daniels Canyon-Strawberry areas show varying structural trends intermediate between the north-south Wasatch Mountain type and the east-west Uinta Mountain trends. This condition is to be expected because of their proximity to the Wasatch Mountain region.

The Porcupine Mountain region is well removed and approximately equidistant from the Wasatch and Uinta mountains and, hence, would not necessarily be expected to take such a north-south trend as it exhibits.

The minor transverse folds, developed primarily on the flanks of the Uinta Mountain arch itself, as well as the north-south trends of the adjacent minor folds, clearly show that: (1) Uinta Mountain deep-seated stresses were localized and quite effectively controlled by the well-defined trough; (2) minor folds are, in reality, foreland folds of the "Wasatch Mountain type"; and (3) prevalent west or southwest tangential stresses readily controlled even deformation on the flanks of the Uinta Mountain arch.

It is also of interest to note that, in the Rock Springs area (12), the folding trends swing gradually from a north-south strike into an easterly direction as the Uinta arch is approached (Pl. 4). That this swing is to be seen on the southern end of the uplift, rather than on the north, further

sustains the theory that the compressive deep-seated stresses producing the east-west trends came from a southerly direction.

### DETAILED CONSIDERATION OF UINTA MOUNTAIN STRUCTURE

*Western portion.*—Because the plunge of the Uinta Mountain fold is not uniform throughout, but shows minor reversals, and also because it does not plunge east and west from the center of the range, the western and eastern portions, as delimited by this major reversal, will be considered separately. In general, the pitch to the west is about twice as steep as that to the east.

The structure of the western portion of the Uinta Range is clearly an expression of the fact that the Uinta trough was well defined and deep near its western end.

In this portion, the anticlinal structure is a uniform broad arch, trending slightly west-southwest, which has, as a rule, relatively low dips on both flanks. Dips on the north flank are, for the most part, greater than those on the south. The pitch gradually increases to the west. Because the Uinta Mountain geosyncline, on projection to the west, carries its somewhat greater depth very definitely into the central Wasatch Mountain trough, structural lineaments of the Uinta Mountain trends within the Wasatch Range must also be considered.

If the Uinta Mountain axis be projected into the Wasatch Range, the uniformity of the Uinta Mountain arch disappears. The general westerly trends swing very decidedly to the northwest and southwest (Pl. 4) and broaden out to cover a much wider area. An eastward-pitching anticlinal axis—the projected Uinta Mountain axis—can be traced to the point where it disappears under the extrusive flows west of Kamas Valley.

Deep-seated stresses of the Uinta Mountain type, acting from probably a general southerly direction, it seems, were sufficiently strong to persist into the Wasatch Mountain region because of the localized, originally well-defined, east-west geosynclinal trough. The contemporaneous tangential Wasatch Mountain type of stresses from the west, which prevailed in the region, was opposed by the prism of sediments in this localized trough. Although these east-west stresses caused a well-defined sag along the Uinta Mountain axis, as shown by the marked reversal of pitch near Kamas, Utah, and also produced a general "fanning" out of the Uinta Mountain trends, they were evidently subordinate to those that produced the Uinta Range.

*Eastern portion.*—The gradual eastward-shallowing of the Uinta Mountain trough, together with a slight southeastward swing of its trend, has been definitely reflected in the folding in the eastern part of the range. Thus, the folds are less uniform in both length and form and cover a wider

area than do those farther west. These features are shown by the Uinta Mountain arch proper, the Yampa Plateau-Split Mountain structure (6), the Raven Park fold (7), and also by numerous smaller folds along the flanks of the major structure. Eastward, the trends of all folds gradually swing more and more to the southwest. The steepest dips are usually on the north flank.

The plunge of the major fold is, in general, quite low to the east and southeast, and can be traced until it reverses abruptly on projection into the Cross Mountain area (11).

The Cross Mountain fold is very near the eastern limits of the true Uinta Mountain geosyncline. This anticline, which trends northeast-southwest, is about 4 miles long.

The Yampa Plateau-Split Mountain (6) and Raven Park (7) folds show, as a rule, the broad, open east-west folding of the Uinta Mountain type. In all these folds the westward pitch is the steeper.

Deep-seated, localized stresses of the Uinta type, acting from probably a southerly direction, and controlled by the well-defined Uinta trough, became progressively smaller as the trough shallowed eastward. These stresses gradually lost their potency to the east-west stresses prevailing throughout the Rocky Mountain region. The result of the combination of these stress relations, together with the southeastward swing of the trough, has caused all the folds in this area to trend southeast.

### FAULTING

The writer postulates that some of the faulting took place during folding. However, as post-folding movements have taken place along most of the faults, it is difficult, with certain exceptions, to determine the relation of the faulting to the folding.

Evidence that the faulting and folding are, in part, contemporaneous is as follows: (a) In some instances, as in the case of the Uinta or Crest Fault, the faults show a marked parallelism to the folds and are on the steepest part of the fold, where the arch might reasonably be expected to break; (b) certain *en échelon* fault zones appear to have been developed during folding.

Because the major faults, as now exposed, have characteristics that can best be explained by post-folding adjustments, and because post-folding displacements of considerable magnitude are apparent (p. 657; Pl. 3), it seems that faulting during folding was only of lesser importance.

The presence and nature of the faults developed contemporaneously with the folding, however, give some information about the stresses acting on the area. Thus, the *en échelon* faults, particularly on the south flank in the general vicinity of the supplementary noses of the Split Mountain section (6), indicate a torsional or compressive stress from the south or

southwest. Moreover, the relative scarcity of low-angle reverse faults points to deep-seated stresses—that is, stresses acting in a deep zone, where shortening would be at a minimum as compared to the shallow zones where tangential stresses give marked overturning and thrusting.

### TIME OF FOLDING

The time of folding of the Uinta Mountains has been variously placed from late Cretaceous to Eocene. Field evidence brings out the following facts:

(1) Laramie deposits are absent from all places in the Uintas where they might be expected.

(2) Wasatch (Eocene) sediments are in marked unconformity with the Mesaverde group and, in a few places, with the Montana group of the upper Cretaceous.

(3) The Uinta Mountain type folds project into the Wasatch Mountain area.

(4) The trends of minor structures swing from Wasatch Mountain trends to Uinta Mountain trends and *vice versa*.

These features indicate that Wasatch and Uinta Mountain folding developed at the same time and represent Laramide deformation.

Folding in the Axial Basin region (10), however, did not take place at this time, because, according to Sears,[62] Laramie sediments are conformable with the lower Wasatch formation. This indicates deposition during Uinta Mountain folding, and also that there was no major deformation before Wasatch time. The Axial Basin region was, therefore, folded later than the Laramide Revolution. This age relationship is further evidence that, eastward, the Uinta Mountain folding, as such, ends at Cross Mountain.

Various writers in the past have proposed other hypotheses to explain the folding of the Uinta Mountains. Beeson[63] postulates folding as the result of laccolithic doming at the time of emplacement of the intrusive bodies of the central Wasatch Mountains. As has been shown, this postulate of Beeson's is untenable, particularly when it is remembered that the andesitic flows of the region (which are genetically related to the Wasatch Mountain intrusives) were extruded on an erosion surface developed after the first Uinta Mountain uplift.

Lawson[64] does not specifically consider the direction of stress, although he does mention underthrusting, but he concludes that the Uinta Range

[62] J. D. Sears: *Geology and oil and gas prospects of part of Moffat county, Colorado, and southern Sweetwater county, Wyoming*, U. S. Geol. Surv., Bull. 751-G (1924) p. 291-292; *Relations of the Wasatch and Green River formations in northwestern Colorado and southern Wyoming*, U. S. Geol. Surv., Prof. Paper 132-F (1924) p. 95.

[63] J. J. Beeson: *Mining districts and their relation to structural geology*, Am. Inst. Min. Metall. Eng., Tr., no. 1500-I (1925) p. 24.

[64] A. C. Lawson: *Folded mountains and isostasy*, Geol. Soc. Am., Bull., vol. 38 (1927) p. 268-271.

represents folding developed on the south side of his "Wyomid" basin, as the result of a greater accumulation of Cretaceous sediments in the center of the basin. As has been shown, the Uinta Range is over an old trough, which, in thickness of the total sedimentary section, far surpasses the sections to the north and south.

De Lyndon,[65] Ver Wiebe,[66] and various other writers have reported a marked overturning of the Uinta anticline to the north. De Lyndon and Ver Wiebe mention low-angle thrust faulting on the north flank and postulate that the Uintas have been moved several miles to the north. They suggest stresses acting from a southerly direction, evidently of a tangential nature, in order to develop this overturning and thrusting. The writer's field work reveals no such widespread low-angle thrusting, nor is overturning by folding stresses in any degree comparable to that postulated. Further evidence to refute the conclusion, that the range has ridden several miles to the north, is obtained from a study of sedimentary thicknesses shown in Figure 1. The major axis of the folding is in close proximity to the axis of the old depositional "deep", and is not displaced several miles to the north, as it would be if the north flank had overridden the margin of the range.

The Axial Basin region has been considered by many geologists to represent an eastward continuation of the Uinta Mountain structure. It has been shown that this area was deformed later than the Uinta Range and, therefore, cannot properly be part of the true Uinta Mountain structure.

Consideration of the facts that have been presented leads the writer to conclude that deep-seated, compressive or torsional stresses, acting from southerly and southwesterly directions on the sediments deposited in the Uinta Trough, produced the upfolding of the Uinta Range.

The effects of these assumed stresses are thought to have been closely controlled and localized by the trough. They appear to represent stresses that were subsidiary to, or resultant from, those acting in a general east-west direction, which were prevalent over the region as a whole. They apparently were resolved into a northerly or a northeasterly direction, primarily because of the east-west trend of the old well-defined Uinta Trough, which, in turn, formed a distinct contrast to the usual north-south geosynclinal trends over most of the Rocky Mountain region.

### POST-FOLDING EROSIONAL HISTORY

At the beginning of folding, erosion began on the center of the uplifted area, and the transported debris was contemporaneously deposited in the

[65] F. De Lyndon: *Discussion of "The isostasy of the Uinta Mountains"* by Andrew C. Lawson, Jour. Geol., vol. 40, no. 7 (1932) p. 664-666.

[66] W. A. Ver Wiebe: *Oil fields in the United States*, 1st ed. (1930) p. 485-487. McGraw-Hill.

adjacent basins on all sides, as the earliest fresh-water Tertiary beds. As folding continued, the area of erosion was gradually and progressively widened. This, in turn, caused a reworking of part of the earliest Tertiary sediments and, consequently, developed a noticeable unconformity between the Eocene and the Mesozoic formations. Topographic relief, as the result of folding, was certainly not even approximately equal to that of the present. This uplift was not sufficient to permit erosion to expose the quartzitic and more indurated members of the lower part of the stratigraphic section. Therefore, the lower Eocene sediments were derived primarily from the breakdown and redeposition of Mesozoic formations,[67] although, undoubtedly, the Paleozoic beds were somewhat incised in certain places. Erosion was rapid in these relatively soft shales and sandstones of the Mesozoic, and, as it was progressing with uplift, it is certain that the 10,000 to 12,000 feet of uplift caused by folding was never approximated topographically. When folding ceased, erosion continued cutting down and lowering the gradients, and the region was eventually reduced to a stage of maturity. This old erosion surface may be observed where later materials have covered and preserved it, as, for instance, under the extrusive andesites along the Weber River near Peoa and Wanship and east of Heber City on Lake Fork Creek. On the south flank of the range, between Longitude 109° 50′ and 110° 30′ West, a notable re-entrant of Duchesne River (Oligocene) sediments is unconformable on all older beds and has preserved an old transverse, mature, drainage channel, which was fully developed by late Eocene.

Because of the numerous structural and erosional events that have taken place in the region since Eocene time, it is difficult to detail the exact extent of this erosion surface over the range. The erosional epoch was brought to a close, in late Eocene, by major uplift and large-scale faulting.

### VERTICAL UPLIFT AND LARGE-SCALE FAULTING

*General statement.*—It is generally recognized that most mountain ranges show at least two periods of uplift, the first, caused by folding, being separated from a later major uplift by an interval of erosion.

That there was such a major uplift in the Uinta Mountain area, later than the folding, is shown by the following relationships:

(1) Extensive tilting and warping of Eocene sediments, which demonstrate that at least part of the uplift was later than the first folding.

(2) Marked vertical displacements of beds, ranging in age up to and including Eocene sediments, along major strike faults, as, for example, Bridger and Green River (Eocene) formations in contact with Paleozoic sediments along a considerable portion of the North Flank and Uinta, or

[67] J. D. Sears: *Relation of the Browns Park formation and the Bishop conglomerate, and their rôle in the origin of Green and Yampa rivers*, Geol. Soc. Am., Bull., vol. 35 (1924) p. 286.

Crest, faults (Pl. 3). The major faults have strain characteristics, which can best be explained by vertical movement—that is, adjustments by tensional, vertical stresses rather than by compressive, folding stresses. These characteristics are: (a) the high angle of dip of all faults; (b) the marginal faults, on both flanks of the range, which are normal faults and dip away from the axial portion of the range; and (c) the Yampa Fault, which is normal and dips steeply toward the axial region of the main Uinta arch.

*Extent and intensity of uplift.*—Not only the Uintas, but also the Axial Basin anticline and the Rock Springs uplift, as well as the Wasatch Mountain region and the Coalville-Weber River and Daniels Canyon-Strawberry areas, show post-folding uplift. For convenience, this uplift is discussed under several general headings.

*Uinta Mountain area.*—The vertical uplift has elevated the central portion of the range approximately 25,000 feet as a maximum. This maximum is where the pitch of the axis reverses, and, because this is somewhat closer to the western limits of the range, the westward pitch is greater than that to the east.

This uplift cannot be measured merely by totalling the throws of the strike faults. Indeed, it is here suggested that a relatively small portion of the displacement along the Uinta, or Crest, Fault may be the result of movement during the folding or first major uplift of the range. This partially, at least, accounts for the previously mentioned greater throw shown by the north flank faults as compared to those of the south flank. Much of the vertical uplift is accounted for by pronounced drag along the major faults, where, in most places, it is better developed on the upthrown side, and by pronounced warping, which steepens the previous dips along both flanks of the Uinta Mountain structure. These features readily explain the difference between the postulated uplift of nearly 25,000 feet and the amount shown by the throws of the strike faults in Plate 4. It is because of this pronounced drag and steepening of dips that a marked accentuation has been given to the dips on the north limb of the major anticline. For instance, the upward drag on the south edge of the fault block between the North Flank and the Crest faults and the downward drag along the north of this block have given it a marked northward tilt. Drag is generally better developed within this block than in adjacent blocks to the north and to the south. These features have led many writers to interpret the Uinta structure as resulting from marked overturning during folding. Where the previous folding was most pronounced, this later vertical uplift is also of greatest magnitude, and, as the folding decreases in intensity, the uplift progressively diminishes.

Uplift in the western half of the Uinta Mountain area is characterized by marked block faulting, and the central, or axial, portion of the range is upthrown with respect to the flanks. As the western limits of the Uinta Mountain anticlinal structure are approached, these fault blocks gradually disappear. In the eastern half of the range, the uplift has been more differential warping, and block faulting is correspondingly less common. Certain areas, such as Yampa Plateau-Split Mountain and Cross Mountain, may have risen higher than the center of the range. Although steepening of dips through drag and tilting is most pronounced on the north flank of the range, the same features are found, to a lesser degree, on the south flank, as, for instance, the abrupt flexing of formations on the south flank of the Yampa Plateau-Split Mountain area. All the major strike faults gradually decrease in throw toward the outer limits of the previous folding.

If it be assumed that an active or moving fault block will develop more drag than marks the adjacent passive block, it may be reasoned that the range as a whole was generally uplifted, rather than that the basin regions to the north and south subsided. With this assumption, it can be further deduced, by the drag along the Yampa Fault, that the Yampa Plateau area was uplifted higher than the axial region of the range (Pls. 3 and 4).

Some slumping of the region after the vertical uplift, is suggested. For example, drag along the north side of the Crest Fault, particularly in the area to the west, where block faulting is prominent, suggests a subsidence of the north flank (including some of the basin area), with respect to the axial portion of the range. Sears [68] cites evidence of subsidence of the center of the Uinta Mountains in the eastern part of the range. Although his evidence is largely correct for the north flank, a study of field relations over the whole range makes certain modifications necessary (p. 662).

*Wasatch Mountain area.*—Indications of uplift after folding along the projection of the Uinta Mountain axis into the Wasatch Mountain area, of a kind other than that of the Basin and Range type of uplift, have been noted by several writers, as, for instance, Stillman [69] and Beeson.[70] Stillman writes that "Thus . . . normal faulting resulted from the vertical stress exerted by the intruding magma, the strike and dip being controlled by the strains during folding", and Beeson states that "The evidence is quite clear that this uplift (post Cretaceous) . . . was coincident with deformation caused by igneous intrusions . . . in the Wasatch and Oquirrh Mountains."

---

[68] J. D. Sears: *op. cit.*, p. 287, 290-300.

[69] F. B. Stillman: *A reconnaissance of the Wasatch Front between Alpine and American Fork canyons, Utah*, Jour. Geol., vol. 36, no. 1 (1928) p. 54.

[70] J. J. Beeson: *op. cit.* p. 23-24.

The uplift of the whole Wasatch Mountain region was evidently more widespread and not so localized as that of the Uinta Mountain area, and Eocene rocks have not there been so greatly warped.

*Coalville-Weber River and Daniels Canyon-Strawberry areas.*—The Coalville-Weber River area was affected by this post-folding uplift to a greater degree than was the Daniels Canyon-Strawberry region. Faults along the Weber River are upthrown on the north side, a fact which partly explains the reversal of throw on the west end of the North Flank Fault; thus the effect of the Uinta Mountain uplift decreased and that of the Wasatch Mountain uplift increased. The Wasatch (Eocene) formations dip, both to the north and to the south from Coalville, at a greater rate than can be accounted for by original depositional slopes. This suggests that the Coalville area was warped and faulted during post-folding uplift.

In the Daniels Canyon-Strawberry area, steeply dipping Eocene formations have been observed, which can best be explained by such a post-mountain-folding uplift.

*Axial Basin region.*—It has been established by Sears [71] that the Axial Basin region participated in uplift after the deposition of early Eocene sediments and at least before Browns Park time. This uplift caused gentle anticlinal warping of the area, uplift by fault displacements being relatively insignificant. That release of pressure on the uplifted, warped portion probably followed is postulated on the basis of the relationship of the strike faulting in the northern portion of the region. This fault zone shows the south side, which was the elevated side during warping, as now the downthrown side. Inasmuch as the Axial Basin region adjoins the Uinta Range on the east but was not folded during the Laramide Revolution, the writer suggests that the Uinta Mountain vertical uplift caused the warping in the region.

*Rock Springs area.*—The major cross faults of the Rock Spring area are roughly parallel to the faults of the Uinta Mountains and are probably later than the folding.[72] Perhaps the uplifted and consequent faulting of the region was genetically related to the major uplift of the Uintas to the south.

*Time of vertical uplift.*—The following evidence indicates that this post-folding uplift took place near the close of the Eocene: (1) Close association of the marked warping with the intrusive bodies of late Eocene or early Oligocene age in the Wasatch Mountains; (2) steepening and warping of Eocene formations in the Coalville and Strawberry areas; and

[71] J. D. Sears: *Geology and oil and gas prospects of part of Moffat County, Colorado, and southern Sweetwater County, Wyoming*, U. S. Geol. Surv., Bull. 751-G (1924) p. 295, 300.

[72] A. R. Schultz: *Oil possibilities in and around Baxter Basin, in the Rock Springs uplift, Wyoming*, U. S. Geol. Surv., Bull. 702 (1920) p. 47-48; map.

(3) observations by Wegemann,[73] indicating that the uplift in the Coalville area was in post-Wasatch time. In the Uinta Range, warping and displacement of Eocene sediments, and not of Oligocene formations, as, for instance, on the south flank of the range, indicate late Eocene uplift. The Bishop (Miocene?) and Browns Park (Pliocene?) formations in places cover the strike faults without disturbance. Moreover, there is a preservation of the Eocene erosion surface by later Eocene and early Oligocene extrusive flows in the western part of the region. As has already been pointed out, the warping of the Axial Basin region was post-early Eocene and pre-Browns Park time. Relaxational movements occurred after the culmination of vertical rise, but evidently not at the same time throughout the whole region. There was subsidence of the north flank in the zone of block faulting, certainly before the end of Bishop (Miocene?) time, inasmuch as the Bishop conglomerate, with no apparent displacement, mantles the fault trace in several localities. Sears [74] has given evidence of subsidence at least as late as Browns Park time, along the north flank in the eastern part of the range. Field relations show that it was certainly not later than Pliocene time.

Summarizing all this evidence, vertical uplift in the Uinta Range and in adjacent areas evidently may be dated as late Eocene or early Oligocene.

*Theory as to cause of vertical uplift.*—There have been several theories advanced to explain such vertical uplifts. It has been suggested [75] that such uplifts take place after folding and a marked erosional interval and at the time of emplacement of a batholithic core within the mountain range. Field relations in the Uinta Mountain area seem to accord with this theory.

Although no batholithic core is exposed, indications of its presence are: (1) Hydrothermal alteration of the Mississippian formations along the Uinta River, and the presence of metalliferous vein deposits in close proximity to the fault zones in several localities in the range; (2) the close association of intrusive igneous bodies with marked uplift in the Wasatch Range; and (3) the great size, breadth, and simplicity of the Uinta Mountain anticline, with its attendant marginal faults.

Therefore, it appears that a major uplift of the Uinta Range took place in late Eocene or early Oligocene time and was genetically associated with the emplacement of a batholithic core in the area previously deformed by folding.

---

[73] C. H. Wegemann: *The Coalville coal field, Utah*, U. S. Geol. Surv., Bull. 581 (1915) p. 171.

[74] J. D. Sears: *Relation of the Browns Park formation and the Bishop conglomerate, and their rôle in the origin of the Green and Yampa rivers*, Geol. Soc. Am., Bull., vol. 35 (1924) p. 287.

[75] C. M. Nevin and E. B. Mayo: *Nature and genesis of batholiths* (abstract), Geol. Soc. Am., Pr., 1934 (1935) p. 101.

### POST-VERTICAL UPLIFT EROSIONAL HISTORY

In the moist Oligocene period, during, and after, culmination of vertical uplift, erosion was active in the relatively non-resistant shaly formations of the lower Mesozoic. Much of the detrital material from the elevated portions was transported some distance into the flanking basins before deposition. Indeed, Bradley [76] suggests that most of the material was carried out of the basins and into the sea or into the Great Plains region. In the old mature transverse stream channel on the south flank, however, there was deposition of the Duchesne River (Oligocene) well up into the range.

Because of the active erosive and depositional forces at work, a rather uniform level, which sloped gradually away from the axial line of ridges forming the crest of the Uintas, was soon developed. Evidence of the surface can readily be observed at the present time throughout much of the range, particularly in the western half of the area. Rich,[77] Eardley,[78] and others have, likewise, noted this surface. In the eastern portion of the range, which had never been so highly uplifted as the central and western parts, trunk drainage had evidently succeeded in breaching the anticline and establishing a fairly well defined course along the axial region of the range. Thus was developed the old depression of Browns Park.

With the advent of the Miocene and its characteristically dry climate, conditions of erosion and weathering were changed. Rainfall on the Uinta Mountain divide area was probably still quite abundant and of a torrential nature, whereas the adjoining regions were progressively more arid away from the divide. These features of an arid climate, combined with the highly jointed old quartzitic formations being extensively eroded, and the relatively steep gradient, at least near the divide area, produced the blocky, poorly sorted Bishop conglomerate as an alluvial fan upon an extensive pediment. This conglomeratic material is widespread and probably extended far up toward the divide. These general conclusions have also been reached by Bradley [79] and Eardley.[80] This erosion still further reduced the relief of the whole area and enlarged the Browns Park longitudinal drainage channel into a mature valley.

It is postulated that, at the beginning of Browns Park (Pliocene) time, the axial portion of the eastern part of the range underwent some release from pressure. Subsidence was more or less periodic and has been defi-

---

[76] W. H. Bradley: *personal communication.*

[77] J. L. Rich: *The physiography of the Bishop conglomerate, southwestern Wyoming,* Jour. Geol., vol. 18 (1910) p. 601-612.

[78] A. J. Eardley: *personal communication.*

[79] W. H. Bradley: *oral communication.*

[80] A. J. Eardley: *personal communication.*

nitely established by Sears,[81] on the north flank of the structure during, or at the close of, Browns Park time. This may explain the apparent insufficient height, as noted by Rich,[82] of the divide area to serve as a source for the Bishop conglomerate. Thus, it is not necessary, at this time, for the range to be uplifted again, as suggested by Rich,[83] inasmuch as the crest area was, no doubt, high enough to supply the coarse material and has since subsided to a considerably lower elevation, in addition to being reduced somewhat by subsequent erosion.

Sinking of the area within which the old longitudinal drainage was established, reduced the gradient and, combined with the low relief of the region as a whole, induced the deposition of the relatively finer Browns Park formation in the old river channel and over wide expanses farther east.

The Uintas were reduced to low relief and, indeed, approached peneplanation, away from the divide area of the range. This divide area was still marked by a line of axial peaks in the western portion, but eastward, in the area that had never been so highly elevated, and which locally had recently dropped down somewhat, the topography had become essentially uniform. Over this region the streams were able to meander with little regard to structure. Cross Mountain was incised by superposition of a stream; the transverse drainage of the present Green River across the Uinta Mountain anticline was developed, possibly to some extent by breaching; and the Yampa River meandered to its junction with the Green River, the combined waters flowing along the axis of Split Mountain and eventually wandering away to the southwest.

Sears [84] postulated graben faulting of the axial portion of the eastern part of the Uinta Range, at the close of Browns Park time. He bases his hypothesis on the theory that the Yampa Fault was formed at that time, as well as on the theory of subsidence by faulting on the north flank of the range; thus, the axial portion dropped as a graben. To support his argument, he states that the Yampa Fault guided the flow of the Yampa River in the area west of Cross Mountain. The writer believes that Sears' conclusion is untenable, inasmuch as the Yampa River meanders across the Yampa Fault south of Zenobia Peak. The river's crossing and recrossing of the faulted zone can best be explained by previous peneplanation of the structure or by superposition in rocks of equal resistance; and, under the existing conditions, it cannot be thus explained at all, if the fault is late enough to have guided the stream channel. Moreover, the drag

[81] J. D. Sears: *op. cit.*, p. 287.
[82] J. L. Rich: *op. cit.*, p. 620.
[83] *Op. cit.*, p. 618.
[84] J. D. Sears: *op. cit.*, p. 290-291, 301-303.

indicates that the south, or footwall, block rose rather than that the north block subsided.

Soon after the establishment of the drainage systems, another uplift of regional proportions commenced.

#### CONTINENTAL UPLIFT IN LATE PLIOCENE OR EARLY PLEISTOCENE

*General Plateau area.*—A far-reaching uplift is known to have taken place throughout this whole general region in late Tertiary or early Quaternary time. This uplift elevated the present high plateaus of Utah, Wyoming, and Colorado, and also the typical Basin Ranges, including the Wasatch Range.

In the region west of the Plateau province, the uplift was differential. Faulting and tilting were the characteristic features, as is shown by the Basin and Range structures. The Plateau province was elevated more uniformly. The Uinta Mountains, therefore, especially if considered as a unit, show no apparent differential uplift with respect to the surrounding regions. Because of this lack of separate elevation, the amount which the Uintas were uplifted at this time can only be approximated by subtracting the previous uplifts of the range from the known total rise of 45,000 feet. By this method, a rise of from 8,000 to 10,000 feet is obtained. This amount of uplift corresponds to estimates made by other writers in studies of the adjacent Wasatch Range.

Direct evidence of this uplift in the Uinta Range is shown by a marked entrenchment of the meandering Green, Yampa, and other master rivers of the region. It is now generally accepted [85] that the Green River and its tributaries are later in their development than the first Uinta Mountain uplift. Present field work entirely substantiates this viewpoint.

*Time of continental uplift.*—The beginning of this regional uplift has been variously placed from the Miocene up to the Pleistocene, with additional adjustments being continued up to the present. As information and knowledge become more accurate through detailed studies of the western United States, there has been a noticeable tendency to move the time of uplift nearer to the present.

Blackwelder, in a recent study of the whole Colorado River system, suggests, on the basis of considerable evidence, that the Green River and other master streams were not integrated until the Pleistocene. Such a suggestion agrees with events as postulated in this paper—that is, the Green and the Yampa rivers, in order to maintain their courses, must have been established before this last major uplift began; and this, as

[85] S. F. Emmons: *Origin of Green River*, Science, n. s., vol. 6, no. 131 (1897) p. 19-21.
E. T. Hancock: *The history of a portion of Yampa River, Colorado, and its possible bearing on that of the Green River*, U. S. Geol. Surv., Prof. Paper 90-K (1915) p. 183-189.
J. D. Sears: *op. cit.*, p. 279-304.

has been brought out, had been done at the close of Browns Park (Pliocene) time.

This widespread elevation began, therefore, at the close of the Pliocene and delineates in this general region the beginning of the Quaternary, which has been a period of notable continental elevation.

## BIBLIOGRAPHY


Beeson, J. J.: *Mining districts and their relation to structural geology,* Am. Instit. Min. Metall. Eng., Tr., no. 1500-I (1925) 36 pages.

Berkey, C. P.: *Stratigraphy of the Uinta Mountains,* Geol. Soc. Am., Bull., vol. 16 (1905) p. 516-530.

Blackwelder, Eliot: *Origin of the Colorado River,* Geol. Soc. Am., Bull., vol. 45 (1934) p. 551-566.

Boutwell, J. M.: *Iron ores in the Uinta Mountains,* U. S. Geol. Surv., Bull. 225 (1904) p. 221-228.

———: *Geology and ore deposits of the Park City district, Utah,* U. S. Geol. Surv., Prof. Paper 77 (1912) 231 pages.

———: *The Salt Lake region,* 16th Internat. Geol. Congr., Guidebook 17, Excur. C-1 (1933) p. 25-98.

Butler, B. S., et al: *The ore deposits of Utah,* U. S. Geol. Surv., Prof. Paper 111 (1920) 672 pages, 57 plates.

De Lyndon, F.: *Discussion of "The isostasy of the Uinta Mountains" by A. C. Lawson,* Jour. Geol., vol. 40, no. 7 (1932) p. 664-669.

Dutton, C. E.: *Report on the geology of the high plateaus of Utah,* U. S. Geol. Geog. Surv. Rocky Mtn. Reg. (1880) 307 pages.

Emmons, S. F.: *Descriptive geology,* U. S. Geol. Expl. 40th Par. (King), vol. 2 (1877) 890 pages; vol. 1 (1878) 803 pages.

———: *The origin of Green River,* Science, n. s., vol. 6, no. 13 (1897) p. 19-21.

———: *Uinta Mountains,* Geol. Soc. Am., Bull., vol. 18 (1907) p. 287-302.

Fenneman, N. M.: *Physiography of western United States* (1931) 534 pages. McGraw-Hill.

Forrester, J. D.: *Structure of the Wasatch front between Rock canyon and Slate canyon, near Povo City, Utah* (unpublished manuscript).

Gale, H. S.: *Geology of the Rangely oil district, Rio Blanco County, Colorado,* U. S. Geol. Surv., Bull. 350 (1908) 61 pages.

———: *Coal fields of northwestern Colorado and northeastern Utah,* U. S. Geol. Surv., Bull. 341 (1909) p. 283-315.

———: *Coal fields of northwestern Colorado and northeastern Utah,* U. S. Geol. Surv., Bull. 415 (1910) 265 pages.

Hancock, E. T.: *The history of a portion of Yampa River, Colorado, and its possible bearing on that of the Green River,* U. S. Geol. Surv., Prof. Paper 90-K (1915) p. 183-189.

———: *Geology and coal resources of the Axial and Monument Butte quadrangles, Moffat County, Colorado,* U. S. Geol. Surv., Bull. 757 (1925) 134 pages.

Heaton, R. L.: *Ancestral Rockies and Mesozoic and late Paleozoic stratigraphy of Rocky Mountain region,* Am. Assoc. Petr. Geol., Bull., vol. 17, no. 2 (1933) p. 109-168.

Hinds, N. E. A.: *Ep-Archean and Ep-Algonkian intervals in western North America,* Carnegie Instit. Washington, Publ. no. 463 (1935) p. 1-52.

Hintze, F. F.: *The Proterozoic-Paleozoic contact in the western Uinta and central Wasatch Mountains, Utah,* Utah Acad. Sci., Pr., vol. 11 (1934) p. 165-166.

Kay, J. L.: *The Tertiary formations of the Uinta Basin, Utah,* Carnegie Mus., Ann., vol. 23 (1934) p. 357-372.

Lawson, A. C.: *Folded mountains and isostasy,* Geol. Soc. Am., Bull., vol. 38 (1927) p. 253-273.

———: *The isostasy of the Uinta Mountains,* Jour. Geol., vol. 39, no. 3 (1931) p. 264-276.

Leith, C. K., and Van Hise, C. R.: *Pre-Cambrian geology of North America,* U. S. Geol. Surv., Bull. 360 (1909) 939 pages.

Lupton, C. T.: *The Deep Creek district of the Vernal coal field, Uinta County, Utah,* U. S. Geol. Surv., Bull. 471 (1912) p. 579-594.

———: *The Blacktail (Tabby) Mountain coal field, Wasatch County, Utah,* U. S. Geol. Surv., Bull. 471 (1912) p. 592-628.

Nevin, C. M.: *Principles of structural geology* (1931) 303 pages. John Wiley and Sons, New York.

——— and Mayo, E. B.: *Nature and genesis of batholiths,* Geol. Soc. Am., Pr. 1934 (1935) p. 101.

Powell, J. W.: *Report on the geology of the eastern portion of the Uinta Mountains and a region of country adjacent thereto,* U. S. Geol. Geog. Surv. Terr., II Div. (1876) 218 pages.

Rich, J. L.: *The physiography of the Bishop conglomerate, southwestern Wyoming,* Jour. Geol., vol. 18 (1910) p. 601-632.

Schneider, Hyrum: *A discussion of certain geologic features of the Wasatch Mountains,* Jour. Geol., vol. 33 (1925) p. 28-48.

Schultz, A. R.: *A geologic reconnaissance of the Uinta Mountains, northern Utah, with special reference to phosphate,* U. S. Geol. Surv., Bull. 690-C (1918) p. 31-94.

———: *Oil possibilities in and around Baxter Basin, in the Rock Springs uplift, Wyoming,* U. S. Geol. Surv., Bull. 702 (1920) 107 pages.

Sears, J. D.: *Geology and oil and gas prospects of part of Moffat County, Colorado, and southern Sweetwater County, Wyoming,* U. S. Geol. Surv., Bull. 751-G (1924) p. 269-319.

———: *Relations of the Browns Park formation and the Bishop conglomerate, and their rôle in the origin of Green and Yampa rivers,* Geol. Soc. Am., Bull., vol. 35 (1924) p. 279-304.

———: *Geology of the Baxter Basin gas field, Sweetwater County, Wyoming,* U. S. Geol. Surv., Bull. 781-B (1926) p. 13-27.

——— and Bradley, W. H.: *Relations of the Wasatch and Green River formations in northwestern Colorado and southern Wyoming,* U. S. Geol. Surv., Prof. Paper 132-F (1924) p. 93-107.

Stanton, T. W.: *The Colorado formation and its invertebrate fauna,* U. S. Geol. Surv., Bull. 106 (1893) 288 pages.

Stillman, F. B.: *A reconnaissance of the Wasatch front between Alpine and American Fork canyons, Utah,* Jour. Geol., vol. 36, no. 1 (1928) p. 44-55.

Veatch, A. C.: *Geography and geology of a portion of southwestern Wyoming, with special reference to coal and oil,* U. S. Geol. Surv., Prof. Paper 56 (1907) 178 pages.

Ver Wiebe, W. A.: *Oil fields in the United States,* 1st ed. (1930) 629 pages. McGraw-Hill.

———: *Present distribution and thickness of Paleozoic systems,* Geol. Soc. Am., Bull., vol. 43 (1932) p. 495-540.

———: *Present distribution and thickness of Mesozoic systems*, Geol. Soc. Am., Bull., vol. 44 (1933) p. 827-864.

Weeks, F. B.: *Stratigraphy and structure of the Uinta Range*, Geol. Soc. Am., Bull., vol. 18 (1907) p. 427-448.

Wegemann, C. H.: *The Coalville coal field, Utah*, U. S. Geol. Surv., Bull. 581 (1915) p. 161-184.

Geological Dept., Anaconda Copper Mining Co., Butte, Mont.
Manuscript received by the Secretary of the Society, May 1, 1936.
Accepted by the Committee on Publications, 1936.

BULLETIN OF THE GEOLOGICAL SOCIETY OF AMERICA
VOL. 48, PP. 667-722, 25 PLS., 7 FIGS. MAY 1, 1937

# ETCH FIGURE INVESTIGATIONS WITH OPTICALLY ACTIVE SOLVENTS

BY ARTHUR P. HONESS AND J. ROBERT JONES

## CONTENTS

Page

Introduction ... 668
Acknowledgments ... 669
Discussion of experimental results ... 670
General statement ... 670
Etching phenomena of calcite ... 671
General statement ... 671
Scalenohedron (6281) ... 672
Rhombohedron (1011) ... 677
Prism (1010) ... 681
Rhombohedron (0112) ... 683
Rhombohedron (0221) ... 683
Basal pinacoid (0001) ... 683
Etching phenomena of smithsonite ... 685
Scalenohedron (2131) ... 685
Rhombohedron (1011) ... 686
Etching phenomena of rhodochrosite and siderite ... 686
Etching phenomena of dolomite ... 687
Etching phenomena of celestite ... 693
Etching phenomena of hemimorphite ... 695
Summary and conclusions ... 697

## ILLUSTRATIONS

Figure Page

1. Calcite etched by citric acid ... 672
2. Calcite etched by dilute laevo malic acid ... 673
3. Calcite etched by lactic acid ... 684
4. Rhodochrosite from Alicante, Colorado ... 686
5. Symmetry relations of calcite ... 692
6. Celestite etched by a potassium hydroxide solution of laevo aspartic acid ... 694
7. Hemimorphite etched by D-glucono-delta-lactone ... 695

Plate Facing page

1. Etched calcite ... 674
2. Etched calcite and smithsonite ... 676
3. Calcite structure models ... 678
4. Etching phenomena on calcite and dolomite ... 700
5. Etching phenomena on scalenohedron faces of calcite ... 701
6. Etch figures of calcite cleavage rhombohedron ... 702
7. Etch figures of calcite cleavage rhombohedron ... 703
8. Etch figures of calcite cleavage rhombohedron ... 704

9. Etch figures of calcite cleavage rhombohedron ..... 705
10. Etch figures of calcite cleavage rhombohedron and prism ..... 706
11. Calcite etchings on the base and prisms ..... 707
12. Calcite etchings on the first order prism ..... 708
13. Etching figures of calcite and smithsonite ..... 709
14. Etching figures of smithsonite, rhodochrosite, and dolomite ..... 710
15. Etch figures on dolomite cleavage rhombohedron ..... 711
16. Abnormal etching phenomena of dolomite cleavage rhombohedron ..... 712
17. Abnormal etching phenomena of dolomite cleavage rhombohedron ..... 713
18. Abnormal etching phenomena of dolomite cleavage rhombohedron ..... 714
19. Abnormal etching phenomena of dolomite cleavage rhombohedron ..... 715
20. Etching phenomena of dolomite and celestite ..... 716
21. Etching figures on the celestite base ..... 717
22. Etching figures of celestite and hemimorphite ..... 718
23. Etch figures on the brachy pinacoid of hemimorphite ..... 719
24. Etch figures on the brachy pinacoid of hemimorphite ..... 720
25. Etching phenomena of dolomite and hemimorphite ..... 721

## INTRODUCTION

The idea has been expressed that some substances, on a basis of their physical and chemical properties, may be classifiable simultaneously into two crystal classes.[1] Such minerals as sylvite, sulfur, diamond, cuprite, and others have been stated to show conflicting properties when tested by various methods. Etch figure studies especially have not always led to conclusions that were in agreement with certain properties known to characterize some crystals. It is significant, however, that inconsistencies of this sort have arisen in some cases because of insufficient data or misinterpretation of the evidence at hand. In recent years, some attention has been given to the methods of crystal etching involving the use of optically active solvents, and, although published accounts of such investigations are scarce, the etch figure data thus far considered seem to have an important bearing on the problem of dual symmetry of crystals. Some of the earlier experimental work was done by Hettich,[2] who reported the development of asymmetric etchings on sylvite by the addition of certain organic optically active substances to the solvents employed. Friedel[3] concluded that the asymmetric configuration of crystals, either through growth or solution, is a composite result of two factors—namely, the symmetry of the crystal and that of the solution. Evidence, contradictory to that obtained by Hettich, has been set forth by Lowry and

[1] E. T. Wherry: *The assignment of crystals to symmetry classes*, Wash. Acad. Sci., Jour., vol. 8 (1918) p. 480-487.

[2] A. Hettich: *Uber die Auszere Scheinbare Unsymmetrie der Alkalihalogenide*, Zeitschr. Krist., vol. 64 (1926) p. 265-295.

[3] G. Friedel: *Sur la controverse récente entre Hettich et Valeton. Les formes hemièdres holoaxes n'impliquent pas nécessairement l'hémiédrie du cristal*, Acad. Sci., C. R., vol. 184 (1927) p. 789-791.

Vernon,[4] who observed no difference in the etch figures of sylvite obtained with pure water and those produced by water that contained optically active substances in solution. Tomkeieff [5] has described, in detail, a method of determining the "leptonic structure" of aragonite by the etch method. No mention is made, however, of the use of optically active solvents, and the structure of aragonite, as proposed by him, does not explain fully the intensities of X-ray spectra. This discrepancy, he suggests, may be explained in the partial transformation of aragonite to calcite in its natural occurrence. Royer [6] describes the etching phenomena of several minerals, including calcite, dolomite, hemimorphite, and sulfur. A considerable number of optically active acids was employed by him, but, as the study of calcite was apparently limited to the cleavage rhombohedron, it has seemed desirable to investigate this mineral further, and to consider the etching phenomena of additional new species in the light of Royer's work.[7] It is, therefore, the purpose of this paper to present the results of a comprehensive study dealing with optically active solvents as etching agents. The conclusions of Royer have been, for the most part, substantiated, and considerable new evidence has been obtained, which, when considered in the light of X-ray structure studies, affords a tentative basis of agreement regarding the symmetry of several common minerals, as indicated by these two important methods of crystal investigation.

## ACKNOWLEDGMENTS

The authors gratefully acknowledge the assistance of many who have taken an interest in this work, and who have, from time to time, offered helpful suggestions or contributed materials for the investigation. Special thanks are due to the late Professor A. H. Phillips, Princeton University; Dr. G. H. Young, Mellon Institute, Pittsburgh; Mr. Harry Berman, Harvard University; Dr. S. G. Gordon, Academy of Natural Sciences, Philadelphia; Dr. R. S. Dean, United States Bureau of Mines; Dr. W. W. Skinner, United States Department of Agriculture; Professor W. H. Newhouse, Mr. William Parrish and Mr. Robert Butler, of the Massachusetts Institute of Technology; Dr. E. T. Wherry, University of Pennsylvania; and Dr. N. W. Taylor, Dr. Wheeler P. Davey, Dr. A. W. Waldo, and

[4] T. M. Lowry and M. A. Vernon: *The electronic theory of valency.* Pt. VII. *The etch figures of sylvine,* Faraday Soc. London, Tr., vol. 25 (1929) p. 286-291; Philos. Mag., 7th ser., vol. 9 (1930) p. 233-240.

[5] S. I. Tomkeieff: *The structure of aragonite,* Min. Mag., vol. 20, no. 110 (1925) p. 408-434.

[6] N. L. Royer: *Sur la décroissance du cristal dans un milieu isotrope actif,* Soc. franç. Minéral., Bull., vol. 53 (1930) p. 350-374.

[7] After our studies were accepted for publication, continuation of Royer's work appeared in a short note: N. L. Royer: *Nouvelles observations sur la décroissance d'un cristal de calcite dans un milieu isotrope actif; Remarque sur les figures de corrosion dans la dolomite,* Acad. Sci., C. R., vol. 202 (1936) p. 429-431.

Dr. A. K. Anderson, of The Pennsylvania State College. The authors have profited much from the counsel of Dr. M. J. Buerger, of the Massachusetts Institute of Technology, and Dr. S. T. Yuster, of The Pennsylvania State College, who critically read the manuscript. Thanks are due to Mr. Quentin L. Wilcox, for preparation of the ink sketches included in this paper.

Grateful acknowledgment is also made to the Geological Society of America for the generous support given this investigation through the Penrose Bequest.

## DISCUSSION OF EXPERIMENTAL RESULTS

### GENERAL STATEMENT

The vast literature on the subject of etch figures is well known to mineralogists, and methods employed in etching investigations are as old as the science itself. Pioneers in mineralogical study were well aware of the characteristic solution phenomena which crystals exhibit if treated with suitable solvents, and much valuable information respecting many of the common species is to be found in the classic contributions of Baumhauer, Becke, Tschermak, Beckenkampf, and others whose names are inseparable from scientific developments in mineralogy over a period of many years.

With the advent of the new mineralogy and the introduction of the X-ray method of studying crystal structures, however, certain apparent inconsistencies between the old and the new mineralogy have arisen respecting structure interpretations and crystal classification,[8] which have not been, in all cases, satisfactorily explained. Just what the ultimate solution to some of these problems in crystal analysis will be is not readily predictable, but it is the opinion of the writers that a more systematic and more thorough investigation of the possibilities of the etch method is likely to yield profitable results. It is the purpose of this paper to describe and discuss the unusual etching phenomena of several important minerals, which have been treated with optically active acids, and to point out certain "abnormal" solution features in calcite, which may permit explanation on the basis of the structural make-up of this species as determined by X-ray analysis.

Although several minerals have been studied during the progress of this investigation, special attention has been given to calcite because of its ready solubility in the weaker organic acids, its diversity of crystal

[8] E. T. Wherry: *op. cit.*

*See also* a criticism of Wherry's paper by A. E. H. Tutton: *X-ray analysis and the assignment of crystals to symmetry classes*, Wash. Acad. Sci., Jour., vol. 9 (1919) p. 94-99.

E. T. Wherry: *Reply to Dr. Tutton's discussion of the assignment of crystals to symmetry classes*, Wash. Acad. Sci., Jour., vol. 9 (1919) p. 99-102.

form, the unusual smoothness of its crystal faces, and the fact that it represents, from the structural standpoint, the ideal crystal whose atomic configuration is well established. It seemed desirable to plan a study of this kind in such a way as to compare the solution phenomena of certain crystals possessing characteristically different types of structures. However, owing to the great difficulty of obtaining the *d* and *l* forms of the necessary organic acids, the experimental work thus far represents results obtained by optically active acids that could be procured, rather than by those to be desired. This fact has, therefore, restricted the number of minerals that might well have been considered.

### ETCHING PHENOMENA OF CALCITE

*General Statement.*—The mineral calcite is known to possess the crystallographic symmetry characteristic of Class 20 (rhombohedral), and, when etched by suitable optically inactive solvents, such as hydrochloric, nitric, or citric acid, the geometric symmetry is well shown.[9] It is obvious that the etch figures, developed on the several fundamental forms of the crystal, considered together, point conclusively to the presence of three planes of symmetry passing through the composite symmetry axis $\acute{C}$, which accords with the type. However, X-ray studies of this mineral reveal a distribution of the oxygen atoms that apparently reduces the symmetry of the structure to a grade lower than that indicated by the etchings obtained with common laboratory acids. Is it possible, then, to obtain, on the faces of calcite, etch figures that harmonize with the structural features as set up by X-ray studies? If such solution figures can be shown to occur under special conditions of etching, may one reach the conclusion that calcite possesses a dual symmetry—a morphological symmetry including three vertical planes, which is in perfect agreement with the regular distribution of equal interfacial angles known to characterize calcite crystals—and an atomic or structural symmetry of lower grade indicated by X-ray measurements? The geometrical form of a calcite crystal is, most certainly, an inadequate expression of its structural symmetry. Calcite, when etched with citric acid and laevo-malic acid, immediately presents this puzzling picture. The former acid reveals well-defined etchings of characteristic shape and orientation, which accord with the established symmetry of type 20; the latter acid yields solution figures wholly inconsistent with this classification (Figs. 1, 2). Any attempt to explain this marked difference in solution phenomena must, of necessity, give first consideration to the very special character of the optically active acid itself and to the relative position of the oxygen atoms in the calcite structure.

[9] A. P. Honess: *On the etching figures of the dihexagonal alternating type of crystals*, Am. Jour. Sci., 4th ser., vol. 45 (1918) p. 201-221.

In order to ascertain the persistency of such abnormal solution phenomena, numerous optically active solvents of various concentrations and temperatures have been employed, and it is remarkable how persistently this lower grade of symmetry can be shown to appear on the six faces of the cleavage rhombohedron for different conditions of etching, where optically active reagents are involved. There are a few exceptions, which may be mentioned here in a general way, such as citric acid—itself optically inactive—which, when used as a solvent for some optically active acids, renders the solution inactive, and the figures produced with such a solvent reveal the full symmetry of calcite. However, d-glucono-delta-lactone with a rather strong re-solution can be dissolved in nitric or hydrochloric acid, with the result that the etching figures are distinctly asymmetric, although it can be shown that the degree of asymmetry is a function of the concentration for this particular optically active substance. Other exceptions will be noted in the discussions that follow.

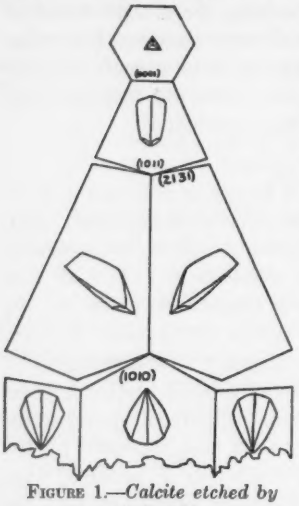


FIGURE 1.—*Calcite etched by citric acid*

Certain of the etching agents used in this work are, in reality, combinations of alkali salts, such as sodium, potassium, lithium, and ammonium, plus an excess of the optically active acid. These solvents have been referred to in this paper as alkaline solutions of the optically active substances, for the express purpose of indicating the method of preparation of the etching solutions. The fact that the presence of the alkali salt, in many instances, apparently quickens the etching action of the solvent is probably due to the increased concentration of the optically active ion.

*Scalenohedron (6281).*—It has been possible to study in detail several of the fundamental forms of calcite, but in no case have the results been more strikingly interesting than in those of the scalenohedral faces. These planes, having an asymmetric atomic configuration individually, when grouped in pairs at either end of the crystal, are symmetrical to a plane passed between them. Etching investigations, where common laboratory acids or examination of naturally etched crystals are employed, appear to confirm this view. However, when optically active acids, such as malic, tartaric, or lactic, are employed, the solution phenomena on adjacent scalenohedral planes are strikingly at variance with all recorded

data for this form. It has long been the conception of mineralogists that all faces of a given crystal form are alike, and the fact that like planes may show such contrasting solution features as are exhibited by calcite is not without significance. Figures 1 and 2 of Plate 4 represent two adjacent scalenohedral faces of calcite, oriented in correspondence with the arrrangement on the crystal. The etching configuration, as revealed by these photographs, was produced by immersion of the calcite crystal for about two hours in a cold concentrated water solution of d-glucono-delta-lactone. It is obvious that the two have not reacted to the solvent in the same manner. The face to the left appears to be more readily soluble, and, by its etchings, indicates a more violent solvent action than that which may be observed on the face to the right. It is also clear that solution maximum on the two planes is not the same. On the face to the left the figures are elongated in the direction of the vertical scalenohedral edge, but those of the opposite face are elongated at right angles to this direction. Figure 1 of Plate 5 shows the effects of solution on the same crystal faces by the same solvent, but in this case the time of immersion was much less. The crystal was so mounted that a direct comparison of the etching phenomena of the two planes can be made by focusing the microscope slightly below their line of intersection, marked CC on the photograph. The difference in solubility, so clearly shown by the right and left faces, is apparently not a case of delayed equilibrium, as this unusual solution feature became visible even in the early stages of solution and further attack by the solvent only tended to accentuate it. This condition is repeated three times at one end of the crystal, each pair of scalenohedral faces showing distinctly different etch figures on the right and the left planes. Doubly terminated scalenohedral crystals were not available for study. Therefore, it has not been possible to work out the distribution of planes, showing like solution, for the entire crystal.

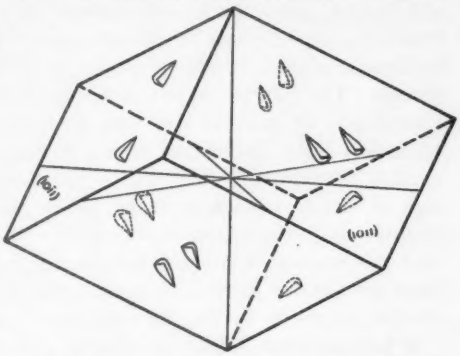


FIGURE 2.—*Calcite etched by dilute laevo-malic acid*

In order to test the validity of this peculiar solution, another crystal of scalenohedral habit was carefully cleaned in alcohol and immersed in a dilute solution of laevo-lactic acid prepared by adding 3 cc. of l-lactic acid (39 per cent solution by titration) to 10 cc. of water. The solvent

was then placed in a hot water bath, and the etching action was allowed to continue for half an hour. The results may be seen in Figure 1 of Plate 1, which shows a pair of scalenohedral faces. The differential solution of the various forms on the crystal is noticeable at an early stage of solution. The cleavage rhombohedron first yields to the attack, and, after a few minutes, becomes covered with prominent asymmetric etch figures, which are rapidly intergrown with continued solution. The first-order prism is less soluble but dissolves more readily than the scalenohedral planes, which, strangely enough, do not react alike to the solvent. The face to the left etches readily to form asymmetric quadrilateral pits of unusual size and definiteness. The face to the right assumes a luster and etched appearance more nearly resembling that of another crystal form. It is dull, striated, and marked by scattered etchings of simple triangular shape wholly inconsistent with the solution features of the adjacent scalenohedral plane. It is obvious, however, that this unusual solution is consistently repeated on the three pairs of faces terminating the calcite crystal, and it is in accord with the etching phenomena shown by the cleavage rhombohedron.

It has been stated that laevo-lactic acid was employed for the experiment. In view of the marked individuality of optically active acids and their peculiarly selective solvent action upon crystals, it seemed logical to assume that if dextro-lactic acid were employed in lieu of the laevo form and the etching were allowed to proceed under like conditions, solution effects should be reversed on the two adjacent scalenohedral planes, and enantiomorphous etchings would result. Another calcite crystal was, accordingly, selected from the same crystal group and was etched under like conditions of temperature and concentration. The results are shown in Figure 2 of Plate 1. It is clear that the etch figures are similar to those produced by the laevo acid, but etching conditions have been repeated in reverse order (compare Figures 1 and 2 of Plate 1). On the crystal treated with laevo-lactic acid, the left scalenohedral face is bright and definitely etched; with dextro-lactic acid the bright face appears to the right. This difference in luster and general appearance of the two planes is so striking that it can be detected readily by the unaided eye, while the crystal is being turned with the fingers.

In the case of malic acid, the etching phenomena are also remarkably different on the scalenohedral faces. A calcite crystal, immersed for eight minutes in a dilute, hot water solution of laevo-malic acid, reveals a differential reaction of adjacent scalenohedral planes. The face to the right in corresponding pairs is characterized by numerous definitely shaped etch figures; the face to the left is without definite eching configuration of any kind; in fact, there is no evidence to indicate that the face

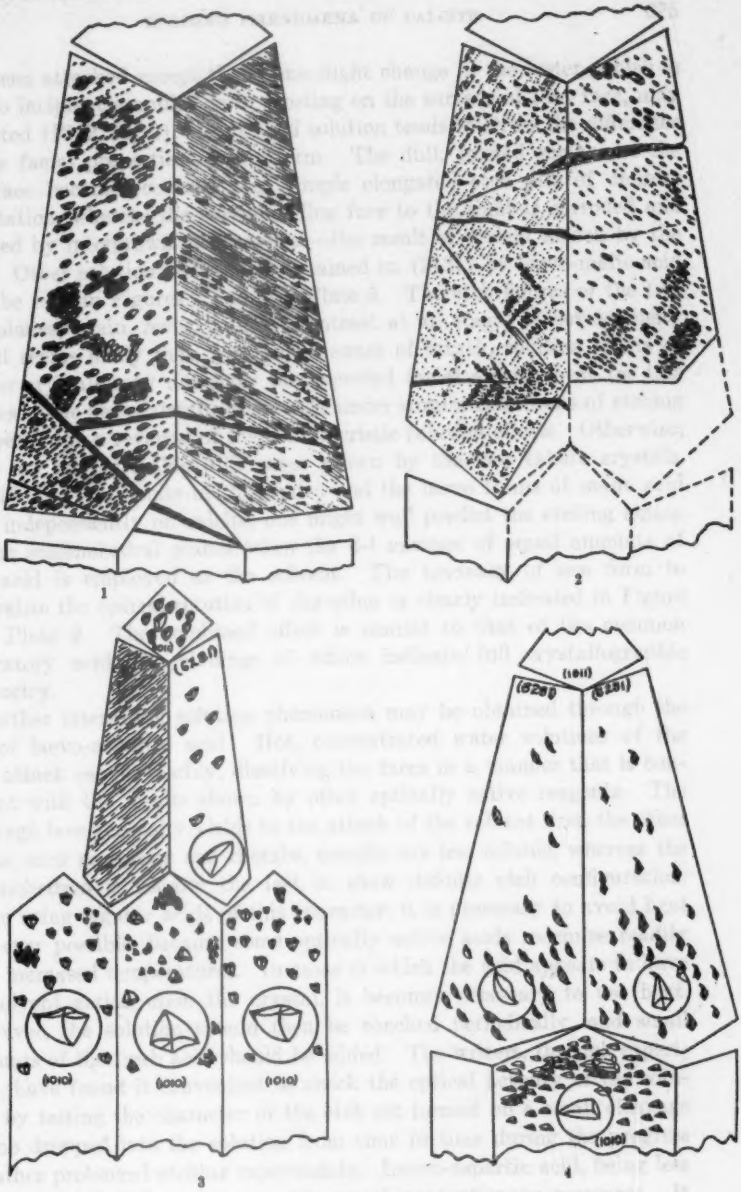


1 2 3 4

ETCHED CALCITE

has been attacked except that some slight change in the luster, which is due to incipient granulation or frosting on the surface of that face, may be noted (Pl. 2, fig. 2). Continued solution tends to stress the difference in the facial properties of this form. The dull, frosted surface of the left face becomes covered with simple elongated etch pits of definite orientation, whereas the corresponding face to the right is corroded and marked by intergrown etch cavities—the result of violent attack by the acid. Other solution phenomena obtained on (2131) by laevo-malic acid may be seen in Figures 2 and 3 of Plate 5. The etch figures of the two like planes, again, reveal marked contrast at all stages of development, and it seems likely that, with this manner of attack, solution relicts of former crystals may not show the expected facial arrangement for this species. The use of dextro-malic acid under similar conditions of etching also results in a reversal of the characteristic solution effects. Otherwise, there are no noticeable differences shown by the two calcite crystals. Considering the results of the dextro and the laevo forms of malic acid used independently on calcite, one might well predict the etching action on the scalenohedral planes when the d-l mixture of equal amounts of this acid is employed as the solvent. The tendency of one form to neutralize the optical rotation of the other is clearly indicated in Figure 1 of Plate 2. The combined effect is similar to that of the common laboratory acid, the etchings of which indicate full crystallographic symmetry.

Further interesting solution phenomena may be obtained through the use of laevo-aspartic acid. Hot, concentrated water solutions of the acid attack calcite readily, dissolving the faces in a manner that is consistent with the results shown by other optically active reagents. The cleavage face generally yields to the attack of the solvent first, the other forms, such as prisms and rhombs, usually are less soluble, whereas the scalenohedron is usually the last to show definite etch configuration. When using organic acids of this character, it is necessary to avoid heat wherever possible, because some optically active acids racemize readily with increased temperatures. In cases in which the acid appears to have no solvent action upon the crystal, it becomes necessary to use heat. However, the solution should then be checked periodically, and small amounts of the fresh acid should be added. The writers, through experience, have found it convenient to check the optical activity of the solution by testing the character of the etch pit formed on a small cleavage rhomb dropped into the solution from time to time during the progress of rather prolonged etching experiments. Laevo-aspartic acid, being less readily soluble in hot water, requires such precautionary measures. It can be used, however, to give excellent results, especially if dissolved in

alkaline solutions. The etching reactions obtained on several crystal forms are shown in Figure 3 of Plate 1. The selective action of the acid is here indicated in the contrasting character of the etch figures on adjacent scalenohedral faces. Figure 4 of Plate 1 shows the etching reactions on these faces after immersion of a calcite crystal in a hot water solution of d-arabono-lactone for a period of thirty minutes. It is obvious that the figures of the prism correspond to the diminished symmetry shown by the scalenohedron. It is evident from the etching reactions just described that optically active acids are capable of most selective solvent action upon the faces of the most general form of calcite. Although the indicated symmetry is not at all consistent with etch results obtained by common laboratory acids or with the geometrical form of calcite itself, the reduced symmetry indicated by these special acids is probably a close approximation to the true structural symmetry of this mineral. The consistency with which these asymmetric etchings may be produced—all different, but all indicating the same structural feature—is testimony to this fact.

The results obtained from the use of simple water solutions of the several organic acids proved to be of such unusual character that it seemed desirable to prepare new solvents by dissolving the optically active acids in alkali hydroxides. In many instances, such solutions proved to be excellent solvents, capable of indicating the lower grade of symmetry by distinctive etching configuration entirely different from that obtained through the use of the simple aqueous solution of the acid. In some cases, the change in the type of figure was not apparent, the solvent action being retarded or accelerated without marked effect on the ultimate etching design of the crystal. The solvent effect of the d-glucono-delta-lactone was not especially changed by the addition of the hydroxide of lithium. However, the results were altered when ammonium hydroxide was employed, but the symmetry indications remained the same (Pl. 5, figs. 4 and 5, oriented in correspondence to the facial arrangement on the crystal). That the results obtained from the two types of solution may be very different can be readily observed in Figure 1 of Plate 1 and in Figure 3 of Plate 2, in which the etchings of the aqueous solution of the lactic acid may be compared with those of the sodium hydroxide solution of this acid. The difference in the etch figures of corresponding faces suggests that, within those planes, there are structural characteristics that are not accidental; these characteristics can be indicated by the etching phenomena of many solvents of different chemical constitution and concentration. It should be emphasized, however, that the abnormal etchings shown here can be obtained only through the use of optically active solvents. The figures produced on like crystal

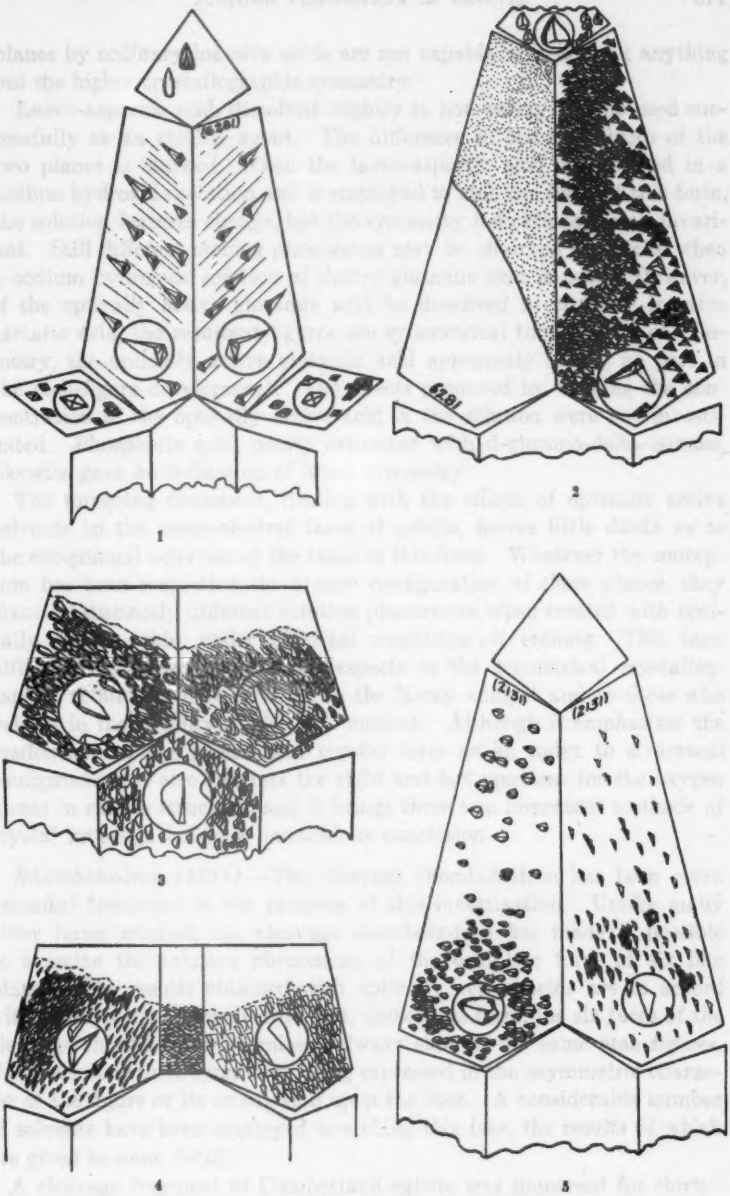


1 2 3 4 5

ETCHED CALCITE AND SMITHSONITE

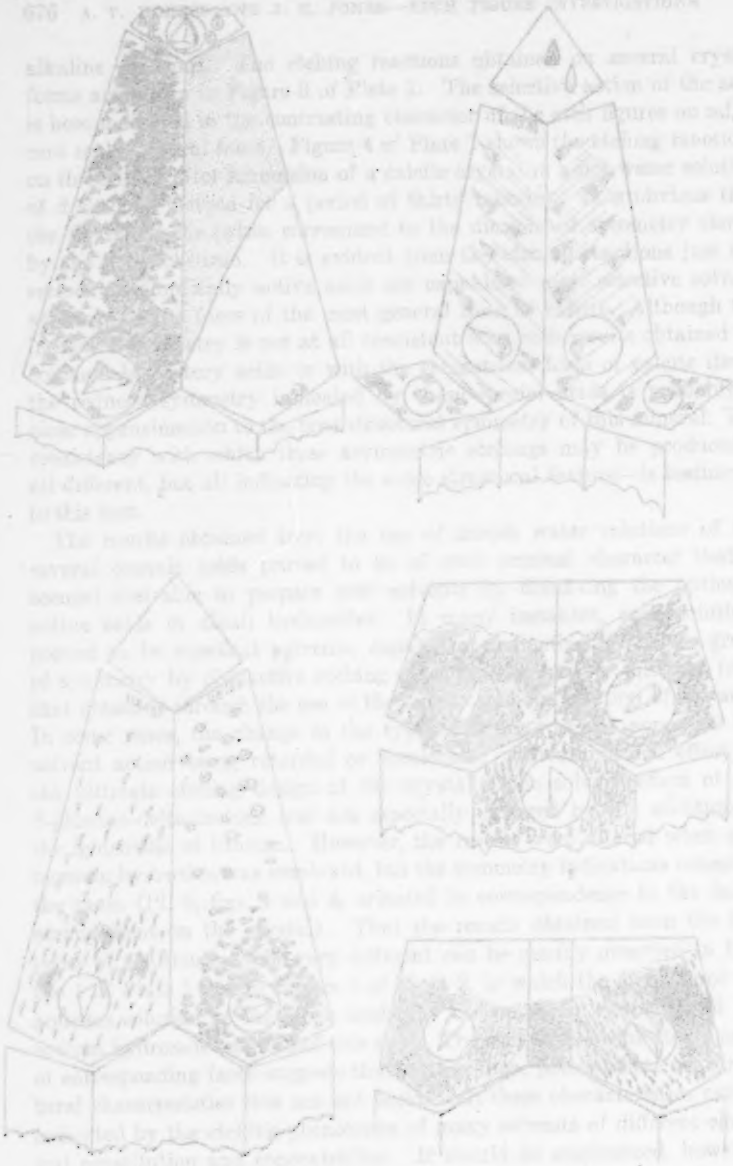

planes by ordinary inactive acids are not capable of indicating anything but the higher crystallographic symmetry.

Laevo-aspartic acid, dissolved slightly in hot water, may be used successfully as an etching agent. The difference in the solubilities of the two planes is marked. When the laevo-aspartic acid is dissolved in a sodium hydroxide solution and is employed to etch the faces of this form, the solution features change, but the symmetry indications are an invariant. Still different etching phenomena may be observed on calcite when a sodium hydroxide solution of dextro-glutamic acid is used. However, if the optically active glutamic acid be dissolved in citric or inactive tartaric acid, the resultant figures are symmetrical to the plane of symmetry, the optically active glutamic acid apparently taking no part in the etch-figure development. The effects produced by varying the concentration of the optically active acid in the solution were not investigated. Phosphoric acid, nearly saturated with d-glucono-delta-lactone, likewise gave no indication of lower symmetry.

The foregoing discussion, dealing with the effects of optically active solvents on the scalenohedral faces of calcite, leaves little doubt as to the exceptional behavior of the faces of this form. Whatever the conception has been respecting the atomic configuration of these planes, they manifest distinctly different solution phenomena when treated with optically active acids, under identical conditions of etching. This fact, although disappointing in some respects to the geometrical crystallographer, should be most welcome to the X-ray analyst and to those who believe in the validity of the etch method. Although it emphasizes the inadequacy of the geometrical crystal form as an index to structural configuration, it also suggests the right and left positions for the oxygen atoms in calcite structure, and it brings these two important methods of crystal investigation to a harmonious conclusion.

*Rhombohedron (1011).*—The cleavage rhombohedron has been given extended treatment in the progress of this investigation. Unlike many other forms studied, the cleavage rhombohedron has made it possible to examine the solution phenomena of the complete form of six like planes. The results obtained with optically active acids are in accord with those of the scalenohedron, but, unlike this form, the six faces of the cleavage rhomb, when examined, always showed the same etch figures, the lower structural symmetry being expressed in the asymmetric character of the figure or its orientation upon the face. A considerable number of solvents have been employed in etching this face, the results of which are given in some detail.

A cleavage fragment of Cumberland calcite was immersed for thirty-five seconds in a warm, concentrated water solution of d-glucono-delta-

lactone. The resultant etchings, which are definite and uniform, give expression to two important facts—namely, the like solubility of the six cleavage planes and the definitely asymmetric character of the etch configuration (Pl. 6, fig. 1). The etch figures, in the mature stage of development, are composed of four facets meeting in a common point well to one side of the pit. They are elongated parallel to the shorter diagonal of the rhomb face and possess an asymmetric outline, which clearly indicates the absence of any symmetrical atomic configuration for the face upon which they are found. This fact is significant. When the etch figures are considered on the six faces, it becomes clear that their mutual relationship imparts a simple trigonal symmetry to the Ć crystallographic axis. The alternating character of this axis is lost. The three axial directions through the rhomb, which correspond to the digonal symmetry axes of calcite, are, however, indicated by these figures. The net result, therefore, has been a reduction in the symmetry to a grade that corresponds to that of the quartz class (Fig. 2). An examination of the atomic arrangement in the structure model of calcite, represented in Figure 1 of Plate 3, shows that the same symmetry elements are present, and, although the atomic structure as determined by X-ray studies and that suggested by etching phenomena obtained by optically active acids seem to be in agreement, it is not consistent with the symmetry shown by the geometrical crystal form of calcite.

If acetic acid be used to dissolve the d-glucono-delta-lactone and this solution be used for etching, the figures produced on the cleavage faces of calcite are distinctly different but characteristically asymmetric (Pl. 6, fig. 2). When the cleavage fragment is etched in a cold saturated solution of d-glucono-delta-lactone acidified with hydrochloric acid, the figures resulting are without symmetry planes; in outline and arrangement of facets, they are unlike the etchings obtained with other solvents (Pl. 6, fig. 3). They are triangular and definitely asymmetric in the mature stage of development, but in the less mature figures the asymmetry is not well marked (compare A and B). The asymmetric character is, therefore, a function of the stage of development and, as will be shown later, a function of the concentration of the optically active acid.[10] For the purpose of determining what effects, if any, different concentrations of the solvent would have upon the etching figures of the calcite cleavage rhomb, a saturated solution of the d-glucono-delta-lactone was added to commercial hydrochloric acid of various strengths, and, although slight differences in the amount of dilution did not result in apparent modification of the etch figures, rather marked changes in the concentration of the

[10] Jiří Novák: *Ein Beitrag zur Symmetrieverminderung der Korrosionfiguren durch optisch aktive Zusätze*, Zeitschr. Krist., vol. 90 (1935) p. 385-391.

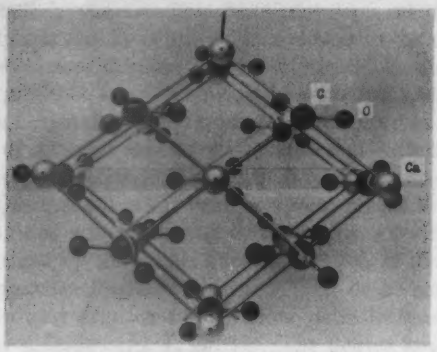


FIGURE 1. VIEWED 45 DEGREES TO THE HORIZONTAL

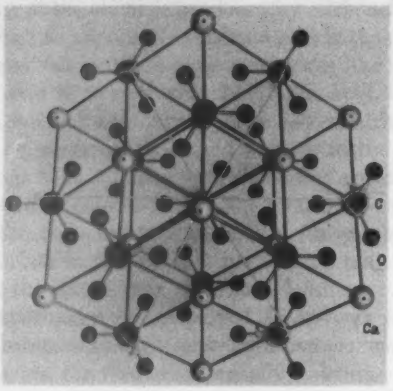


FIGURE 2. VIEWED PARALLEL TO THE VERTICAL AXIS

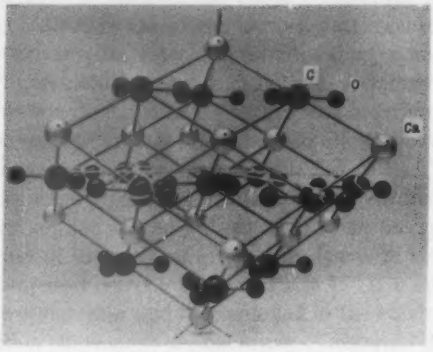


FIGURE 3. VIEWED HORIZONTALLY

CALCITE STRUCTURE MODELS

solvent did result in characteristic facial development of the etch pits. This modification is usually expressed in a change in the angle formed by the facet intersections within the figures. Hydrochloric acid alone always produces etch pits that are symmetrical to a vertical plane and oriented according to full crystallographic symmetry. As may be expected, nitric acid solutions of different concentration, saturated with d-glucono-delta-lactone, gave results similar to those of the hydrochloric acid treated with the lactone. Commercial acetic acid, however, diluted to one tenth with water and saturated with d-glucono-delta-lactone, gave figures identical with those obtained by the simple aqueous solution of the lactone (Pl. 6, fig. 4). If a cleavage fragment of iceland spar be immersed in a warm saturated citric acid solution of d-glucono-delta-lactone, however, the results are very different (Pl. 7, fig. 1). The figures are perfectly symmetrical to a vertical plane passed through the rhomb face, and, as they resemble so closely those etchings produced by citric acid alone, the optically active lactone has apparently taken no part in the reaction. Dextro-glutamic acid, dissolved in dilute citric acid, gives like results, and, when inactive tartaric acid is treated with d-glutamic acid, the figures resulting from such a solvent are only slightly asymmetric. Whether such solvents as inactive acids can be mixed with optically active substances to produce etchings that conform with the lower symmetry of calcite is apparently answered, at least in part. The results depend upon the chemical nature and the concentration of both acids employed. Therefore, considerable variation in the solution phenomena may be expected, and in some instances the results may be most indefinite.

Where alkali hydroxides are employed as solvents for such optically active organic substances as d-glucono-delta-lactone, malic, aspartic, lactic, and tartaric acids, the results are usually a definite expression of the lower symmetry. A few examples may be cited to emphasize this fact. A cleavage fragment of Cumberland calcite, immersed in a hot concentrated solution obtained by dissolving laevo-aspartic acid in dilute sodium hydroxide solution, reveals, after five minutes time, a beautifully etched surface. The figures are triangular in outline, definitely asymmetric to the vertical vibration direction of the rhomb, and are alike on all cleavage faces. Their shape and mutual relations indicate a symmetry lower than the morphological symmetry of calcite (Pl. 7, fig. 2). The results obtained with potassium hydroxide solution nearly saturated with laevo-aspartic acid are similar, the only distinction being the more acute angle made by the lines of intersection of the etch facets in the upper portion of the pits. Compare Figures 2 and 3 of Plate 7. If a sodium hydroxide solution of dextro-glutamic acid be employed in the etching of the calcite rhomb, the solution phenomena are definitely of asymmetric character and

different from those produced by other optically active solvents (Pl. 7, fig. 4). The photograph shows the figures in all stages of development. In Figure 1 of Plate 8 can be seen the etched surface of the cleavage rhomb, after immersion of the mineral in an ammoniacal solution of d-gluconodelta-lactone for a period of seven minutes. The etch figures are apparently no different from those obtained with the simple aqueous solution of the lactone. However, when a lithium hydroxide solution of the lactone is used, the etch figures assume a new form with a characteristic arrangement of the facets (Pl. 8, fig. 2); for comparison with etchings obtained by an inactive acid—d-l-malic acid—see Pl. 8, fig. 3.

Another feature of the etching phenomena of the cleavage rhomb that deserves special mention is the evidence of enantiomorphous solvent action exhibited by these planes when the *d* and the *l* forms of some suitable organic acid are employed. Dextro-tartaric acid, if dissolved in water to a concentrated solution, yields asymmetric etching figures of roughly triangular outline, bearing two distinct lines of intersection within the etch cavity. One of these intersections makes a small angle with the vertical vibration direction of the rhomb; the other intersection extends to the left. The etch figures produced by the laevo-tartaric acid are identical, but are mirror images of those obtained by the dextro acid (Pl. 8, figs. 4 and 5). The dextro and the laevo forms of malic acid have proven excellent solvents for the more soluble carbonate minerals, and the etching phenomena obtained on the cleavage rhomb of calcite reveal in a striking manner the right and left properties of these acids (Pl. 9, figs. 1 and 2). Ammoniacal solutions of this acid yield results that are not markedly different (Pl. 9, figs. 4 and 5). Etchings obtained with hot laevo-lactic acid (prepared by adding 1 cc of acid (39 per cent by titration) to 9 cc of water) after three minutes are of exceptional size and definition (Pl. 10, fig. 1). They are rounded, asymmetric oval forms, elongated parallel to the vertical vibration direction of the crystal. The etch faces of prominence lie in a zone at right angles to $\dot{C}$ and intersect in a definite straight line—the most prominent feature of the figures. They are definitely left-handed in general appearance, in contrast to those produced by the dextro lactic acid. Somewhat exceptional are the etching figures of this form obtained with dextro tartaric acid dissolved in a dilute citric acid. The figures are definitely asymmetric and offer a striking contrast to those obtained by concentrated citric acid (Pl. 10, fig. 3). The etchings obtained by the citric acid solution of dextro-tartaric acid are shown in Figure 2 of Plate 10.

To test further the use of optically active solvents in crystal studies, the cleavage rhomb was investigated by means of other solvents, one of which—dextro leucin—is of special character and, as might be expected,

gave etch figures of vastly different shape and orientation (Pl. 9, fig. 3). The attack of the solvent is represented by etch cavities, which, individually, may be considered symmetrical to one plane, but the orientation of the figures upon the crystal face is such as to preclude the possibility of symmetrical atomic configuration according to calcite morphology. The fact that the rhomb cleavage face reacts in such a spectacular manner to solvents of this character suggests some special feature of the crystal face, which may have its explanation in the right and left positions of the oxygen atoms of the calcite structure. These asymmetric etching phenomena suggest an analogy between such solution features and the re-solution of a d-l by a *d* base. In this latter case, the half neutralization by the addition of the *d* base to the d-l acid results in the production of a d-l salt and an *l* acid. It may be possible that the *d* and the *l* etching agents remove from the crystal the corresponding *l* and *d* atomic groups, resulting in etch figures of symmetry lower than that shown by the geometrical form. If this suggestion proves valid, this peculiar enantiomorphous solvent action may be a feature of only certain planes, and some crystal faces may not be expected to reveal, by their etch figures, lower grades of symmetry. One also wonders if all minerals having asymmetric atomic groups of any kind may not reveal etchings of lower symmetry grade on some faces, if optically active solvents are employed. Etching results of other minerals, discussed in a later section of this paper, may contribute useful information bearing on this problem.

When optically active solvents are employed, therefore, the cleavage rhombohedron of calcite is characterized by asymmetric etch figures. Unlike dolomite, the six cleavage faces show no difference in solubility or etching phenomena, and, although the chemical character of the solvent may be changed, there is a persistent recurrence of etching design, which accords with the results obtained on the scalenohedron. The data, as obtained from these two forms, suggest a lower symmetry than that indicated by the crystal form itself or by the etchings obtained by optically inactive acids.

*Prism (1010).*—The first-order prism faces of calcite have long been used to demonstrate the alternating symmetry of the $\dot{C}$ axis of this mineral. Its geometrical form of six like faces, when etched by optically inactive solvents such as citric, nitric, or acetic acid, always shows like etch figures on all faces of the prism, but, on adjacent faces, they reveal a reciprocal orientation. On the first-order prism, such figures are always symmetrical to a vertical plane (Pl. 10, fig. 4, by citric acid), but on the second-order form the etchings are asymmetric (Pl. 11, fig. 1). The etchings produced upon the basal pinacoid indicate the positions of the first- and second-

order zones, as only the first-order forms reveal monosymmetric etchings when optically inactive solvents are employed (Pl. 11, fig. 2). The departure from etching phenomena of this sort is obvious when optically active acids are employed to etch the prisms. The base proves to be an interesting exception, as may be observed upon comparison of Figure 2 of Plate 11 with text Figure 3. A saturated solution of laevo-aspartic acid may be diluted with water to one half strength and used to obtain excellent etching phenomena on the faces of the prism $10\bar{1}0$ (Pl. 11, fig. 3). The figures are distinct cavities of asymmetric design, so oriented on adjacent faces as to indicate a simple trigonal symmetry for the $\dot{C}$ axis, in contrast to the alternating character expressed in the etching figures of citric acid previously referred to. The plane of symmetry indicated in Figure 4 of Plate 10, where citric acid was employed, is likewise absent, according to the solution figures obtained by laevo-aspartic acid. When the crystallized laevo-aspartic acid is dissolved in a dilute sodium hydroxide solution, the solvent action is expressed by sharp polygonal forms of asymmetric outline, oriented on the six prism faces according to the trigonal symmetry of the $\dot{C}$ axis (Pl. 1, fig. 3; Pl. 11, fig. 4). Dextro-glutamic acid dissolved in dilute sodium hydroxide to a nearly saturated solution affords an excellent etching solvent, especially if heated. A calcite crystal of scalenohedral-prismatic habit illustrates the low-symmetry configuration of several important forms, if the crystal be allowed to remain in the hot solvent for about an hour. The prism, in this instance, reacts favorably to the acid, revealing etch figures of exceptional definition (Pl. 12, fig. 1). Their outline and orientation accord with all previous results where optically active acids have been employed. Further tests were made on the prism faces by an ammoniacal solution slightly acidified by laevo-lactic acid. The crystal is usually placed in the test tube of alkali, to which the desired optically active acid is added, drop by drop, until slight effervescence takes place. The acidified solution bearing the crystal is then gradually warmed in a water bath to aid solvent action. The time necessary to etch the crystal successfully depends, of course, upon the nature and the temperature of the solvent, but, usually, half an hour is sufficient. The results obtained when using various alkaline solutions as the solvents for the acid may be seen in Figures 2, 3, and 4 of Plate 12, and in Figure 1 of Plate 13. The general appearance of these figures for the four solvents is the same. They are, however, asymmetric and so oriented on adjacent prism faces as to indicate trigonal symmetry for the C axis. This form, therefore, like the scalenohedron and the cleavage rhomb, reacts with optically active solutions in a manner that accords with a lower grade of symmetry.

*Rhombohedron (0112).*—This form, although commonly present on the calcite crystals studied, was usually so striated as to make it undesirable for etching purposes. However, in a quarry at Hollidaysburg, Pennsylvania, a limited number of crystals were found, which possessed this form with an excellent luster. It was, accordingly, etched with dextro and laevo-lactic acids, and the mirror image relationship of the figures was readily demonstrated. When the solution phenomena of the basal pinacoid are discussed, reference will be made to etch figures of this form.

*Rhombohedron (0221).*—Another rhomb (0221), lying in the zone of the first-order prism, appears as a small face, and, during the experimental work, etchings of unique character were often observed on this form. However, as no special effort was made to investigate this face thoroughly, a single photograph will suffice to show the asymmetric orientation of the etch figures developed upon it. Figure 2 of Plate 13 shows this face after the calcite crystal had been immersed in a cold sodium hydroxide solution of d-glucono-delta-lactone for a period of nineteen hours. The extinction directions of the rhomb face are indicated by the crosshairs shown in photograph. This should be compared with Figure 3 of Plate 13, which represents the etchings of this form obtained by the optically inactive chlor-brome-acetic acid. The contrasting character of the etchings obtained by the different solvents is evident.

*Basal Pinacoid (0001).*—The rarity of the basal pinacoid form has limited the study of it. Very few specimens have been available that were not complexly twinned, corroded, or otherwise rendered unfit for etch figure studies. Several specimens from Patterdale, England, and one large tabular crystal from Bisbee, Arizona, have been treated with several optically active organic acids, the results of which have been so unexpected that the experimentation dealing with this form will be described in detail.

A large tabular crystal of calcite from Bisbee, Arizona, having a prominent base with well-developed faces of the rhombohedron "e" (0112), was placed beneath the microscope, where small isolated areas of the basal pinacoid were etched separately by a dilute solution of dextro and laevo-lactic acids for a period of forty minutes. Etching by this method has several advantages, one of which is the opportunity to observe the figures in their various developmental stages. With higher magnifications the effects of the solvent can be observed almost at once, as microscopic triangular pits are scattered over the surface of the basal plane. Their orientation is fixed with respect to the crystalline edges, and it is significant that not only are the facets of the etch figures developed in the zone 0001/1010, indicating the full crystallographic symmetry, but there

is no distinction between the etchings of the dextro acid and those of the laevo-lactic acid, either in facial arrangement or in orientation on the face of this form (Fig. 3). In view of the arrangement of the oxygen groups

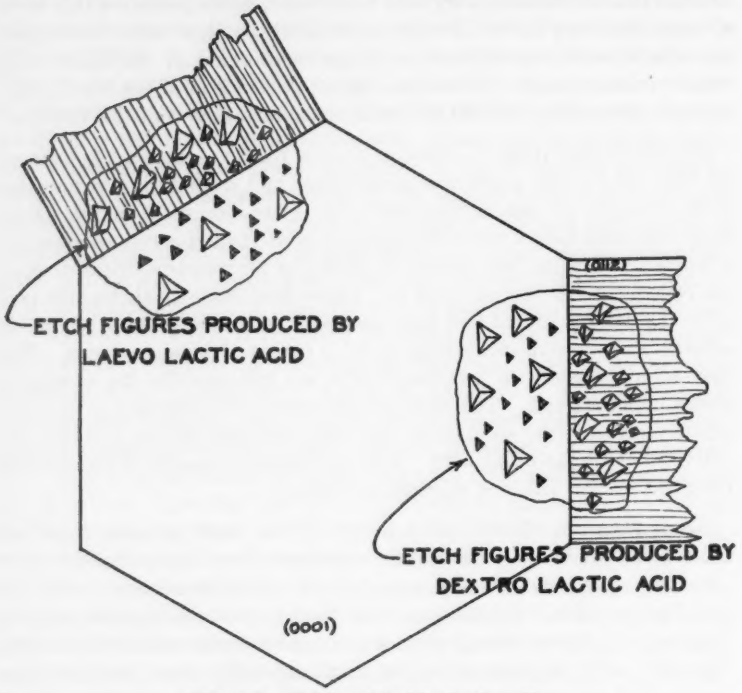


FIGURE 3.—*Calcite etched by lactic acid*

in a plane parallel to the base, these figures are very suggestive of some relationship, which may exist between the asymmetric atoms of the acid and the relative right and left bond directions of the oxygen-carbon atoms. No other face of calcite has given results of this kind, and no other plane in the calcite structure is so constituted of alternate planes of carbonate groups and calcium atoms. The base shows a neutrality with respect to oxygen direction bonds, and upon this face the dextro and laevo forms of lactic acid are not individually selective. When the rhomb faces (0112) of this specimen are etched with the opposite active forms of the lactic acid, in the manner already described, the figures are not only definitely asymmetric, but, on adjacent rhomb faces, the figures are enantiomorphously identical, indicating the individual selectivity of the optically active acids. This plane, however, possesses right and left oxygen-carbon bond

directions, which may have influenced the solvent. Several other solvents of varying chemical constitution, employed in the investigation of this form, failed to give results that could, in any way, be interpreted as contradictory to the data already described. It would seem, however, that before a positive statement can be given regarding the exceptional solution phenomena of the base of calcite, a more extended study should be made.

### ETCHING PHENOMENA OF SMITHSONITE

*Scalenohedron (2131).*—The isomorph of calcite was selected for study in order to obtain further information respecting the fundamental forms of this crystal class, and, although only a limited amount of suitable material was available, additional data were obtained respecting the scalenohedron and cleavage rhomb. The solvents that gave best results were dextro-glucono-delta-lactone, laevo-malic, dextro-tartaric, and laevo-lactic acids, dissolved in water. The solubility of smithsonite is much less marked in these acids than is that of calcite; a longer period of immersion was therefore required. If allowed to react with the crystal for two hours, concentrated d-glucono-delta-lactone etches the scalenohedral faces, and, although the resulting figures are small, they possess a definiteness that, under high magnification, leaves no doubt respecting the marked difference in the solubility of these two planes (Pl. 2, fig. 5). The solution feature is as marked as is that of calcite. Another smithsonite crystal was etched for half an hour in a hot water solution of laevo-malic acid. The solution was prepared by dissolving 26.82 grams of crystallized acid in 100 cc of water; the solution resulting gave a rotation of 0°-55′. The crystal was then immersed in the acid, and the temperature was raised by allowing the test tube to stand in a beaker of boiling water. The etchings so produced on adjacent scalenohedral faces are similar, but their orientation differs. Dextro-tartaric acid, likewise, develops this unusual solution feature upon the scalenohedral faces of smithsonite. The etchings are, in some respects, alike on adjacent planes, but their orientation expresses the diminished symmetry in a manner quite in accord with that of calcite (Pl. 2, fig. 4). The results obtained with dextro and laevo-lactic acids were not conclusively of low symmetry character, and the reason for this is not clear. Two small smithsonite crystals were carefully etched with these acids, and in both instances the figures appeared symmetrical to the plane of symmetry passed between the scalenohedral planes. Whether this result is due to improper concentration of the solvent, to minute differences in the figures, which are not readily recognizable on such small crystals, or to the possible racemization of the acid after long heating, is not known. Usually, the etching phenomena obtained by optically

active acids are very definite in their expression of lower symmetry features. It should be recalled, however, that the asymmetry has been shown to be a function of the concentration of the optically active substances, at least in some instances, and it seems necessary to investigate the lactic-acid figures more thoroughly.

*Rhombohedron (1011).*—The cleavage rhombohedron of smithsonite also gave etching phenomena that would permit fairly definite interpretation. Cleavage fragments immersed in laevo-lactic acid of medium strength and heated for several hours appear as shown in Figure 4 of Plate 13. The surface is well covered with simple triangular pits, which do not appear to be in alignment with the vibration directions of the crystal. All faces of the rhomb, however, react alike to the solvent. Etch figures obtained upon this form by means of the sodium hydroxide solution of laevo-lactic acid are decidedly of asymmetric configuration, in accord with etchings on the calcite rhomb (Pl. 14, fig. 1). Smithsonite, therefore, possessing a structure similar to that of calcite, when etched by optically active acids, reacts in much the same manner. Difficulty experienced in obtaining suitable material has restricted the study of the etching reactions of this mineral; consequently, additional data for the rhomb would be desirable.

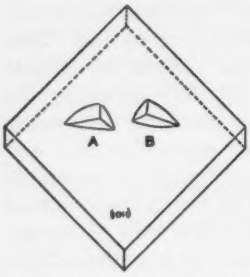


FIGURE 4. — *Rhodochrosite from Alicante, Colorado*

### ETCHING PHENOMENA OF RHODOCHROSITE AND SIDERITE

Other minerals of the calcite group, such as rhodochrosite and siderite, were considered briefly. Small lustrous rhombohedral crystals of the manganese carbonate from Alicante, Colorado, react readily to laevo-lactic acid, prepared by adding 3 cc of lactic acid (39 per cent solution by titration) to 10 cc of water. In order to accelerate the solvent action, it is necessary to heat the acid over a water bath for about forty-five minutes, after which the crystal surface is well covered with definite triangular etch figures of asymmetric outline (Pl. 14, fig. 2). The orientation of the etch figures, considered on all faces of the form, like those of calcite, indicates a trigonal symmetry. A solution prepared by adding 3 cc dextro-lactic acid (52 per cent solution by titration) to 10 cc of water also developed triangular etch figures, on the cleavage rhomb, which are identical in outline to, but exact mirror images of, those produced by the laevo form of this acid (Fig. 4). In order that a comparison may be made of the solvent action of optically active and inactive acids, a small cleavage rhomb of rhodochrosite was carefully

treated with dilute chlor-brome-acetic acid. The etch figures resulting from this solution are perfectly symmetrical forms, divisible by a vertical plane of symmetry (Pl. 14, fig. 3). Here, the solvent action of the two types of solution may be compared.

No attempt was made to investigate the cleavage rhomb of siderite with a number of solvents. D-glucono-delta-lactone, however, if sufficiently concentrated, attacks the mineral slightly, after five hours immersion. The figures so produced suggest a lower symmetry, but no definite statement can be made without further experimentation.

The etching results just described seem to show that optically active acids are capable of indicating isomorphous relationships. The unusual phenomena revealed by calcite have been shown to characterize other members of the calcite group; indeed, it may be suggested that peculiarities of atomic structures characteristic of certain species or mineral groups apparently may be indicated by the etch method. It seems to the writers that a definite plan of study could be followed, which would have for its main purpose the careful examination of several fundamental planes, with a view to classification of such planes, by etch studies, according to certain structural features known to exist in the species examined. It has been suggested earlier in this paper that the only crystal face of calcite that, with optically active acids, always revealed high symmetry figures, is the basal pinacoid. Is it not significant that this is the only plane in the calcite structure that is constituted of alternating layers of carbonate groups and calcium atoms (Pl. 3, figs. 2 and 3), and should not other members of the calcite group, whose structures are similar, be expected to show this exceptional etch phenomenon? Further investigation of this and other groups should contribute valuable information.

### ETCHING PHENOMENA OF DOLOMITE

The investigation of dolomite illustrates further the exceptional solution phenomena which minerals may show when immersed in optically active solvents. It will be remembered that the scalenohedron of calcite exhibits unlike etch figures on different faces and that the twelve faces of the form may be divided into two groups, according to the manner of solution. An anomaly of a different kind can be shown to appear on the cleavage rhombohedron faces of dolomite; this is so unusual that a full description of it seems warranted.

For the purpose of etching studies, a large rhombohedral crystal of dolomite, from Styria, Austria, was broken into small cleavage fragments, which were sufficiently smooth and transparent to permit microscopic study of the solution phenomena. These fragments were etched with many different solvents, in an effort to determine the regularity of etch

figure development under different conditions of concentration and temperature. The more striking features of these experiments will be described.

The cleavage rhomb etched for forty-five minutes in hot concentrated laevo-malic acid reveals a definite etch pattern, which appears to be the same for all faces of the rhomb, indicating an absence of symmetry planes. The orientation of the figures, however, indicates a center of symmetry, which accords with the crystallographic symmetry of dolomite (Pl. 14, fig. 4). There can be no doubt that the etchings of the upper three rhomb faces are identical, and, if there is a distinction to be made between the figures of the three upper and those of the three lower rhomb faces, this difference must be slight. Their general appearance is the same. When a concentrated solution of dextro-tartaric acid is employed to etch dolomite, the figures are also much alike on the six faces of the rhomb (Pl. 15, fig. 1). They are asymmetric and triangular in outline, apparently indicating the full dolomite symmetry. It should be stated here, however, that lower magnifications, such as were used, may not reveal slight differences in etch figure development. With d-glucono-delta-lactone, there is a slight difference of solubility noticeable on opposite parallel rhomb faces; the figures, however, appear similar, indicating full symmetry (Pl. 15, fig. 2).

Laevo-aspartic acid, likewise, fails to show any apparent differences in the etch figures of opposite parallel cleavage faces. There may be some difference in the intensity of the etching configuration, but, certainly, there is no marked distinction to be made in the etchings of opposite faces. The figures are irregular quadrilateral pits, which appear to indicate the full dolomite symmetry (Pl. 15, fig. 3). That the figures produced by inactive acids also are asymmetric may be seen in Figure 4 of Plate 15, where chlor-brome-acetic acid has been employed as the solvent. The results obtained with laevo-lactic acid are strikingly at variance with all phenomena on dolomite, already described. The solvent was prepared by adding two or three drops of laevo-lactic acid to 10 cc of water. The cleavage rhomb was then immersed, and the acid was heated for several minutes. With this treatment the solvent shows a preference for certain of the rhomb faces; this divides the crystal form into two groups of planes—those surrounding the positive termination of the $\dot{C}$ axis respond alike to the solvent, but those opposite respond differently. This puzzling phenomenon can be readily observed beneath the microscope by focusing first on the upper rhomb face, where the etch figures appear as in Figure 1 of Plate 25, after which the tube may be dropped slightly to catch the face opposite, where the etchings appear as in Figure 2 of Plate 25. The marked dissimilarity of the figures of

these faces, which are usually considered to be alike, presents an interesting problem concerning the structure of dolomite. Further illustration of this feature will be given.

The dextro-lactic acid, as would be expected, reacts with the crystal to produce etch figures identical to those obtained with the laevo form. However, on the same face, the *d* and *l* solvents develop etch figures that are mirror images of each other. With the exception of lactic acid, then, the simple aqueous solutions of the organic acids employed in this work do not appear to show exceptional solution features; in some instances, alcohol was used as the solvent for these acids, with similar results. It is noteworthy, however, that when alkaline hydroxide solutions of the optically active substances served as the etching reagents, this abnormal solvent action appeared in a more positive manner. A few illustrations will serve to emphasize this fact. Figures 1 and 2 of Plate 16 represent opposite faces of the rhomb, etched by a solution obtained by dissolving laevo-malic acid in an aqueous solution of sodium hydroxide. The solubility difference expressed by these figures is marked, compared to the solution phenomena obtained on this mineral by laevo-malic acid dissolved in water. On one face, the etchings are distinctly quadrilateral and asymmetric; on the opposite face, they appear as trapezoidal pits entirely different in outline and orientation. In the complexly twinned portions of the crystal, one may observe both types of figures on a single face, marking definite areas separated by an irregular line or twin boundary, marked *a*——*b* in Figure 3 of Plate 16. When lithium hydroxide is used as the solvent for the laevo-malic acid, the results are again different. The figures on opposite faces of the rhomb are exceptionally well defined but are different in outline (Pl. 4, figs. 3 and 4). Dextro-tartaric acid gives little evidence of abnormal solution, but, if dissolved in sodium hydroxide, the etchings are not the same on parallel faces (Pl. 17, figs. 1 and 2). Here, there is a pronounced preference indicated by the solvent, one face being more soluble than the other. A potassium hydroxide solution of dextro-tartaric acid attacks dolomite violently on one cleavage face, producing characteristic corrosion configuration most unlike the etching of the opposite parallel plane (Pl. 17, figs. 3 and 4). The preferential solution shown by dextro-tartaric acid in the experiments just mentioned is, therefore, emphasized by the addition of alkali hydroxides.

To further illustrate the effect of alkali hydroxides on the solvent action of the acids, d-glucono-delta-lactone may be mentioned. It will be recalled that this optically active substance, dissolved in water to form an acid solution, gives little or no evidence of abnormal solution phenomena. However, a sodium hydroxide solution of the lactone attacks the

crystal in a peculiar manner (Pl. 18, figs. 1 and 2). One cleavage face is characterized by numerous etchings of elongated habit, extending parallel to the vertical vibration direction; the other face bears many blade-shaped pits, much larger and oriented with their long edge 25 degrees to the vertical extinction position of the crystal. Compare with potassium hydroxide solution of this lactone (Pl. 18, figs. 3 and 4). In those experiments where ammonia was used as a solvent for the lactone, dolomite gave positive evidence of a lower symmetry (Pl. 19, figs. 1 and 2). The etch figures of opposite faces are most dissimilar, a fact in contrast to the etching phenomena of these planes when treated with an aqueous solution of this optically active substance. Equally as interesting results may be obtained with a potassium hydroxide solution of d-glucono-delta-lactone, where marked differences in the solubility of the faces may be obtained. Laevo-aspartic acid dissolved in lithium hydroxide produces an etching configuration of marked dissimilarity on dolomite cleavage faces (Pl. 19, figs. 3 and 4). Finally, lactic acid, dissolved in an aqueous solution of sodium hydroxide, shows no exception to this rule. The three faces terminating one end of the crystal are marked by terraced etch pits of irregular triangular design. But those faces of the crystal terminating the opposite end are characterized by etch figures of distinctly different type (Pl. 20, figs. 1 and 2).

Other solvents of varying chemical nature have been tried, both in water and in hydroxide solutions, and the results have been consistent. A few exceptions have been noticed, where the use of an optically active acid has failed to indicate the diminished symmetry by preferential solution of different faces of a single form. However, as the asymmetry of the figure may be a function of the concentration of the active substance, etching results at times may not permit definite interpretation. The etch method, however, is not restricted in its use of solvents, and, before final conclusions are drawn, the crystal faces should be examined with a number of different solutions, in order to determine the degree of regularity in the etching phenomena of selected faces. Abnormal solution features, contradictory as they may first seem, always permit explanation when sufficient data are available. In fact, such unusual features are always more interesting.

The solution phenomena already discussed are of special significance, both from the viewpoint of the X-ray analyst and from that of the mineralogist. The development of etch figures by optically active substances is a comparatively new method of attack and requires more systematic research, but there can be no doubt that the very limited amount of experimental data already available indicates clearly some of the important results that may be expected from future investigations.

The solvent action of organic acids, as reviewed in the foregoing pages, represents definitely four types of etching phenomena, which have been developed on the fundamental planes of several carbonate minerals. The asymmetric etch figures of the cleavage rhombohedron are alike on all faces of the form, such as those of the species of the calcite group. Etch figures obtained on this form with inactive solvents, such as nitric or citric acids, are symmetrical to a vertical plane, in accord with the geometrical crystal form. The second kind of etching phenomena, developed by optically active solvents, is represented by marked difference in the solubility of the individual faces composing the scalenohedron. Each pair of faces forming a polar edge on calcite and smithsonite is capable of indicating two differently etched surfaces, in marked contrast to the solvent action of these faces treated with common laboratory acids. Thirdly, there is the unusual solution feature shown by dolomite, where unmistakable evidence is presented that clearly portrays the unlike solubility of the cleavage faces of this mineral. The three upper rhomb faces react alike to the solvent, but the lower three faces react in a manner fundamentally different. Finally, there is that type of solution shown by the base of calcite, where repeated attempts to obtain asymmetric etchings with several optically active acids were unsuccessful.

It is obvious, then, that the use of optically active acids in the etching of the carbonates has usually resulted in an etching design that indicates a diminished symmetry. Calcite, considered from the etch figures of its several forms, is reduced in its classification to that of the trigonal holoaxial point group. Those forms whose atomic configuration is characterized by right and left oxygen atoms or bond directions appear to show preferential attack by the dextro and laevo forms of a given acid, suggesting the influence of single oxygen atoms rather than that of the carbonate group as a whole. The differential attack on the scalenohedron may be due to the oxygen-carbon bond direction of these faces. With the aid of a structure model of calcite, it can be shown that these bonds of the carbonate group may lie in a direction nearly parallel to the plane of one face; whereas, on the adjacent scalenohedral plane, this oxygen-carbon bond may be more nearly normal to the plane (Pls. 3 and Fig. 5). In view of the very special right and left properties of optically active acids, these abnormal solution phenomena may have their explanation in selective attack of the dextro and laevo solvents. The fact that the etch figures are mirror images when obtained by right and left acids and are wholly symmetrical when the racemic optically neutral acid is employed lends support to this idea. Another fact of considerable importance in this connection is the etching phenomena revealed on the basal

plane of calcite by the dextro and laevo-lactic acids. This plane is apparently the one form on calcite that fails to show, under varied conditions of etching, any figures indicative of a diminished symmetry. May not

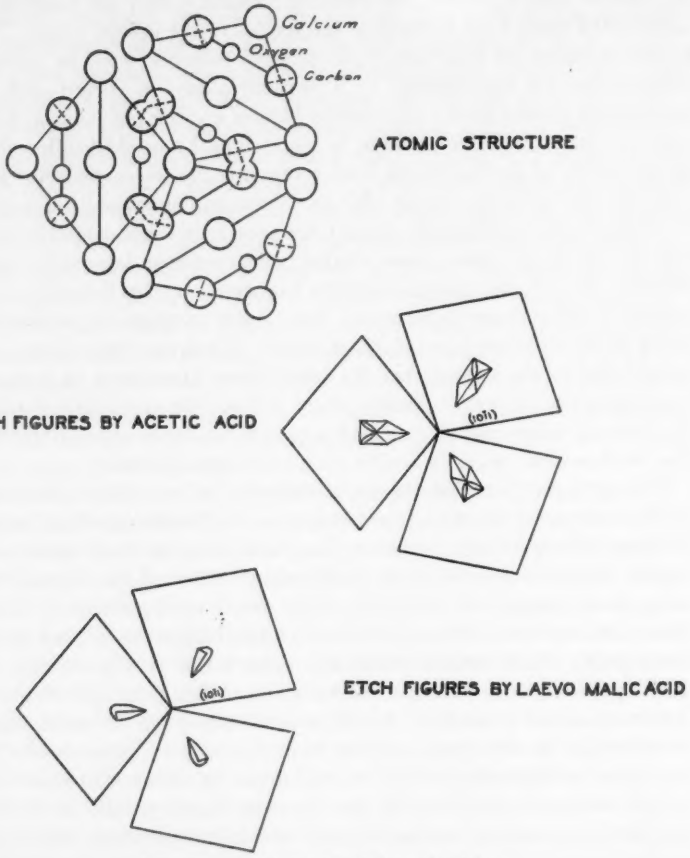


FIGURE 5.—*Symmetry relations of calcite*

this condition be explained by the neutrality of the oxygen atoms that mark the configuration of this face? If further experimentation lends support to this suggestion, may not any crystal, which contains asymmetric atomic groups in its structural make-up, show, at least on one plane, under favorable conditions of etching, solution phenomena indicative of a symmetry lower than that of the geometrical form? Just what the etching of minerals with simple ionic structures may contribute to

this problem is not known, but several etching tests on halite and fluorite, made by the writers, are suggestive.

With respect to dolomite, the lower crystallographic symmetry precludes the possibility of obtaining etch figures on any form with any solvent other than those that are asymmetric in outline. Necessarily, then, the use of optically active acids may not be expected to show a downward change in the dolomite etch figure. The diminished symmetry must, therefore, be expressed by some other solution phenomenon. This has been demonstrably shown in the unlike solvent action of parallel cleavage planes, a fact that may indicate a polarity of the $\dot{C}$ axis. It is not clear from the structure model of dolomite why certain optically active solvents should react as they do with respect to the rhomb face. The phenomena of like parallel planes developing different etch configuration simultaneously under like conditions call up structural properties not contained in calcite, as this mineral does not show different etch figures on opposite rhomb faces; this solution feature has not been observed on any of the species examined, except on those of carbonate composition. Further study of this group may clarify this interesting problem.

### ETCHING PHENOMENA OF CELESTITE

During the investigation of celestite, special attention was given to the basal pinacoid. There were no assurances that unusual etching phenomena would be obtained on this form, but the fact that it was a face well developed and smooth on the material available readily suggested its use. The etch figures obtained by a variety of solvents will be discussed.

This form, if treated with common inorganic acids, reveals bi-symmetrical figures, but optically active solvents often show asymmetric etchings indicating a diminished symmetry. This fact can be demonstrated by immersion of a tabular celestite crystal in a solution prepared by dissolving d-glucono-delta-lactone in lithium hydroxide and heating over a water bath for two hours. The figures so produced are small but fairly definite (Pl. 20, fig. 3). The small facets at the ends of the pits apparently eliminate the two planes of symmetry characteristic of this class. The etchings do, however, indicate the digonal symmetry of the vertical axes, and on opposite basal faces the figures are alike and oriented to show the binary symmetry of the two horizontal axes. The same optically active substances, dissolved in sodium or potassium hydroxide solution, reveal similar etchings on this form (Pl. 20, fig. 4; Pl. 21, fig. 1). However, an ammoniacal solution reveals a distinct change in the shape of the etch figures. They are of irregular diamond-shaped out-

line, with the interior facet arrangement that marks the lower symmetry (Pl. 21, fig. 2). Laevo-aspartic acid dissolved in alkali hydroxide is also capable of developing characteristic etchings, which do not indicate the full crystallographic symmetry. Figure 3 of Plate 21 shows the etching configuration on the base of celestite after a two-hour immersion in a concentrated potassium hydroxide solution of laevo-aspartic acid. Obviously, the solvent action on this crystal records the diminished symmetry, not in the figure itself, which is symmetrical to two planes, but in its orientation upon the faces of this form. The positions of the etch figures on opposite (001) planes are indicated in Figure 6. The diagonal symmetry of the three axes is clearly shown, but there is no evidence of symmetry planes. The same symmetry can be shown by a sodium hydroxide solution of laevo-aspartic acid. The etch figures, in this case, are of a different kind but are definite and are asymmetrically oriented to the principal crystallographic directions (Pl. 21, fig. 4).

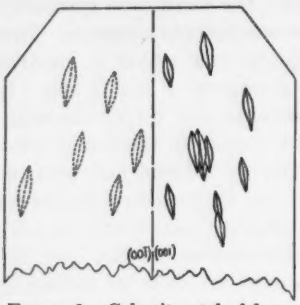


FIGURE 6.—*Celestite etched by a potassium hydroxide solution of laevo-aspartic acid*

Dextro-tartaric acid may also be used in alkali hydroxide solvents, to show these solution features of celestite. The solvent effects upon the base are shown in Figure 1 of Plate 22. The figures are asymmetric and show beak development at the acute angles. The full axial symmetry is indicated in these figures, the planes being absent. Dextro-tartaric acid dissolved in an ammoniacal solution yields etchings distinctly asymmetric but different in outline from those obtained by other solvents (Pl. 22, fig. 2). This acid dissolved in sodium hydroxide is not so definite in its expression of lower symmetry. There is, however, the suggestion of asymmetry in the etchings of Figure 3 of Plate 22. Other solvents have been employed in this work, but the results have not been fundamentally different. There is some tendency on the part of these organic acids to react like inactive solvents, when they are dissolved in water. The hydroxide solutions, however, usually bring out the diminished symmetry in a more marked manner. It should also be noted that, for celestite, as for calcite and other minerals studied, the etch figures, as obtained by the organic acids, although distinctly different from those produced by common inactive acids, are consistent in their symmetry indications, a fact that implies a diminution in symmetry elements. Where the crystallographic symmetry includes planes, this symmetry is usually changed downward by elimination of the planes. This is true of calcite, smithsonite, celestite, and other species. In the case of dolomite, where no

planes of symmetry exist, the change downward is effected by etch figures, which eliminate the symmetry center and give the $\dot{C}$ axis a trigonal polar character. There has not been a single instance where a hemihedral crystal revealed etch figures indicating a higher symmetry than that of the geometrical crystal form.

### ETCHING PHENOMENA OF HEMIMORPHITE

In order to test the etching phenomena of organic acids in connection with polar symmetry, the hemihedral zinc silicate was chosen. A great amount of etch-figure data has been obtained with respect to the pinacoid 010, but only a summarized discussion of the more important facts will be given. As may be expected, the etch figures of this form can be shown to vary considerably with different solvents, but when a change in symmetry is indicated, as before, it is downward. The feature that characterizes this change in celestite, calcite, and others—namely, a loss of symmetry planes—is further shown in the etching phenomena of hemimorphite.

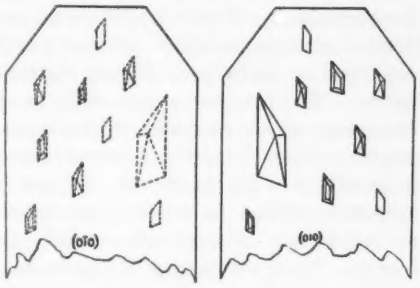


FIGURE 7.—*Hemimorphite etched by D-glucono-delta-lactone*

The crystals used in this study are from Dona Ana County, New Mexico, and, although their striated character renders them less suitable for etching, it is believed that the results obtained are sufficiently definite and accurate to warrant discussion.

Several of the organic solvents diluted with water have given excellent results. Figure 4 of Plate 22 shows the surface of (010) etched for ten minutes in laevo-aspartic acid. The figures, although definitely polar in character, do not show the vertical plane of symmetry commonly observed on the faces of this form. The opposite faces bear etch figures, identical but reversed in position according to the binary symmetry of the $\dot{C}$ axis. The asymmetric character of the figure, of course, eliminates both the vertical symmetry planes. Dextro-glucono-delta-lactone dissolved in water produces etchings as shown in Figure 1 of Plate 23. The solvent action is much different from that observed in the previous photograph, but the asymmetric outline of the etch figures is definite. The relation of the figures on opposite (010) faces is clearly shown in Figure 7. With dextro-arabono-lactone, the outer contour of the etchings is not especially asymmetric; the internal ar-

rangement of the etch figure facets, however, is definitely so. The solution of several of these active substances in various hydroxides, as in some other species studied, appears to produce solvents that clearly bring out the asymmetry. Dextro-arabono-lactone, dissolved in sodium hydroxide and allowed to stand at room temperatures, in contact with the crystal of hemimorphite for two hours, etches the crystal as shown in Figure 2 of Plate 23. Dextro-glucono-delta-lactone, dissolved in potassium hydroxide and allowed to react with the crystal in the cold for fifty minutes, produces an excellent etched surface, showing an asymmetric design (Pl. 23, fig. 3). These figures appear to be identical with those obtained in Figure 1 of Plate 23, in which only a water solution of this lactone was employed. Figure 4 of Plate 23 represents the etchings developed on (010) by a sodium hydroxide solution of d-glucono-delta-lactone. The figures are apparently no different (Pl. 23, figs. 1 and 3). The same lactone, used with lithium hydroxide, also produces a similarly etched surface. There is, however, some slight difference to be noticed in these figures (Pl. 24, fig. 1). Dextro-tartaric acid dissolved in sodium hydroxide affords an effective solvent for hemimorphite. The figures on (010) were obtained after a fifteen-minute immersion in the cold solvent. Their asymmetric character is expressed both in the figure contour and in the internal facet arrangement (Pl. 24, fig. 2). If, however, dextro-tartaric acid be dissolved in ammonium hydroxide and employed to etch this mineral, the figures of (010) are distinctly different from those of the sodium hydroxide solution. Their asymmetry is marked (Pl. 24, fig. 3). A solution of d-l malic acid, prepared by dissolving the acid in sodium hydroxide, gives etch figures, which develop according to the full symmetry (Pl. 24, fig. 4). Finally, lactic acid dissolved in water gave further evidence of the diminished symmetry. A concentrated solution of laevo-lactic acid was dropped on a glass slide, placed beneath the microscope, and a small hemimorphite crystal was immersed in it. The attack of the acid and the developmental stages of etch figure growth can be carefully traced by this method. Figure 3 of Plate 25 represents the etched surface (010) after approximately fifteen minutes of attack by the acid. The figures are regular and of definite asymmetric shape and orientation. On opposite faces of the form, they are alike but are oriented according to the binary symmetry of the vertical polar axis. A similar experiment, performed with the dextro-lactic acid, reveals the right and left solvent action of these acids. Compare Figures 3 and 4 of Plate 25 and note the slope of the contour at the broad end of the figures. The racemic mixture of the two acids results in a symmetrical attack by the solvent. This mineral, therefore, is capable of indicating structural features that permit preferential solvent action on the brachy

pinacoid, resulting in etch phenomena unlike those produced by common inorganic solvents.

Having investigated, by means of optically active acids, the etching figures of several minerals representing different crystal symmetries, it seemed desirable to gain some knowledge of the solvent action of these acids on crystals of more simple structural arrangement. Because of lack of time and inability to secure the necessary acids, it was not possible to progress far in this direction. However, the etching phenomena revealed on fluorite by means of concentrated dextro and laevo-lactic acids indicate a solvent action comparable to that of the common inorganic acids. It was necessary to heat the solvent for many hours, in order to obtain even small etch figures, but, under high magnification, distinct isolated etch pits were plainly visible; these assumed high symmetry orientation on the cube face. There is no distinction between the figures of the dextro and those of the laevo acids, either in shape or in orientation. They are, like the etchings on the base of calcite by these acids, identical. On halite, only a single experiment, which resulted in a like manner, was performed. The cubical etch pits are definitely oriented in the zone of 001/010, indicating full symmetry. The suggestion that simple structural types may not show the diminished symmetry is apparently one which may well be further investigated.

The scarcity of published data bearing on the use of optically active solutions as etching agents of crystals suggested to the writers the necessity of reporting in full the results of the experimental work carried out during the progress of this investigation. In order to make the discussion more understandable and to facilitate comparative studies of the various etching phenomena, the report is fully illustrated by photomicrographs and ink sketches.

## SUMMARY AND CONCLUSIONS

Certain conclusions reached in this paper may meet with some criticism, especially as regards the interpretation of certain structural features of crystals as set up by X-ray analysts. It seems desirable to state, in this connection, that in the discussion of results embodied in this paper, a plane of symmetry implies coincidence of points in space by reflection, without translation or rotation of any kind. Symmetry of this sort is demonstrated in the sodium chloride structure, where no asymmetric ionic groups are found, but, in the case of the calcite structure, the presence of asymmetric carbonate groups requires gliding or translation before coincidence of like points may be obtained by reflection. In other words, the carbonate groups assume right and left positions in alternating planes, which fact precludes the possibility of true reflective symmetry as regards the oxygen atoms. This can be demonstrated by etching phe-

nomena, although the external form of calcite gives no evidence of this feature. The scalenohedron, as a geometrical form, possesses true symmetry planes, revealed by the symmetrical distribution of equal interfacial angles, striae, and etch figures obtained by many of the commoner inorganic acids.

Etch figures on the surface of calcite crystals, obtained by optically active solvents, have been shown to be of distinctly different character from those produced by optically inactive acids. It is believed by some that the etching itself is the result of interaction between the solvent and the crystal at the interface and is, therefore, the expression of two symmetries—that of the crystal and that of the solvent or environment—and does not necessarily represent the true symmetry of the crystal structure. If this be true, is it not a striking coincidence that the etch figures of calcite, when developed by many organic solvents of extreme contrasting chemical character, do, nevertheless, consistently indicate, by their shape and orientation on the fundamental forms, this asymmetric structural feature of calcite, not observed on the external form? And is it not significant that these special solvents do not impose their symmetry upon the etching figures of the basal pinacoid, but only on those planes that possess the enantiomorphic atomic configuration? It would seem that the figure design is ultimately controlled by the crystal structure itself and that the optically active solvent is the agent by which this structure may be exposed. If this suggestion seems warranted, further investigation should show that those substances possessing slight irregularities of structure, not only of oxygen groups, but of asymmetric ions of any kind, may react to optically active solvents in such manner as to expose this special atomic configuration. It should be kept in mind, however, that these special structural features will influence the solution only on those planes where the configuration of atoms will permit preferential attack by the asymmetric ions of the solvent. As a result of this, it may become necessary to investigate several crystal forms, before any generalizations can be made regarding the structural features of the crystal. But, having done this, one should be able, by the etch method, to predict the presence of asymmetric atomic groupings. One should also be able to determine those planes in the structure in which the effects of the ionic groups neutralize each other. The result of this neutralization is that only the higher symmetry figures can be developed on such planes, even when optically active etching agents are used.

The experimental results on etching described in this paper seem to show that:

(1) Crystals may show two symmetries—the geometrical and the atomic—and each of these may be definitely indicated by etch figures.

The geometrical symmetry will always be revealed in the etching figures produced by optically inactive solvents. The atomic symmetry may be revealed by etching figures obtained by optically active solvents under favorable conditions of etching. The results of the two may differ widely.

(2) When a change of symmetry is indicated by means of etch figures produced by optically active solvents, the change is in the direction of a lower symmetry; the result is effected by loss of symmetry planes, by loss of symmetry center, or by development of conditions that resemble polarity along a major axis.

(3) The most general geometrical crystal form may be an inadequate expression of the structural symmetry of that crystal class. In the case of calcite, celestite, smithsonite, and rhodochrosite, experiments with optically active acids show exactly the symmetry required by the well-known and universally accepted structures found by X-ray methods. Exactly similar experiments on these crystals, with optically inactive acids, show the symmetry required by the geometrical exterior of the crystals, but not that required by the accepted X-ray data.

(4) An optically active solvent gives etch figures of reduced symmetry only on certain planes of the crystal. Other planes of the same crystal may not show this selective action. For instance, in calcite, the basal pinacoid always shows full symmetry etching phenomena for all optically active solvents. This may be due to the orientation of the triangles of oxygen atoms in the basal plane.

(5) Crystal structures, with special conditions of etching, are capable of showing enantiomorphous etch figures on the same plane, indicating a right and left structural arrangement, at least of certain atomic groups.

(6) In general, if the concentration of a given optically active solvent is less than some characteristic value, the etch figures will show full geometric symmetry. If the concentration exceeds this limiting value, the reduced symmetry is found on the proper crystal faces. This probably is a result of the degree of chemical activity of the solvent material. In some cases, such as laevo-malic acid in water, the minimum value of concentration required to give a perceptible asymmetry is extremely small.

(7) Some minerals, such as halite and fluorite, because of their simple ionic structures, may react alike to both optically active and optically inactive solvents, revealing only full symmetry. Such a result would be consistent with the well-known structures found by X-ray crystal analysis. This feature, recognized from the experiments described, should be further investigated.

THE PENNSYLVANIA STATE COLLEGE, STATE COLLEGE, PA.
MANUSCRIPT RECEIVED BY THE SECRETARY OF THE SOCIETY, AUGUST 8, 1936.
ACCEPTED BY THE COMMITTEE ON PUBLICATIONS, 1936.
Project Grant 100-34.

# EXPLANATION OF PLATES

## PHOTOMICROGRAPHS OF ETCH FIGURES

*Note:* Unless otherwise indicated, the C axis is vertical in all photomicrographs except those of the basal pinacoid.

### PLATE 4

### ETCHING PHENOMENA ON CALCITE AND DOLOMITE

Figures 1 and 2. Calcite. Adjacent scalenohedral faces etched simultaneously by a concentrated solution of d-glucono-delta-lactone in water. The etch figures of the like planes are markedly different. The photos are mounted in correspondence with the facial arrangement on the crystal. x 70

Figures 3 and 4. Dolomite. Opposite parallel faces of the cleavage rhombohedron etched simultaneously by lithium hydroxide solution of l-malic acid. x 350

1

2

3

4

ETCHING PHENOMENA ON CALCITE AND DOLOMITE

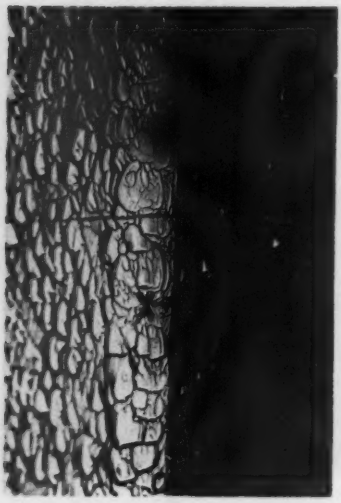

1

2

3

4

5

ETCHING PHENOMENA ON SCALENOHEDRON FACES OF CALCITE

## PLATE 5

### ETCHING PHENOMENA ON SCALENOHEDRON FACES OF CALCITE

**Figure 1.** Same as figures 1 and 2, of Plate 4, with shorter period of immersion in the solvent. Scalenohedral edge formed by the right and left faces may be observed at x on the photo. Note unlike solubility of adjacent planes. x 70

**Figures 2 and 3.** Calcite. Adjacent scalenohedral faces etched simultaneously by l-malic acid. Figure 2 represents the face to left; figure 3, the face to right. The etch figures are oriented to correspond with their relative positions on the faces of the crystal. x 70

**Figures 4 and 5.** Calcite. Adjacent scalenohedral faces etched simultaneously by an ammoniacal solution of d-glucono-delta-lactone. x 70

## PLATE 6

### ETCH FIGURES OF CALCITE CLEAVAGE RHOMBOHEDRON

Figure 1. Calcite. Cleavage rhombohedron etched by d-glucono-delta-lactone. The mature etching appears at a, the immature figure at b. x 70

Figure 2. Calcite. Cleavage rhombohedron etched by acetic acid solution of d-glucono-delta-lactone. x 70

Figure 3. Calcite. Cleavage rhombohedron etched by d-glucono-delta-lactone acidified with hydrochloric acid. Various stages of etch figure growth may be observed. Compare etchings A and B. x 70

Figure 4. Calcite. Cleavage rhombohedron etched by d-glucono-delta-lactone acidified with acetic acid. Etchings are similar to those obtained by water solution of this lactone. x 70

1

2

3

4

ETCH FIGURES OF CALCITE CLEAVAGE RHOMBOHEDRON

1

2

3

4

ETCH FIGURES OF CALCITE CLEAVAGE RHOMBOHEDRON

## PLATE 7

### ETCH FIGURES OF CALCITE CLEAVAGE RHOMBOHEDRON

**Figure 1.** Calcite. Cleavage rhombohedron etched by citric acid solution of d-glucono-delta-lactone. Etch figures indicate full crystallographic symmetry. x 70

**Figure 2.** Calcite. Cleavage rhombohedron etched by sodium hydroxide solution of l-aspartic acid. Etchings are definitely asymmetric. x 70

**Figure 3.** Calcite. Cleavage rhombohedron etched by potassium hydroxide solution of l-aspartic acid. x 70

**Figure 4.** Calcite. Cleavage rhombohedron etched by sodium hydroxide solution of d-glutamic acid. Note various developmental stages of figures. x 70

PLATE 8

ETCH FIGURES OF CALCITE CLEAVAGE RHOMBOHEDRON

Figure 1. Calcite. Cleavage rhombohedron etched by ammoniacal solution of d-glucono-delta-lactone. Note the marked likeness of etch figures to those of Plate 7, figure 4. x 70

Figure 2. Calcite. Cleavage rhombohedron etched by lithium hydroxide solution of d-glucono-delta-lactone. x 70

Figure 3. Calcite. Cleavage rhombohedron etched by d-l malic acid (optically inactive). Compare with figures 1 and 2 of Plate 9. x 70

Figure 4. Calcite. Cleavage rhombohedron etched by l-tartaric acid. x 70

Figure 5. Calcite. Cleavage rhombohedron etched by d-tartaric acid. Compare enantiomorphous etching A of figure 4 with etching B of figure 5. x 70

1

2

3

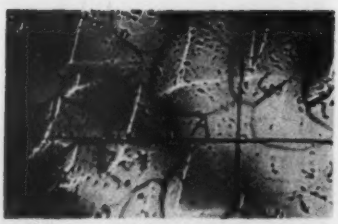

4

5

ETCH FIGURES OF CALCITE CLEAVAGE RHOMBOHEDRON

1

2

3

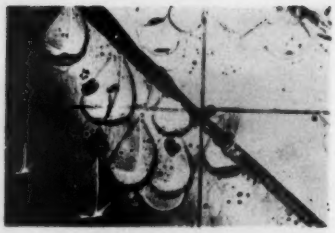

4

5

ETCH FIGURES OF CALCITE CLEAVAGE RHOMBOHEDRON

## PLATE 9

### ETCH FIGURES OF CALCITE CLEAVAGE RHOMBOHEDRON

**Figure 1.** Calcite. Cleavage rhombohedron etched by d-malic acid. x 70

**Figure 2.** Calcite. Cleavage rhombohedron etched by l-malic acid. Compare with figure 1. x 350

**Figure 3.** Calcite. Cleavage rhombohedron etched by water solution of d-leucin. x 350

**Figure 4.** Calcite. Cleavage rhombohedron etched by ammoniacal solution of d-malic acid. x 70

**Figure 5.** Calcite. Cleavage rhombohedron etched by ammoniacal solution of l-malic acid. x 70

PLATE 10

ETCH FIGURES OF CALCITE CLEAVAGE RHOMBOHEDRON AND PRISM

Figure 1. Calcite. Cleavage rhombohedron etched by l-lactic acid. x 70

Figure 2. Calcite. Cleavage rhombohedron etched by citric acid solution of d-tartaric acid. x 85

Figure 3. Calcite. Cleavage rhombohedron etched by concentrated citric acid (optically inactive). x 70

Figure 4. Calcite. First order prism etched by concentrated citric acid. x 310

1

2

3

4

ETCH FIGURES OF CALCITE CLEAVAGE RHOMBOHEDRON AND PRISM

1

2

3

4

CALCITE ETCHINGS ON THE BASE AND PRISMS

## PLATE 11

### CALCITE ETCHINGS ON THE BASE AND PRISMS

**Figure 1.** Calcite. Second order prism etched by concentrated citric acid. x 310

**Figure 2.** Calcite. Basal pinacoid etched by concentrated citric acid. x 30

**Figure 3.** Calcite. First order prism etched by l-aspartic acid. Compare etchings of figures 3 and 4 with those of figure 4 of Plate 10 and note diminished symmetry when optically active solvents are employed. x 70

**Figure 4.** Calcite. First order prism etched by sodium hydroxide solution of l-aspartic acid. x 70

PLATE 12

CALCITE ETCHINGS ON THE FIRST ORDER PRISM

Figure 1. Calcite. First order prism etched by d-glutamic acid dissolved in sodium hydroxide. x 70

Figure 2. Calcite. First order prism etched by ammoniacal solution of l-lactic acid. x 70

Figure 3. Calcite. First order prism etched by sodium hydroxide solution of l-lactic acid. x 70

Figure 4. Calcite. First order prism etched by lithium hydroxide solution of l-lactic acid. x 70

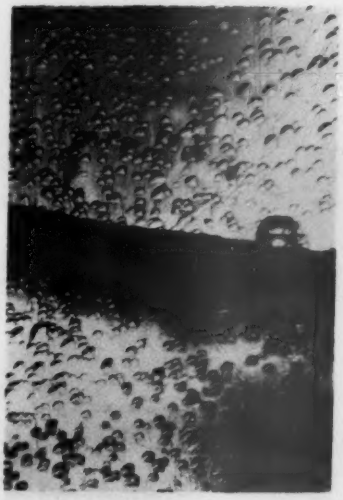

1

2

3

4

CALCITE ETCHINGS ON THE FIRST ORDER PRISM

1

2

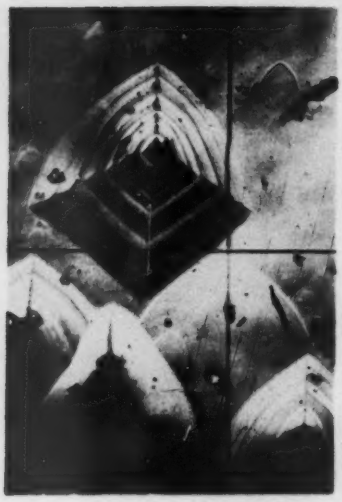

3

4

ETCHING FIGURES OF CALCITE AND SMITHSONITE

PLATE 13

ETCHING FIGURES OF CALCITE AND SMITHSONITE

**Figure 1.** Calcite. First order prism etched by potassium hydroxide solution of l-lactic acid. x 70

**Figure 2.** Calcite. Acute rhombohedron f. etched by sodium hydroxide solution of d-glucono-delta-lactone (optically active). x 70

**Figure 3.** Calcite. Acute rhombohedron f. etched by chlor-brome-acetic acid (optically inactive). Compare with figure 2. x 70

**Figure 4.** Smithsonite. Cleavage rhombohedron etched by l-lactic acid. x 350

PLATE 14

ETCHING FIGURES OF SMITHSONITE, RHODOCHROSITE, AND DOLOMITE

Figure 1. Smithsonite. Cleavage rhombohedron etched by sodium hydroxide solution of l-lactic acid. x 70

Figure 2. Rhodochrosite. Cleavage rhombohedron etched by l-lactic acid. x 350

Figure 3. Rhodochrosite. Cleavage rhombohedron etched by optically inactive chlor-brome-acetic acid. Compare with figure 2. x 350

Figure 4. Dolomite. Cleavage rhombohedron etched by l-malic acid. x 70

1

2

3

4

ETCHING FIGURES OF SMITHSONITE, RHODOCHROSITE, AND DOLOMITE

1

2

3

4

ETCH FIGURES ON DOLOMITE CLEAVAGE RHOMBOHEDRON

PLATE 15

ETCH FIGURES ON DOLOMITE CLEAVAGE RHOMBOHEDRON

**Figure 1.** Dolomite. Cleavage rhombohedron etched by d-tartaric acid. x 350

**Figure 2.** Dolomite. Cleavage rhombohedron etched by d-glucono-delta-lactone. x 350

**Figure 3.** Dolomite. Cleavage rhombohedron etched by l-aspartic acid. x 70

**Figure 4.** Dolomite. Cleavage rhombohedron etched by chlor-brome-acetic acid (optically inactive). x 70

PLATE 16

ABNORMAL ETCHING PHENOMENA OF DOLOMITE CLEAVAGE RHOMBOHEDRON

Figures 1 and 2. Dolomite. Opposite parallel faces of the cleavage rhombohedron etched by sodium hydroxide solution of l-malic acid. x 350

Figure 3. Dolomite. Twinned face of the cleavage rhombohedron etched by sodium hydroxide solution of l-malic acid. Compare etch figures above and below line a—b. x 350

1

2

3

ABNORMAL ETCHING PHENOMENA OF DOLOMITE CLEAVAGE RHOMBOHEDRON

1

2

3

4

ABNORMAL ETCHING PHENOMENA OF DOLOMITE CLEAVAGE RHOMBOHEDRON

PLATE 17

ABNORMAL ETCHING PHENOMENA OF DOLOMITE
CLEAVAGE RHOMBOHEDRON

**Figures 1 and 2.** Dolomite. Opposite parallel faces of the cleavage rhombohedron etched simultaneously by sodium hydroxide solution of d-tartaric acid. x 350

**Figures 3 and 4.** Dolomite. Opposite parallel faces of the cleavage rhombohedron etched simultaneously by potassium hydroxide solution of d-tartaric acid. x 350

PLATE 18

ABNORMAL ETCHING PHENOMENA OF DOLOMITE
CLEAVAGE RHOMBOHEDRON

Figures 1 and 2. Dolomite. Opposite parallel faces of the cleavage rhombohedron etched simultaneously by sodium hydroxide solution of d-glucono-delta-lactone. x 350

Figures 3 and 4. Dolomite. Opposite parallel faces of the cleavage rhombohedron etched simultaneously by potassium hydroxide solution of d-glucono-delta-lactone. x 350

1

2

3

4

ABNORMAL ETCHING PHENOMENA OF DOLOMITE CLEAVAGE RHOMBOHEDRON

1

2

3

4

ABNORMAL ETCHING PHENOMENA OF DOLOMITE CLEAVAGE RHOMBOHEDRON

PLATE 19

ABNORMAL ETCHING PHENOMENA OF DOLOMITE
CLEAVAGE RHOMBOHEDRON

**Figures 1 and 2.** Dolomite. Opposite parallel faces of the cleavage rhombohedron etched simultaneously by ammoniacal solution of d-glucono-delta-lactone. x 350

**Figures 3 and 4.** Dolomite. Opposite parallel faces of the cleavage rhombohedron etched simultaneously by lithium hydroxide solution of l-aspartic acid. x 350

PLATE 20

ETCHING PHENOMENA OF DOLOMITE AND CELESTITE

Figures 1 and 2. Dolomite. Opposite parallel faces of the cleavage rhombohedron etched simultaneously by sodium hydroxide solution of l-lactic acid. x 350

Figure 3. Celestite. Basal pinacoid. Etched by lithium hydroxide solution of d-glucono-delta-lactone. x 350

Figure 4. Celestite. Basal pinacoid. Etched by sodium hydroxide solution of d-glucono-delta-actone. x 70

1

2

3

4

ETCHING PHENOMENA OF DOLOMITE AND CELESTITE

1

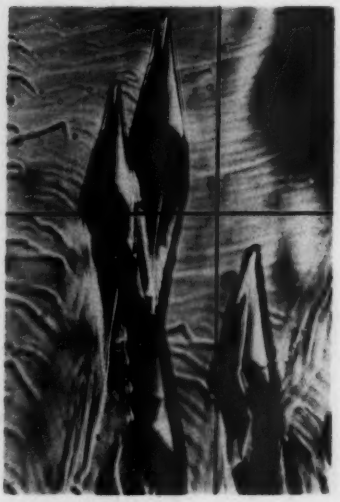

2

3

4

ETCHING FIGURES ON THE CELESTITE BASE

PLATE 21

ETCHING FIGURES ON THE CELESTITE BASE

**Figure 1.** Celestite. Basal pinacoid. Etched by potassium hydroxide solution of d-glucono-delta-lactone. x 70

**Figure 2.** Celestite. Basal pinacoid. Etched by ammoniacal solution of d-glucono-delta-lactone. x 350

**Figure 3.** Celestite. Basal pinacoid. Etched by potassium hydroxide solution of l-aspartic acid. x 350

**Figure 4.** Celestite. Basal pinacoid. Etched by sodium hydroxide solution of l-aspartic acid. x 350

PLATE 22

ETCHING FIGURES OF CELESTITE AND HEMIMORPHITE

Figure 1. Celestite. Basal pinacoid. Etched by d-tartaric acid dissolved in potassium hydroxide. x 350

Figure 2. Celestite. Basal pinacoid. Etched by ammoniacal solution of d-tartaric acid. x 70

Figure 3. Celestite. Basal pinacoid. Etched by sodium hydroxide solution of d-tartaric acid. x 350

Figure 4. Hemimorphite. Brachy pinacoid. Etched by l-aspartic acid. x 350

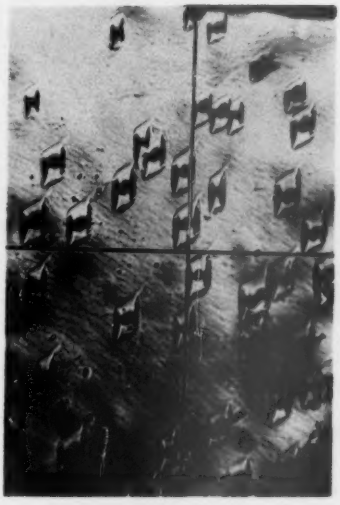

1

2

3

4

ETCHING FIGURES OF CELESTITE AND HEMIMORPHITE

1

2

3

4

ETCH FIGURES ON THE BRACHY PINACOID OF HEMIMORPHITE

PLATE 23

ETCH FIGURES ON THE BRACHY PINACOID OF HEMIMORPHITE

**Figure 1.** Hemimorphite. Brachy pinacoid. Etched by d-glucono-delta-lactone. x 350

**Figure 2.** Hemimorphite. Brachy pinacoid. Etched by sodium hydroxide solution of d-arabono-lactone. x 350

**Figure 3.** Hemimorphite. Brachy pinacoid. Etched by potassium hydroxide solution of d-glucono-delta-lactone. x 350

**Figure 4.** Hemimorphite. Brachy pinacoid. Etched by sodium hydroxide solution of d-glucono-delta-lactone. x 350

PLATE 24

ETCH FIGURES ON THE BRACHY PINACOID OF HEMIMORPHITE

Figure 1. Hemimorphite. Brachy pinacoid. Etched by lithium hydroxide solution of d-gluconodelta-lactone. x 350

Figure 2. Hemimorphite. Brachy pinacoid. Etched by sodium hydroxide solution of d-tartaric acid. x 350

Figure 3. Hemimorphite. Brachy pinacoid. Etched by ammoniacal solution of d-tartaric acid. x 350

Figure 4. Hemimorphite. Brachy pinacoid. Etched by racemic d-l malic acid. (Figures symmetrical.) x 350

1

2

3

4

ETCH FIGURES ON THE BRACHY PINACOID OF HEMIMORPHITE

1

2

3

4

ETCHING PHENOMENA OF DOLOMITE AND HEMIMORPHITE

PLATE 25

ETCHING PHENOMENA OF DOLOMITE AND HEMIMORPHITE

**Figures 1 and 2.** Dolomite. Opposite parallel faces of the cleavage rhombohedron etched by l-lactic acid. x 70

**Figure 3.** Hemimorphite. Brachy pinacoid. Etched by l-lactic acid. (Etch figures are enantiomorphous to those of figure 4.) x 350

**Figure 4.** Hemimorphite. Brachy pinacoid. Etched by d-lactic acid. x 350